



A User's Guide to the PLTEMP/ANL Code

Version 4.2

Nuclear Engineering Division

About Argonne National Laboratory

Argonne is a U.S. Department of Energy laboratory managed by UChicago Argonne, LLC under contract DE-AC02-06CH11357. The Laboratory's main facility is outside Chicago, at 9700 South Cass Avenue, Argonne, Illinois 60439. For information about Argonne and its pioneering science and technology programs, see www.anl.gov.

DOCUMENT AVAILABILITY

Online Access: U.S. Department of Energy (DOE) reports produced after 1991 and a growing number of pre-1991 documents are available free via DOE's SciTech Connect (<http://www.osti.gov/scitech/>)

Reports not in digital format may be purchased by the public from the National Technical Information Service (NTIS):

U.S. Department of Commerce
National Technical Information Service
5301 Shawnee Rd
Alexandria, VA 22312
www.ntis.gov
Phone: (800) 553-NTIS (6847) or (703) 605-6000
Fax: (703) 605-6900
Email: orders@ntis.gov

Reports not in digital format are available to DOE and DOE contractors from the Office of Scientific and Technical Information (OSTI):

U.S. Department of Energy
Office of Scientific and Technical Information
P.O. Box 62
Oak Ridge, TN 37831-0062
www.osti.gov
Phone: (865) 576-8401
Fax: (865) 576-5728
Email: reports@osti.gov

Disclaimer

This report was prepared as an account of work sponsored by an agency of the United States Government. Neither the United States Government nor any agency thereof, nor UChicago Argonne, LLC, nor any of their employees or officers, makes any warranty, express or implied, or assumes any legal liability or responsibility for the accuracy, completeness, or usefulness of any information, apparatus, product, or process disclosed, or represents that its use would not infringe privately owned rights. Reference herein to any specific commercial product, process, or service by trade name, trademark, manufacturer, or otherwise, does not necessarily constitute or imply its endorsement, recommendation, or favoring by the United States Government or any agency thereof. The views and opinions of document authors expressed herein do not necessarily state or reflect those of the United States Government or any agency thereof, Argonne National Laboratory, or UChicago Argonne, LLC.

A User's Guide to the PLTEMP/ANL Code

Version 4.2

by
A. P. Olson and M. Kalimullah
Nuclear Engineering Division, Argonne National Laboratory

July 7, 2015

This work is sponsored by the
U.S. Department of Energy, National Nuclear Safety Administration (NNSA),
Office of Material management and Minimization (NA-23) Reactor Conversion Program

TABLE OF CONTENTS

LIST OF FIGURES	vii
LIST OF TABLES	viii
ABSTRACT	ix
1. INTRODUCTION	1
2. DEVELOPMENT OF PLTEMP/ANL	1
2.1. Improvements and Extensions Introduced in PLTEMP/ANL	1
2.2. Corrections made to PLTEMP/ANL	6
3. FURTHER DEVELOPMENT OF PLTEMP/ANL	6
3.1. Solution of the Temperature Profile	6
3.2. Radial Geometry	7
3.3. Thermodynamic Properties of Coolants	8
3.4. Output Edits	8
3.5. Processing Engineering Hot-Channel Factors	8
3.6. Flow Excursion Instability	13
3.7. Friction Factors for Smooth Pipes and Rough Pipes	13
3.8. New Treatment of Bypass Channels	14
3.9. Natural Circulation Flow	15
3.10. Search Capability	17
3.11 Modeling a Central Solid Fuel Rod Inside Multiple Coaxial Fuel Tubes	18
3.12 Organization of the Output File	18
3.13. Other Changes to Input and Output	21
4. VALIDATION	22
5. LIMITS OF CODE OPERATION	24
6. CLEANUP/MODERNIZATION OF SOURCE CODE	24
7. COMPUTER HARDWARE REQUIREMENTS	24
REFERENCES	26
APPENDIX I. PLTEMP/ANL V4.2 INPUT DESCRIPTION	55
APPENDIX II. INPUT DATA FOR AXIAL POWER SHAPE IN EACH STRIPE OF ALL FUEL PLATES	88
APPENDIX III. HEAT CONDUCTION EQUATIONS FOR 1-D RADIAL GEOMETRY USED IN BROYDEN SOLUTION	93
APPENDIX IV. HEAT TRANSFER CORRELATIONS	95

APPENDIX V.	HOT CHANNEL FACTORS TREATMENT OPTION 2	108
APPENDIX VI.	ANALYTICAL SOLUTION FOR TEMPERATURE DISTRIBUTION IN A FLAT FUEL PLATE ASSEMBLY	118
APPENDIX VII.	EXCURSIVE FLOW INSTABILITY PREDICTION	123
APPENDIX VIII.	ANALYTICAL SOLUTION FOR RADIAL TEMPERATURE DISTRIBUTION IN A MULTI-TUBE FUEL ASSEMBLY.....	140
APPENDIX IX.	HEAT TRANSFER COEFFICIENT AND FRICTION FACTOR IN CHANNELS HAVING LONGITUDINAL INNER FINS	150
APPENDIX X.	COMPARISON OF BABELLI-ISHII FLOW INSTABILITY CRITERION WITH 75 TESTS DONE BY WHITTLE AND FORGAN.....	167
APPENDIX XI.	CALCULATION OF NATURAL CIRCULATION FLOW RATE	194
APPENDIX XII.	VERIFICATION AND APPLICATION OF SEARCH CAPABILITY	227
APPENDIX XIII.	ANALYTICAL SOLUTION FOR RADIAL TEMPERATURE DISTRIBUTION IN AN ASSEMBLY OF MULTIPLE FUEL TUBES EACH MADE OF FIVE MATERIAL REGIONS.....	242
APPENDIX XIV.	NORMALIZATION OF POWER IN LONGITUDINAL STRIPES OF A FIVE-LAYER THICK FUEL PLATE	256

LIST OF FIGURES

Figure 1.	Cross Section of a Typical Fuel Assembly Having Six Fuel Plates Modeled by PLTEMP/ANL Code (A single fuel plate is shown at the top).....	30
Figure 2.	Fuel Plate Geometry modeling in PLTEMP/ANL Code.....	31
Figure 3.	Cross Section of a Typical Fuel Assembly Having Four Coaxial Fuel Tubes Modeled by PLTEMP/ANL Code.....	32
Figure 4.	Geometry of a Fuel Tube with Different Claddings on the Left and Right Sides of the Fuel Meat in Two Cases: (1) Without Gap Between Meat and Cladding, and (2) With Gap Between Meat and Cladding.....	33
Figure 5.	Subroutine Calling Hierarchy in PLTEMP/ANL Version 4.2 Code.....	34
Figure 6.	Logical Flow Diagram of the Main Program of PLTEMP/ANL Code.....	35
Figure 7.	Logical Flow Diagram of Subroutine PLTEMPX, the Pre-Search Main Driver.	36
Figure 8.	Logical Flow Diagram of Subroutine WORK in PLTEMP/ANL Code.	37
Figure 9.	Geometrical Representation of ONB Ratio for a Fuel Plate Axial Node in PLTEMP/ANL Code.....	41
Figure 10.	Geometrical Representation of ONB Ratio for a Fuel Plate Axial Node, Including the Effect of Hot Channel Factors.....	42
Figure 11.	Coolant Flow Path in a Fuel Assembly and Chimney Modeled in PLTEMP/ANL (Multiple Axial Regions Downstream of the Heated Section Are Allowed).....	43

LIST OF TABLES

Table 1. Purpose of Major Subroutines in PLTEMP/ANL V4.2 Code	44
Table 2. Check of Peak Fuel Temperature in Slab Geometry	23
Table 3. Definition of Important FORTRAN Variables in the Code	48

A USERS GUIDE TO THE PLTEMP/ANL V4.2 CODE

Arne P. Olson and M. Kalimullah
Argonne National Laboratory
Argonne, Illinois 60439 USA

ABSTRACT

PLTEMP/ANL V4.2 is a FORTRAN program that obtains a steady-state flow and temperature solution for a nuclear reactor core, or for a single fuel assembly. It is based on an evolutionary sequence of "PLTEMP" codes in use at ANL for the past 20 years [1-7]. Fueled and non-fueled regions are modeled. Each fuel assembly consists of one or more plates or tubes separated by coolant channels. The fuel plates may have one to five layers of different materials, each with heat generation. The width of a fuel plate may be divided into multiple longitudinal stripes, each with its own axial power shape. The temperature solution is effectively 2-dimensional. It begins with a one-dimensional solution across all coolant channels and fuel plates/tubes within a given fuel assembly, at the entrance to the assembly. The temperature solution is repeated for each axial node along the length of the fuel assembly. The geometry may be either slab or radial, corresponding to fuel assemblies made of a series of flat (or slightly curved) plates, or of nested tubes. A variety of thermal-hydraulic correlations are available with which to determine safety margins such as Onset-of- Nucleate boiling (ONB), departure from nucleate boiling (DNB), and onset of flow instability (FI). Coolant properties for either light or heavy water are obtained from FORTRAN functions rather than from tables. The code is intended for thermal-hydraulic analysis of research reactor performance in the sub-cooled boiling regime. Both turbulent and laminar flow regimes can be modeled. Options to calculate both forced flow and natural circulation are available. A general search capability is available (Appendix XII) to greatly reduce the reactor analyst's time.

1. INTRODUCTION

PLTEMP/ANL V4.2 is descended from the original PLTEMP code authored by Mishima, *et al.* [1-5]. The original PLTEMP was created to obtain a 1-dimensional steady-state temperature solution for a reactor core consisting of a group of nuclear reactor fuel assemblies, each comprised of multiple flat plates separated by coolant channels. Bypass flow was also modeled. It was intended for analysis of “MTR-type” fuel assemblies. The code was first applied to the Kyoto University Reactor (KUR), which is a light water-moderated, tank-type nuclear research reactor in current operation. The power of the KUR is 5 MWt and the mean thermal neutron flux is 3.2×10^{13} n/cm²/s. The KUR core consists of enriched uranium fuel of MTR-type. The original PLTEMP was designed to represent flow and temperature conditions in a single hot channel, a single fuel assembly, or a reactor core consisting of up to five different types of fuel assemblies, and up to 30 fuel assemblies of each type. It was assumed that the coolant temperature was that at the outlet. This assumption gave conservative estimates for the peak fuel temperature and clad surface temperatures of each plate, and for the safety-related margin to critical heat flux.

The full fuel assembly or core flow was modeled with entrance and exit hydraulic pressure losses. Flow distribution was calculated to obtain uniform pressure drops across all flow paths, either in the core or in a given fuel assembly. Axial power peaking factors were supplied for each fuel plate of each fuel assembly. Bypass flow through non-fueled channels could also be specified. There was no axial power distribution imposed on the heat generation by the fuel. Engineering hot channel factors were accounted as follows: F_b for bulk water temperature rise, F_q for heat flux, and F_h for heat transfer coefficient. Physical properties for the coolant (saturation temperature, enthalpy, viscosity, and thermal conductivity) were obtained by interpolation from supplied tables. Thermal conductivity of a variety of uranium-aluminum alloy fuels was available from interpolation or from fitted equations. A series of calculations could be performed in one run to span a desired range of pressure drops.

2. DEVELOPMENT OF PLTEMP/ANL

Section 2.1 describes the improvements and extensions made to the PLTEMP code and introduced in the PLTEMP/ANL version of the code. Section 2.2 describes the various corrections made to the PLTEMP/ANL code.

2.1. Improvements and Extensions Introduced in PLTEMP/ANL

One important extension was to provide one or multiple imposed axial heat production profiles from which to calculate axial temperature profiles. Another feature was a revision of the coolant property library tables: they were made identical to those used by the PARET/ANL code [7, 8]. A broader selection of clad alloys with clad conductivity data was added. Friction factor parameters and the integral flow instability parameter η were made input options. Additional heat transfer correlation choices were also added, including the Carnavos correlation for finned channel (Appendix IX). The Petukhov correlation [9] and another Russian correlation as used in their ASTRA code for the single-phase heat transfer coefficient have been added as options, and the Weatherhead correlation [10] has been added to the selection of Departure from Nucleate Boiling (DNB) choices. The Forster-Greif correlation [12] has been added as a second choice for

the detection of Onset-of-Nucleate Boiling (ONB). Because of the variation in the fuel meat conductivity with fuel type, loading and burnup, this parameter must be determined by the user.

The location (fuel assembly, fuel plate and flow channel) where the hot channel factors apply may now be specified by fuel type with full fuel assemblies, multiple fuel assemblies, and multiple fuel types. A single hottest plate may still be modeled with the hot channel factors included. Also it should be recognized that not all of the components of the heat flux hot channel factor apply over the entire axial length of the fuel meat. Thus, the heat flux hot channel factor may now be split into global and local components, with the local component applied at a selected single axial node or over a selected axial range of nodes. The local and global components are combined statistically where the local component applies axially and in the original (single-node, non-axial) portion of the code.

Given an input frictional pressure drop from the inlet to exit of an assembly, the code computes and edits the flow rate for each flow path (fuel and bypass), the heat flux on each side of each fuel plate, and the temperatures of coolant, cladding and fuel meat. Running the code in this way is referred to as the *pressure drop driven mode*. As an alternate option to the pressure drop driven mode, the flow rate by channel may be input directly, and running the code the latter way is referred to as the *flow driven mode*. The margins to DNB and to Flow Instability (FI) based on outlet coolant temperature values are calculated. Given an axial relative power distribution, the code computes the heat flux profile and corresponding temperatures for the fuel, clad and coolant. Nodes in sub-cooled nucleate boiling and fully developed nucleate boiling based on either the Bergles-Rohsenow or the Forster-Greif correlation and the Jens-Lottes correlation, respectively, are flagged in the output. The power at ONB can be determined manually. An edit of the dynamic bubble detachment parameter, ETA, as a function of the local coolant temperature, heat flux and flow velocity is also provided at each node.

In all versions of PLTEMP, the fuel plate dimensions are input in terms of the width or arc length of the fuel meat and the unfueled length of the plate. The geometry is shown in Figs. 1 to 4. This gives the user the freedom to describe flat plates, or curved plates of varying size and extends to concentric cylinders of fuel with no unfueled region. With radii that are large compared with the thickness of the plate, the plate geometry solution is still a good approximation for curved plates or cylinders. The solution allows a choice of single-phase heat transfer coefficients that include the Sieder-Tate [13], Dittus-Boelter [14] and Colburn [15] correlations. The Critical Heat Flux (CHF) options include the Mirshak-Durant-Towell [16], Bernath [17], Labuntsov [18], Mishima [19] correlations, the Groeneveld tables [32], a combined Mishima-Mirshak-Labuntsov scheme, Shah [35] and Sudo-Kaminaga [38] correlations. The Flow Instability (FI) options include the Whittle-Forgan correlation [20] and the Babelli-Ishii-Zuber criterion [26]. The Jens-Lottes [21] correlation is imposed for two-phase heat transfer, and the Forster-Greif [12] or Bergles-Rohsenow [22] correlations are used to detect the Onset-of-Nucleate Boiling (ONB).

PLTEMP/ANL added the Mishima [19] and Weatherhead [10] CHF correlations, and two Russian heat transfer correlations: Petukhov [9] and a slightly modified Dittus-Boelter correlation of the form $Nu = 0.021 Re^{0.8} Pr^{0.43} (Pr/Pr_w)^{0.25}$.

As a new option, a series of calculations could be performed in one run to span a desired range of powers. The purpose of major subroutines of the code is given in Table 1 (see p. 44), and the calling hierarchy of the major subroutines is shown in Fig. 5. The logic flow diagrams of the code are shown in Figs. 6 to 8.

PLTEMP/ANL V2.0 was documented in a User's Guide dated June 12, 2003 (RERTR Project internal memorandum). PLTEMP/ANL V2.14 was documented in a User's Guide dated Feb. 25, 2005 (RERTR Project internal memorandum). The improvements made since then are:

1. The 1995 Groeneveld critical heat flux (CHF) look-up table has been replaced by the 2006 Groeneveld [31, 32] CHF table. The 2006 table was implemented as the same option (option 5) for calculating CHF ratio. The RMS error of the 2006 table (based on all data used in deriving the table) is quoted as 7.10 % when the table is used at constant inlet condition, or 38.93% when the table is used at constant local quality [32]. An auxiliary code is used to convert data in digital matrix form (one matrix per pressure, containing CHF values vs. mass flux and quality) into a double precision binary file *groen2.bin*. The coding for the implementation was also improved so that the 2006 or any other CHF table could also be used in PLTEMP/ANL V4.2, simply by replacing the input binary file *groen2.bin*. The correction factor applied to the base Groeneveld CHF table (for a hydraulic diameter of 8 mm) to account for variation in hydraulic diameter is also changed from $K_1 = (0.008/D_h)^{1/3}$ to $K_1 = (0.008/D_h)^{1/2}$.

Other effects such as from the use of bundles (K_2), grids (K_3), heated length variation (K_4), axial flux distribution factor (K_5), radial or circumferential flux distribution factor (K_6), flow-orientation factor (K_7), and vertical low-flow factor (K_8), have been developed [31] for use with the CHF tables. Only K_1 is accounted for in V4.2. As used in PLTEMP/ANL V4.2, the CHF lookup tables are appropriate for pressures ranging from 0.100 MPa to 21 MPa, mass fluxes from 0 to 8000 kg/m²/s, and quality from -0.5 to 1.0. Because V4.2 is only valid for 1-phase flow, it is used for quality from -0.5 to 0.0. The tables can be used for upflow or downflow.

A three-dimensional (3-D) linear interpolation in pressure, mass flux, and quality is used to find the CHF at the pressure, mass flux, and quality in each heat transfer node of a coolant channel. For this 3-D interpolation in the (quality, mass flux, and pressure) space, the eight nearest tabular values or points that surround the desired heat transfer node are located first. Then a 3-D interpolation within these 8 points is used to calculate the value of CHF for the node. Extrapolation is not permitted. Instead, if the nodal conditions are out of range, the CHF values at the end-points of the tabulated ranges for pressure, mass flux, and quality are used and a warning message is printed.

2. One-sided heat transfer can be modeled for first and last coolant channels in a fuel assembly (this is important for laminar flow only) [33]:

$$Nu = 4.86$$

3. Laminar flow heat transfer coefficient is computed and compared with turbulent flow value. The larger heat transfer coefficient is then used. The ORNL laminar forced convection correlation is [34]:

$$\text{Nu} = 7.63$$

4. Channel friction factors can now be computed for laminar flow, and for the transition between laminar and turbulent flow.
5. The usage of hot channel factor F_h is changed; it is now applied globally rather than locally.
6. Carnavos correlation is incorporated in the code to calculate the heat transfer coefficient and friction factor in internally finned coolant channels (like the MIT Reactor).
7. A capability was added in PLTEMP/ANL V4.2 to calculate natural circulation flow, up through the fuel assemblies and down through the flow area in the reactor pool/vessel outside the fuel assemblies. See Appendix XI for documentation.
8. The Collier correlation for Nusselt number was implemented in PLTEMP/ANL V4.2 to account for buoyancy-induced enhancement of cladding-to-coolant heat transfer. The implementation provides full control to the code user to change the values of the coefficients and exponents in the correlation. To use this capability, set the input MORE on Card 0200 to 2.
9. A chimney model was implemented in PLTEMP/ANL V4.2. To use this capability, set the input MORE on Card 0200 to 1. See Appendix XI for documentation.
10. The six hot channel factors treatment (input option IHCF = 2) is also available in the case of natural circulation calculation.
11. The volume-average fuel meat temperature is calculated for each fuel plate and each fuel assembly.
12. A general search capability (input option ISRCH = 1) is available to get a specific target value for a specified code output variable (e.g., reactor coolant flow rate) by changing a user-specified input datum (e.g., applied pressure drop).
13. An error was corrected in the critical heat flux (CHF) option 3 that is based on Mishima's suggested CHF *lower bound*¹⁹ for mass velocity from 350 kg/m²-s downward to 70 kg/m²-s upward, at close to atmospheric pressure, in a rectangular channel.
14. A CHF option was added to the code that uses Mishima's fit to his CHF test data¹⁹ for mass velocity $G < 600$ kg/m²-s, uses the smaller of the Mirshak¹⁶ and Labuntsov¹⁸ correlations for $G > 1500$ kg/m²-s, and interpolates between the Mishima fit at $G=600$ kg/m²-s and the smaller of the Mirshak and Labuntsov correlations at $G=1500$ kg/m²-s

for the intermediate range $600 < G < 1500 \text{ kg/m}^2\text{-s}$. This correlation is good for natural circulation flow rates *and near-atmospheric pressure* in rectangular coolant channels.

15. The Shah correlation for CHF was added to the code as the input option 7.
16. The 1998 CHF correlation of Sudo and Kaminaga^{37,38} was implemented into the code. This correlation is an improvement of Mishima's fit¹⁹ (CHF input option 6), and is tested for the mass velocity range from $25800 \text{ kg/m}^2\text{-s}$ downflow through stagnant flow to $6250 \text{ kg/m}^2\text{-s}$ upflow, and the pressure range from 1 to 7.2 bar. It is recommended for use at natural circulation flow rates in rectangular coolant channels.
17. The CHF is computed at each axial heat transfer node on both sides (left and right hand sides) of each fuel plate of each fuel assembly modeled by the input data file. The nodal CHF is obtained as the ratio of the critical heat flux at an axial node of the coolant channel on the left (or right) hand side of the fuel plate divided by the operating heat flux in the node on the plate's left (or right) hand surface. The nodal CHF is defined and calculated using this method, irrespective of the critical heat flux correlation chosen. This improvement is made in the exact solution option (KSOLNPR = 0) only, not in the Broyden solution option (KSOLNPR \geq 1) of the code.
18. The CHF correlation previously available in the code as the Weatherhead correlation (option 4) was replaced by Eq. (9) reported in ANL-6675 by R. J. Weatherhead [Ref. 10] because the previous correlation was not found documented in any publication.
19. Given a CHF correlation, an option (ITRNCHF=1) was added to the code to calculate the nodal CHF at the nodal thermal-hydraulic condition when the fuel plate power has been raised by an iteratively determined factor (keeping the axial power shape unchanged) such that the nodal heat flux equals the value of CHF. Basically, the node achieves a CHF condition when the iteration has converged. If the iteration requires the plate power to be raised by such a large factor that the limit of applicability of the given CHF correlation is reached before the nodal heat flux equals CHF, then the iteration is stopped without exceeding the applicability limit, and the value of CHF calculated in the last iteration is used.
20. An error in the code V3.3.1 and older versions in the implementation of the simplified Babelli-Ishii flow instability criterion was corrected in the code V3.4. The error was related to the adjustment (to account for axially non-uniform heat flux) of the dimensionless non-boiling length. To adjust the uniform-heat-flux-based non-boiling length for heat flux non-uniformity, it may be divided by the peak/average heat flux ratio in the channel, but it was incorrectly divided by the peak heat flux. This was corrected.
21. In the case of Colburn heat transfer correlation, the coolant viscosity (variable VISC) at the bulk temperature was used in the code V3.3.1 and older versions (in routines HCOEF and HCOEF1) whereas the viscosity at the film temperature should be used in this correlation. This was corrected in the code V3.4.

22. In the case of Mishima *lower bound* for critical heat flux (input option ICHF = 3), the code V3.7 and older versions had an error. In the equation for q_f (critical heat flux at zero mass velocity), the coolant channel heated perimeter was used (incorrectly) instead of using the channel width (the longer dimension of the channel cross section). This was corrected in the code V3.8.

2.2. Changes in PLTEMP/ANL V4.2 Compared to the Previous Release

1. On the input card 200, two new critical heat flux options were added. These are the extended Groeneveld 2006 CHF table (ICHF = 9), and the Hall-Mudawar inlet conditions correlation (ICHF = 10). The ICHF=9 is recommended.
2. On the input card 200, the meaning of option NAXDIS = 2 has changed. Now the axial power shape file may have any filename that is supplied on a new input card 702A. If the card 702A is not supplied, the code assumes a default filename of *axial.power.shape*.
3. On the input card 200, the option IGOM=1 was improved to model solid fuel rod, as described in Section 3.11 of the PLTEMP/ANL Users Guide.
4. D₂O liquid viscosity had an error of about 50% in the code V4.1. This has been corrected in V4.2.
5. On the input card 200, an additional hot channel factors option (IICF = 3) is available. Some input data related to this option is provided on card 306C.
6. On the input card 203, an additional double search option (NSRCH = 26) is available.
7. The code V4.2 is modified to stop with a message if a bulk coolant temperature greater than 340 °C is encountered during the calculation. The code V4.1 continued in this situation. This usually happened (with a warning message) in search problems with a wide input reactor power range. If no such warning message was printed in the finally converged searched solution, the results calculated by V4.1 were correct.
8. On the input card 300, a new option IBERN is added to use the Bernath CHF correlation in *half* channels.
9. On the input card 305, an additional input FPOVRD, a multiplier for turbulent heat transfer coefficient, is available.
10. On the input card 307, the user may set the value of AFF(I,1), the flow area of the first coolant channel, to less than 10^{-15} m² when modeling a solid fuel rod. This is described in Section 3.11 of the PLTEMP/ANL Users Guide.
11. The code V4.2 checks the input data file for the presence of unprintable characters. The code stops with a message if such a character is found.
12. Two improvements speed up the solution of search problems: (i) Not writing debug output files during search iterations, and (ii) Entering the search convergence criteria XCONV and YCONV as input data (on card 500) so that the user may relax these criteria to speed up the solution.

3. FURTHER DEVELOPMENT OF PLTEMP/ANL

3.1. Solution of the Temperature Profile

The procedure used in earlier versions of PLTEMP estimated the location of the peak fuel temperature within a given plate from channel-average heat fluxes on either side. This process

was inconsistent in that the peak fuel temperature within a given plate could be predicted from each side, but the location and value of the peak fuel temperature was not corrected to eliminate the mismatch. PLTEMP/ANL V2.1 added a new iterative procedure to find the location and value of the peak temperature in the fuel, for every axial node. This location influences every other predicted temperature and heat flux. Now the code has two solution methods: the above-mentioned iterative procedure (referred to as the Broyden method), and an exact method described in Appendix VI. In the former method, the solution process is iterative, assuming conditions for the coolant entering a particular axial node are known and that the heat production rate within the node is also known. First, the standard PLTEMP solution is obtained, and used as a basis for further refinement. A globally convergent technique known as Broyden method [23] is used to solve the equation $\mathbf{F}(\mathbf{x}) = 0$, where \mathbf{F} is a vector of peak fuel plate temperature differences as obtained from either side and \mathbf{x} is the solution vector containing the fractional position of the peak in each plate. This method numerically determines the Jacobian matrix of partial derivatives that is needed to refine the vector \mathbf{x} . The solution proceeds iteratively until the peak fuel temperature differences are all less than a specified tolerance (typically results are good to less than 0.01 degree). While this process is ongoing, all heat transfer coefficients, coolant temperatures, clad temperatures, and fuel temperatures are continuously updated. The final temperature solution is therefore self-consistent. This method models 3-material layer thick plates.

Besides the method described above, two analytical methods are also available in the code. The second method models 3-material layer thick plates and is based on an analytical solution of heat conduction and convection equations in slab geometry (Appendix VI), and an analytical solution in radial geometry (Appendix VIII). This method assumes a single axial power shape for all fuel plates. The third method models 5-material layer thick fuel tubes and is based on an analytical solution of heat conduction and convection equations in radial geometry (Appendix XIII). This method uses the axial power shape of each of a number of longitudinal stripes in each fuel plate, and a partial mixing of the coolant sub-channels adjacent to the fuel plate stripes. All coolant, cladding and fuel temperatures in an axial slice of an assembly are simultaneously calculated without iteration (for given material thermal properties and convective heat transfer coefficients), avoiding any convergence difficulty. The former method is based on searching for the position an adiabatic plane in the fuel meat of each plate, and should not be used if there is no such plane in one of the fuel plates of an assembly (i.e. if the fractional position x is 0.0 or 1.0). This happens if the heat flux (into a cladding) caused by fuel meat power density is smaller than the heat flux into that cladding from a *hotter* coolant in the adjacent channel. The second method may be used for all problems, including such low power density cases. The second and third methods also account for volumetric heat sources in the cladding and coolant.

3.2. Radial Geometry

Another extension to the capabilities concerns adding an option to permit curved plates or annular fuel tubes. The temperature profile can now be obtained at user option in either slab or radial geometry. The three methods (Broyden method for 3-layer plates, the analytical method for 3-layer plates, and the analytical method for 5-layer plates) are available in radial geometry in the code V4.2. The radial geometry analytical methods are described in Appendices VIII and XIII. In the Broyden method and the analytical method for 3-layer fuel tubes, the fuel and

cladding thicknesses are assumed to be the same for all tubes of a given fuel assembly type. The analytical method for 5-layer fuel tubes accounts for the tube-to-tube variation of the thicknesses of fuel meat, gas gap, and cladding in a given fuel assembly type. To specify the fuel assembly geometry, it is necessary to provide the radius of curvature of the *fuel meat* centerline of each tube. The mathematical equations solved are changed to account for curvature, as are the heat fluxes. In the Broyden method and the analytical method for 3-layer plates, the code detects the sequence of the tubes: from the largest to the smallest radius of curvature, or vice-versa. Internal logic and equations permit the user to specify the problem in either orientation in both methods. In the analytical method for 5-layer fuel tubes, the radii of curvature of meat centerline are currently specified in the increasing order because the option to specify in the decreasing order is not yet implemented.

3.3. Thermodynamic Properties of Coolants

A new capability added to PLTEMP/ANL V2.1 is the elimination of fluid properties derived by interpolation within supplied tables. Instead, the user selects the coolant choice, and the code now generates all required fluid properties from FORTRAN functions [7]. This eliminates some inaccuracies introduced by interpolation from tables, but also frees the user from restricted pressure and temperature ranges in tables.

The user must still exercise judgment over which heat transfer, boiling, and CHF correlation options are appropriate, although the code now includes checks on limits of operation and will so inform the user if outside the range of applicability.

3.4. Output Edits

For ease of iteration, the entire solution set of axial nodal properties are now written to a binary direct-access file where each record corresponds to conditions at that node. This also facilitated generation of new output tables for each plate and node, since this direct-access file can be simply edited as desired. Selected use of lower-case characters was added to the edits. This is helpful for denoting SI units such as MPa, J/kg, and MW/m² (since FORTRAN output has no subscripts or superscripts, this is given as MW/m^2).

The margin to Onset-of-Nucleate Boiling (ONB) is now edited for each channel and node, for both sides of each channel. This is the ratio of power at which ONB will occur to the requested power, based on extrapolation from conditions at the present state point. In general, the variation of ONB with power is non-linear. One can vary the power until ONB=1, to get the true power limit without extrapolation.

3.5. Processing Engineering Hot-Channel Factors

Historically, engineering Hot Channel Factors (HCF) have been used to estimate the safety implications of deviations from fuel and core design specifications that are caused by either random effects or by specific physical effects. In PLTEMP/ANL code, there are two options for hot channel factors treatment:

Option IHCF = 1, an older method that is described in Section 3.5.1, and

Option IHCF = 2, the recommended method described in Section 3.5.2 and in Appendix V.

3.5.1. Option 1 for Hot Channel Factors Treatment

This treatment uses four hot channel factors. F_b is the hot channel factor (HCF) for the global bulk coolant temperature rise. F_h is the HCF for the heat transfer coefficient to the coolant. F_q is the hot channel factor for heat flux from the meat. The PLTEMP/ANL V2.1 code permits the user to use any or all of F_q , F_b , and F_h . But the solution technique is new.

In the event that hot channel factors differing from unity are provided:

- (i) The base case conditions are solved without HCF's (titled "STEP= 1" on the output file);
- (ii) Then the HCF's are applied to the base condition solution, *without alteration of the location of the peak fuel temperature points* (titled "STEP= 2" on the output file);
- (iii) Then the HCF's are applied to the base condition solution, with a full solution permitting everything to vary in order to reach the new steady-state solution. All three problem conditions are solved in a single run (titled "STEP= 3" on the output file).

The results from solution Step 2 are recommended as being most conservative. Step 3 permits heat sharing between the affected channel with hot channel factors and its neighbors that have no hot channel factors. Step 3 represents the physically correct solution to the actual heat flow problem. Step 2 results are more like the original use of hot channel factors for a single hot channel representation, that could be computed by hand.

In PLTEMP/ANL V1.0, F_q was applied to either side of a fuel plate meat when calculating the heat flux moving left and right. The ratio of heat fluxes was used to estimate the location of the peak fuel temperature point from:

$$\delta = t_{\text{meat}} / (1 + Q_r / Q_l)$$

Consequently, the width of the fuel meat section to which F_q was applied varied with the problem. For ease of understanding, the methodology is now changed to assure that F_q is applied to either the left or right half of the fuel meat. In that event, it is clear that the location of the peak fuel temperature should be shifted from plate center toward the side with higher power.

Consider the problem of solving for the temperature profile in fuel meat for the excess heat produced by $F_q > 1$. Assume that the excess heat, $(F_q - 1)s \text{ W/m}^3$, is produced on the *left half* of fuel meat. In slab geometry, the excess heat flux (W/m^2) on the left side will be:

$$Q_l = (F_q - 1)s x_{\text{max}}$$

where s is the nominal volumetric heat source strength (W/m^3), x_{max} is the location of fuel peak temperature in meat thickness from the left, t_f is the fuel meat thickness, and $0 \leq x_{\text{max}} \leq t_f / 2$

Assuming that the fuel temperature is T_1 on the left surface of the meat and T_3 on the right surface, and T_m is the maximum, then it can be shown that

$$T_m - T_3 = \{(F_q - 1)s / (2 k_f)\} \{3t_f^2 / 4 - 2 x_{\max} t_f + x_{\max}^2\}$$

Here k_f is the meat thermal conductivity. Defining the non-dimensional location $X = x_{\max} / t_f$, we get

$$T_m - T_3 = \{(F_q - 1)s t_f^2 / (2 k_f)\} \{3/4 - 2X + X^2\}, \text{ for } 0 \leq X \leq 1/2.$$

For $X > 1/2$, all of the excess heat from $(F_q - 1)s$ flows to the left (recall that it exists only for $X \leq 1/2$). In that case, the contribution to $T_m - T_3$ is zero. On the left hand side,

$$T_m - T_1 = \{(F_q - 1)s t_f^2 / (2 k_f)\} \{X^2\}, \text{ for } 0 \leq X \leq 1/2.$$

By substituting $Y = 1 - X$, one obtains the symmetrical equations for F_q applied on the right.

The code V4.2 has changed how F_h is used. Now it is applied globally to all fuel plates, rather than just to the plate identified on the input card type 0302. If there are uncertainties in power and/or flow measurement, it is best to leave them out of the calculation of the hot channel factors, and apply corrections later. That is because power and flow errors are global, not local.

3.5.2. Option 2 for Hot Channel Factors Treatment

This treatment [24] uses the following six hot channel factors, three global and three local. It does not use the hot channel factors input for option 1.

Global (reactor system-wide) factors:

1. FPOWER = A factor to account for uncertainty in total reactor power measurement.
2. FFLOW = A factor to account for uncertainty in total reactor flow measurement.
3. FNUSLT = A factor to account for uncertainty in Nu number correlation.

Local (random hot spot) factors:

4. FBULK = A factor for local bulk coolant temperature rise. It is denoted by the symbol F_{bulk} in the equations that follow.
5. FFILM = A factor for local temperature rise across the coolant film. It is denoted by the symbol F_{film} in the equations that follow.
6. FFLUX = A factor for local heat flux from cladding surface. It is denoted by the symbol F_{flux} in the equations that follow.

A method of obtaining these factors from a number of sub-factors, and a suggested method of incorporating the factors in a thermal-hydraulic analysis is described Appendix V. The method of implementation consists of the following three steps:

Step 1. A nominal or best estimate calculation

Step 2. A calculation that incorporates only the reactor-wide uncertainties in power, flow, and

heat transfer coefficient

This calculation is done using the outermost loop in the code (the power loop), by directly multiplying the nominal reactor power by the input uncertainty factor FPOWER, reducing the channel flow rates (that were computed in step 1 using the subroutines CNLFLO or CNLFLO_NC) by the input uncertainty factor FFLOW (skipping the call to subroutines CNLFLO and CNLFLO_NC that usually compute channel flows), and reducing the convective heat transfer coefficient in subroutines HCOEF and HCOEF1 by the uncertainty factor FNUSLT.

Figure 9 shows how the margin to Onset-of-Nucleate Boiling, i.e., the ONB ratio, for a heat transfer axial node is found using the steady-state bulk coolant and cladding surface temperatures obtained in this step. The figure is a T_w vs. q'' diagram (cladding surface temperature versus heat flux) that shows a point A representing the operating condition of a node. It also shows a plot of ONB at the local pressure of the node, based on the Bergles-Rohsenow correlation. The origin of the diagram is located at the point ($T_w = T_{in}$, $q'' = 0.0$), implying that the cladding surface temperature at the node equals coolant inlet temperature if the heat flux at the node is zero. The operating cladding surface temperature is less than the coolant saturation temperature T_{sat} , and therefore some margin to ONB exists. The diagram shows two ways of quantifying the amount of this margin:

- (i) If the reactor flow decreases at constant power, the heat flux at the node remains constant; the cladding surface temperature increases; the operating condition of the node moves along line AD as shown in Fig. 9 till it reaches the ONB line at some reduced flow. The margin to ONB can be quantified in this case by the ratio of temperature change BD to the temperature change BA, i.e., $(T_{onb,D} - T_{in}) / (T_{w,op} - T_{in})$.
- (ii) If the reactor power increases at constant flow, the convective heat transfer coefficient remains practically constant (except for small changes due to temperature dependence of coolant properties). If the total reactor power is increased by a factor r , the heat flux at the node increases by the same factor r ; the bulk coolant temperature rise gets multiplied by r ; the film temperature rise gets multiplied by r ; the operating condition of the node moves in direction OA as shown in Fig. 9 till it reaches the ONB line at some value of the factor r . The margin to ONB can be quantified in this case by the value of factor r corresponding to point E in Fig. 9. This movement of the operating conditions is described by Eqs. (1) to (3).

$$q'' = r q''_{op} \quad (1)$$

$$T_b - T_{in} = r (T_{b,op} - T_{in}) \quad (2)$$

$$T_w - T_b = r (T_{w,op} - T_{b,op}) \quad (3)$$

Adding Eqs. (2) and (3), one gets

$$T_w = T_{in} + r (T_{w,op} - T_{in}) \quad (4)$$

Setting the nodal wall temperature of Eq. (4) equal to the ONB temperature corresponding to the heat flux $r q''_{op}$ (in W/m^2), one gets the following equation for r .

$$T_{in} + r (T_{w,op} - T_{in}) = T_{sat} + (5/9)[r q''_{op} / (1082.9 P^{1.156})]**(P^{0.0234/2.16}) \quad (5)$$

where P is the nodal coolant pressure in bar. The value of r obtained by solving Eq. (5) is the ONB ratio for the axial node under consideration. The ONB ratio for each fuel plate node is found in this way and tabulated.

Step 3. A final calculation that incorporates the effects of local random uncertainties into the solution obtained in step 2

Given the cladding and coolant temperatures calculated in step 2, and given the point A on the T_w-q'' diagram (Fig. 10) that represents the operating conditions of a heat transfer node, the purpose now is to define a point H which represents the incorporation of local random uncertainties to the point A. This is done by accounting for three user-input local hot channel factors (F_{bulk} , F_{film} and F_{flux}). The resulting bulk coolant temperature rise and film temperature rise are given by the following equations:

$$T_{b,hc} - T_{in} = F_{bulk} (T_{b,op} - T_{in}) \quad (6)$$

$$T_{w,hc} - T_{b,hc} = F_{film} (T_{w,op} - T_{b,op}) \quad (7)$$

Adding Eqs. (6) and (7), one gets the wall temperature in hot channel

$$T_{w,hc} = T_{in} + F_{bulk} (T_{b,op} - T_{in}) + F_{film} (T_{w,op} - T_{b,op}) \quad (8)$$

The heat flux in the hot channel is given by

$$q''_{hc} = F_{flux} q''_{op} \quad (9)$$

Equations (8) and (9) define a point H on the T_w-q'' diagram (Fig. 10) that represents the heat transfer node after incorporating the local uncertainties.

Two ONB ratios can be found for point H by following the arguments used in step 2. If the reactor flow decreases at constant power, the margin to ONB can be quantified the ratio of temperature change JF to the temperature change JH, i.e., $(T_{onb,F} - T_{in}) / (T_{w,hc} - T_{in})$. If the reactor power increases at constant flow, the ONB ratio r for the axial node, after incorporating the input local uncertainties, is given by the following equation.

$$T_{in} + r \{F_{bulk} (T_{b,op} - T_{in}) + F_{film} (T_{w,op} - T_{b,op})\} = T_{sat} + (5/9)[r F_{flux} q''_{op} / (1082.9 P^{1.156})]**(P^{0.0234/2.16}) \quad (10)$$

where P is the nodal coolant pressure in bar. The ONB ratio for each fuel plate node can be found in this way and tabulated. Currently, the code tabulates the ONB ratio found from Eqs. (5)

and (10). To implement this, two new subroutines ONBRATIO and FINLRD6 have been added to the code.

3.6. Flow Excursion Instability

The code edits flow excursion instability using three methods: (1) the Whittle and Forgan Flow Instability Ratio (FIR) correlation [20], (2) the Flow Excursion Ratio (FER) proposed by the ORNL Advanced Neutron Source Reactor design team (discussed in Appendix VII), (3) the criterion proposed by Babelli and Ishii and a simplified form of their criterion. The ORNL FER is really a prediction of Onset of Significant Void (OSV). OSV always occurs at a lower power than does flow instability. As a result, the ORNL FER prediction should be conservative relative to the FIR predicted by the Whittle and Forgan Correlation. Appendix VII, Tables VII-6 and VII-7, compare PLTEMP results of FIR versus FER for six experimental CHF tests and for 10 flow excursion tests.

Recent work by Babelli and Ishii [25, 26] on flow excursion instability in downward flow systems provides a new approach to this problem. According to this, the code computes a ratio $N_{\text{sub}}/N_{\text{zu}}$ where N_{sub} is the subcooling number for the channel, N_{zu} is the Zuber number, and the channel flow is *stable* if the ratio $N_{\text{sub}}/N_{\text{zu}}$ on the left hand side of the following equation is greater than the quantity on the right hand side, and *unstable* if the ratio $N_{\text{sub}}/N_{\text{zu}}$ is smaller.

$$\frac{N_{\text{sub}}}{N_{\text{zu}}} = \left(\frac{L_{\text{nvg}}}{L} \right)_{\text{critical}} + \frac{A_{\text{F}}}{\zeta_{\text{H}} L} \begin{cases} 0.0022 \text{Pe} & \text{if } \text{Pe} < 70000 \\ 154 & \text{if } \text{Pe} > 70000 \end{cases} \quad (11)$$

A simplified form their criterion is that the ratio $N_{\text{sub}}/N_{\text{zu}}$ must exceed 1.36 for stability. See Appendix X for a detailed description and testing of these flow instability criteria. For editing, the dimensionless non-boiling length L_{nvg}/L is calculated. The available energy gain to onset of boiling is then compared with the actual power supplied to the channel, corrected by the axial heat flux peaking factor. Finally, the value of $L_{\text{nvg}}/L + (E\text{-available})/(E\text{-provided}) \times A/A_{\text{h}}$ is computed. Here, A is the channel flow area, and A_{h} is the heated area. $E\text{-available}$ is the product of mass flow rate \times (enthalpy at ONB at channel exit – enthalpy at inlet).

3.7. Friction Factors for Smooth Pipes and Rough Pipes

For turbulent flow, friction factors for sections of reactor fuel assemblies and bypass channels can be obtained from:

$$f = A * \text{Re}^{-B} \quad (12)$$

given A and B from experiment. Coefficients A and B account for surface roughness and actual geometry. If no such fitted data exists, PLTEMP/ANLV4.2 will now obtain default friction factors f appropriate for hydraulically smooth pipes from Moody [27].

The equation for the Fanning friction factor f' at Reynolds number Re satisfies:

$$1/\sqrt{f'} = 4. * \text{Log}_{10}[\text{Re} \sqrt{f'}] - 0.4 \quad (13)$$

Mathematica was used to solve this expression for f' :

$$f' = 6.25002 / (1. - 8.68591 \text{Log}_e[\text{Re} \sqrt{f'}] + 18.8612 (\text{Log}_e [\text{Re} \sqrt{f'}])^2) \quad (14)$$

This expression for f' can easily be solved recursively starting with a trial value of f' , typically in less than 10 recursions, for relative error $< 1.0 \times 10^{-5}$. Then the Darcy-Weisbach friction factor $f = 4f'$, as given by Moody, follows directly.

For rough pipes, the user supplies the relative surface roughness e/D_e as a parameter ($0 \leq \text{ROUGH}(I) \leq 0.1$). This f' is solved iteratively using the smooth pipe result as a starting guess.

$$f' = 0.331369 / \{ \text{Log}_e[0.27027e/D_e + 1.255/(\text{Re} \sqrt{f'})] \}^2 \quad (15)$$

Then the Darcy-Weisbach friction factor $f = 4f'$, as given by Moody, follows directly.

3.7.1. Laminar Flow and the Transition from Laminar to Turbulent Flow

The laminar friction factor in a narrow channel is calculated from:

$$f = 96/\text{Re}, \text{ for } 0 < \text{Re} < 2200 \quad (16)$$

Correlations for a circular flow channel or for a thick annulus are available theoretically but are not yet implemented.

In the transition region between laminar and turbulent flows, the friction factor is computed by reciprocal interpolation as

$$f_{\lambda,T} = (3.75 - 8250/\text{Re})(f_{t,3000} - f_{l,2200}) + f_{l,2200} \quad 2200 < \text{Re} < 3000 \quad (17)$$

where $f_{l,2200}$ is the laminar factor at a Reynolds number of 2200, $f_{t,3000}$ is the turbulent friction factor at a Reynolds number of 3000. The turbulent friction factor $f_{t,3000}$ is found as defined in Section 3.7.

3.8. New Treatment of Bypass Channels

The code was formerly fixed-dimensioned with a limit of 5 different types of bypasses. The arrays involving bypass flow are now variably-dimensioned, and limited to 50 different types of bypasses at this time. Increasing the limit is now trivial, because only one FORTRAN statement need be changed. Hydraulic problems such as finding the flows for a given uniform pressure drop may now be solved that have no heated fuel at all: all flow paths can be bypass channels.

3.9. Natural Circulation Flow

Figure 11 shows the coolant flow paths, and flow resistances in a fuel assembly modeled in PLTEMP/ANL. The hydraulic equations based on the Bernoulli equation and a method of solution for calculating the natural circulation flow, without any approximation about the coolant density and viscosity, are given in Sections 2 to 3 of Appendix XI. This method is implemented in PLTEMP/ANL V4.2. The method requires iteration (referred to as outer iteration) between the hydraulic and the thermal calculations of the code. An approximation (given in Section 5 of Appendix XI) of the general hydraulic equations is used in the first outer iteration to start the calculation. The general and the approximate methods are summarized below. The derivation of these equations, the definition of the symbols used, the solution strategy, and some testing and verification of the code are given in Appendix XI.

General Method: The general method solves the following N_c+3 simultaneous equations N_c+3 unknowns variables P_2 , P_3 , W and $W_{c,k}$. Here, N_c is the number of coolant channels in the fuel assembly.

$$P_2 - P_3 + \frac{W^2}{2 \rho_1 A_1^2} - \frac{W^2}{2 \rho_3 A_3^2} = g \int_{\text{Channel } k} \rho_{c,k}(z) dz + \frac{K_2 W_{c,k}^2}{2 \rho_{c,k} A_{c,k}^2} + \frac{W_{c,k}^2}{2 D_{hc,k} A_{c,k}^2} \int_{\text{Channel } k} \frac{f_{c,k} dz}{\rho_{c,k}(z)} \quad (k = 1, 2, \dots, N_c) \quad (18)$$

$$W = \sum_{k=1}^{N_c} W_{c,k} \quad (19)$$

$$P_2 = P_1 - \frac{W^2}{2 \rho_1 A_1^2} - g \rho_1 L_1 - \left(K_1 + \frac{f_1 L_1}{D_{h,1}} \right) \frac{W^2}{2 \rho_1 A_1^2} \quad (20)$$

$$P_3 = P_4 - \frac{W^2}{2 \rho_3 A_3^2} + g \rho_3 L_3 + \left(K_3 + \frac{f_3 L_3}{D_{h,3}} \right) \frac{W^2}{2 \rho_3 A_3^2} \quad (21)$$

where

P_1 = Absolute pressure of the creeping coolant in the pool at the assembly inlet level, Pa

P_2 = Absolute coolant pressure just before the inlet to the heated section, Pa

P_3 = Absolute coolant pressure just after the exit from the heated section, Pa

P_4 = Absolute pressure of the creeping coolant in the pool at the assembly exit level, Pa

W = Flow rate in the assembly (total flow in all coolant channels), kg/s

$W_{c,k}$ = Flow rate in the k^{th} coolant channel, kg/s

$\rho(z)$ = Coolant density as a function of axial position z , kg/m^3

These hydraulic equations are solved using two kinds of iteration, inner iteration and outer iteration. The inner iteration is performed *at a fixed set of coolant channel temperature profiles*, to find a consistent set of channel flow rates $W_{c,k}$ and assembly flow rate W satisfying the hydraulic equations. The outer iteration is that in which a *new multi-fuel-plate heat transfer*

calculation is done, using an available set of channel flow rates. After each heat transfer calculation, the inner iteration is performed again, using a new set of coolant channel temperature profiles, to satisfy the hydraulic equations, obtaining another consistent set of channel flow rates $W_{c,k}$ and assembly flow rate W . The problem is solved when the consistent set of channel flow rates and assembly flow rate change by a negligible amount, from an outer iteration to the next.

In order to assure convergence of outer iterations, only a fraction ε (e.g., 0.6) of the coolant temperature change from the previous outer iteration is used to find the temperature-dependent coolant properties and friction factor during the inner iterations, as shown by Eq. (22) below. The coolant properties and friction factor used in evaluating the integrals in Eq. (18), are evaluated at the temperature $T_{c,k,used}(z)$.

$$T_{c,k,used}(z) = T_{c,k,L-1}(z) + \varepsilon [T_{c,k,L}(z) - T_{c,k,L-1}(z)] \quad (22)$$

Here, $T_{c,k,L}(z)$ is the coolant temperature profile obtained by the multi-fuel-plate heat transfer calculation done *just before* outer iteration L . The coolant channel temperature profile $T_{c,k,L}(z)$ is not available for $L = 1$. In outer iteration 2, when the coolant temperature profiles $T_{c,k,2}(z)$ and $T_{c,k,1}(z)$ are both needed in Eq. (22), the coolant temperature $T_{c,k,1}(z)$ in each channel of the heated section is assumed to vary linearly from T_{in} to T_{out} (assembly outlet temperature). In the third outer iteration and onwards ($L \geq 3$), the coolant temperature profiles $T_{c,k,L-1}(z)$ and $T_{c,k,L}(z)$, both calculated by the multi-fuel-plate heat transfer calculation, are available.

Approximate Method: In this approximation, it is assumed that the coolant density and viscosity are uniform over each axial region in a fuel assembly. The coolant properties are evaluated (i) at the inlet temperature in axial region 1 ($n = 1$), (ii) at the mean temperature $0.5(T_{in} + T_{out})$ in the heated section ($n = 2$), and (iii) at the assembly exit temperature in all axial regions downstream ($n \geq 3$) of the heated section. Then the Bernoulli equation for the fuel assembly from its inlet to exit (i.e., Eq. (6) of Appendix XI) simplifies to Eq. (22) below. The gravity head terms are collected on the left hand side of this equation. The quantity on the left hand side is called buoyancy which drives the *natural circulation flow*.

$$gL_2(\rho_1 - \rho_a) + gL_3(\rho_1 - \rho_3) = \left[\left(K_1 + \frac{f_1 L_1}{D_{h,1}} \right) \frac{\rho_a}{\rho_1 A_1^2} + 2 \rho_a R_{eqv} + \left(K_3 + \frac{f_3 L_3}{D_{h,3}} \right) \frac{\rho_a}{\rho_3 A_3^2} \right] \frac{W^2}{2 \rho_a} \quad (23)$$

where

T_{in} = Coolant temperature at the assembly inlet, °C

T_{out} = Coolant temperature at the assembly outlet, °C

ρ_1, μ_1 = Coolant density and dynamic viscosity in axial region 1

ρ_a, μ_a = Coolant density and dynamic viscosity in the heated section (axial region 2)

ρ_3, μ_3 = Coolant density and dynamic viscosity in axial region 3 and others downstream of the heated section

Equation (23) is the approximate hydraulic equation for calculating the assembly flow rate W due to natural circulation, under the assumptions made in this section. The middle term on the

right hand side of Eq. (23) is the frictional pressure drop over the heated section. The equivalent hydraulic resistance R_{eqv} in the middle term is given by Eq. (28) of Appendix XI without any assumption about coolant properties. Under the assumptions made, that equation simplifies to

$$\frac{1}{2 \rho_a R_{\text{eqv}}} = \left[\sum_{k=1}^{N_c} \frac{A_{c,k}}{\left(K_2 + \frac{f_{c,k} L_2}{D_{hc,k}} \right)^{0.5}} \right]^2 \equiv \frac{1}{\text{DENOF}_2} \quad (24)$$

Equation (23) also holds for *forced flow* if the buoyancy, i.e., the quantity on the left hand side of the equation, is replaced by the user input DP0 (on card type 0500).

3.10. Search Capability [Coauthors: B. Dionne and E. E. Feldman]

To save the reactor analyst's time, a general search capability (input option ISRCH = 1) has been implemented to get a user-specified target value for a specified code output variable (e.g., reactor coolant flow rate) by adjusting a specified input datum (e.g., applied pressure drop). Two basic types of searches are implemented: (1) Single search in which *one* input datum is adjusted to achieve a target value for *one* output variable; and (2) Double search in which *two* input data are adjusted to achieve target values for *two* output variables. Figure 6 shows a logic flow diagram of how a search is performed by the main program of the code. Basically, each search is performed using the *interval-halving technique*. Appendix XII describes in detail a verification and an application of this capability.

In a single search using this technique, the specified input datum is first set at its lower limit $X1=XLOW$ (which is an input); an input data file is written on a scratch file; and the *pre-search* code is run to find the corresponding value $Y1$ for the specified output variable. The specified input datum is then reset at its upper limit $X2=XHIGH$ (an input); another input data file is written over the scratch file; and the *pre-search* code is re-run to find the corresponding value $Y2$ for the output variable. The interval between $X1$ and $X2$ is then halved, and the specified input datum is reset at the arithmetic mean $X3$ of its lower and upper limits $X1$ and $X2$; a third input data file is written over the scratch file; and the *pre-search* code is re-run to find the corresponding value $Y3$ for the output variable. If the user-specified target value $YTARGT$ of the output variable lies between $Y1$ and $Y3$, then $X2$ is set equal to $X3$; or if the target value $YTARGT$ lies between $Y3$ and $Y2$, then $X1$ is set equal to $X3$. The interval between $X1$ and $X2$ is halved again, and the process (of writing an input data file and running the *pre-search* code) is repeated to get another pair of values, $X3$ and $Y3$, for the input datum and the output variable. This process is repeated to achieve a convergence, i.e., either the gap between $X1$ and $X2$ is a very small fraction of $(XHIGH - XLOW)$, or $Y3$ is very close to $YTARGT$. This process is carried out in the subroutine SEARCH1. A single search converges in about 15 to 30 runs of the pre-search code.

In a double search using this technique, the same process is carried out in the main program MAINSRCH (Fig. 6) in order to achieve a user-specified target value $YTARGT2$ of *the second*

of the two output variables, by adjusting *the second* of the two specified input data (e.g., reactor power in the case of search type 21). In the main program, instead of running the pre-search code, the subroutine SEARCH1 is called each time to run a single search to adjust *the first* specified input datum (e.g., applied pressure drop in the case of search type 21) to achieve *the first* output variable's specified target value. The process in the main program is repeated till either the gap between the lower and upper limits of the second datum is a very small fraction of (XHIGH2 – XLOW2), or the value of the second output variable at the interval mid-point is very close to YTARGT2. A double search converges in about 300 to 400 iterations, i.e., runs of the pre-search code.

Currently, 12 single searches and 6 double searches are available. The different types of single search and double search currently available in the code are listed with the input data required by the search option (Cards 0203 and 0204) in the Input Description in Appendix I. These searches adjust the input applied pressure drop or/and reactor power to get target values of any one or any two of these calculated quantities: total flow rate, minimum ONBR, minimum DNBR, minimum flow instability power ratio, maximum cladding surface temperature, and maximum coolant exit temperature. The implementation of the search capability is such that new searches can be easily added.

3.11. Modeling a Central Solid Fuel Rod Inside Multiple Coaxial Fuel Tubes

A central solid fuel rod (with or without multiple coaxial fuel tubes around the fuel rod) can be modeled by the code using the input IEND=1. This option uses a new heat transfer routine capable of handling nested fuel tubes each made of 5 materials (described in Appendix XIII). The input data for this heat transfer routine allows unequal cladding thicknesses on the two sides of each fuel tube.

It should be noted that the basic structure of the code has a coolant channel on both the inner and outer sides of each fuel tube (having NCHNF channels and NCHNF-1 fuel tubes). Therefore, to model a fuel rod, the flow area of the innermost channel is supplied to be less than 10^{-15} m^2 , the inner cladding thickness is supplied to be zero, and the code then internally sets the convective heat transfer coefficient to be $1.0 \text{ W/m}^2\text{-}^\circ\text{C}$ for the innermost channel.

In the output file, the structure of tables printed for the solid fuel rod is kept the same as that for printing the tables for fuel tubes. Therefore, for the solid fuel rod (alone or inside nested coaxial fuel tubes), the innermost coolant channel is physically meaningless. In addition to this, if the innermost cladding thickness is zero, then the innermost cladding surface temperature is also physically meaningless and is discarded by the code in obtaining the maximum cladding temperature. The innermost channel is also ignored in determining the reactor safety margins like the minimum ONBR (onset of nucleate boiling ratio), FIR (flow instability ratio) and CHF (critical heat flux ratio).

3.12. Organization of the Output File [Coauthor: E. E. Feldman]

The important results calculated for each axial node are first saved on a direct-access scratch file when the problem is being solved. The results on the scratch file are read and edited later. This scratch file is saved on the logical unit 20 for the Broyden method of heat transfer calculation, on

the logical unit 19 for the analytical heat transfer method for 3-layer fuel plates or tubes, and on the logical unit 11 for the analytical heat transfer method for 5-layer fuel tubes.

The output for the nominal case (without hot channel factors) is printed in the same order as the output for the case including the hot channel factors (HCFs). The nominal case is printed first, followed by the case including the HCFs. Since the core consists of NFTYP types of fuel assemblies, with NELF(I) assemblies of type I, with NLSTR(I) longitudinal stripes in a fuel plate of type I, the output file is organized to clearly present the results for all fuel plates. The output (nominal or with HCFs) is printed in increasing order of assembly types, for each type in increasing order of assembly number, and for each assembly in increasing order of longitudinal stripe number. This organization of the output file is shown below in detail. The data for each stripe is printed fuel plate by fuel plate, and ordered as shown in the text boxes below the organization. At the very end of the output file, there is printed a two-line summary of the results. The first line is for the nominal case and the second line is for the case including the global and local HCFs. This summary contains the safety margins ONBR, FIR, CHFR, reactor power and flow rate etc.

Organization of the Code Output File

■ Results for type 1 assemblies

- Fuel assembly 1 of type 1
 - ◆ Longitudinal stripe 1
 - ◆ Longitudinal stripe 2
 - ◆ Longitudinal stripe 3 and so on all NLSTR(1) stripes.
- Fuel assembly 2 of type 1
 - ◆ Longitudinal stripe 1
 - ◆ Longitudinal stripe 2
 - ◆ Longitudinal stripe 3 and so on all NLSTR(1) stripes.
- Fuel assembly 3 of type 1
 - ◆ Longitudinal stripe 1
 - ◆ Longitudinal stripe 2
 - ◆ Longitudinal stripe 3 and so on all NLSTR(1) stripes.
- and so on all NELF(1) assemblies of type 1.

■ Results for type 2 assemblies

- Fuel assembly 1 of type 2
 - ◆ Longitudinal stripe 1
 - ◆ Longitudinal stripe 2
 - ◆ Longitudinal stripe 3 and so on all NLSTR(2) stripes.
- Fuel assembly 2 of type 2
 - ◆ Longitudinal stripe 1
 - ◆ Longitudinal stripe 2
 - ◆ Longitudinal stripe 3 and so on all NLSTR(2) stripes.
- Fuel assembly 3 of type 2
 - ◆ Longitudinal stripe 1
 - ◆ Longitudinal stripe 2

- ◆ Longitudinal stripe 3 and so on all NLSTR(2) stripes.
- and so on all NELF(2) assemblies of type 2.

■ **Results for type 3 assemblies**

- Fuel assembly 1 of type 3
 - ◆ Longitudinal stripe 1
 - ◆ Longitudinal stripe 2
 - ◆ Longitudinal stripe 3 and so on all NLSTR(3) stripes.
- Fuel assembly 2 of type 3
 - ◆ Longitudinal stripe 1
 - ◆ Longitudinal stripe 2
 - ◆ Longitudinal stripe 3 and so on all NLSTR(3) stripes.
- Fuel assembly 3 of type 3
 - ◆ Longitudinal stripe 1
 - ◆ Longitudinal stripe 2
 - ◆ Longitudinal stripe 3 and so on all NLSTR(3) stripes.
-
- and so on all NELF(3) assemblies of type 3.

-
- and so on the results for assemblies of all NFTYP types.

Order of Data for each Stripe in the Nominal Case

1. Coolant, cladding and fuel temperatures, plate by plate
2. Flow instability power ratio by channel
3. ONBR on both surfaces of all plates
4. CHF and CHF on both surfaces of all plates
5. Heat fluxes on both surfaces of fuel plate, plate power split, and coolant pressure at each heat transfer node center, plate by plate. The pressure printed above the first node center is the pressure at the heated section inlet. The pressure printed below the last node center is the pressure at the heated section exit.

Order of Data for each Stripe in the Case with Hot Channel Factors

1. Coolant, cladding and fuel temperatures, plate by plate, with only global HCFs
2. Flow instability power ratio by channel
 - (i) With only global HCFs
 - (ii) with global and local HCFs
3. ONBR on both surfaces of all plates, with only global HCFs
4. Coolant, cladding and fuel temperatures, plate by plate, with global and local HCFs
5. ONBR on both surfaces of all plates, with global and local HCFs
6. CHF and CHF on both surfaces of all plates, with global and local HCFs
7. Heat fluxes on both surfaces of fuel plate, plate power split, and coolant pressure at each heat transfer node center, plate by plate, with only global HCFs. The pressure printed above the first node center is the pressure at the heated section inlet. The pressure printed below the last node center is the pressure at the heated section exit.

3.13. Other Changes to Input and Output

New features include the ability to process multiple cases per run, and the ability to enhance the readability of the input file with liberal use of comment lines anywhere in the file. The user-supplied input file is read on unit 5, as before. But now it is examined for comment cards. Any line beginning with a '!' in column 1 is treated as a comment. That is, a new (scratch) input file is created from a copy of the supplied input file, minus the comment lines, and written to a temporary file on unit 1. All subsequent reading by the 'input' routine is performed on unit 1. The job is complete when an 'end of file' is read on unit 1. In option NAXDIS=2, the axial power shapes by stripe are supplied in a separate file (named by a character variable APSHF supplied on the input Card 0702A) which must be present in the code running directory.

It should be noted that card type 500 (of the input file is read on unit 5) consists of two cards, not only one as in the V2.0 of the code (see the input description given in Appendix I). A second card must be added to an older input data file.

A new edit is provided which shows the power density in each axial node of each plate, for each fuel assembly. Also, the volume-weighted radial power peaking factor is now edited.

As the input is being processed, an auxiliary output file named bug.out is created which begins by listing the input file, and then shows the progress in processing the input by showing which card types are being read, as well as listing key variables used to determine the length of input arrays. As each card type (and record) is read, the data is examined for reasonableness. If a variable is not within known limits, an error message is created which indicates the variable name and its incorrect value. The job then terminates. A successful job may contain much more debug information on bug.out, and on another file named aux1.out.

The number of different types of fuel assemblies is now increased from 5 to 60.

The following files are used:

Name	Unit	Purpose
input.short	1	A of copy of the user-supplied input file, minus the comment cards (i.e., the lines with ! in column 1)
input.modified	2	A copy of the input file with one or two user-specified input values modified for search.
output.srch	3	Search output.
input string APSHF	4	Input file of axial power shapes by fuel plate stripe. The string APSHF is entered on the input Card 0702A.
input	5	The user-supplied input file (or the file supplied on the run command line as < input.file).
output	6	The standard output. The code will overwrite any pre-existing file named <i>output</i> . Save your work before running a second case.
groen2.bin	9	CHF lookup table binary (double precision) file from Groeneveld.
--	11	A direct-access scratch file used to save all key variables

		for each axial node in the <i>exact</i> solution method (IEND=1) for 5-layer fuel plates with axial power shape by stripe (in order to solve the problem first and edit it later).
ASME	15	A short ASME light water table for P= 0.1(0.025)0.2; 0.3(0.1)1; 1.2(0.2)2 MPa, and T=0(1)120 C. (Reference: ASME Steam Tables, Sixth Edition, 1993, ASME Press, New York).
ASME.TBOIL	16	A short ASME steam table of H, S, density, Cp, and conductivity at boiling vs. pressure. P=0.1(.025)2 MPa.
ASME.out	17	Input tables and derived values from data on units 15 and 16.
--	18	A direct-access scratch file to which are copied all the data that was saved on logical unit 19 in the <i>previous outer iteration</i> . The coolant temperatures found in the previous outer iteration are needed in calculating the channel flow rates caused by natural circulation.
--	19	A direct-access scratch file used to save all key variables for each axial node in the <i>exact</i> solution method for 3-layer plates (in order to solve the problem first and edit it later).
--	20	A direct-access scratch file used to save all key variables for each axial node in the <i>Broyden</i> solution method (in order to solve the problem first and edit it later).
bug.out	21	An auxiliary output file of value for debugging user errors in the input file, as well as to contain additional debugging information for the run.
aux1.out	22	Additional debugging information.

4. VALIDATION

The validation of PLTEMP/ANL V2.1 is described in Reference [47] and in this section, whereas the verification of the models added later (in the code V3.0 and later versions) are given in Appendices. Appendix VII provides a verification of the Whittle and Forgan flow instability correlation, and the ORNL flow instability correlation. Appendix VIII provides a description and a reference to a verification of the analytical method for calculating temperature distribution. Appendix IX provides a verification of the heat transfer coefficient and friction factor used in coolant channels with fins. Appendix X provides a verification of the Babelli-Ishii flow instability criteria.

A computation of energy going out of all coolant channels was added in order to confirm the energy balance: heat going out = heat coming in.

At user option, the fluid specific heat and density can be fixed for the run. This has been of some assistance when comparing results with those from other codes.

Mathematica was used to determine the correct equations to use for radial geometry. It was also used to perform validations of some specific temperature profiles. For example, calculations were performed for variations on the IAEA Generic 10 MW Reactor [28] to check the peak fuel temperature from the code vs. results from *Mathematica* (see Table 2). A single axial node model was used for this check. The general solution for the peak fuel temperature in slab geometry with flat heat source volumetric strength s , conductivity k , thickness d , and boundary temperatures t_1 and t_2 (in *Mathematica* notation) is:

$$\text{pf}[t_1, t_2, k, s, d] := \{4k^2(t_1 - t_2)^2/d^2 + (4k s)(t_1 + t_2) + s^2 d^2\} / (8k s)$$

The location of the peak fuel temperature is:

$$x \rightarrow (2k t_1 - 2k t_2 + s x_1^2 - s x_2^2) / (2s(x_1 - x_2))$$

Table 2. Check of Peak Fuel Temperature in Slab Geometry.

Power, MW	Clad/Fuel Temp., C	Peak Fuel Temp., C PLTEMP/ANL 4.2	Peak Fuel Temp., C <i>Mathematica</i>
0.01	69.9454	103.014	103.014
0.02	89.5427	155.680	155.690
0.03	108.8295	208.036	208.036

In radial geometry, with flat heat source volumetric strength s , conductivity k , x_1 and x_2 the radii of the two exterior surfaces with boundary temperatures t_1 and t_2 , the general solution for the peak fuel temperature (in *Mathematica* notation) is:

$$\begin{aligned} \text{r}[t_1, t_2, k, s, x_1, x_2] := & \\ & \{2(4k t_2 + s x_2^2)\text{Log}[x_1] - 2(4k t_1 + s x_1^2)\text{Log}[x_2] + \\ & (4k(t_1 - t_2) + s(x_1^2 - x_2^2)) \\ & \{-1 + 2 \text{Log}[-C1/C2]\}\} / (8k(\text{Log}[x_1/x_2])); \end{aligned}$$

$$C1 = \sqrt{4k(t_2 - t_1) + s(x_2^2 - x_1^2)}$$

$$C2 = \sqrt{2s \text{Log}[x_2/x_1]}$$

The location of the peak fuel temperature is:

$$x \rightarrow \sqrt{4k[t_2 - t_1] + s[x_2^2 - x_1^2]} / \sqrt{2s(\text{Log}[x_2] - \text{Log}[x_1])}$$

The hydraulic solution for unheated pipe flow was validated against analytical solutions for mass flow rate obtained versus desired pressure drop, given bypass dimensions.

5. LIMITS OF CODE OPERATION

Fluid properties are generated by a set of function routines. For light water, if the temperature exceeds 340 °C, there may be an error message of failure. The saturation pressure of water was taken from [29]. For heavy water, the properties functions come from [30].

The cladding surface to coolant heat transfer coefficient is based on single-phase convection. Since the increase in heat transfer coefficient downstream of the onset-of-nucleate-boiling (ONB) axial position is not calculated, the cladding surface and fuel meat temperatures downstream of the ONB position are not very accurate. The effect of the increased friction to coolant flow due to vapor bubbles over the channel length downstream of the ONB axial position is also not accounted for. Hence, the resulting increase in pressure drop and decrease in flow rate due to vapor bubbles are ignored.

The Broyden method of calculating temperature distribution is limited to problems having heat fluxes *directed out* of both surfaces of all fuel plates, which is usually true for research reactors. The method fails if the heat flux at any location is directed in the *reversed direction*, i.e., into the fuel plate rather than out of the plate, which may happen for a fuel plate generating a very small power compared to an adjacent plate.

6. CLEANUP/MODERNIZATION OF SOURCE CODE

The source code for PLTEMP/ANL V1.0 was written in FORTRAN 77. A number of obsolete FORTRAN features that were eliminated. The new features added for user convenience are:

- The date and time of the run appear on the output;
- The output contains a listing of the input;
- The input data is checked for errors before the calculations begin. Detected errors are clearly noted on the “output” file, and the run is terminated. Generally, the card type and variable name are given along with the erroneous value.
- Asterisks ‘*’ were removed from output edits unless an error has occurred.
- File processing errors are detected; diagnostic error messages will result.
- Conversion to dynamic memory allocation is partially completed. When completed, code maintenance will be simplified as the need for extensions and improvements continue.

7. COMPUTER SOFTWARE REQUIREMENTS

The code was developed in FORTRAN 77 on a Linux computer system. No nonstandard library routines are used. The program has been compiled with Lahey Fortran 95 compilers for Linux and Windows PC. Other advanced Fortran compilers can be used but will require minor changes in clock timer and date routines, the Lahey intrinsic function TRIM, some arguments of OPEN statements, and INTENT statements. The code has been tested to run on Windows 7, Windows XP and Linux computers running the CENTOS distribution.

To execute the code on Windows, create a working directory and copy files pltemp.exe (the executable of the code), ASME, groen2.bin, ASME.TBOIL, and axial power shape file (if NAXDIS = 2) to it. Change to that directory. Use the same process for linux. Create an input file of any name, e.g. input.test. To run from the command line, type:

```
pltemp.exe < input.test
```

REFERENCES

1. K. Mishima, K. Kanda and T. Shibata, "Thermal-Hydraulic Analysis for Core Conversion to the Use of Low-enrichment Uranium Fuels in the KUR," KURRI-TR-258, Research Reactor Institute, Kyoto University (December 7, 1984).
2. K. Mishima, K. Kanda and T. Shibata, "Thermal-Hydraulic Analysis for Core Conversion to the Use of Low-Enriched Uranium Fuels in the KUR," ANL/RERTR/TM-6, CONF-8410173, p. 375 (1984).
3. W. L. Woodruff and K. Mishima, "Neutronics and Thermal-Hydraulics Analysis of KUHFR," ANL/RERTR/TM-3, CONF-801144, p. 579 (1980).
4. W. L. Woodruff, "Some Neutronics and Thermal-hydraulics Codes for Reactor Analysis Using Personal Computers," Proc. Int. Mtg. on Reduced Enrichment for Research and Test Reactors, Newport, RI, Sept. 23-27, 1990, CONF-9009108 (ANL/RERTR/TM-18), Argonne National Laboratory (1993).
5. W. L. Woodruff, J. R. Deen and C. Papastergiou, "Transient Analyses and Thermal-hydraulic Safety Margins for the Greek Research Reactor (GRR1)," Proc. Int. Mtg. on Reduced Enrichment for Research and Test Reactors, Williamsburg, VA, Sept. 19-23, 1994, CONF-9409107 (ANL/RERTR/TM-20), Argonne National Laboratory (1997).
6. W. L. Woodruff, "A Kinetics and Thermal-hydraulics Capability for the Analysis of Research Reactors," Nucl. Technol., **64**, 196 (1983).
7. W. L. Woodruff and R. S. Smith, "A Users Guide for the ANL Version of the PARET Code, PARET/ANL (2001 Rev.)," ANL/RERTR/TM-16 (March 2001).
8. "International Association for the Properties of Steam (IAPS)," H. J. White, Secretary, National Bureau of Standards, Washington, D.C., 1977 (revised 1983).
9. B. S. Petukhov and V. N. Popov, "Theoretical Calculation of Heat Exchange in Turbulent Flow in Tubes of an Incompressible Fluid with Variable Physical Properties," High Temp., **1**, No. 1, pp 69-83 (1963).
10. R. J. Weatherhead, "Nucleate Boiling Characteristics and the Critical Heat Flux Occurrence in Subcooled Axial-flow Water Systems," ANL-6675, Argonne National Laboratory, Argonne, IL, USA (1963).
11. R. J. Weatherhead, "Heat Transfer, Flow Instability, and Critical Heat Flux for Water in a Small Tube at 200 psia," ANL-6715, Argonne National Laboratory, Argonne, IL, USA (June 1963).
12. Roger Ricque and Roger Siboul, "Ebullition Locale De L'eau En Convection Forcee," Report CEA-R-3894, CEA Grenoble (May 1970).

13. E. N. Sieder and G. E. Tate, "Heat Transfer and Pressure Drop of Liquids in Tubes," *Ind. Eng. Chem.*, **28**, 1429 (1936). See also W. M. Rohsenow, J. P. Hartnett, and Y. I. Cho, "Handbook of Heat Transfer," The McGraw-Hill Company, New York, p. 5.26 (1998).
14. F. W. Dittus, and L. M. K. Boelter, "Heat Transfer in Automobile Radiators of the Tubular Type," University of California Press, *Eng.*, **2** (13), 443 (1930).
15. A. P. Colburn, "A Method of Correlating Forced Convection Heat Transfer Data and a Comparison with Fluid Friction," *Trans. AIChE* **29**, 174 (1933).
16. S. Mirshak, W. S. Durant, and R. H. Towell, "Heat Flux at Burnout," E. I. du Pont de Nemours & Co., DP-355, Available from Office of Tech. Services, U. S. Dept. Commerce, Washington, D. C. (February 1959).
17. L. Bernath, "A Theory of Local Boiling Burnout and Its Application to Existing Data," *Chem. Eng. Prog. Symp. Series*, **56** (30), 95 (1960).
18. D. A. Labuntsov, "Critical Thermal Loads in Forced Motion of Water Which is Heated to a Temperature Below the Saturation Temperature," *Soviet J. of Atomic Energy (English Translation)* Vol. 10, No. 5, pp. 516-518 (May 1961).
19. K. Mishima, H. Nishihara, and T. Shibata, "CHF Correlations Related to the Core Cooling of a Research Reactor," *Proc. International Meeting on Reduced Enrichment for Research and Test Reactors*, 24-27 October, 1983, Tokai, Japan, JAERI-M-84-073, 311 (1983).
20. R. H. Whittle and R. Forgan, "A Correlation for the Minima in the Pressure Drop Versus Flow-Rate Curves for Subcooled Water Flowing in Narrow Heated Channels," *Nucl. Eng. Design* **6**, 89 (1967).
21. W. H. Jens and P. A. Lottes, "Analysis of Heat Transfer, Burnout, Pressure Drop and Density Data for High-Pressure Water," ANL-4627 (May 1951).
22. A. E. Bergles and W. M. Rohsenow, "The Determination of Forced-Convection Surface-Boiling Heat Transfers," *Trans. ASME, J. Heat Transfer* **86**, 365 (1964).
23. William H. Press, Saul A. Teukolsky, William T. Vetterling, and Brian P. Flannery, "Numerical Recipes in FORTRAN, The Art of Scientific Computing, Second Ed., Cambridge University Press, Chapter 9 (1992).
24. E. E. Feldman, "Recommended Treatment of Hot Channel Factors in the PLTEMP Code", Intra-Laboratory memorandum, Nuclear Engineering Division, Argonne National Laboratory (January 9, 2006)
25. Ibrahim Babelli and Mamoru Ishii, "Flow Excursion Instability in Downward Flow Systems. Part I. Single-phase Instability," *Nucl. Eng. Design* **206**, 91 (2001).

26. Ibrahim Babelli and Mamoru Ishii, "Flow Excursion Instability in Downward Flow Systems. Part II. Two-phase Instability," Nucl. Eng. Design **206**, 97 (2001).
27. L. F. Moody, Trans. ASME, 66, 671 (1944).
28. Interatom, "Safety Analysis for the IAEA Generic 10 MW Reactor," IAEA-TECDOC-643, 11 (April 1992).
29. Report NASA TN D-7391, National Aeronautics and Space Administration (1973).
30. "Heavy Water – Thermophysical Properties," Kernforschungsanlage (KFA), Julich GMBH. These functions span 0-100 MPa, and 0-800 C.
31. D. C. Groeneveld et al., "Lookup Tables for Predicting CHF and Film-Boiling Heat Transfer: Past, Present, and Future," Nuclear Technology 152, 87 (Oct. 2005).
32. D. C. Groeneveld et al., "The 2006 CHF Look-up Table," Nuclear Engineering and Design, 237, pp. 1909-1922 (2007).
33. W. M. Kays, Convective Heat and Mass Transfer, McGraw-Hill Book Co., New York, Table 8-2, p. 117 (1966).
34. ORNL Monthly Progress Report, ORNL/ANS/INT-5/V19, Oak Ridge National Laboratory, Oak Ridge, Tennessee, USA (October 1989).
35. M. M. Shah, "Improved General Correlation for Critical Heat Flux during Upflow in Uniformly Heated Vertical Tubes," International Journal of Heat and Fluid Flow, Vol. 8(4), pp. 326-335 (1987).
36. J. G. Collier and J. R. Thome, "Convective Boiling and Condensation," Third Edition, Clarendon Press, Oxford (1994).
37. M. Kaminaga, K. Yamamoto, and Y. Sudo, "Improvement of Critical Heat Flux Correlation for Research Reactors using Plate-Type Fuel," J. of Nuclear Science and Technology, Vol. 35, No. 12. pp. 943-951 (1998).
38. Y. Sudo and M. Kaminaga, "A New CHF Correlation Scheme Proposed for Vertical Rectangular Channels Heated From Both Sides in Nuclear Research Reactors," Transactions of the ASME, J. of Heat Transfer, Vol. 115, pp. 426-434 (1993).
39. N. I. Kolev, "Multiphase Flow Dynamics 2: Thermal and Mechanical Interactions," 2nd. Edition, Springer-Verlag, Berlin, Germany, p. 517 (2005).
40. H. C. Kim, W. P. Baek, and S. H. Chang, "Critical Heat Flux of Water in Vertical Round Tubes at Low Pressure and Low Flow Conditions," Nucl. Eng. Des., Vol. 199, pp. 49-73 (2000).

41. F. P. Incropera, D. P. Dewitt, T. L. Bergman, and A. S. Lavine, "Introduction to Heat Transfer," 5th. Edition, John Wiley and Sons, Hoboken, NJ (2007).
42. G. P. Celata, F. D'Annibale, A. Chiaradia, and M. Cumo, "Upflow Turbulent Mixed Convection Heat Transfer in Vertical Pipes," *Int. J. Heat Mass Transfer*, Vol. 41, pp. 4037-4054 (1998).
43. M. Kalimullah, E. E. Feldman, A. P. Olson, B. Dionne, J. G. Stevens, and J. E. Matos, "An Evaluation of Subcooled CHF Correlations and Databases For Research Reactors Operating at 1 to 50 bar Pressure," RERTR 2012 – 34th International Mtg. on Reduced Enrichment for Research and Test Reactors, Warsaw, Poland (October 14-17, 2012).
44. D. D. Hall and I. Mudawar, "Critical Heat Flux for Water Flow in Tubes – II. Subcooled CHF Correlations," *Intern. J. Heat and Mass Transfer*, Vol. 43, pp. 2605-2640 (2000).
45. N. E. Todreas and M. S. Kazimi, "Nuclear Systems Volume 1: Thermal Hydraulic Fundamentals," pp. 444-447, Hemisphere Publishing Corporation, USA (1990).
46. S. Kakac, R. K. Shah, and W. Aung, "Handbook of Single-Phase Convective Heat Transfer," John Wiley & Sons, New York, USA (1987).
47. M. Kalimullah, A. P. Olson, E. E. Feldman, N. Hanan, and B. Dionne, Argonne National Laboratory, unpublished information, 2014.
48. V. Gnielinski, "New Equations for Heat and Mass Transfer in Turbulent Pipe and Channel Flows," *Int. Chem. Eng.* 16. pp. 359–368 (1976).
V. Gnielinski, "Neue Gleichungen für den Wärme- und den Stoffübergang in turbulent durchströmten Röhren und Kanälen. *Forschung im Ingenieurwesen*," Bd. 41, Nr. 1: 8–16 (1975).
49. G. P. Celata, M. Cumo, and A. Mariani, "The Effect of the Tube Diameter on the Critical Heat Flux in Subcooled Flow Boiling," *Intern. J. of Heat and Mass Transfer*, Vol. 39, pp. 1755-1757 (1996).
50. A. Tanase, S. C. Cheng, D. C. Groeneveld, and J. Q. Shan, "Diameter Effect on Critical Heat Flux," *Nucl. Eng. Des.*, Vol. 239, pp. 289-294 (2009).

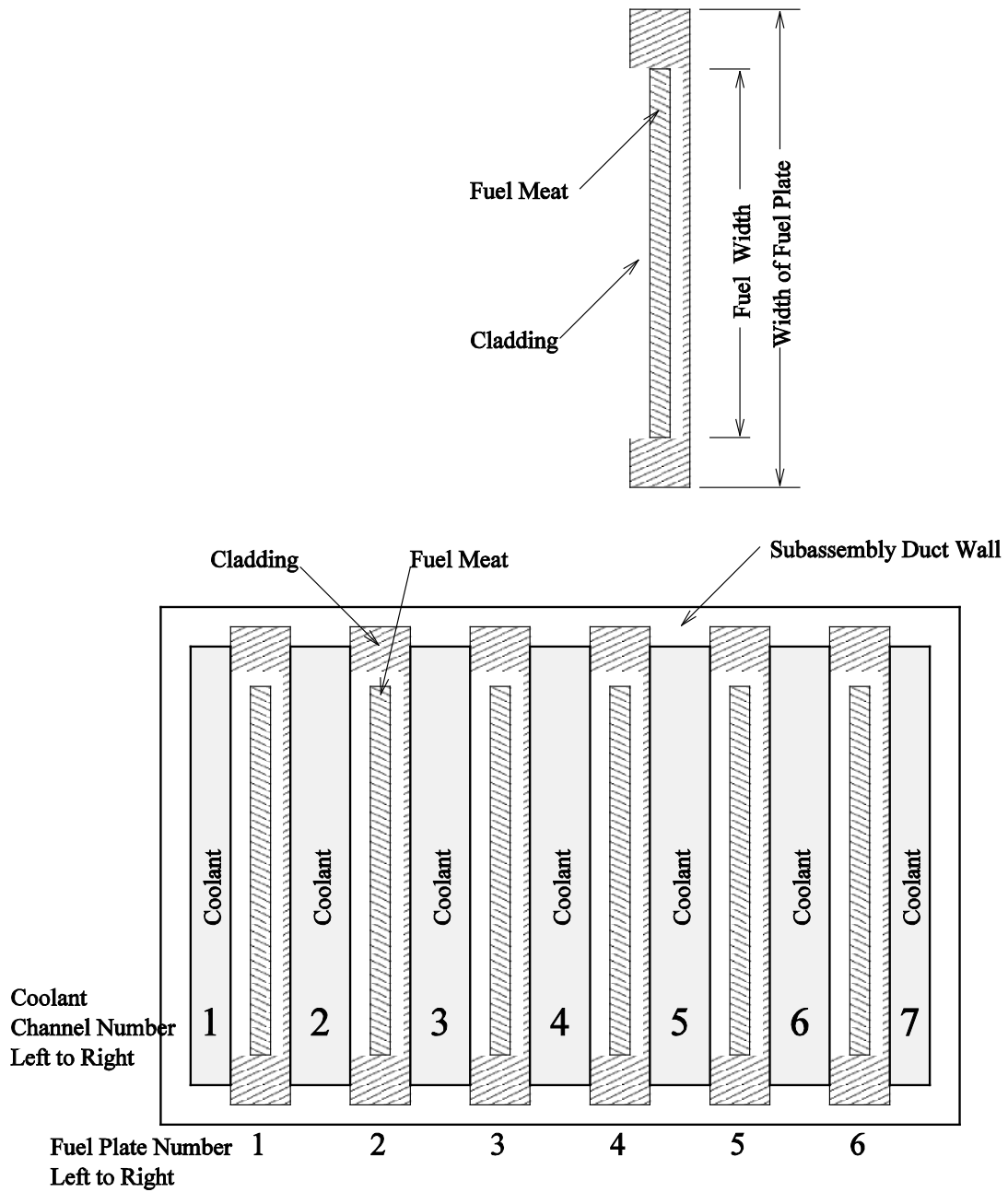


Figure 1. Cross Section of a Typical Fuel Assembly Having Six Fuel Plates Modeled by PLTEMP/ANL Code (A single fuel plate is shown at the top).

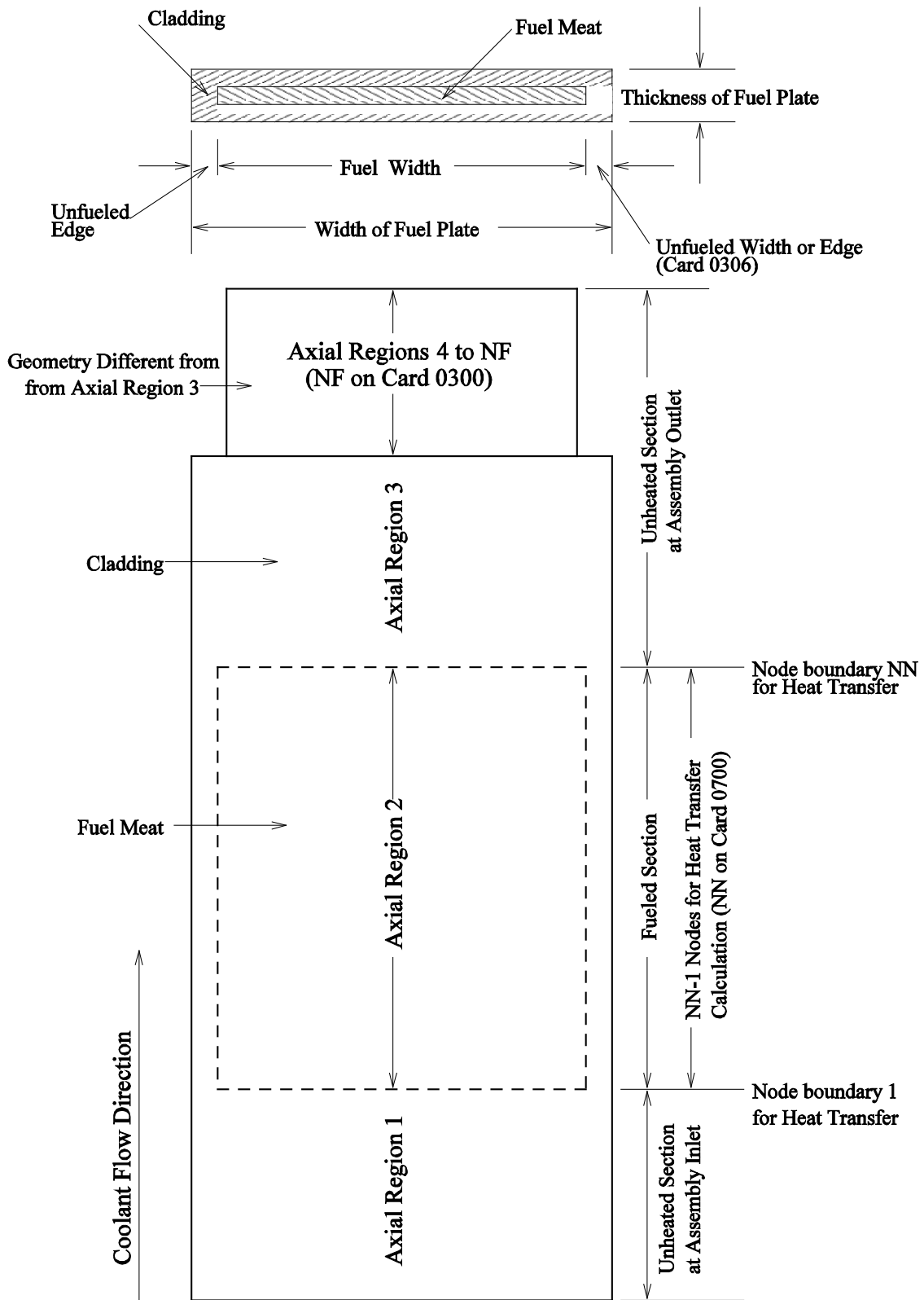


Figure 2. Fuel Plate Geometry modeling in PLTEMP/ANL Code.

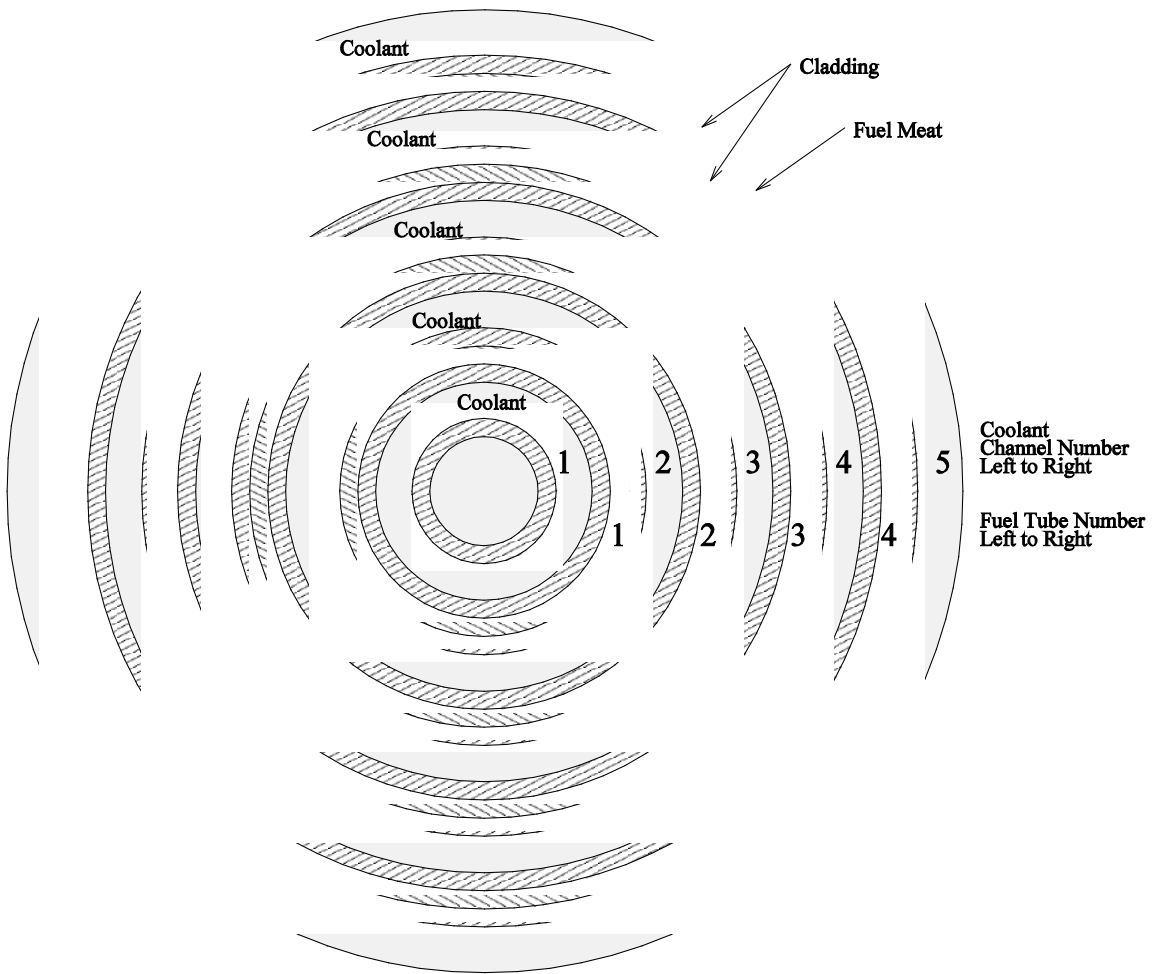


Figure 3. Cross Section of a Typical Fuel Assembly Having Four Coaxial Fuel Tubes Modeled by PLTEMP/ANL Code.

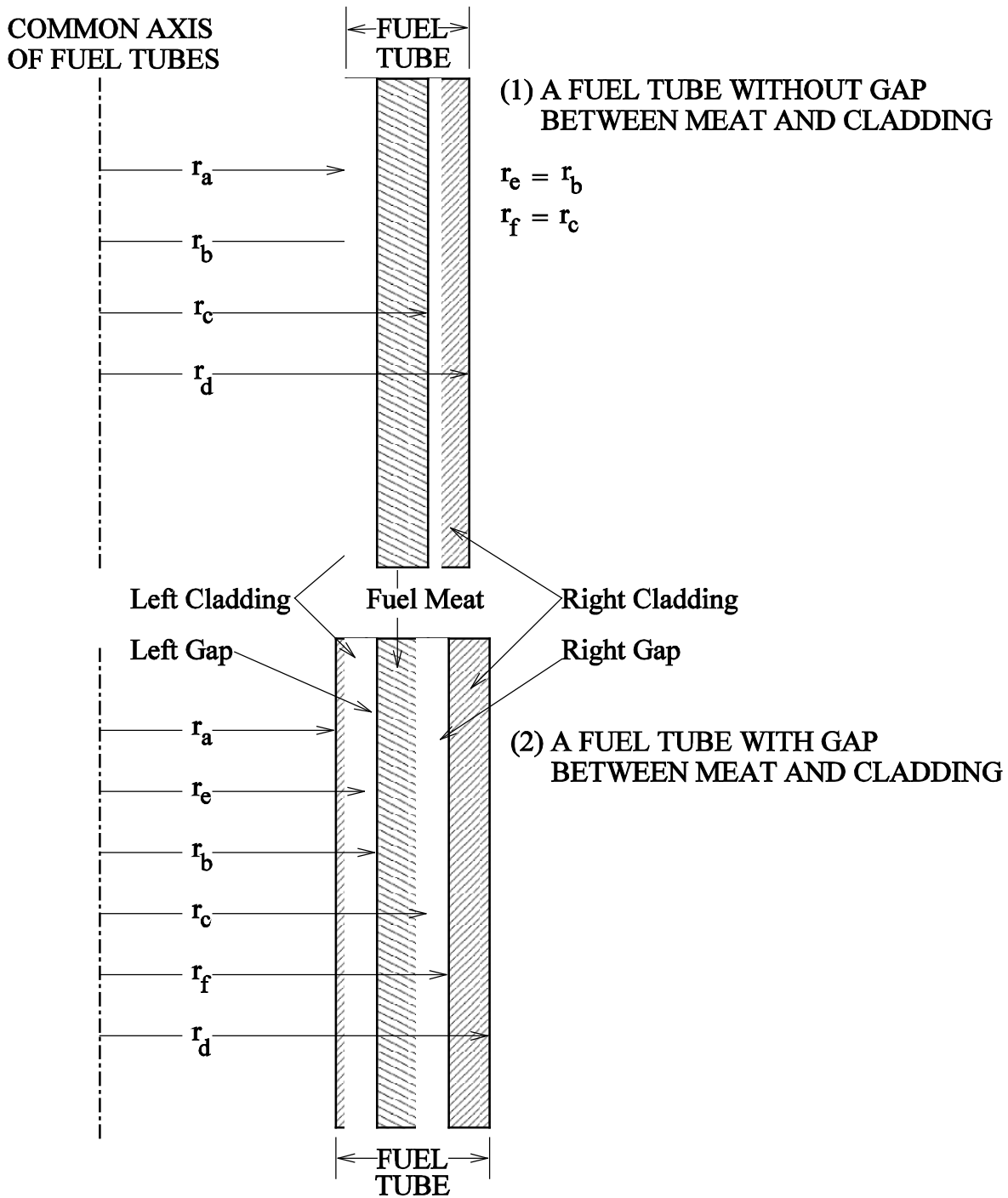


Figure 4. Geometry of a Fuel Tube with Different Claddings on the Left and Right Sides of the Fuel Meat in Two Cases: (1) Without Gap Between Meat and Cladding, and (2) With Gap Between Meat and Cladding.

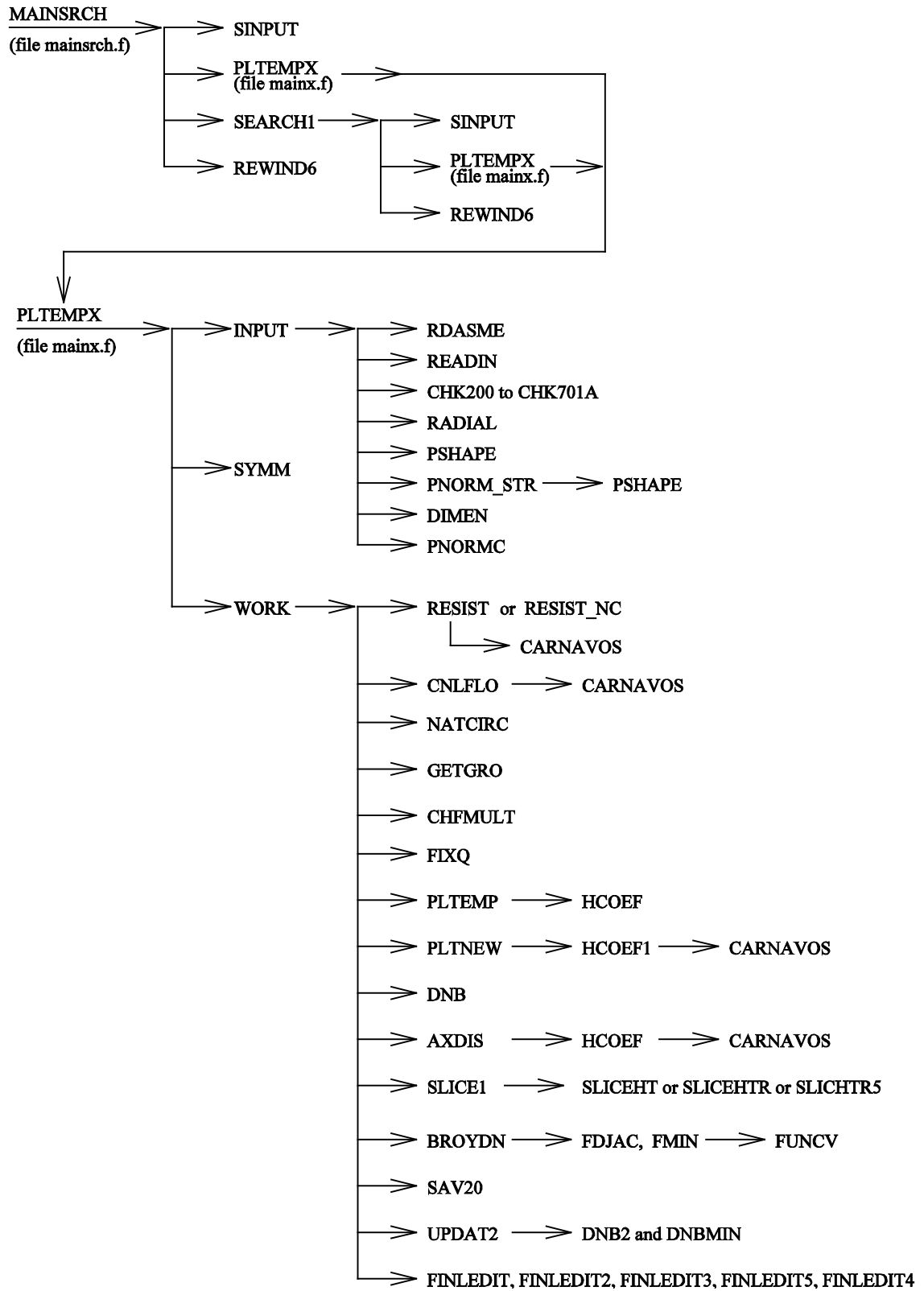


Figure 5. Subroutine Calling Hierarchy in PLTEMP/ANL Version 4.2 Code.

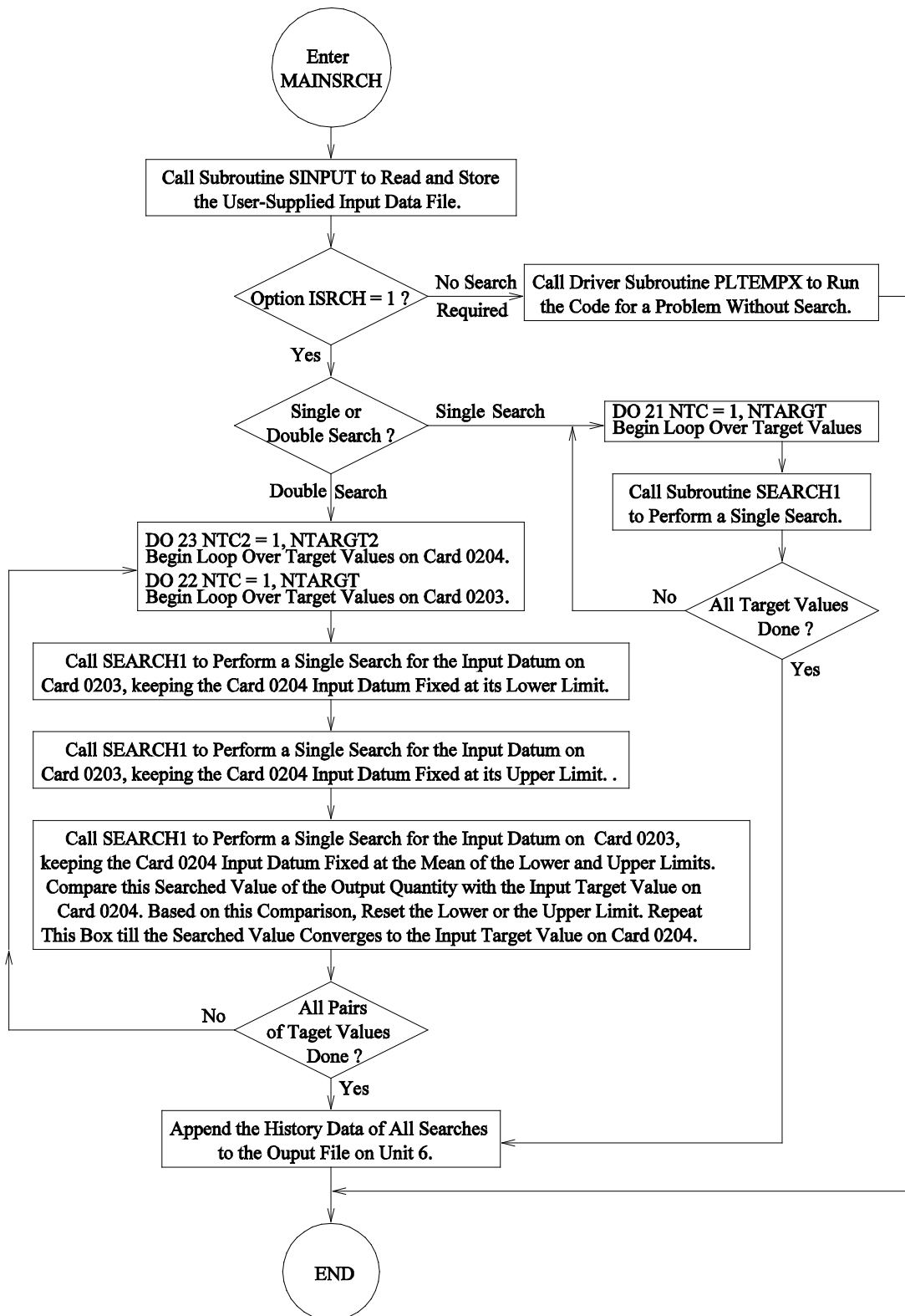


Figure 6. Logical Flow Diagram of the Main Program of PLTEMP/ANL Code.

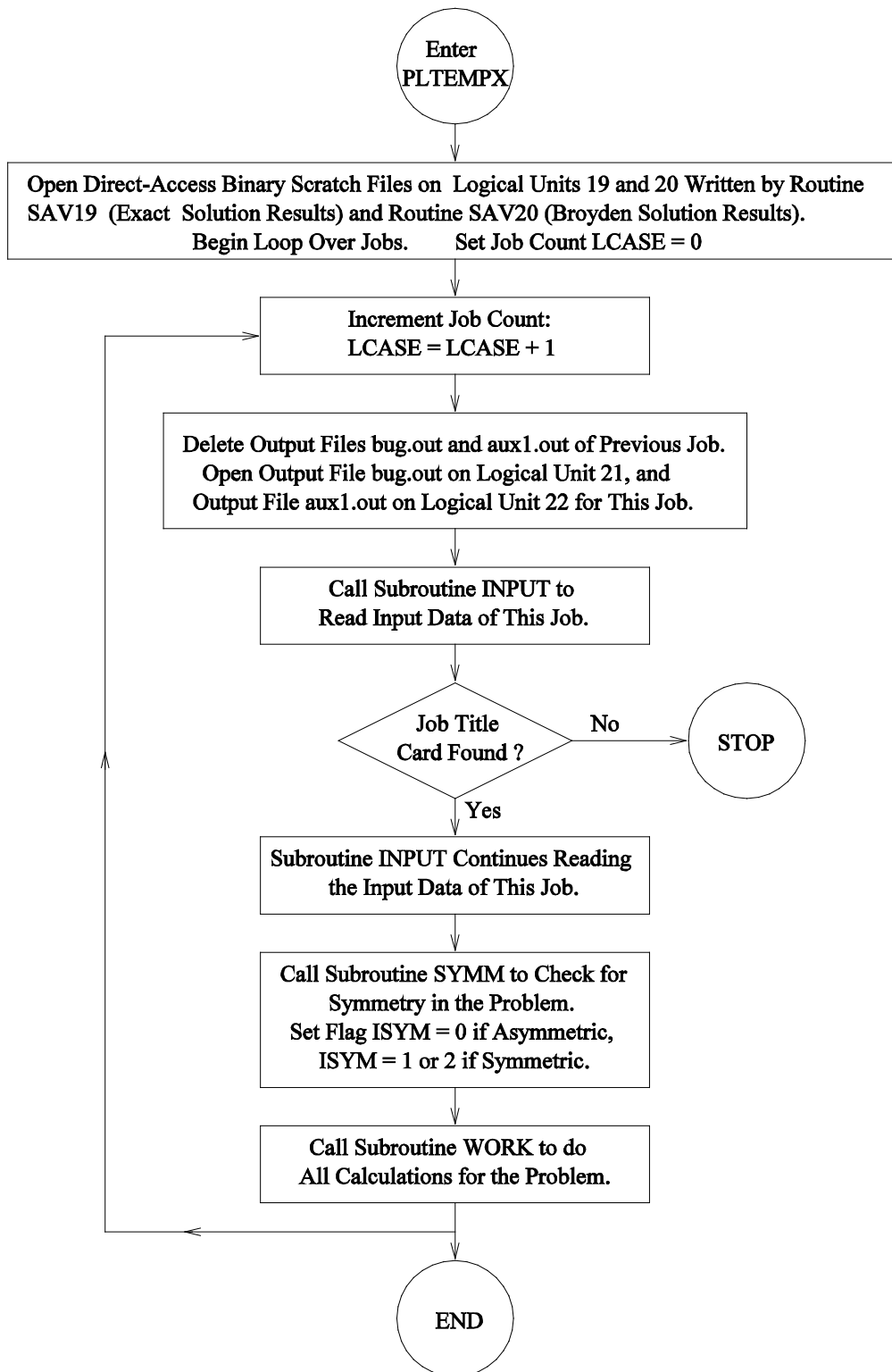


Figure 7. Logical Flow Diagram of Subroutine PLTEMPX, the Pre-Search Main Driver.

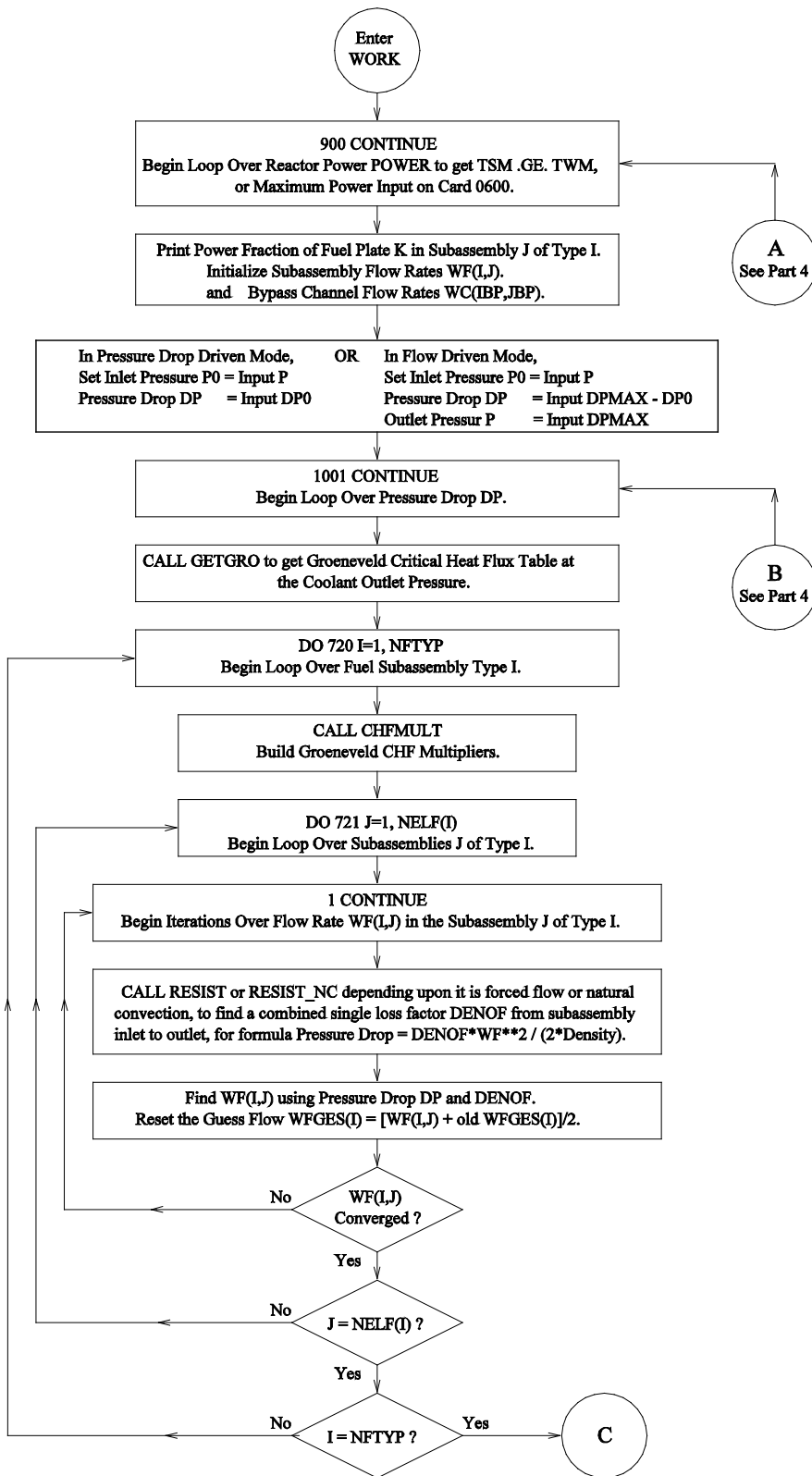


Figure 8. Logical Flow Diagram of Subroutine WORK in PLTEMP/ANL Code.

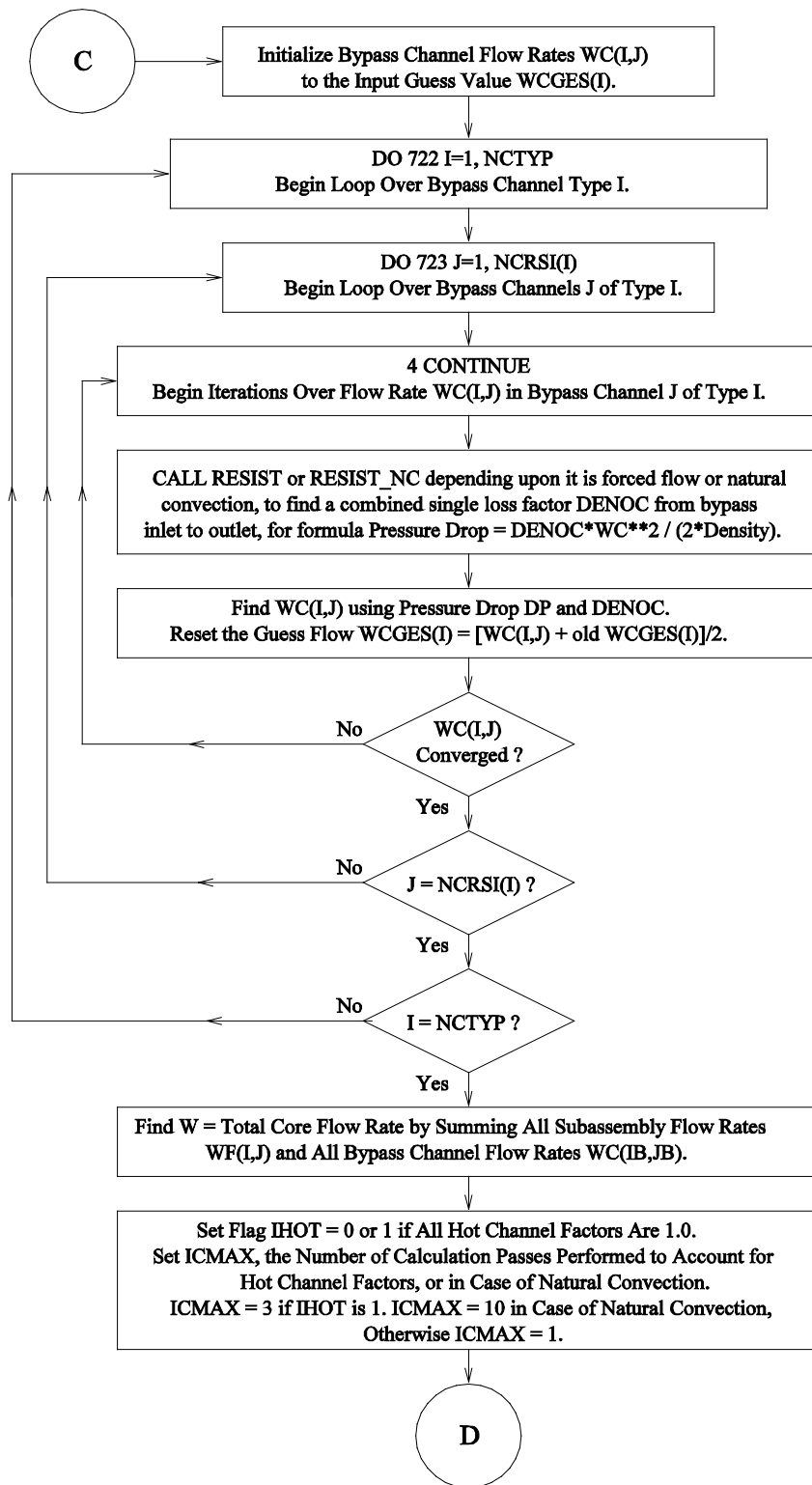


Figure 8. Continued, Part 2

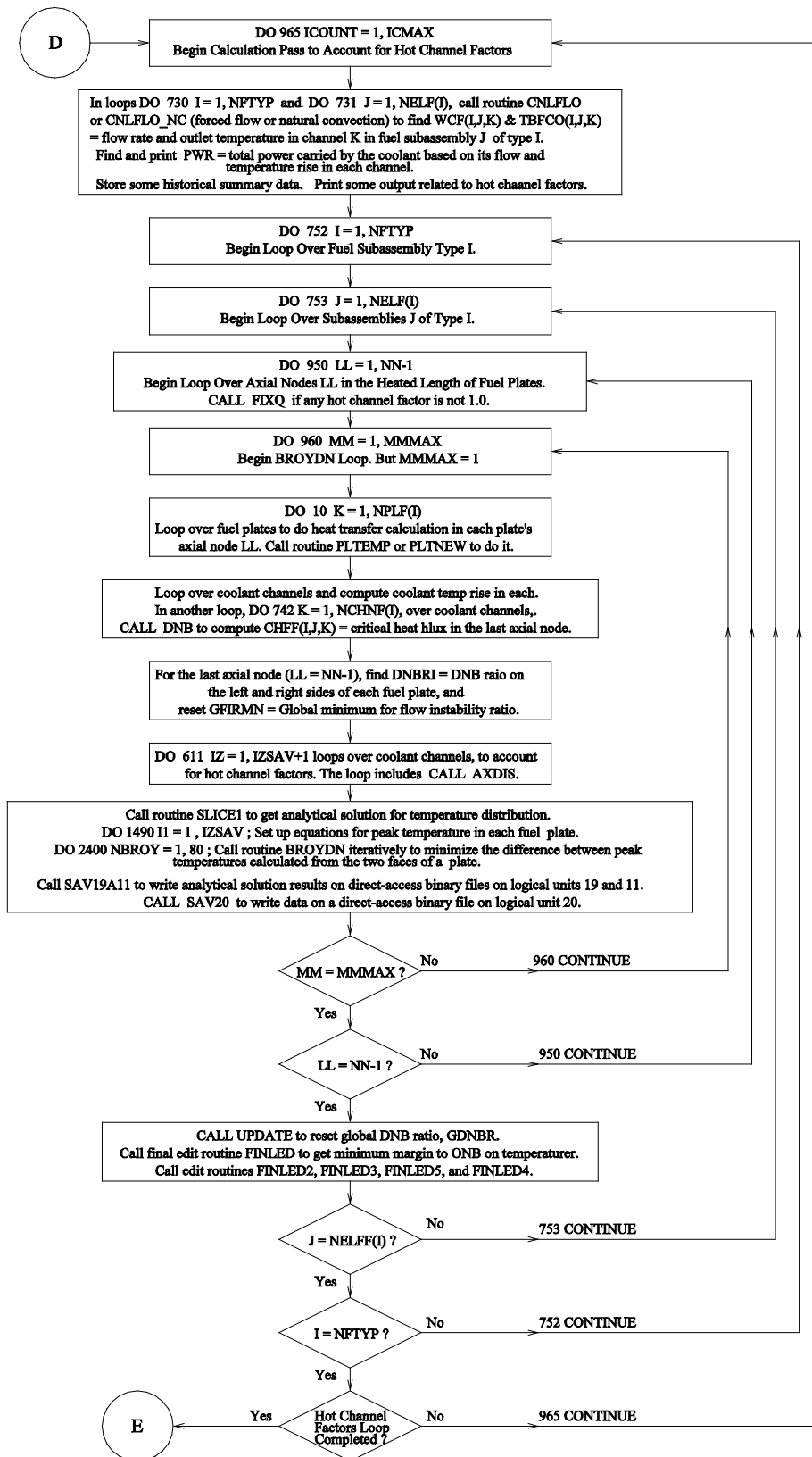


Figure 8. Continued, Part 3.

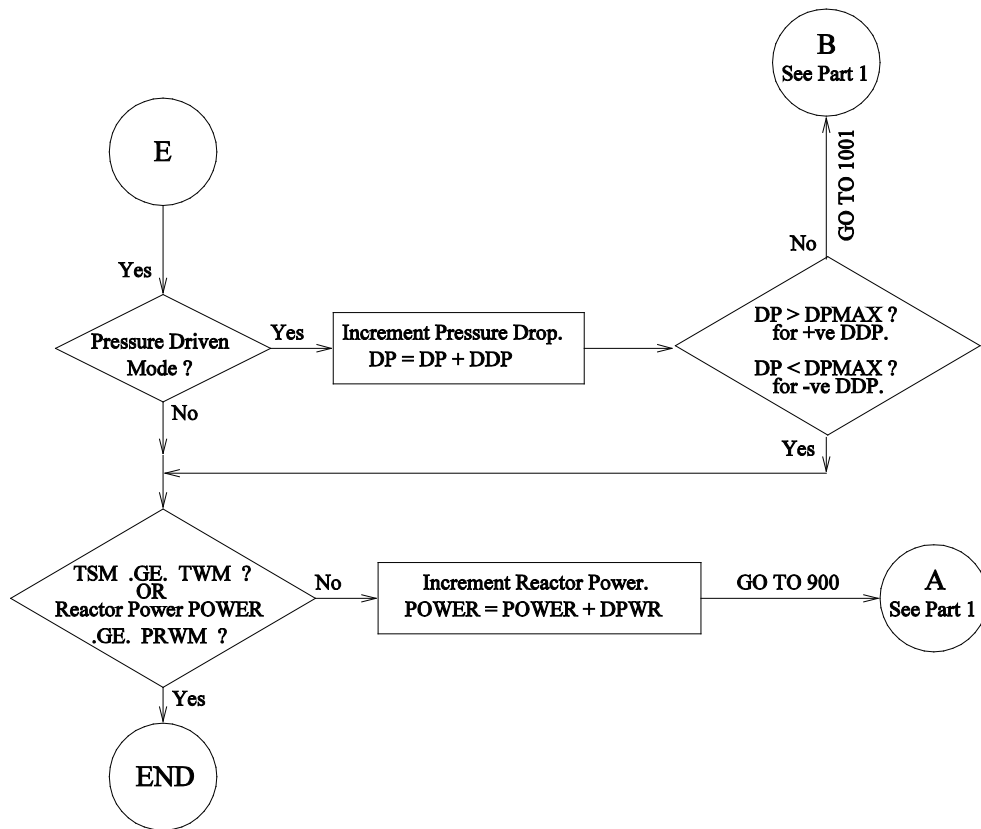
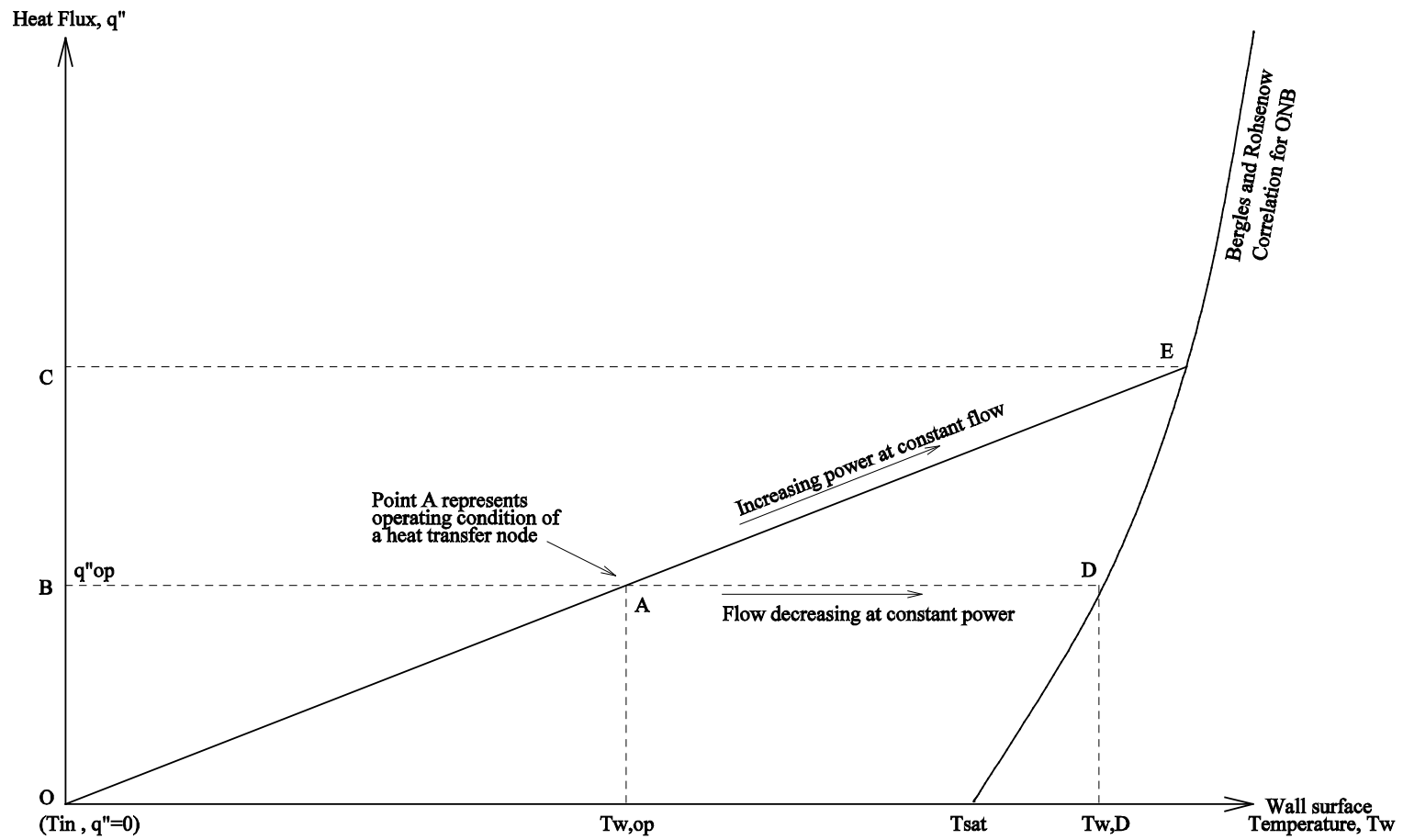
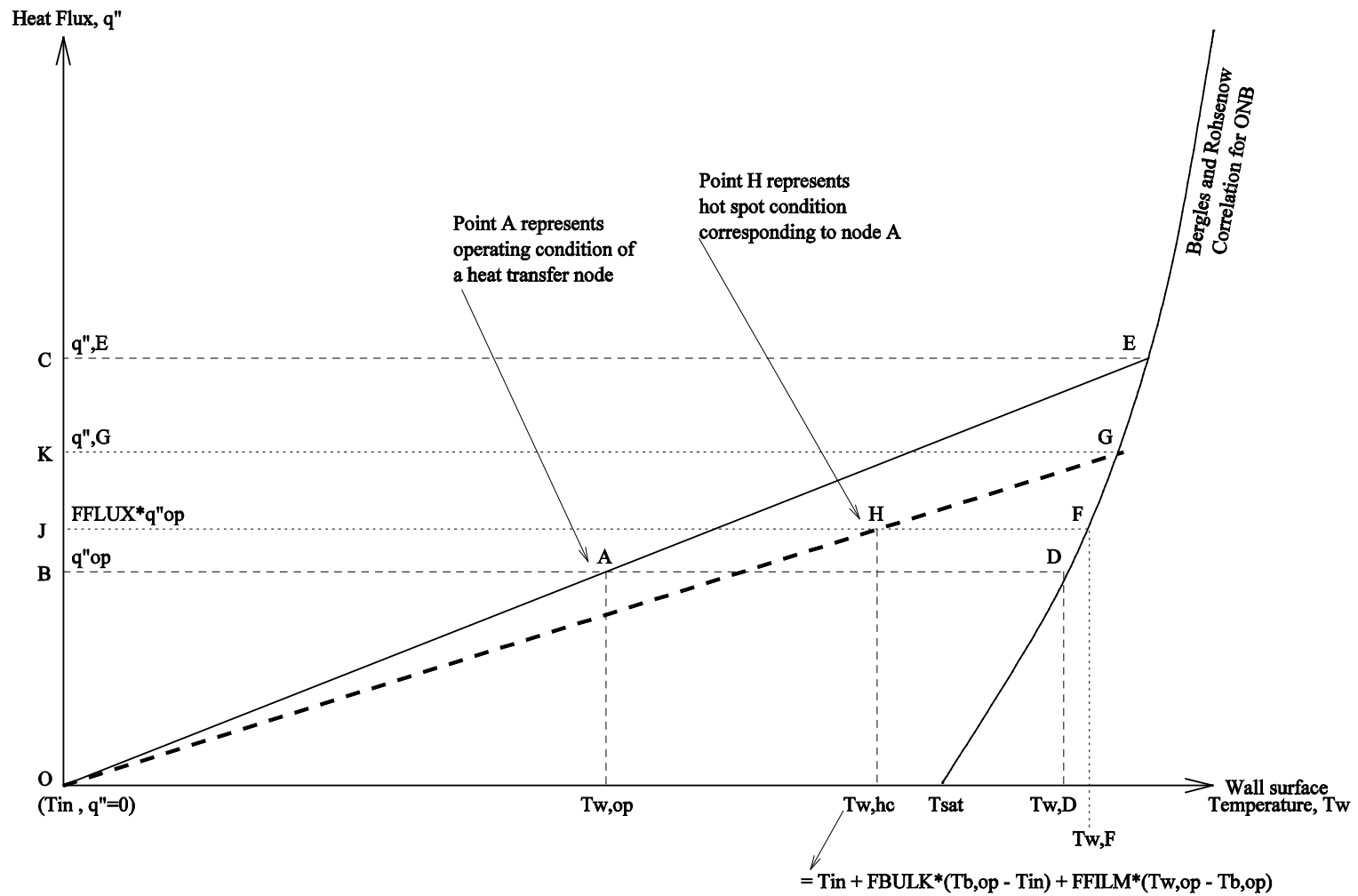


Figure 8. Continued, Part 4.



For flow decreasing at constant power, ONB Ratio = $(T_{w,D} - T_{in}) / (T_{w,op} - T_{in})$
 For increasing power at constant flow, ONB Ratio = $q''_E / q''_{op} = CO/BO$

Figure 9. Geometrical Representation of ONB Ratio for a Fuel Plate Axial Node in PLTEMP/ANL Code.



For flow decreasing at constant power, ONB Ratio for Point H = $(T_{w,F} - T_{in}) / (T_{w,hc} - T_{in})$

For increasing power at constant flow, ONB Ratio for Point H = $q''_G / q''_H = KO/JO$

Figure 10. Geometrical Representation of ONB Ratio for a Fuel Plate Axial Node, Including the Effect of Hot Channel Factors

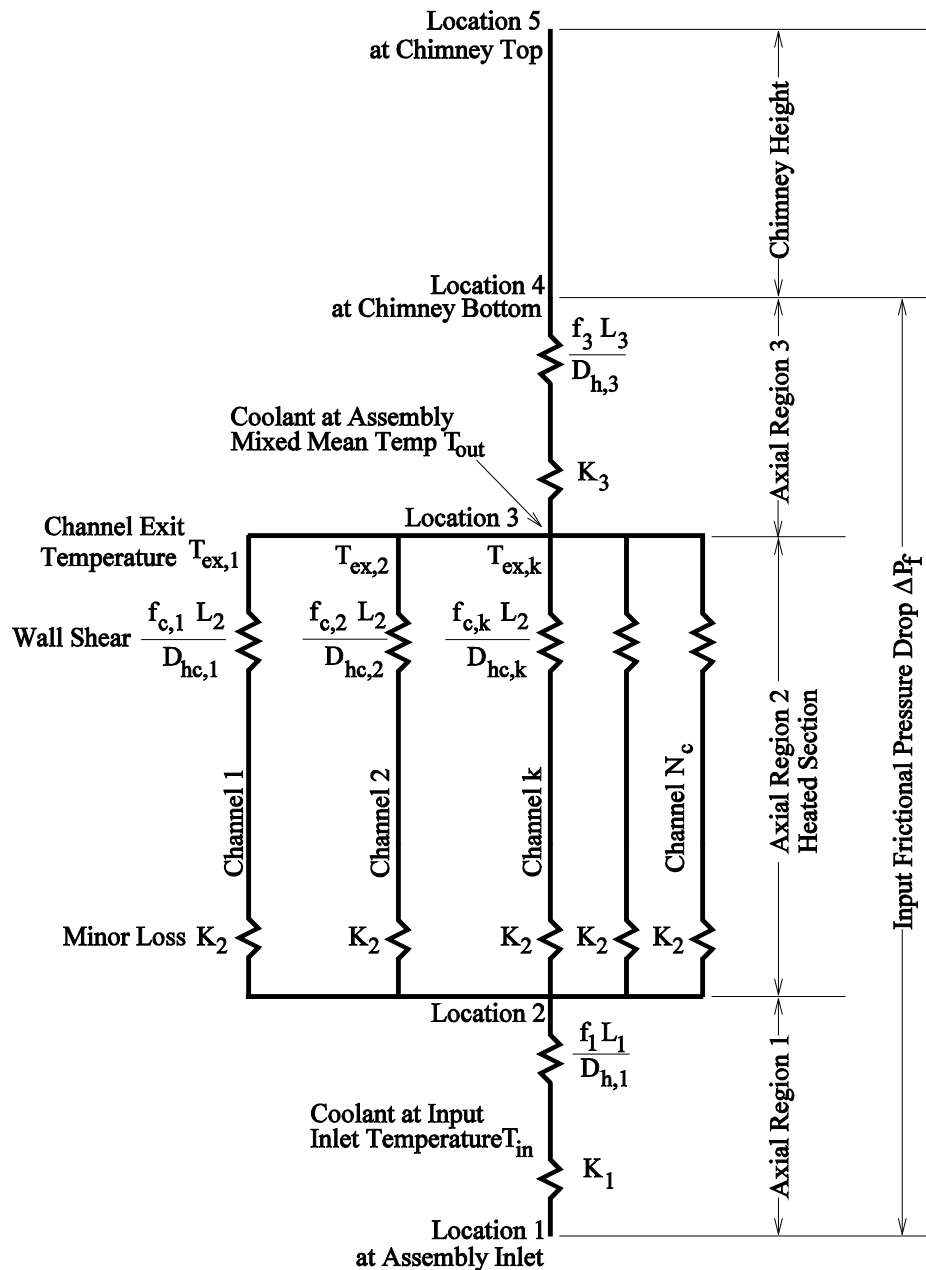


Figure 11. Coolant Flow Path in a Fuel Assembly and Chimney Modeled in PLTEMP/ANL (Multiple Axial Regions Downstream of the Heated Section Are Allowed)

Table 1 . Purpose of Major Subroutines in PLTEMP/ANL V4.2 Code

Subroutine	Purpose of the Subroutine
PLTEMP2	This is the main routine and has the filename <i>mainsrch.f</i> . It calls the subroutine SINPUT to read the user-supplied input data and write an input data file <i>input.modified</i> having one datum modified for the search of input option ISRCH; and then calls the driver subroutine PLTEMPX (the main routine of the pre-search versions of the code) to run the code for the modified input data file.
PLTEMPX	This is the driver subroutine in file <i>mainx.f</i> . It was the main program of the code before adding the search capability. It calls the subroutine INPUT to read the input data; calls the subroutine SYMM to check for symmetry; and then calls the subroutine WORK which does all the calculation work.
AXDIS	This subroutine calculates axial temperature distributions. It obtains a low order solution, not the final answer. Only some numbers in the solution obtained are important.
BROYDN	This subroutine implements Broyden method to iteratively solve for the vector containing the fractional position of the fuel temperature peak in each plate. The method proceeds iteratively until the difference between the peak fuel temperatures predicted from each side of any fuel plate is less than a specified tolerance. BROYDN calls a routine LNSRCH which contains a numerically important control on the limits of the maximum fuel temperature position in fuel meat thickness (see array X). For the code to converge, these limits on array X must be reasonable for the problem being solved (and may need to be changed).
CARNAVOS	This subroutine calculates turbulent heat transfer coefficient and friction factor for a circular or rectangular coolant channel having longitudinal inner fins of trapezoidal cross section. If the input IH = -1, it is called by subroutines HCOEF, HCOEF1 to get the heat transfer coefficient, and by subroutines RESIST and CNLFLO to get the friction factor.
CHFMULT	This subroutine computes the Groeneveld critical heat flux (CHF) table lookup multipliers for each coolant channel, assuming plate-geometry fuel without grid spacers with vertical flow.
CHK200 to CHK701A	This is a group of 19 subroutines (filename <i>chk.f</i>) used to check input data of various card types. The name of each subroutine in the group ends with a three-digit number which is the card type checked by that subroutine.
CNLFLO	This subroutine calculates the flow distribution and temperature rise in the fuel channels.
CNLFLO_NC	This subroutine is based on CNLFLO but modified for natural circulation. It calculates the flow distribution and temperature rise in the fuel channels.
DATE_AND_TIME	This subroutine provides calendar date, time of day, and time zone.
DIMEN	This subroutine calculates total flow area and average hydraulic diameter of fuel coolant channels from the input dimensions of the channels.
DNB	This subroutine calculates critical heat flux (CHF).
DNB2	This subroutine calculates CHF using the nodal or channel exit temperatures. This subroutine has more CHF correlations than the subroutine DNB.
DNBMIN	This subroutine finds minimum DNB ratio (DNBR).

FINLEDIT	This is one of the final edit subroutines. It finds and edits (a) the Onset-of-Nucleate Boiling (ONB) margin, (b) the average coolant temperature rise if core and bypass flows are recombined.
FINLEDIT2	This is one of the final edit subroutines. It finds and edits (a) dimensionless non-boiling length (LNBL and LNBR on right and left sides of the channel), (b) the ratio of Zuber number to Subcooling number, N_{sub}/N_{Zu} .
FINLEDIT3	This is one of the final edit subroutines. It prepares input for the PARET/ANL V7.0 code by treating each fuel plate as two "half-plates" within the context of a PARET "channel".
FINLEDIT4	This is one of the final edit subroutines. It finds and edits Reynolds number and Prandtl number.
FINLEDIT5	This is one of the final edit subroutines. In natural circulation, it is used to edit several variables including temperatures, pressures, thermal properties, buoyancy force, frictional force over the active fuel height.
FINLEDIT6	This is one of the final edit subroutines. It tabulates ONB ratio at all heat transfer nodes in a fuel assembly.
FIXQ	This subroutine sets up special conditions over a range of axial heat transfer nodes where the local hot channel factor also applies (in addition to the global hot channel factor).
GETDATA	This subroutine reads the temperature and heat flux distribution data calculated by subroutine SLICHTR5 in assemblies made of 5-layer fuel tubes, and brings the data to the editing subroutines FINLEDIT, FINLEDIT2, ... FINLEDIT6, and UPDAT2.
GETGRO	This subroutine reads the Groeneveld critical heat flux (CHF) tables in binary format. Then it interpolates and prints a CHF table at the system pressure. See D. C. Groeneveld, L. K. H. Leung, A. Z. Vasic, Y. J. Guo, S. C. Cheng, Nuclear Engineering and Design 225 (2003) pp 83-97
INPUT	This subroutine calls the subroutine RDASME to read an ASME steam table for water, and calls the subroutine READIN to read the input data file stripping out the comments. It checks the input data cards using 19 subroutines named CHK200, CHK300 ... CHK701A. It also calls the subroutine RADIAL to determine effective cladding thickness for radial geometry; calls the subroutine DIMEN to calculate total flow area and average hydraulic diameter of coolant channels from the input dimensions; and calls the subroutine PNORMC to normalize the input radial power peaking factors for fuel plates.
INTERP3D	This subroutine does a 3-dimensional interpolation (using 8 CHF data points) of the Groeneveld CHF array GRALL(NN1,NN2,NN3) to find the CHF at a desired point, i.e., given values of the coolant quality, mass flux, and pressure
NATCIRC	In the natural circulation option, this subroutine performs the inner iterations to calculate channel flow rates. See the solution strategy described in Section 3 of Appendix XI.
ONBRATIO	This function solves Eq. (10) of Section 3.5.2 to find the Onset-of-Nucleate Boiling ratio for a heat transfer node. It is called by subroutine FINLED6 repetitively for each node, to print a table for a fuel assembly.
PLTEMP	This subroutine calculates fuel plate temperatures for a single axial segment, not the entire channel length.

PLTNEW	This subroutine calculates fuel plate temperatures for a single axial segment, not the entire channel length, using data from the prior pass after the whole solution is known.
PNORMC	This subroutine normalizes the input radial power peaking factors for fuel plates of all assembly types.
PNORM_STR	This subroutine normalizes the axial power density shapes by stripe read from the input axial power shape file, using Eqs. (12) and (34) of Appendix XIV for 5-layer thick plates.
PSHAPE	This subroutine reads axial power density shapes by fuel plate stripe from the input axial power shape file. To speed up code execution, it reads data for one specific fuel type.
RADIAL	This subroutine determines effective cladding thickness for radial geometry.
RDASME	This subroutine reads an ASME steam table for water.
READIN	This subroutine reads the input data file and strips out comments.
RESIST	This subroutine calculates (in case of forced flow) for a given assembly J of type I, a flow resistance parameter $DENOF(I,J)$, using the geometrical data on card 0304, where $DENOF = \sum (K_{loss} + f L/D_h) / A^2$, the sum being over all axial regions $NF(I)$, such that the pressure drop P is related to mass flow rate W as: $P = DENOF * (W^2 / 2\rho)$.
RESIST_NC	This subroutine calculates (in case of natural circulation) for a given assembly J of type I, a flow resistance parameter $DENOF(I,J)$, using the geometrical data on card 0304, where $DENOF = \sum (K_{loss} + f L/D_h) / A^2$, the sum being over all axial regions $NF(I)$, such that the pressure drop P is related to mass flow rate W as: $P = DENOF * (W^2 / 2\rho)$.
REWIND6	This subroutine is used during a search to backspace the file on unit 6 to the beginning of all the output written by each PLTEMPX run prior to the search convergence.
SAV20	This subroutine writes the common block to a direct access file on logical unit 20, and also edits to the file <i>bug.out</i> on unit 21.
SEARCH1	This subroutine performs a single search of any given type. It calls SINPUT to prepare an input file, calls PLTEMPX to run the pre-search code, and then calls REWIND6 to get rid of the printed output, except the output for the run with the search converged.
SINPUT	This subroutine reads and stores the user-supplied input file. During a single or double search, it is used to write a modified input file with one or two input data changed.
SLICE1	If the option IEND = 0 (3-layer fuel plates), this subroutine drives subroutines SLICEHT and SOLVER to set up and solve Eq. (22) of Appendix VI to find the <i>exact solution</i> (see input option KSOLNPR) for the node-center coolant bulk temperatures in <i>all</i> channels in an axial slice of a fuel assembly in slab geometry. It also handles the radial geometry option IGOM = 1 by using SLICEHTR instead of SLICEHT.
SLICEHTR	If the option IEND = 0 (3-layer fuel plates), this subroutine is called by SLICE1 to set up and solve Eq. (26) of Appendix VIII to find the <i>exact solution</i> for the node-center coolant bulk temperatures in <i>all</i> channels in an axial slice of a fuel assembly in radial geometry.
SLICHTR5	If the option IEND = 1 (5-layer fuel plates), this subroutine is called by SLICE1 to set up and solve Eq. (37) of Appendix XIII to find the exact solution for the node-center coolant

bulk temperatures in *all channels in each stripe* of an axial slice of a fuel assembly in radial geometry.

SYMM	This subroutine checks for symmetry to left and right, which can lead to a zero Jacobian in the subroutine BROYDN. If the problem is symmetric, then calling BROYDN is not needed.
UPDAT2	This subroutine uses the subroutine DNB2 to calculate a table of critical heat flux ratios (CHFR) at each heat transfer axial node on both surfaces of each fuel plate.
WORK	This is the subroutine which does all the calculation work in the program.
ZERO	This subroutine sets a three-dimensional array to zero.
ZERO1	This subroutine sets a one-dimensional array to zero.
ZERO2	This subroutine sets a two-dimensional array to zero.

Table 3. Definition of Important FORTRAN Variables in the Code

Variable	Description of the Variable
CHFF(I,J,K)	Critical heat flux in the last axial node of coolant channel K of assembly J of fuel type I, $W/m^2\text{-}^\circ C$
DENOC	Equivalent flow resistance of <i>bypass</i> assembly J of type I, calculated in the subroutine resist.f such that the assembly inlet-to-outlet frictional pressure drop $DP = DENOC * WC(I,J)^2 / (2 * RHO)$, where RHO is coolant density (kg/m^3) at the input inlet temperature.
DENOF	Equivalent flow resistance of <i>fuel</i> assembly J of type I, calculated in the subroutine resist.f such that the assembly inlet-to-outlet frictional pressure drop $DP = DENOF * WF(I,J)^2 / (2 * RHO)$, where RHO is the coolant density (kg/m^3) at mean temperature of heated section.
DP	Frictional pressure drop ($f L/D +$ minor losses, excluding the gravity head) in an assembly, Pa
DPF(I,J,J1)	Frictional pressure drop (MPa) in axial region J1 of assembly J of type I
GFIRMN	Global minimum value of flow instability ratio
GPM	Total flow rate in the reactor core and bypass, gpm
HFLMAX	Maximum heat flux over all fuel plates in a single fuel assembly which is currently being edited
HIST(*,1)	Driving pressure drop, MPa. The first index in array HIST and the companion array IHIST is 1 for the calculation without hot channel factors (the nominal case), and is 2 for the calculation with all six hot channel factors applied.
HIST(*,2)	Total flow rate in the core, kg/s
HIST(*,3)	Total flow rate in all bypass assemblies, kg/s
HIST(*,4)	Total flow rate in the reactor core and bypass, kg/s
HIST(*,5)	Minimum Onset Nucleate Boiling Ratio (ONBR). It is the minimum over all fuel assemblies in the reactor.
HIST(*,6)	Minimum Departure from Nucleate Boiling Ratio (DNBR), also called Minimum Critical Heat Flux Ratio (CHFR). It is the minimum over all fuel assemblies in the reactor.
HIST(*,7)	Total flow rate in the reactor core and bypass, m^3/hr
HIST(*,8)	Reactor power, MW
HIST(*,9)	Minimum Flow Instability Ratio (FIR). It is the minimum over all fuel assemblies in the reactor.
HIST(*,10)	Maximum cladding surface temperature in the core, $^\circ C$. It is the maximum over all fuel assemblies in the reactor.
HIST(*,11)	Maximum coolant bulk temperature in the core, $^\circ C$. It is the maximum over all fuel assemblies in the reactor.
HIST(*,12)	Maximum heat flux in the core, MW/m^2 . It is the maximum over all fuel assemblies in the reactor.
HIST(*,13)	Maximum fuel meat temperature in the core, $^\circ C$. It is the maximum over all fuel assemblies in the reactor.
HIST(*,14)	Currently unused

HIST(*,14)	Currently unused
IHIST(*,1)	Fuel assembly type in which the minimum ONBR occurs. The first index in array HIST and the companion array IHIST is 1 for the calculation without hot channel factors (the nominal case), and is 2 for the calculation with all six hot channel factors applied.
IHIST(*,2)	Fuel assembly type in which the minimum DNBR occurs
IHIST(*,3)	Fuel plate number on which occurs the maximum cladding surface temperature
IHIST(*,4)	Coolant channel number in which occurs the maximum coolant bulk temperature
IHIST(*,5)	Fuel plate number on which occurs the maximum heat flux
IHIST(*,6)	Fuel plate number on which occurs the maximum fuel meat temperature
IHIST(*, 7 to 15)	Currently unused
IMINF	Channel number with the minimum flow instability ratio RFLOWMIN in a single fuel assembly which is currently being edited, for the nominal case or with only three global hot channel factors
IMINF2	Channel number with the minimum flow instability ratio RFLOWMIN2 in a single fuel assembly which is currently being edited, with all six (both global and local) hot channel factors
IWF	An internally defined integer flag to indicate flow mode. IWF = 0 indicates pressure drop driven mode; IWF = 1 indicates flow driven mode.
KSW	An internally defined integer flag to indicate the order of fuel tube radii in the input data. KSW=0 if the radii are in the descending order. KSW=1 if the radii are in the ascending order.
NCTEX	Coolant channel number which has the maximum coolant temperature TEXMAX
NPHFL	Fuel plate number which has the maximum heat flux HFLMAX
NPTCS	Fuel plate number which has the maximum cladding surface temperature TCSMAX
NPTF	Fuel plate number having the maximum fuel meat temperature TFMAX
ONBR2(I,N)	ONBR at coolant-cladding interface I in axial heat transfer node N, with the ONBR defined as ONB heat flux divided by operating heat flux. This array is for the case <i>when only the global hot channel factors are applied</i> .
ONBR3(I,N)	ONBR at coolant-cladding interface I in axial heat transfer node N, with the ONBR defined as ONB heat flux divided by operating heat flux. This array is for the case <i>when both the global and local hot channel factors are applied</i> .
P0	Pressure (MPa) at assembly inlet. It is set internally (once for ever) equal to the input datum P for the assembly inlet pressure. It is important to note that the input variable P is not kept unchanged, rather is reset in subroutine <i>work.f</i> to the heated section outlet pressure.
P	Input datum for the assembly inlet pressure (MPa) in the pressure driven mode. It should be noted that the input value of P is not kept unchanged, rather is reset in subroutine <i>work.f</i> to the heated section outlet pressure.
PINTERF(LL)	Coolant pressure at the entry to axial node LL, bar
RFLOWMIN	Minimum flow instability ratio in single fuel assembly which is currently

	being edited, for the nominal case or with only three global hot channel factors
RFLOWMIN2	Minimum flow instability ratio in single fuel assembly which is currently being edited, with all six (both global and local) hot channel factors
TCSMAX	Maximum cladding surface temperature over all fuel plates of a single fuel assembly which is currently being edited
TEXMAX	Maximum coolant temperature over all fuel plates in a single fuel assembly which is currently being edited
TFMAX	Maximum fuel meat temperature over all fuel plates in a single fuel assembly which is currently being edited
TINY	An internally set negligible flow area (currently set as 10^{-15} m^2) that is used in modeling a solid fuel rod (with or without coaxial fuel tubes around the fuel rod). If the input flow area of the innermost coolant channel (at the center) is smaller than TINY, the coolant temperature and the safety margins (ONBR, FIR, CHFR) associated with the central channel are ignored in determining their minima.
UF(I,J,K)	Coolant velocity (m/s) in channel K of assembly J of type I
W	Total flow rate in the reactor core and bypass, kg/s
WBP	Total flow rate in all bypass assemblies, kg/s
WC(I,J)	Flow rate in a bypass assembly J of type I, kg/s
WCF(I,J,K)	Flow rate in coolant channel K of assembly J of fuel type I, kg/s
WCORE	Total flow rate in the reactor core and bypass, kg/s (same as W)
WF(I,J)	Flow rate in a fuel assembly J of type I, kg/s
WT	Total flow rate in the core, kg/s
ZMINL	Smallest ONBR on the left side of all plates in a fuel assembly, with the ONBR calculated as the ratio $(T_{w,ONB} - T_{in}) / (T_{w,operating} - T_{in})$
ZMINR	Smallest ONBR on the right side of all plates in a fuel assembly, with the ONBR calculated as the ratio $(T_{w,ONB} - T_{in}) / (T_{w,operating} - T_{in})$
ZMIN	Minimum ONBR in a given longitudinal stripe of a fuel assembly. It equals $\text{MIN}(ZMINL, ZMINR)$.
ZPR(0)	Pressure at inlet to the heated section (at $z = 0.0$) which is edited in the output file
ZPR(LL)	Pressure (bar) <i>at center</i> of heat transfer mesh interval LL ($LL=1, NN-1$). It is defined in line 1436 of subroutine <i>work.f</i> (see lines 1412 to 1436). It is used throughout the code in heat transfer, ONBR, and CHFR calculations, and edited in the output file as part of the heat flux table.
ZPR(NN)	Pressure at exit of the heated section [at $z = LF(I,2)$] which is edited in the output file
ZONBL(I)	ONBR on the left side of fuel plate I in a fuel assembly, with the ONBR calculated as the ratio $(T_{w,ONB} - T_{in}) / (T_{w,operating} - T_{in})$
ZONBR(I)	ONBR on the right side of fuel plate I in a fuel assembly, with the ONBR calculated as the ratio $(T_{w,ONB} - T_{in}) / (T_{w,operating} - T_{in})$

Temperature arrays used in the Broyden heat transfer method:

DTSATL	ONB temperature minus saturation temperature on the <i>left side</i> of a fuel plate, °C
--------	--

DTSATR	ONB temperature minus saturation temperature on the <i>right side</i> of a fuel plate, °C
ETAPRL	Whittle and Forgan parameter η (dimensionless) on the <i>left side</i> of a fuel plate, calculated as $\eta = (\text{Coolant velocity}) * (T_{\text{sat}} - \text{Coolant temp.}) * (\text{Coolant density}) C_p / (4 * \text{Heat flux})$
ETAPRR	Whittle and Forgan parameter η (dimensionless) on the <i>right side</i> of a fuel plate, calculated as $\eta = (\text{Coolant velocity}) * (T_{\text{sat}} - \text{Coolant temp.}) * (\text{Coolant density}) C_p / (4 * \text{Heat flux})$
XMAX(K)	Location (m) of fuel maximum temperature in fuel meat thickness
TSAT	Coolant saturation temperature, °C
ZCOOLM(K)	Coolant temperature in channel K at the center of node LL, °C
ZCSL(K)	Cladding left surface temperature, °C
ZFT(K)	Fuel maximum temperature in meat thickness, °C
ZCSR(K)	Cladding right surface temperature, °C
ZHL(K), ZHR(K)	Convective heat transfer coefficients on the left and right cladding surfaces, $W/m^2 \cdot ^\circ C$

Temperature arrays used in heat transfer subroutine SLICEHT for 3-layer fuel plates:

AA(K), BB(K), CC(K), DD(K)	Coefficients in the linear simultaneous algebraic equations for the node-center bulk coolant temperatures in a horizontal slice of a fuel assembly
AAH1(K)	Left cladding-to-coolant heat transfer surface area (m^2) in axial node N from plate K into channel K
AAH2(K)	Right cladding-to-coolant heat transfer surface area (m^2) in axial node N from plate K into channel K+1
CKK1(K), CKK2(K)	Thermal conductivity of left and right claddings of plate K, $W/m \cdot ^\circ C$
CPW(K)	Coolant specific heat in axial node N of channel K, $J/kg \cdot ^\circ C$
DHDPXDP(K)	$(\partial h / \partial P) * (\delta P) = (\text{Partial derivative of coolant enthalpy with respect to pressure}) * (\text{Pressure change})$ in axial node N of channel K
FKK(K)	Thermal conductivity of fuel meat of plate K, $W/m \cdot ^\circ C$
FRAQFC(I,J,K)	Normalized power fraction generated in K-th plate in J-th fuel assembly of type I.
FUELX(K)	XMAX(K) expressed as a fraction of fuel meat thickness
HCONV1(K), HCONV2(K)	Convective heat transfer coefficients on left and right cladding surfaces, $W/m^2 \cdot ^\circ C$
IDHDP	An internally set flag (0 or 1) to include or ignore $(\partial h / \partial P)_T$, the derivative of coolant enthalpy with respect to pressure
KK	Number of coolant channels in the assembly
KK-1	Number of fuel tubes in the assembly
LL	Axial node number
QC1(K), QFL(K), QC2(K)	Volumetric heat sources in left cladding, fuel meat, and right cladding of plate K, W/m^3
QWC(K)	Volumetric heat source in coolant of channel K, W/m^3
QFL(K)	Power density (W/m^3) in axial node LL of plate K, in fuel subassembly J of type I.

TBCX(K)	Coolant temperature in channel K at the center of node LL, °C
TCLADL(K)	Cladding left surface temperature, °C
TCLADR(K)	Cladding right surface temperature, °C
TC1(K), TC2(K)	Thicknesses of left and right claddings of fuel plate K, m
TFL(K)	Thickness of fuel meat in fuel plate K, m
TFUEL(K)	Fuel maximum temperature in meat thickness by plate, °C
TTB(K)	Coolant temperature in channel K at the lower boundary (entry) of the heat transfer axial node LL of a subassembly slice, °C
TTB1(K)	Coolant temperature (°C) in channel K at the upper boundary (outlet) of the heat transfer axial node LL of a fuel assembly slice
TTC1(K), TTC2(K)	Temperatures (°C) of cladding surface on left, and on right of fuel plate K, needed for calculating heat transfer coefficients
VVW(K)	Volume of coolant in axial node N of coolant channel K, m ³
WWC(K)	Coolant flow rate in channel K, kg/s
XMAX(K)	Location (m) of maximum temperature in fuel meat thickness by plate
ZDZ(J)	Fraction of fuel plate power generated in axial node J.
ZPOWER	Reactor power, W

Temperature arrays used in heat transfer subroutine SLICHTR for 3-layer fuel plates:

The FORTRAN variable names in common blocks used in this radial geometry exact solution begin with the string TUBE or TUB or at least T. This was done to differentiate these variables from the flat plate exact solution variables.

AAH1(K)	Left cladding-to-coolant heat transfer surface area in axial node N from fuel tube K into channel K
AAH2(K)	Right cladding-to-coolant heat transfer surface area in axial node N from fuel tube K into channel K+1
ALFA(K)	Symbol α in Appendix VII of the Users Guide
CKK1(K)	Thermal conductivity of inner cladding of fuel tube K, W/m-°C
CKK2(K)	Thermal conductivity of outer cladding of fuel tube K, W/m-°C
CPW(K)	Coolant specific heat in axial node N of channel K
FKK(K)	Thermal conductivity of fuel meat of fuel tube K, W/m-°C
FUELX(K)	Areal fraction in the meat thickness at the meat's maximum temperature
HCONV1(K)	Convective heat transfer coefficient on inner cladding surface, W/m ² -°C
HCONV2(K)	Convective heat transfer coefficient on outer cladding surface, W/m ² -°C
HFLUXR(K)	Symbol q_1'' in Appendix VII of the Users Guide
HFLUXL(K)	Symbol q_2'' in Appendix VII of the Users Guide
QC1(K), QFL(K), QC2(K)	Volumetric heat source in inner cladding, fuel meat, and outer cladding of tube K, W/m ³
QQ(K)	Symbol Q in Appendix VII of the Users Guide
QWC(K)	Volumetric heat source in coolant of channel K, W/m ³
TBCX(K)	Node-center bulk coolant temperature in channel K in a slice, °C
TFUEL(K)	Fuel maximum temperature in meat thickness by fuel tube, °C
TTB(K)	Coolant bulk temperature in channel K, at the lower boundary of node LL (at node inlet), °C

TTB1(K)	Coolant bulk temperature in channel K, at the upper boundary of node LL (at node outlet), °C
TUBERR(K)	Symbol R in Appendix VII of the Users Guide
TUBESS(K)	Symbol S in Appendix VII of the Users Guide
TUBERA(K)	Inner radius of fuel tube K, m
TUBERB(K)	Inner radius of fuel meat in tube K, m
TUBERC(K)	Outer radius of fuel meat in tube K, m
TUBERD(K)	Outer radius of fuel tube K, m
TUBEBC(K)	Symbol B in Appendix VII of the Users Guide
VVW(K)	Volume of coolant in axial node N of coolant channel K
WWC(K)	Coolant flow rate in channel K, kg/s
XMAX(K)	Radial position (meter) of fuel maximum temperature, measured from the fuel meat's inner surface.

Temperature arrays used in heat transfer subroutine SLICHTR5 for 5-layer fuel plates:

AA(K), BB(K), CC(K), DD(K)	Coefficients in the linear simultaneous algebraic equations (shown below) for node-center coolant bulk temperatures TBCX_S(K,LS) of <i>all channels</i> in the axial slice currently being computed, for a stripe LS of a fuel assembly: $AA(K)*TBCX_S(K-1,LS) + BB(K)*TBCX_S(K,LS) + CC(K)*TBCX_S(K+1,LS) = DD(K)$
ALFA(K,LS)	Symbol ALFA in Appendix XIII of the Users Guide, for stripe LS in channel K
FUELX_S(K,LS)	Areal fraction in the meat thickness at the meat's maximum temperature
HFLUXR_S(K,LS)	Symbol q1" in Appendix XIII of the Users Guide, for stripe LS in channel K
HFLUXL_S(K,LS)	Symbol q2" in Appendix XIII of the Users Guide, for stripe LS in channel K
QQ(K,LS)	Symbol Q in Appendix XIII of the Users Guide, for stripe LS in channel K
TBCX_S(K,LS)	Node-center coolant bulk temperature in the axial slice currently being computed, for stripe LS in channel K (without any effect of mixing), °C
TTB1_S(K,LS)	Node-exit-boundary coolant bulk temp. in the axial slice currently being computed, for stripe LS in channel K (without any effect of mixing), °C
TBCX_P(K,LS)	Node-center coolant bulk temperature in the axial slice currently being computed, for stripe LS in channel K, found by partially mixing TBCX_S(K,LS), °C
TCRUDL_S(K,LS)	Inner cladding (inside on the crud) surface temperature, °C
TCRUDR_S(K,LS)	Outer cladding (outside on the crud) surface temperature, °C
TFUEL_S(K,LS)	Fuel maximum temperature in meat thickness by fuel tube, °C
TTB1_P(K,LS)	Node-exit-boundary coolant bulk temperature in the axial slice currently being computed, for stripe LS in channel K, found by partially mixing TTB1_S(K,LS), °C
TBCX_M(K)	Mixed mean node-center coolant bulk temperature in channel K of the axial slice currently being computed, found by averaging TBCX_S(K,LS) over all stripes, °C

TTB1_M(K)	Mixed mean node-exit-boundary coolant bulk temp. in channel K of the axial slice currently being computed, found by averaging TTB1_S(K,LS) over all stripes, °C
TUBERR(K,LS)	Symbol R in Appendix XIII of the Users Guide, for stripe LS in channel K
TUBESS(K,LS)	Symbol S in Appendix XIII of the Users Guide, for stripe LS in channel K
TUBEBS(K,LS)	Symbol B in Appendix XIII of the Users Guide, for stripe LS in channel K
XMAX_S(K,LS)	Radial position (meter) of fuel maximum temperature, measured from the fuel meat's inner surface

Note: The meanings of FORTRAN variables for temperatures and heat fluxes at 10 interfaces across a fuel plate thickness are given in the subroutine SLICHTR5, beginning at line number 778. Look for the string “Explanation of Heat Flux & Temp Symbols like YYC1A, ZZC1E”.

APPENDIX I. PLTEMP/ANL V4.2 INPUT DESCRIPTION

Definition of Terms Used in Code Output and FORTRAN Source:

- Fuel plate A single plate (flat or curved, or a tube) having three layers in its thickness, where the middle layer is fuel meat and the outer two layers are cladding.
- Fuel element A bundle of several fuel plates fastened mechanically together, that is loaded into the reactor as a unit. It is called assembly or subassembly at ANL.

Ease of use and intelligibility are enhanced by two new features: the use of comment cards, and multiple-case capability. The user may intersperse any number of additional comment records (a line beginning with ‘!’ in column 1) anywhere in the input file. These comments will be skipped automatically. Input for multiple cases can now be stacked sequentially. Additional comments can be added to most input records in columns beyond 80, since those columns have no effect on input data processing. The exception is card type 0310, which is list-directed input.

“Tab” keys should never be used anywhere in the input file. Use “space” instead. Each input card type is followed by an integer within parentheses and a four-digit card type. The integer within the parentheses is the number of input cards required of this type.

Card (1) 0100..... Problem title

ANAME

Format (20A4)

ANAME Alphanumeric descriptive title of the problem or the case

Card (1) 0200..... Major code options

IH, IB, ICHF, NFTYP, NCTYP, NEDIT, NAXDIS, IFLOW, IGOM, ICP, IFLUID, IEND, IPARET, IBROYDN, IHCF, KPRINT, ISRCH, KSOLNPR

Format (20I4)

1. IH Single phase heat transfer correlation selector
- = -1 Carnavos correlation for channels having longitudinal internal fins. The fins are assumed to be in the heated length only (axial region 2). Fin geometry data are required on Card 0202. See Appendix IX.
 - = 0 Sieder-Tate. See Appendix IV for the temperature at which coolant properties are evaluated.
$$\text{Nu} = 0.027 \text{Re}^{0.8} \text{Pr}^{1/3} [\mu/\mu_w]^{0.14}$$

= 1 Dittus-Boelter, good for small ($T_{wall}-T_{bulk}$). Instead use option 9 for large ($T_{wall}-T_{bulk}$) at high heat flux.

$$Nu = 0.023 Re^{0.8} Pr^{0.4}$$

= 2 Colburn

$$Nu = 0.023 Re^{0.8} Pr^{0.3}$$

= 3 Petukhov & Popov

The Darcy friction factor f_D is approximated as

$$f_D = [1.0875 - 0.1125 (4A/P^2)]/[1.82 \log_{10} Re_b - 1.64]^2$$

then the forced-convection heat transfer coefficient is:

$$Nu = (f_D/8)Re_b Pr_b (\mu_b/\mu_w)^{0.11} / [(1+3.4 f_D)+(11.7 + 1.8/Pr_b^{1/3})(f_D/8)^{1/2} (Pr_b^{2/3}-1.0)]$$

= 4 Russian

$$Nu = 0.021 Re^{0.8} Pr^{0.43} [Pr/Pr_w]^{0.25}$$

= 5 Natural circulation, using Nu for fully developed laminar flow in rectangular ducts without entrance effects, Nu_{FD}

= 51 Natural circulation, using mixed convection Nusselt number from [Collier and Thome, "Convective Boiling and Condensation", p. 185 (1994)]. *Here the buoyancy assists the static head-driven flow.* The minimum laminar Nu is **CL1**. The values of parameters are: CL1 = 4.0, CL2 = 0.17, CL3 = 0.33, CL4 = 0.43, CL5 = 0.25, CL6 = 0.1, RE1 = 2000, RE2 = 2500. These values may be modified by setting MORE=2 and supplying the input Card 0200B.

$$Nu = \begin{cases} Nu_L \equiv \max \left[CL1, CL2 * Re_b^{CL3} Pr_b^{CL4} \left(\frac{Pr_b}{Pr_w} \right)^{CL5} \left(\frac{g \beta \rho^2 D_e^3 (T_w - T_b)}{\mu^2} \right)^{CL6} \right] & \text{if } Re < RE1 \\ Nu_T \equiv 0.023 Re_b^{0.8} Pr_b^{0.4} & \text{if } Re \geq RE2 \\ Nu_L + \frac{(Re - RE1)}{(RE2 - RE1)} \{Nu_T(RE2) - Nu_L(RE1)\} & \text{if } RE1 \leq Re < RE2 \end{cases}$$

= 52 Same as option IH = 51, except that the minimum laminar Nu is Nu_{FD} used in option IH = 5.

= 53 Natural circulation, using Churchill-Chu Nu Correlation Nusselt number

$$\overline{Nu}_L \equiv \frac{\bar{h} L}{k} = \left[0.825 + \frac{0.387 Ra^{1/6}}{\{1 + (0.492/Pr)^{9/16}\}^{8/27}} \right]^2$$

It should not be used if the boundary layers on the pair of fuel plates making the coolant channel interfere with each other.

- = 54 Natural circulation, using the China Institute of Atomic Energy (CIAE) correlation for natural convection heat transfer, based on measurements in the Miniature Neutron Source Reactor (MNSR).
- = 6 Natural circulation, using Nu for developing laminar flow in rectangular ducts with entrance effects (**Not Yet Modeled**); Option IH = 6 is currently the same as option IH = 5.
- = 7 Celata correlation [1998] for *mixed* turbulent convection to account for buoyancy. See Appendix IV for the correlation.
- = 8 Sleicher-Rouse correlation [1975]. It accounts for temperature-dependence of coolant properties, important at high heat flux.

$$\text{Nu}_{\text{bulk}} = 5 + 0.015 (\text{Re}_{\text{film}})^a (\text{Pr}_{\text{wall}})^b$$

$$a = 0.88 - 0.24 / (4 + \text{Pr}_{\text{wall}}), \quad b = 1/3 + 0.5 \exp(-0.6 \text{Pr}_{\text{wall}})$$

- = 9 Dittus-Boelter correlation improved to account for temperature-dependence of coolant properties, important at high heat flux.

$$\text{Nu} = 0.023 \text{Re}^{0.8} \text{Pr}^{0.4} [\mu/\mu_w]^{0.11}$$

- = 10 Gnielinski correlation for Nusselt number at axial position z from the beginning of heated length⁴⁸.

(Not Yet Implemented)

$$\text{Nu}(z) = \frac{(f_D/8) (\text{Re} - 1000) \text{Pr}}{1 + 12.7(f_D/8)^{0.5} (\text{Pr}^{2/3} - 1)} \left[1 + \frac{(D_h/z)^{2/3}}{3} \right] \left(\frac{\text{Pr}}{\text{Pr}_w} \right)^{0.11}$$

where f_D is Darcy friction factor. The following average

$$\text{Nusselt number } \overline{\text{Nu}}(L) = \frac{1}{L} \int_0^L \text{Nu}(z) dz \text{ over any length } L$$

is obtained by integrating the above correlation.

$$\overline{\text{Nu}}(L) = \frac{(f_D/8) (\text{Re} - 1000) \text{Pr}}{1 + 12.7(f_D/8)^{0.5} (\text{Pr}^{2/3} - 1)} \left[1 + \left(\frac{D_h}{L} \right)^{2/3} \right] \left(\frac{\text{Pr}}{\text{Pr}_w} \right)^{0.11}$$

Note: Options 1 to 4 and 7 to 9 apply to forced flow. Options 5 and 6 apply to natural circulation flow. In options 1 to 4, the code computes the turbulent heat transfer coefficient h_{turb} and the laminar heat transfer coefficient h_{lam} as well, and uses $\text{MAX}[h_{\text{lam}}, h_{\text{turb}}]$. In options 5 and 6, the code allows for the laminar, transition, and turbulent friction factors.

The subscript “w” refers to fluid film at the wall temperature; subscript “b” refers to bulk fluid; k is thermal conductivity; h is heat transfer coefficient; D_e is equivalent diameter, $4A/P$ where A is flow area and P is wetted perimeter; Re is Reynolds number; Pr is Prandtl number.

2. IB Boiling correlation selector (used for ONB thermal margin)

- = 0 Bergles-Rohsenow
- = 1 Forster-Greif
- = 2 Russian Modified Forster-Greif

3. ICHF

CHF correlation selector used for calculating CHF. Kolev³⁹ has reported that there are more than 500 empirical correlations for CHF in forced convection in heated tubes and channels, demonstrating that the final understanding of this phenomenon is not yet reached. The code has only some of the correlations that are successful in limited ranges of thermal-hydraulic variables given in Appendix IV. The selected CHF correlation should be valid for four thermal-hydraulic variables: (1) Geometry (channel thickness), (2) Pressure, (3) Mass velocity, and (4) Exit subcooling (or exit quality). At coolant velocities less than ~1 m/s, other variables such as the flow direction and one-sided/two-sided heating may also be important in selecting the CHF correlation. See also option ITRNCHF for CHF calculating method.

- = 0 Mirshak-Durant-Towell
- = 1 Bernath
- = 2 Labuntsov
- = 3 Mishima *lower bound*, for mass velocities from 350 kg/m²-s downward to 350 kg/m²-s upward, at ~1.0 bar pressure, in a rectangular channel. In downflow, Eqs. (9), (10), and (14) of Ref. 19 are used, and in upflow Eq. (18) is used.
- = 4 Weatherhead, Eq. (9) of [Ref. 10]
- = 5 Groeneveld 2006 lookup table for CHF as a function of quality, mass flux, and pressure.
- = 6 Mishima-Mirshak-Labuntsov. Use Mishima's fits to his *CHF test* data¹⁹ for mass velocity $G < 600$ kg/m²-s, and use the smaller of the Mirshak¹⁶ and the Labuntsov¹⁸ correlations for $G > 1500$ kg/m²-s. For the intermediate range $600 < G < 1500$ kg/m²-s, interpolate between Mishima's fit at $G=600$ kg/m²-s and the smaller of the Mirshak and the Labuntsov correlations at $G = 1500$ kg/m²-s.
- = 7 M. M. Shah, Eq. (8.41) of J. G. Collier and J. R. Thome, "Convective Boiling and Condensation," Clarendon Press, Oxford (1994). H. C. Kim⁴⁰ has shown that Shah correlation reasonably predicts CHF at low pressure and low flow.
- = 8 Sudo-Kaminaga 1998 correlation³⁷, for rectangular channels, the thickness must be between 2.25 and 5.0 mm.
- = 9 Extended Groeneveld 2006 lookup table recommended after a review of post-1993 CHF literature⁴³.

= 10 Hall-Mudawar subcooled CHF inlet conditions correlation⁴⁴.

4. NFTYP Number of different *types* of fuel assemblies. In a given *type*, the fuel assemblies must have the same geometry and the same axial power distribution shape (input on cards 0700 and 0701). But the radial power peaking factors (input on Card 0309) and flow in the fuel assemblies of a given *type* may be different. The flow may be different whether the code is run in the *pressure drop driven mode*, or in the *flow driven mode*.
($0 \leq \text{NFTYP} \leq 60$).
NFTYP can be zero, in a pure hydraulic problem that is not heated.
5. NCTYP Number of different types of bypasses ($0 \leq \text{NCTYP} \leq 50$)
6. NEDIT Number of pressure drop increments between detailed edits when the code is run in the *pressure drop driven mode*. **(Disabled)**
7. NAXDIS Axial power shape indicator
- = 1 Use the same axial power shape for *every* fuel plate. Supply the axial power shape on the card series 0700.
- = 2 Use a different axial power shape for every fuel plate. Supply a file containing the axial power shapes for all longitudinal stripes of all fuel plates. The filename is the string APSHF supplied on the input Card 0702A. See the file structure in Appendix II .
8. IFLOW Flow direction indicator
- = 0 Downward
- = 1 Upward
9. IGOM Geometry indicator
- =0 Slab geometry
- =1 Radial geometry (See Section 3.11 to model solid fuel rod)
10. ICP Coolant specific heat (C_p) and density option
- =0 Temperature and pressure dependent coolant C_p and density obtained from built-in functions.
- =1 Set coolant $C_p=4,180.0$ J/kg-C and density= 1000 kg/m³
 Do not use this option with IH=5 and 6 (natural circulation).
11. IFLUID Coolant choice option

- =0 light water
- =1 heavy water

12. IEND

Number of layers in fuel plate and special end plate

- =0 Normal, i.e., the fuel plate has 3 material layers. Supply Cards 0306. The claddings on both sides of the fuel meat have equal thickness and thermal conductivity, and all fuel plates in assemblies of a fuel type have the same meat thickness, cladding thickness, and thermal conductivity.
- =1 The fuel plate has 5 material layers. (IEND=1 is not allowed in slab geometry. However, see the note below.) Supply Cards 0306A and 0306B. The claddings and gaps on both sides of the fuel meat may have different thicknesses and thermal conductivities. Also, the meat thickness, cladding thickness, and their thermal conductivities may differ from plate to plate in a fuel assembly. This option uses a new analytical heat transfer solution for five-layer fuel plates. This option is not allowed for IGOM=0.

Note: To run a slab geometry problem (IGOM = 0), run it in radial geometry using very large values for meat mid-thickness radii (i.e., using RMID on Card 0308A = ~50 meters).

- = 2 The fuel plate has 3 material layers with *different* claddings on both sides of a fuel plate, with data supplied on Cards 0306A and 0306B. The claddings of a plate have different thicknesses and thermal conductivities on both sides, and the meat thickness, cladding thickness, and their thermal conductivities may differ from plate to plate in a fuel assembly. This option uses the analytical heat transfer solution for 3-layer fuel plates. **(Not Yet Implemented)**

Heat Transfer Option	Single Axial Power Shape NAXDIS=1	Axial Power Shapes by Stripe NAXDIS=2
IEND = 0	Analytical Solution for Assembly Having 3-Layer Fuel Plates, using Plate Geometry Input on Cards 306	Not Allowed
IEND = 1	Not Allowed	Analytical Solution for Assembly Having 5-Layer Fuel Tubes
IEND = 2	Not Allowed	Analytical Solution for Assembly Having 3-Layer Plates, using Plate by Plate Axial Power Shapes & Plate Geometry Input on Cards 306A and 306B.

13. IPARET

Transient code PARET model edit option

- =0 no edit
- =1 provide PARET model detailed edit (not yet implemented in this version)

14. ITRNCHF

Iteration option in calculating CHF

- = 0 Do not iterate to make the nodal heat flux equal to the nodal CHF obtained from the correlation selected by option ICHF. It is the direct substitution method (DSM).
- = 1 Iterate to make the nodal heat flux equal to the nodal CHF obtained from the selected correlation. Currently, it is done for ICHF=0, 1, 2, 4, 5, and 7 only. Not done for ICHF=3, 6, and 8 because these correlations do not depend on coolant exit temp in some cases. It is the heat balance method (HBM).

15. IHCF

Hot channel factors treatment option

- = 1 The older method of treating hot channel factors described in Section 3.5.1 of this report. When using this option, enter the hot channel factors FB, FQ, FH and FQL on Cards 0300 and 0301.
- = 2 The method of treating hot channel factors described in Section 3.5.2 and Appendix V (**Recommended Option**). Input the system-wide hot channel factors FPOWER, FFLOW and FNUSLT on Card 0201, and input local hot channel factors FBULK, FFILM and FFLUX on Card 0300A. When using this option, the hot channel factors used in the older method (i.e., FB, FQ, FH, FQL) must be 1.0.
- = 3 Same as the above option 2 but with channel dependent input local hot channel factors FBULK, FFILM and FFLUX on **Card 0306C**. The system-wide hot channel factors FPOWER, FFLOW and FNUSLT on Card 0201 are used. When using this option, the hot channel factors used in the older method (i.e., FB, FQ, FH, FQL) must be 1.0.

Note: When using the option IHCF = 2, both global and local hot channel factors (FPOWER, FFLOW, and FNUSLT on input Card 0201, and FBULK, FFILM, and FFLUX on input Card 0300A) are used in calculation of Onset of Nucleate Boiling Ratio (ONBR), Departure from Nucleate Boiling Ratio (DNBR), the maximum cladding surface temperature, and the maximum coolant temperature. Only one line of HISTORY DATA is printed at the end of the output file on unit 6 if the option IHCF is 1. However, two lines of HISTORY DATA are printed when using the option IHCF = 2: the first line shows results without incorporating any hot channel factor, and the second line shows results with all six hot channel factors applied.

16. KPRINT

Printed output controlling option

- = 0 Print usually needed output, i.e., print input data and calculated coolant, cladding and fuel temperatures, heat fluxes, coolant flow rates, ONB ratio, CHF ratio, flow instability ratio, warnings for out-of-range usage of CHF correlations, etc.

- = 1 In addition to the above, print input data as it is read card by card, the Groeneveld CHF Table and correction multipliers used in CHF calculation, print power density in coolant by stripe and channel calculated in the 5-layer heat transfer subroutine, tabulate coolant properties, Reynolds number, and Prandtl number.
- = 2 In addition to the output obtained in option 1, some variables useful to code developers are edited, e.g., exact solution debugging output, Churchill-Chu correlation debugging output.

17. ISRCH Option to vary an input datum to search and get a desired value of of an output quantity (e.g., to vary the applied pressure drop to get a given reactor coolant flow rate)
- = 0 No search
 - = 1 Perform search. The search type and the search parameters are entered on cards 0203 and 0204.
18. KSOLNPR Flag to specify the solution to be printed (Exact or Broyden)
- = 0 Print only the exact solution.
 - ≥ 1 Print only Broyden solution making KSOLNPR Broyden iterations. Not allowed in option IEND=1, i.e., with the exact solution for 5-layer fuel plates.
19. NATDBG Debug print option for natural circulation/forced flow calculation
- = 0, No such debug printing
 - = 1, Print hydraulics data (coolant temp, pressure, etc) only after the inner iteration has converged. Also print the thermal calculation results of each outer iteration.
 - = 2, For each inner iteration, print hydraulics data (coolant temp, pressure, etc.) *at channel exits* (not nodal data). Also print the thermal calculation results of each outer iteration.
 - = 3, For each inner iteration, print *nodal* coolant temp, pressure, friction factor, etc. for each heat transfer node during the hydraulic calculation.
 - = 4, Print the above three debug outputs, *excluding* the thermal calculation results of each outer iteration.
20. MORE
- = 0, No additional input card containing major options
 - = 1, Input major data on 1 additional card, Card 0200A
 - = 2, Input major data on 2 additional cards, Card 0200A and Card 0200B

Card (1) 0200A ... Major code options, Continued. Required only if MORE ≥ 1

Format (2I4)

1. ICHIMNY Option to specify the group of fuel assemblies whose exit coolants are mixed in the chimney(s). Enter chimney height on Card 0305.
 - = 1 All fuel assemblies modeled in the input data file are mixed in a single chimney. It is assumed that the reactor design has a *single chimney* for all fuel assemblies modeled.
 - = 2 Fuel assemblies of a fuel type I are mixed in a chimney. It is assumed that the reactor design has a separate chimney for each fuel assembly type I. (**Not yet modeled**)

2. ICOLL = 0 Use the standard values of parameters in the Collier correlation for heat transfer coefficient, used if option IH=51 or 52.
 - = 1 Use the modified values supplied on Card 0200B for the Collier parameters.

**Card (1) 0200B ... User input values of parameters in Collier heat transfer correlation;
See option IH = 51; Required only if MORE ≥ 2**

Ref. J. G. Collier and J. R. Thome, "Convective Boiling and Condensation," Third Edition, p. 185, Clarendon Press, Oxford (1994).

CL1, CL2, CL3, CL4, CL5, CL6, RE1, RE2 as defined in Appendix IV

Format (8F9.3)

- | | |
|-----|--|
| CL1 | Parameter CL1 in the Collier correlation. |
| CL2 | Parameter CL2 in the Collier correlation. |
| CL3 | Parameter CL2 in the Collier correlation. |
| CL4 | Parameter CL3 in the Collier correlation. |
| CL5 | Parameter CL4 in the Collier correlation. |
| CL6 | Parameter CL5 in the Collier correlation. |
| RE1 | Parameter RE1 in the Collier correlation (default = 2000). |
| RE2 | Parameter Re2 in the Collier correlation (default = 2500). |

Card (1) 0201 System-wide hot channel factors used in option IHCF = 2
(Do not input this card if IHCF =1)
 FPOWER, FFLOW, FNUSLT

Format (3E12.5)

- FPOWER A factor to account for uncertainty in total reactor power. It equals 1.0 + (the tolerance fraction for power measurement). For example, see column 6 of Table V-1 in Appendix V.
- FFLOW A factor to account for uncertainty in total reactor flow. It equals 1.0 + (the tolerance fraction for flow measurement). For example, see column 6 of Table V-1 in Appendix V.
- FNUSLT A factor to account for uncertainty in Nu number correlation. It equals 1.0 + (the tolerance fraction for heat transfer coefficient). For example, see column 6 of Table V-1 in Appendix V.

Card (1) 0202 Fin Geometry Data, Required Only if IH = -1
 The fins are assumed over only the heated length (axial region 2).
 EFIN, BFIN, TFIN, AHELIX, NFIN

Format (4E12.5, I4)

- EFIN Fin height (see Fig. 1 in Appendix IX), m
- BFIN Fin thickness at the bottom, m
- TFIN Fin thickness at the tip, m
- AHELIX Helix angle (angle between the fin's longitudinal axis and the channel axis), degrees
- NFIN Number of fins in each coolant channel of fuel assembly

Card (1) 0203 Search Data, Required Only if ISRCH = 1
 NSRCH, XLOW, XHIGH, NTARGET, (YTARGET(NT),NT=1,NTARGET)

Format (I4, 2E12.5, I4, 4E12.5, /, (6E12.5))

- NSRCH Search type to be done. See Types and List of Searches noted below Card 0204.
- XLOW Lowest value of the code input datum varied in the search.

See the list of Code Input and Output Data given below Card 0204.

XHIGH	Highest value of the code input datum varied in the search
NTARGET	Number of desired or target values (≤ 20)
YTARGET	Target values of the output quantity to be achieved by search Note that when the search capability is used with the hot channel factors option IHCF = 2, the input target values are the values (of output quantity) with all six hot channel factors applied.

Note 1: Do not use any other multiple run option of the code with the search capability of the input Card 0203 or 0204. For example, do not stack multiple problems in a single input file; do not run the code for multiple values of driving pressure drop using the values of DDP and DPMAX on input Card 0500. On Card 0600, set DPWR = 0.0 to avoid the power search.

Note 2: During the search, several input data files are written with a modification, using the format 1PE12.5 for floating point input data, thus rounding the user-supplied data to six significant digits in the modified input data files.

**Card (1) 0204 Double Search Data, Required Only if ISRCH = 1, and NSRCH \geq 21
(Skip this card if NSRCH \leq 20)**

XLOW2, XHIGH2, NTARGET2, (YTARGET2(NT2),NT2=1,NTARGET2)

Format (2E12.5, I4, 4E12.5, /, (6E12.5))

XLOW2	Lowest value of the second input datum varied in the double search
XHIGH2	Highest value of the second input datum varied in the double search
NTARGET2	Number of target values of the second output quantity (≤ 20) For example, in search type 21, set NTARGET2 equal to one if only one value of ONBR _{min} (say, 1.0) is desired for all searches in this run (i.e., for all values of total flow rate on Card 0203).
YTARGET2	Target value of the second output quantity to be achieved by search. Note that when the search capability is used with the hot channel factors option IHCF = 2, the input target values are the values (of output quantity) with all six hot channel factors applied.

Types of Searches:

A search is called *single*, when a single specified input to the code is varied to achieve a desired value of a specific computed quantity.

A search is called *double*, when an input is varied to achieve a desired value of a computed quantity, and having achieved that, another specified input is varied to achieve a desired value of a second user-specified computed quantity.

List of Searches:

NSRCH, Search Type	Input Datum Being Adjusted	Output Quantity Whose Target Value is Searched	Comments
<i>Single Searches</i>			
1	Pressure Drop, MPa	Total flow through all fuel assemblies, kg/s, WT	
2	Pressure Drop, MPa	Onset of nucleate boiling ratio, $ONBR_{min}$	Desired $ONBR_{min} \geq 1$
3	Pressure Drop, MPa	Minimum ratio of critical heat flux to reactor heat flux, $DNBR_{min}$	Desired $DNBR_{min} \geq 1$
4	Reactor Power, MW	$ONBR_{min}$	
5	Reactor Power, MW	$DNBR_{min}$	
6	Pressure Drop, MPa	Minimum flow instability power ratio FIR_{min}	Desired $FIR_{min} \geq 1.15$
7	Reactor Power, MW	Minimum flow instability power ratio FIR_{min}	
8	Pressure Drop, MPa	Maximum cladding surface temperature $T_{cs,max}$, °C	
9	Pressure Drop, MPa	Maximum coolant temperature $T_{ex,max}$, °C	
10	Reactor Power, MW	$T_{cs,max}$, °C	
11	Reactor Power, MW	$T_{ex,max}$, °C	
12	Reactor Power, MW	Maximum cladding surface heat flux, MW/m^2	
<i>Double Searches</i>			
21	First Pressure Drop, Then Reactor Power	Total flow WT $ONBR_{min}$	Multiple values of each target may be input in a run.
22	First Pressure Drop, Then Reactor Power	Total flow WT $DNBR_{min}$	
23	First Pressure Drop, Then Reactor Power	Total flow WT FIR_{min}	
24	First Pressure Drop, Then Reactor Power	Total flow WT Maximum cladding surface temperature $T_{cs,max}$	

25	First Pressure Drop, Then Reactor Power	Total flow WT Maximum coolant temperature $T_{ex,max}$
26	First Pressure Drop, Then Reactor Power	Total flow WT Maximum fuel meat temperature $T_{f,max}$

Repeat Cards 0300-0310 NFTYP times (once for each type of fuel assembly).

Card (1) 0300..... Data for Type I fuel assemblies

NELF(I), NF(I), WFGES(I), FB(I), FQ(I), FH(I), IBC(I), IBCA(I), HBC(I),
IBERN(I)

Format (2I4, 4E12.5, 2I4,E12.5,I4)

NELF(I) Number of fuel assemblies of Type I. Each individual assembly *within a type* is identified by an index running from 1 through NELF(I) in the input preparation that follows. (60 max.)

NF(I) Number of axial regions used in coolant flow calculation in fuel assemblies of Type I (10 max.). The flow calculation uses only one region in the unheated inlet section of the assembly, only one region in the heated length of fuel plates, and one or more regions in the unheated outlet section of the assembly.

It is noted that, for the fuel-to-coolant heat transfer calculation, axial region 2 (i.e., the region consisting of multiple fuel plates and coolant channels) is subdivided into NN-1 axial nodes or mesh intervals (keeping unchanged the number of axial regions in the inlet and outlet sections of the assembly). NN is input on card 0700.

In flow calculations, the coolant flowing in axial region 1 is assumed to be at the input inlet temperature, and the coolant flowing in axial regions 3 through NF(I) is at the mixed mean temperature. In axial region 2, the flow rate in each channel is calculated using its axial temperature profile.

WFGES(I) Flow rate guess in an assembly of Type I (kg/s).

If the input WFGES(I) > 0.0, then the code is run in the *pressure drop driven mode* for assemblies of Type I; the pressure drop data on Card 0500 are required, and card 0310 data must not be supplied.

Put in WFGES(I) > 0.0 for a natural circulation problem also.

The code has been tested to work even if the input flow rate guess is 10^{12} times too low or too high.

If the input WFGES(I) = 0.0, then the code is run in the *flow driven mode* for assemblies of Type I; fixed flow rates must be directly input on Card 0310. The inlet and outlet pressures on Card 0500 are still required for use in calculating safety margins like ONB ratio, DNB ratio, etc.

- FB(I) Hot channel factor for the global bulk coolant temperature rise, used in treatment option IHCP = 1. (≥ 1.0). It must be 1.0 if the input option IHCF is 2.
- FQ(I) Hot channel factor for heat flux (Total if FQL is combined statistically; otherwise global), used in treatment option IHCP = 1. (≥ 1.0). It must be 1.0 if the input option IHCF is 2.
- FH(I) Hot channel factor for heat transfer coefficient, used in treatment option IHCP = 1. (≥ 1.0). It must be 1.0 if input option IHCF is 2.
- IBC(I) 0, normal two-sided heating of all channels.
The flag IBC(I) ≥ 1 is used to imply that the first and last channels have 1-sided heating thus reducing the laminar Nusselt number from 7.63 to 4.86.
1, channel 1 has 1-sided heating.
2, channel NCHNF(I) (last channel) has 1-sided heating
3, channel 1 and channel NCHNF(I) have 1-sided heating
- IBCA(I) Flag to set the heat transfer coefficient to a user-input low value on the left surface of the first fuel plate and right surface of the last plate to model adiabatic boundary conditions.
0, normal use of the code computed heat transfer coefficients.
1, use a user-input heat transfer coefficient only on the left surface of the first fuel plate.
2, use a user-input heat transfer coefficient only on the right surface of the last fuel plate.
3, use a user-input heat transfer coefficient on both the left surface of the first fuel plate and the right surface of the last fuel plate.
- HBC(I) The heat transfer coefficient to use if IBCA(I) ≥ 1 . ($\text{W/m}^2\text{-C}$)
(Suggested value: $1.0 \text{ W/m}^2\text{-C}$)
- IBERN(I) It is used in calculating $D/(D + \xi/\pi)$ in Bernath CHF correlation.
0, normal. In calculating $D/(D + \xi/\pi)$, the input value of XIF on Card 0307 is used for ξ for all coolant channels.

- 1, only half of the *first* channel thickness is modeled. In calculating $D/(D + \xi/\pi)$, ξ equals two times the input value of XIF on Card 0307 for the *first* channel.
- 2, only half of the *last* channel thickness is modeled. In calculating $D/(D + \xi/\pi)$, ξ equals two times the input value of XIF on Card 0307 for the *last* channel.
- 3, only half of the *first and last* channel thicknesses are modeled. In calculating $D/(D + \xi/\pi)$, ξ equals two times the input value of XIF on Card 0307 for the *first and last* channels.

Card (1) 0300A Local hot channel factors used in option IHCF = 2

(Skip this card if IHCF is not 2)

FBULK(I), FFILM(I), FFLUX(I)

Format (3E12.5)

- FBULK(I) Hot channel factor for bulk coolant temperature rise, used only in option IHCF = 2. For an explanation, see F_{bulk} in Appendix V.
- FFILM(I) Hot channel factor for temperature rise across the coolant film, used only in option IHCF = 2. For an explanation, see F_{film} in Appendix V.
- FFLUX(I) Hot channel factor for heat flux from cladding surface, used only in option IHCF = 2. For an explanation, see F_q in Appendix V.

Card (1) 0301.....Local heat flux hot channel factor and the axial nodes it applies to.

Not required if option IHCF \neq 1 (but may be present)

IQNODS(I), IQNODF(I), FQL(I)

Format (2I4, E12.5)

- IQNODS(I) Starting axial node for local heat flux hot channel factor ($1 \leq \text{IQNODS}(I) \leq |\text{NN}|$); $|\text{NN}|$ is the number of heat-transfer-node interfaces (number of axial heat transfer nodes = $|\text{NN}| - 1$) over the heated length of fuel plates. NN is input on Card 0700. Set it to 1 if the input option IHCF is 2.
- IQNODF(I) Finishing axial node for local heat flux hot channel factor ($1 \leq \text{IQNODF}(I) \leq |\text{NN}|$). Set it to 1 if the input option IHCF is 2.

FQL(I) Local heat flux hot channel factor. If the value is not 1.0, then the combined heat flux hot channel factor is $1 + \{(FQ-1)^2 + (FQL-1)^2\}^{1/2}$ where FQ is *global* heat flux hot channel factor input on Card 0300, and FQL is this *local* heat flux hot channel factor. It is used in treatment option IHCF = 1. (FQL(I) \geq 1.0). It must be 1.0 if the input option IHCF is 2.

**Card (1) 0302..... The assembly and channel to which the hot channel factors apply.
Not required if option IHCF \neq 1 is used (but may be present)
IELFHF(I), ICHNHF(I), IPLTHF(I)**

Format (3I4)

IELFHF(I) The fuel assembly of Type I to which the hot channel factors apply.
($1 \leq$ IELFHF(I) \leq NELF(I))

ICHNHF(I) Coolant channel to which the hot channel factors apply
($1 \leq$ ICHNHF(I) \leq NCHNF(I))

IPLTHF(I) Fuel plate to which the hot channel factors apply.
The side of the fuel plate chosen is assumed to correspond to the coolant channel selection.
($1 \leq$ IPLTHF(I) \leq NCHNF(I) -1)

**Card (N1) 0303..... Axial power peaking factor by assembly
(FZ(I,J), J=1, NELFI)**

Format (6E12.5)

NELFI = NELF(I) = Number of assemblies of Type I.
N1 = Minimum integer larger than or equal to NELFI/6

FZ(I,J) Axial power peaking factor for the J-th assembly of Type I.
This data must be consistent with the axial power shape input on card 0701. Since a single axial power shape is currently input for all assemblies of Type I, the value of FZ(I,J) does not change with the assembly index J. Therefore, the same value is repeated NELFI times on this card type.
Find the axial peak-to-average power density ratio in each fuel plate of each assembly of Type I. Identify the assembly and the fuel plate giving the maximum ratio. Enter the maximum ratio on this

card, and input the axial power shape of the identified fuel plate on card 0701.

If FZ is not correct, a warning is printed that the peak heat flux edit can be off.

Card (NFI) 0304.....Fuel assembly geometry (one card for each axial region of fuel assembly)

(AF(I,J), DF(I,J), LF(I,J), ZF(I,J), WIDTH(I,J), THICK(I,J), J=1, NFI)

Here, J is axial region index (not an index for assemblies of Type I)

Format (6E12.5)

NFI = NF(I) = Number of axial regions (input on Card 0300) used in hydraulic calculation

- AF(I,J) Flow area of axial region J in an assembly of Type I (m)
Axial region 2 must be the channels between the fuel plates, and axial regions
1, 3, etc. represent entrance and exit regions.
If AF(I,2) is input as zero, then the code finds it from other input data (sum of areas of all coolant channels in an assembly).
- DF(I,J) Hydraulic diameter of axial region J in a Type I assembly (m).
DF(I,2)=0.0 may be entered and the value will be determined from AFF((I,K) and DFF(I,K) (again see Cards 0307).
- LF(I,J) Length of axial region J in a Type I assembly (m).
- ZF(I,J) Sum of entrance and exit resistance coefficients for axial region J in a Type I assembly. Also add to it other loss coefficients if present in the flow path, e.g., due to screens. The input coefficient is multiplied by an average velocity head in the axial region to calculate the minor pressure drop (that is added to the Moody pressure drop fL/D).
- WIDTH(I,J) Width of a *single channel* (along the fuel plate) in axial region J in a Type I assembly (m).
- THICK(I,J) Thickness of a *single channel* (gap between the fuel plates) in axial region J in a Type I assembly (m).

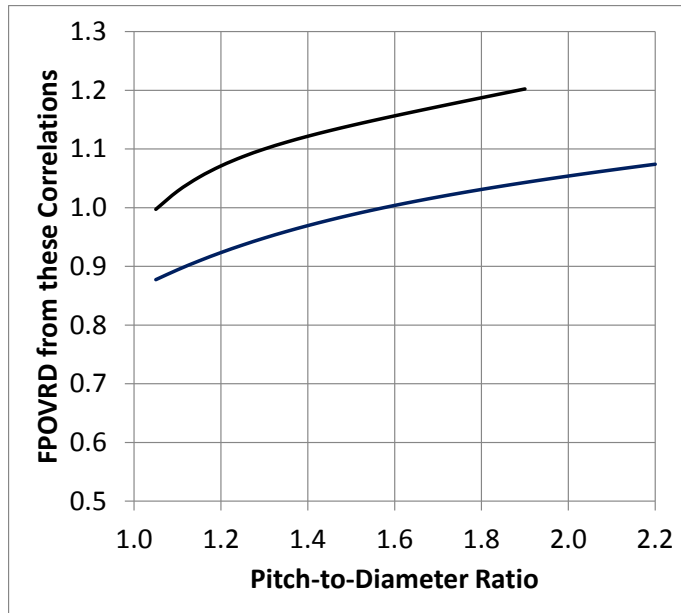
Note: WIDTH and THICK are required if IH is -1, 5, or 6 (the channel has fins, or natural

circulation flow), or the critical heat flux option ICHF = 6, 8.

Card (1) 0305..... Coolant flow friction factor equation, for the assembly Type I
FCOEF(I), FEXPF(I), ROUGH(I), CHIMNY(I), POVERD(I)

Format (5E12.5)

- FCOEF(I) The coefficient in the following equation for Darcy-Weisbach friction factor used in an assembly of Type I
- FEXPF(I) The exponent in the equation for Darcy-Weisbach friction factor used in an assembly of Type I , where
Darcy-Weisbach friction factor $f = \text{FCOEF(I)} \cdot \text{RE}^{(-\text{FEXPF(I)})}$
If *both* FCOEF(I) and FEXPF(I) are 0.0 for a given fuel assembly Type I, the code will default to friction factors appropriate for smooth thin channels, or rough channels of input relative roughness ROUGH(I), as described in Section 3.8 of this Users Guide.
- ROUGH(I) Relative surface roughness, e/D_e , where e is the roughness height and D_e is the equivalent diameter. ($0 \leq \text{ROUGH(I)} \leq 0.1$)
Note that it is used in calculating the friction factor, but not in calculating the film coefficient.
- CHIMNY(I) Chimney height (m), used only in natural circulation calculation, i.e., only if IH = 5, 51, 52, 53, or 6. Use the option ICHIMNY on Card 0200A to specify the group of fuel assemblies whose exit coolants are mixed in the chimney(s).
- FPOVRD(I) A multiplier for turbulent forced convection heat transfer coefficient. This multiplier is used in IGOM=1 only. The multiplier is limited to the range $0.0 < \text{FPOVRD} < 1.6$. If not supplied, it defaults to 1.0 . It can be used to account for the ratio of heat transfer coefficient in a vertical rod bundle in parallel flow to that in a circular tube of equal hydraulic diameter. This multiplier depends on the pitch-to-diameter ratio P/D of the pin array. N. E. Todreas and M. S. Kazimi⁴⁵ provide the following correlations for this multiplier. These correlations are also recommended in the Handbook of Single-Phase Convective Heat Transfer⁴⁶.



$$FPOVRD = 0.9090 + 0.0783 \left(\frac{P}{D} \right) - 0.1283 \exp \left\{ -2.4 \left(\frac{P}{D} - 1 \right) \right\}$$

for infinite triangular array and $1.05 \leq P/D \leq 2.2$

$$FPOVRD = 0.9217 + 0.1478 \left(\frac{P}{D} \right) - 0.1130 \exp \left\{ -7.0 \left(\frac{P}{D} - 1 \right) \right\}$$

for infinite square array and $1.05 \leq P/D \leq 1.9$

Card (1) 0306.....Fuel plate geometry and material properties for assembly Type I

Required if IEND = 0 or 2. Do not put in if IEND = 1.

Fuel plate width or arc length is input not here but on Card 0308.

NCHNF(I), IDC(I), UNFUEL(I), L(I), CLAD(I), TCCLAD(I),

TAEM(I), TCFUEL(I)

Format (2I4, 6E12.5)

NCHNF(I) Number of coolant channels adjacent to the fuel plates in an assembly of Type I. It is one plus number of plates. (50 max).

IDC(I) Clad material indicator (used only if the cladding thermal conductivity TCCLAD input on this card = 0.0)

<u>Indicator</u>	<u>Thermal Conductivity</u>
= 1 ALMG1 (NUKEM)	200 (W/mK)
= 2 ALMG2 (NUKEM)	186 (W/mK)
= 3 6061 (USA)	180 (W/mK)

= 4 AG2NE (CERCA)	162 (W/mK)
= 5 AG3NE (CERCA)	130 (W/mK)
= 6 AG5NE (CERCA)	120 (W/mK)
= 7 Cladding on Grenoble Fuel	146 (W/mK)
= 8 Cladding on Russian Fuel	175 (W/mK)

UNFUEL(I)	Width of the <i>unfueled edges</i> of the fuel plates in an assembly of Type I (2 edges per plate; supply width of one edge only); (m). See Figure 1. Set to zero for uniform round tubes.
L(I)	Length of the fueled region (axial region 2 in Fig. 2) in Type I assemblies (m)
CLAD(I)	Clad thickness in a fuel plate of Type I assemblies (m)
TCCLAD(I)	Thermal conductivity of cladding in a fuel plate of Type I assemblies (W/m-K). If input as zero, then the value based on the input cladding material indicator IDC is used.
TAEM(I)	Fuel meat thickness in a plate of Type I assemblies (m)
TCFUEL(I)	Thermal conductivity of the fuel meat (W/m-K)

Card (1) 0306A... Fuel plate geometry if the claddings on the left and right sides of the plate are different, one card for assembly Type I.

Required if IEND = 1. Do not put in if IEND = 0 or 2.

In the option IEND = 1, the input data for cladding thickness and thermal conductivity on Cards 0306A and 0306B are used for the claddings on the left and right hand sides of fuel plate. The data on Card 0306 is not used.

Note 1 and Fig. 4 show how the various radii are determined in a fuel tube in the radial geometry option (IGOM = 1).

NCHNF(I), UNFUEL(I), L(I)

Format (I4, 2E12.5)

NCHNF(I)	Number of coolant channels in an assembly of Type I. It is one plus the number of fuel plates in an assembly. (50 max)
UNFUEL(I)	Width of the <i>unfueled edges</i> of the fuel plates in an assembly of Type I (2 edges per plate; supply width of one edge only); (m). See Figure 1. Set to zero for uniform round tubes.

L(I) Length of the fueled region (axial region 2 in Figure 2) in Type I assemblies (m).

Card (NPLFI) 0306B...Fuel plate geometry if the claddings on the left and right sides of the plate are different (one Card 0306B for each plate).

Required if IEND = 1. Do not put in if IEND = 0 or 2.

(IDC1(I,K), RCRUD1(I,K), CLAD1(I,K), TCCLAD1(I,K), RGAP1(I,K), GAP1(I,K), TCGAP1(I,K),

IDC2(I,K), RCRUD2(I,K), CLAD2(I,K), TCCLAD2(I,K), RGAP2(I,K), GAP2(I,K), TCGAP2(I,K),

TAEM0(I,K), TCFUEL0(I,K), K=1, NPLFI) on N1 cards

Format (I4, 6E12.5, / , I4, 6E12.5, / , 2E12.5)

NPLFI=NCHNF(I) - 1

N1 = 3*NPLFI

IDC1(I,K) Left hand side cladding material indicator in K-th fuel plate of Type I assemblies (used only if the cladding thermal conductivity TCCLAD1 input on this card = 0.0). Use the indicator values given above for Card 0306.

RCRUD1(I,K) Crud resistance (m^2-K/W) on the *left* cladding surface of K-th fuel plate of Type I.

CLAD1(I,K) Left hand side cladding thickness in K-th fuel plate of Type I assemblies (m)

TCCLAD1(I,K) Thermal conductivity of cladding in a fuel plate of Type I assemblies ($W/m-K$). If input as zero, then the value based on the input cladding material indicator IDC1 is used.

RGAP1(I,K) Gap resistance between the fuel meat and the *left* hand side cladding (m^2-K/W). It is the reciprocal of gap conductance. This thermal resistance is in addition to that due to the thermal conductivity TCGAP1(I,K) of the material in the gap that is supplied on this card below. See Fig. XIII-2 and the Note 1.

Note 1: Temp drop across inner gap

= Meat inner surface temp. - Inner cladding's outer surface temp.

= $RGAP1(I,K) * (\text{Heat flux through gap}) + TCGAP1(I,K) * (\text{Temp. gradient in gap})$

GAP1(I,K) Gap thickness between the fuel meat and the *left* hand side

cladding (m).

TCGAP1(I,K) Thermal conductivity of the gas/material between the fuel meat and the *left* hand side cladding (W/m-K).

START ANOTHER CARD.

IDC2(I,K) Right hand side cladding material indicator in K-th fuel plate of Type I assemblies (used only if the cladding thermal conductivity TCCLAD2 input on this card = 0.0). Use the indicator values given above for Card 0306

RCRUD2(I,K) Crud resistance ($\text{m}^2\text{-K/W}$) on the *right* cladding surface of K-th fuel plate of Type I.

CLAD2(I,K) Right hand side cladding thickness in K-th fuel plate of Type I assemblies (m)

TCCLAD2(I,K) Thermal conductivity of cladding in K-th fuel plate of Type I assemblies (W/m-K). If input as zero, then the value based on the input cladding material indicator IDC2 is used.

RGAP2(I,K) Gap resistance between the fuel meat and the *right* hand side cladding ($\text{m}^2\text{-K/W}$). It is the reciprocal of gap conductance. This thermal resistance is in addition to that due to the thermal conductivity TCGAP2(I,K) of the material in the gap that is supplied on this card below. See Fig. XIII-2 and the Note 2.

Note 2: Temp drop across outer gap

= Meat outer surface temp. – Outer cladding's inner surface temp.

= $\text{RGAP2(I,K)} * (\text{Heat flux through gap}) + \text{TCGAP2(I,K)} * (\text{Temp. gradient in gap})$

GAP2(I,K) Gap thickness between the fuel meat and the *right* hand side cladding (m).

TCGAP2(I,K) Thermal conductivity of the gas/material between the fuel meat and the *right* hand side cladding (W/m-K).

START ANOTHER CARD.

TAEM0(I,K) Fuel meat thickness in a plate of Type I assemblies (m)

TCFUEL0(I,K) Thermal conductivity of the fuel meat (W/m-K)

Note 1: The six radii r_a through r_f of a fuel tube (see Fig. 4 after the main text of the Users Guide) are found from the input data as follows:

$$\begin{aligned}
 r_b &= \text{RMID}(I,K) - 0.5 * \text{TAEM0}(I,K) = \text{Inner radius of the meat in the fuel tube} \\
 r_e &= \text{RMID}(I,K) - 0.5 * \text{TAEM0}(I,K) - \text{GAP1}(I,K) \\
 &= \text{Outer radius of the inner cladding of the fuel tube} \\
 r_a &= r_e - \text{CLAD1}(I,K) = \text{Inner radius of the } K^{\text{th}} \text{ fuel tube} \\
 r_c &= \text{RMID}(I,K) + 0.5 * \text{TAEM0}(I,K) = \text{Outer radius of meat in the fuel tube} \\
 r_f &= \text{RMID}(I,K) + 0.5 * \text{TAEM0}(I,K) + \text{GAP2}(I,K) \\
 &= \text{Inner radius of the outer cladding of the fuel tube} \\
 r_d &= r_f + \text{CLAD2}(I,K) = \text{Outer radius of the fuel tube}
 \end{aligned}$$

Card (1) 0306C Local hot channel factors by channel used in option IHCF = 3

One card for each channel (Skip this card if $\text{IHCF} \neq 3$)

(K, FBULK(I,K), FFILM(I,K), FFILMR(I,K), FFLUX(I,K),
K = 1, NCHNFI)

Format (I4,4E12.5)

K Coolant channel number

FBULK(I,K) Hot channel factor for bulk coolant temperature rise in **channel K**. For an explanation, see F_{bulk} in Appendix V.

FFILM(I,K) Hot channel factor for temperature rise across the coolant film on the **left side of fuel plate K**. For an explanation, see F_{film} in Appendix V. Note that fuel plate K lies between channels K and K+1.

FFILMR(I,K) Hot channel factor for temperature rise across the coolant film on the **right side of fuel plate K**. For an explanation, see F_{film} in Appendix V.

FFLUX(I,K) Hot channel factor for heat flux from cladding surface of **fuel plate K**. For an explanation, see F_q in Appendix V. Note that the last card will have datum for FBULK only.

Card (NCHNFI) 0307..... Coolant channel cross-section data for the fueled region, i.e., axial region 2 (one card for each channel)

The channels and fuel plates are numbered from left to right (the leftmost being number 1) in flat plate geometry problems ($\text{IGOM}=0$, input on Card 0200). The channels and fuel plates are numbered as described in note 2 below in radial geometry problems ($\text{IGOM}=1$). (AFF(I,K), DFF(I,K), PERF(I,K), XIF(I,K), WIDTHH(I,K),

THICKH(I,K), K=1, NCHNFI)

Format

(6E12.5)

NCHNFI=NCHNF(I)

AFF(I,K) Flow area of K-th coolant channel in an assembly of Type I (m^2). When modeling a solid fuel rod, set it to less than 10^{-15} m^2 for the innermost pinhole channel in geometry IGOM=1.

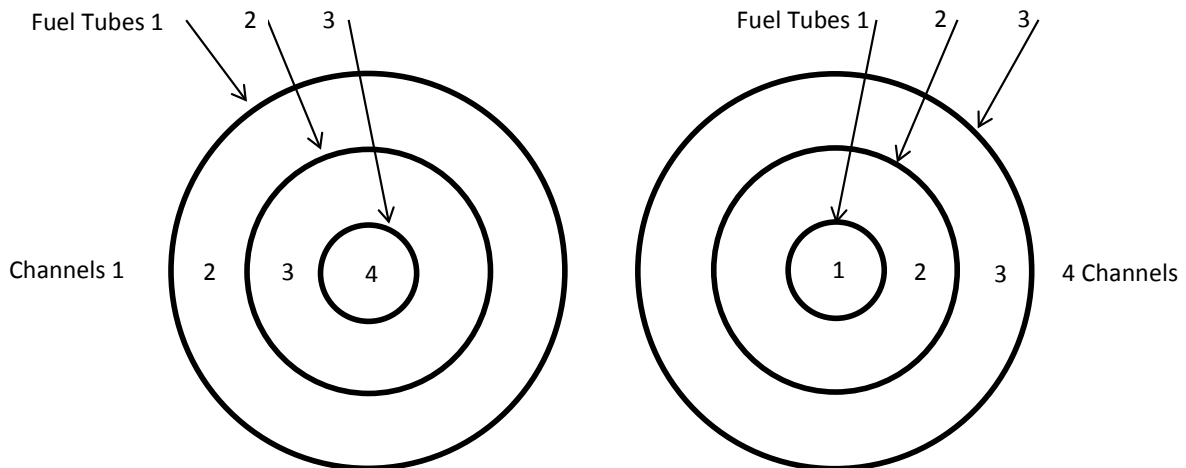
DFF(I,K) Hydraulic diameter of K-th channel in an assembly of Type I (m). If the input value is zero, DFF will be computed by the code from $4*\text{AFF}/\text{PERF}$.

PERF(I,K) Wetted perimeter of K-th channel in an assembly of Type I (m)

XIF(I,K) Heated perimeter of K-th channel in an assembly of Type I (m). If the input value is zero, the code will calculate XIF from other data.

WIDTHH(I,K) Channel width (m)

THICKH(I,K) Channel thickness. Input the full thickness for the first or last channel even if it is a half channel in the model (m)



Two Ways of Numbering the Fuel Tubes of an Assembly in Radial Geometry (IGOM = 1)

Note 1: WIDTHH and THICKH are required if IH is -1, 5, or 6 (the channel has fins, or natural circulation flow), or the critical heat flux option ICHF = 6, 8.

Note 2: In a radial geometry problem (IGOM=1 on Card 0200) using the *exact solution method* (KSOLNPR = 0 or -1), or the *Broyden solution method* (KSOLNPR ≥ 1), the radii of fuel tubes can be input in either ascending order or descending order (inside to outside, or the reverse, as shown the above figure), but must be in sequence. The numbering of fuel tubes and coolant channels is determined by the code from the user-input order of the tube radii. In the code output in radial geometry problems, the tube surfaces are identified as “inner” or “outer” instead of “left” or “right”.

Note 3: If the input value of XIF for the first or last channel is zero, then it is reset by the code as follows, using the fuel plate widths input on Card 0308:

$$XIF(I,1) = CIRCF(I,1) - 2.0 * UNFUEL(I)$$

$$XIF(I,NCHNFI) = CIRCF(I,NCHNFI) - 2.0 * UNFUEL(I)$$

If the input value of XIF(I,K) is zero for an internal channel ($K \neq 1, K \neq NCHNFI$), then it is reset as follows, and two-sided heating applies to channel K.

$$XIF(I,K) = CIRCF(I,K) + CIRCF(I,K-1) - 4.0 * UNFUEL(I)$$

Example 1: The first and last channels have adiabatic boundary, and are heated on only one side. Set XIF(I,1) and XIF(I,NCHNFI) to zero. Supply full channel areas, wetted perimeters, heated perimeters, and mass flow rates (on Card 0310) for these channels.

Example 2: The first and last channels are in a periodic lattice, with two-sided heating for all channels.

Set XIF(I,1) and XIF(I,NCHNFI) to zero. Supply half-channel areas, wetted perimeters, heated perimeters, and flow rates (Card 0310) for these channels, because of symmetry. The hydraulic diameter based on the half-channel data is the same as the full-channel hydraulic diameter.

Card (N2) 0308..... Width or arc length of each fuel plate along the mid-thickness of meat
(CIRCF(I,K), K=1, NPLFI) on N2 cards

Format (6E12.5)

NPLFI=NCHNF(I) – 1 = Number of fuel plates in an assembly of Type I

N2 = Minimum integer larger than or equal to NPLFI/6

CIRCF(I,K) Width or arc length of K-th plate in an assembly of Type I (m)

Card (N2) 0308A.....Radii of coaxial fuel tubes (Required only if IGOM=1 on Card 0200)
 (RMID(I,K), K=1, NPLFI) on N2 cards

Format (6E12.5)

NPLFI=NCHNF(I) – 1 = Number of fuel plates in an assembly of Type I

N2 = Minimum integer larger than or equal to NPLFI/6

RMID(I,K) Fuel meat centerline radius of the K-th plate in an assembly of Type I (m)

Note: If using the exact solution method for 3-layer fuel tubes (KSOLNPR = 0 or -1 and IEND = 0), or the Broyden method (KSOLNPR ≥ 1 and IEND = 0), the radii of fuel tubes can be input in either ascending order or descending order (inside to outside, or the reverse), but must be in sequence. The numbering of fuel tubes and coolant channels is determined by the code from the user-input order of the tube radii. In the code output in radial geometry problems, the tube surfaces are identified as “inner” or “outer” instead of “left” or “right”. If using the exact solution method for 5-layer fuel tubes (KSOLNPR = 0 and IEND = 1), the radii must be input in ascending order if IEND = 1.

Cards 0309 and 0310 are read in pairs, a pair for each assembly, NELF(I) pairs for all assemblies of Type I

Card (N3) 0309.....Radial power peaking factors for fuel plates in assemblies of Type I
 (FACTF(I,J,K), K=1, NPLFI) on N3 cards

Format (6E12.5)

NELFI = NELF(I) = Number of assemblies of Type I in the reactor.

N3 = Minimum integer larger than or equal to NELFI*NPLFI/6

FACTF(I,J,K) Radial power peaking factor of K-th plate in the J-th assembly of Type I, defined as the ratio of the average power density in the K-th plate to the average power density produced in the reactor core, i.e., averaged over all Types of fuel assemblies.

The code sets the power (MW) of any fuel plate (I,J,K) as follows, after reading data for all assembly types:

$$\text{Power of plate (I,J,K)} = \text{FACTF(I,J,K)} * \text{VOLFUEL(I,J,K)} * \text{POWER} / \left[\sum_I \sum_J \sum_K \text{FACTF(I,J,K)} * \text{VOLFUEL(I,J,K)} \right]$$

where POWER is the total reactor power input on card 0500, VOLFUEL(I,J,K) is the fuel volume in plate (I,J,K), and the denominator is the sum of fuel volume times the radial power peaking factors input here over all fuel plates K, all assemblies J, and all assembly Types I.

Note: If FACTF(I,J,K) = 0.0, this plate is disregarded in calculating the core average power density. If the volume-weighted average of all factors is not unity (± 0.0001), all values are normalized by dividing each factor by the volume-weighted average. Total power and relative power densities in each plate are preserved. The output file edits the "PEAK POWER DENSITY" and "VOL. AVG. RADIAL PEAKING FACTOR".

Card (NCHNFI) 0310..... Flow rates in coolant channels of assemblies of Type I

Required only if the flow rate guess WFGES(I) is 0.0 on Card 0300 (WCF(I,J,K), K=1,NCHNFI)

Format (6E12.4)
NCHNFI = NCHNF(I)

WCF(I,J,K) Input mass flow rate for the K-th coolant channel in the J-th assembly of Type I (kg/s).

Begin data for bypasses after the data for all fuel types.

Repeat Cards 0400-0402 NCTYP times (once for each type of bypass).

If NCTYP = 0, omit Cards 0400-0402.

Card (1) 0400..... Data for Type I bypass

NCRS(I), NC(I), WCGES(I)

Format (2I4, E12.5)

NCRS(I) Number of bypass channels of Type I (50 max.)

NC(I) Number of axial regions in Type I bypass (10 max.)

WCGES(I) Guess for flow rate in Type I bypass (kg/s)

Note 1: Bypass channels are assumed to be unheated. A bypass channel is therefore separated from fuel and heated coolant channels by an insulating material boundary such as a vessel wall or flow baffle.

Note 2: In natural circulation problems, bypass channels are modeled to have no upward flow because they do not produce any power. They are not connected to the chimney.

Card (NCI) 0401..... Geometry of Type I bypass, one card for each axial region J

(AC(I,J), DC(I,J), LC(I,J), ZC(I,J), WIDTHC(I,J), THICKC(I,J), J=1, NCI)

Format (6E12.5)

NCI = NC(I) = Number of axial regions in Type I bypass.

AC(I,J)	Flow area of axial region J in Type I bypass (m ²)
DC(I,J)	Hydraulic diameter of axial region J in Type I bypass (m)
LC(I,J)	Length of axial region J in Type I bypass (m)
ZC(I,J)	Sum of entrance and exit resistance coefficients of axial region J in Type I bypass
WIDTHC(I,J)	For natural circulation (IH=5 or 6; must be non-zero): the channel I width to be used for flow resistance, in axial region J
THICKC(I,J)	For natural circulation (IH=5 or 6; must be non-zero): the channel I thickness to be used for flow resistance, in axial region J

Card (1) 0402.....Friction factor in Type I bypass

FCOEC(I), FEXPC(I), ROUGHC(I)

Format (3E12.5)

FCOEC(I)	Friction factor coefficient for Type I bypass
FEXPC(I)	Friction factor exponent for Type I bypass
ROUGHC(I)	Relative surface roughness, e/D_e , where e is the roughness height and D_e is the equivalent diameter. ($0 \leq \text{ROUGH}(I) \leq 0.1$)

Card (2) 0500..... Driving pressure drop, Reactor power, Inlet temperature and pressure

DP0, DDP, DPMAX, POWER, TIN, P,
QFCLAD, QFCOOL, EPSLN, EPSLNI, XCONV, YCONV

Format (6E12.5,/,6E12.5)

DP0	If the input WFGES(I) > 0.0 on card 0300, put in the initial value of the driving pressure drop used to compute flow rates. Then the code
-----	---

runs in the *pressure drop driven mode* to find the flow rate at which the frictional pressure drop from the assembly inlet to the assembly exit equals DP0 (or a range of input values for DP0).

If it is a natural circulation problem (i.e., option IH = 5 or 6 on the input card 0200), put in 0.0 or an estimate of DP0; or

If the input WFGES(I) = 0.0, put in the pressure at the heated surface **outlet**. In this option, the flow rates on card 0310 must be directly supplied, and then the code runs in the *flow driven mode*.

(DP0 > 0.0) (MPa).

DDP	Pressure drop increment for changing the pressure drop value (MPa). It can be either positive or negative. Setting DPWR (on Card 0600) = 0.0 stops running multiple cases of the problem using different values of the driving pressure drop, as described below (see the next input DPMAX). DDP is ignored if WFGES(I) = 0 on card 0300.
DPMAX	In the <i>pressure drop driven mode</i> (i.e., if WFGES(I) > 0), DPMAX is the final value of imposed pressure drop (MPa). The code runs multiple cases of the problem, first using a driving pressure drop of DP0. The driving pressure drop is then set to a value in the series DP0+DDP, DP0+2*DDP, DP0+3*DDP, The final value used for the driving pressure drop \leq DPMAX. In the <i>flow driven mode</i> (i.e., if WFGES(I) = 0), DPMAX is the pressure at the heated surface inlet (MPa).
POWER	Total thermal power (MW). Of this, only a fraction (1.0 - QFCLAD - QFCOOL) is generated in fuel meat, with the remainder directly deposited in cladding and coolant.
TIN	Inlet coolant temperature (C)
P	Inlet pressure (MPa)
	START ANOTHER CARD.
QFCLAD	Fraction of the total input power POWER, that is generated in the cladding (due to gamma heating). Used only if option IEND = 0, otherwise the data on Card 0501 are used. The power generated in the cladding <i>axial nodes</i> on the left and right of a fuel plate are each given by 0.5*QFCLAD*(total power in the fuel plate node).
QFCOOL	Fraction of the total input power POWER, that is generated in the

coolant channels (due to gamma heating).

The power generated in an inner coolant channel *axial node* is computed as $0.5 \cdot Q_{FCOOL} \cdot (\text{sum of total power in the two adjacent fuel plate nodes})$. The power in the first (or last) coolant channel is $0.5 \cdot Q_{FCOOL} \cdot (\text{total power in only one fuel plate, the first or last})$.

EPSLN	Relaxation factor for <i>outer</i> iteration used in natural circulation flow calculation. It is the parameter ϵ used in Eq. (14) in Appendix XI. The code converges usually for EPSLN in the range 0.45 to 0.80. If the input value is zero, a default value of 0.6 is used.
EPSLNI	Relaxation factor for <i>inner</i> iteration used in natural circulation flow calculation. It is the parameter F_{inner} used in Step 6 in Section 3 on the solution strategy given in Appendix XI. The code converges usually for EPSLNI in the range 0.02 to 0.9. If the input value is zero, a default value of 0.5 is used. Use a value smaller than 0.5 if the inner iterations do not converge.
XCONV	Convergence criterion in searching for the target values input on Card 0203. A default value of 10^{-8} is used if the input value is less than 10^{-8} . It may be increased to 10^{-6} for running speed.
YCONV	Convergence criterion in searching for the target values input on Card 0204 in a double search problem. A default value of 10^{-5} is used if the input value is less than 10^{-5} . It may be increased to 10^{-4} for running speed.

Example: How do I determine the mass flow rates through each channel, given a driving pressure drop, or a range of pressure drops? Consider the following values on card 0500:

0.000005 0.000001 0.000005 6.0E-03 30. 0.11

This represents a request for a flow rate calculation driven by a pressure drop of 5 Pa (0.000005 MPa), for a power of 6.0E-3 MW, an inlet temperature of 30 °C, and an inlet pressure of 0.11 MPa. Because DPMAX is the same as DP0, there will only be a single calculation. If DPMAX exceeded DP0+DDP, there would be a series of calculations at steps of 1 Pa until DPMAX is exceeded. To do this flow rate calculation, WFGES(I) must be non-zero on card type 0300, and card 0310 data must not be supplied.

Card (1) 0501..... Power produced in cladding, gap, and coolant

Required only if option IEND = 1. The option IEND is input number 12 on Card 0200.

QFCLAD1, QFCLAD2, QGAP1, QFGAP2, XMIX

Format (5E12.5)

QFCLAD1	Power density in the <i>left</i> cladding as a fraction of the power density in fuel meat (due to gamma heating).
QFCLAD2	Power density in the <i>right</i> cladding as a fraction of the power density in fuel meat (due to gamma heating).
QFGAP1	Power density in the <i>left</i> gap as a fraction of the power density in fuel meat (due to gamma heating).
QFGAP2	Power density in the <i>right</i> gap as a fraction of the power density in fuel meat (due to gamma heating).
XMIX	A mixing parameter used to model coolant mixing among the sub-channels (adjacent to the fuel plate stripes) of a coolant channel. XMIX varies from 0.0 to 1. XMIX = 0.0 implies no mixing among sub-channels, and XMIX = 1.0 implies perfect mixing among all sub-channels in a coolant channel. Intermediate values of XMIX causes partial mixing among the sub-channels of a channel.

Note: Perfect mixing (XMIX = 1.0) was assumed by the code in the past. However, this is not the most conservative option.

Card (1) 0600..... Data used to loop on reactor power to get $TSM \geq TWM$, to the maximum power level input on this card. For each of these power levels, the driving pressure drop is changed as input on card 0500. TSM is cladding surface temperature, and TWM is onset of nucleate boiling (ONB) temperature. ITER, CONV, ETA, DPWR, PWRM

Format (I4,4E12.5)

ITER	Not currently used. Formerly the maximum number of iterations. The code now sets limits of 10 and 20 iterations in subroutines PLTEMP and PLTNEW.
CONV	Convergence criterion for iteration on flow (default 0.0001)
ETA	Parameter η in Whittle-Forgan flow instability correlation; See the recommended procedure for finding the margin to flow instability in Section VI of Appendix VII. (recommended 32.5)
DPWR	Power search increment, MW (≥ 0.0). Set DPWR = 0.0 to avoid the power search.

PWRM Maximum power level in search, MW

Provide Cards 0700 and 0701 if NAXDIS = 1. If NAXDIS = 2, skip Cards 0700 and 0701, and provide Cards 0702A, 0702, and a separate file containing the axial power shapes by stripe as described in Appendix II.

Card (1) 0700..... Number of heat transfer node interfaces in fueled region

NN

Format (I4)

NN Number of heat transfer node interfaces (Nodes + 1) in axial distribution over the heated length of fuel plates. This may be entered as either a positive or negative value. $NN \leq 50$

If NN positive:

Card (NN) 0701..... Axial power shape in the fueled region of a plate, input at interfaces of heat transfer nodes (Required only if NAXDIS = 1)

(ZR(J), QVZ(J), J=1, NN)

Format (2E12.5)

ZR(J) Relative distance of J-th node interface from inlet
Renormalized if ZR(NN) is not 1.0.

QVZ(J) Relative heat generation at J-th interface (should average to 1.0)

If NN negative:

Card (NN) 0701..... Axial power shape in the fueled region of a plate, input at heat transfer nodes (Required only if NAXDIS = 1. See Appendix II if NAXDIS = 2)

(ZR(J), ZAVG(J), QAVG(J), J=1, |NN|)

ZR(J) Relative distance of J-th node interface from inlet
The value of ZR(|NN|) must be entered on the last Card 0701.
Renormalized if ZR(|NN|) is not 1.0.

ZAVG(J) Relative distance of the J-th node center from inlet

QAVG(J) Relative average heat generated in the J-th node
The value QAVG(|NN|) is not entered.

Card (1) 0702A.... Name of the file containing axial power shapes
APSHF

Format (A80)

APSHF Filename of axial power shapes. If this card is absent, the filename will be assumed to be *axial.power.shape* as in the previous version of the code.

Card (1) 0702..... Fueled stripes whose axial power shapes are edited.

Set NIJK to zero if option IEND = 0 on Card 0200. Supply at least one stripe if option IEND \neq 0. The first stripe supplied here must be *fueled*.
NIJK, (NII(N), NJJ(N), NKK(N), NSS(N), N=1,NIJK)

Format (17I4, /, (4X, 16I4))

NIJK Number of stripes whose axial power shape is edited.

NII(N) Fuel assembly type of the N-th stripe to be edited.

NJJ(N) Fuel assembly number of the N-th stripe to be edited.

NKK(N) Fuel plate number of the N-th stripe to be edited.

NSS(N) Stripe number to be edited.

Note: The axial power shape of the first stripe supplied here is used in the Broyden method (of computing temperature distribution) that uses a single axial power shape.

APPENDIX II. INPUT DATA FOR AXIAL POWER SHAPE IN EACH STRIPE OF ALL FUEL PLATES

(Required only if NAXDIS = 2)

Enter in a file (filename: the string APSHF supplied on the input Card 0702A) the axial power shape in each longitudinal stripe of all fuel plates in all fuel assemblies of all fuel types. The following input variables determine the array size of the data in this file. See Fig. II-1.

NFTYP = Number of fuel types (input on Card (input on Card 0200),
NELF(I) = Number of fuel assemblies of type I (input on Card 0300),
NCHNF(I) -1 = Number of fuel plates in an assembly of type I (input on Card 0306),
NLSTR(I) = Number of stripes in a fuel plate of type I (input below on Card 0705),
I = Fuel assembly type index,
J = Axial node number,
NLS = Longitudinal stripe number,
NPL = Fuel plate number,
NFA = Fuel assembly number.

Card (1) 0703 Title for the axial power shape data

TDATA

Format (20A4)

TDATA Alphanumeric descriptive title of the data

Card (1) 0704 Relative distance of heat transfer node interfaces in fueled region, for each fuel assembly Type I

NN, (ZR(J), J=1,|NN|)

Format (I4, /, (6E12.5))

NN Number of heat transfer node interfaces (Nodes + 1) in the axial distribution of power over the heated length of fuel plates. This number must be the same for all fuel plates of all fuel assemblies, and may be entered as either a positive or a negative value. The sign affects the data on Cards 0705. $NN \leq 50$.

ZR(J) Relative distance of the J-th node interface from inlet to the heated length. The value of ZR(|NN|) must be entered. The array will be re-normalized if ZR(I,|NN|) is not 1.0. Do not supply ZR for fuel types I = 2, NFTYP. They are the same as ZR for fuel type 1.

Supply Cards 0705 and 0706 for all fuel assemblies of type 1, then for all fuel assemblies of type 2, and so on for all fuel types. The Cards 0706 for each fuel type *must* end with the Card 0706 for the last assembly's last plate's last stripe of the fuel type.

Card (1) 0705 Fractional widths of stripes in fuel plates of assembly Type I

I, NLSTR(I), (WIDLS1(I,M), M=1, NLSTR(I))

Format (2I4, /, (6E12.5))

I Fuel assembly type number

NLSTR(I) Number of longitudinal stripes in a fuel plate of type I (maximum 30). The heat conduction along the fuel plate width and length is ignored if the input value of NLSTR(I) is 1.

WIDLS1(I,M) Width or arc length of the M-th longitudinal stripe as a fraction of the *first* plate's fueled+unfueled width or arc length CIRCFC(I,1) entered on input Card 0308. A *negative* fraction implies that the stripe is unfueled. Similar width fractions for other plates K are scaled from this input and the inputs UNFUEL(I) and CIRCFC(I,K).

Note 1: The sum of WIDLS1(I,M) over all M with positive values of WIDLS1(I,M) must be $1 - \frac{2 * UNFUEL(I)}{CIRCFC(I, 1)}$, and the sum of |WIDLS1(I,M)| over all M with negative values of

WIDLS1(I,M) must be $\frac{2 * UNFUEL(I)}{CIRCFC(I, 1)}$.

Note 2: Currently, the variation of coolant velocity along the width of coolant channel is ignored, and the fractions WIDLS1(I,M) are used to split the flow rate of a channel into the flow rates associated with the stripes. The flow rate associated with each stripe (subchannel) is used in the heat transfer calculation by stripe in option IEND=1.

If NN positive:

Card (*) 0706..... Axial shape of power density for a contiguous collection of stripes (having the same power density shape) in fuel plates of assemblies of type I. Input data at *interfaces* of heat transfer nodes.

A contiguous collection of stripes is defined by the starting and ending stripes of the collection. Each stripe is identified by specifying its (assembly number, plate number, and stripe number), e.g., (NFA1, NPL1, NLS1) for the starting stripe of the collection, and (NFA2, NPL2, NLS2) for the ending stripe of the collection. Use as many contiguous collections as needed to put in data for all fuel plate stripes in assemblies of type I.

I, NFA1, NFA2, NPL1, NPL2, NLS1, NLS2, (QVEZ(J), J=1, |NN|)

Format (7I4, /, (6E12.5))

Use as many Cards 0706 as needed to enter |NN| values.

I Fuel assembly type for a *contiguous* collection of fuel plate stripes having the same axial power shape that is input on this set of Cards 0706.

NFA1 Starting assembly number of type I for the *contiguous* collection of stripes having the same axial power shape.

NFA2 Ending assembly number of type I for the *contiguous* collection of stripes having the same axial power shape.

NPL1 Starting plate number in assembly NFA1 of type I for the *contiguous* collection of stripes having the same axial power shape.

NPL2 Ending plate number in assembly NFA2 of type I for the *contiguous* collection of stripes having the same axial power shape.

NLS1 Starting stripe number in fuel plate NPL1 of assembly NFA1 of type I for the *contiguous* collection of stripes having the same axial power shape.

NLS2 Ending stripe number in fuel plate NPL2 of assembly NFA2 of type I for the *contiguous* collection of stripes having the same axial power shape.

QVEZ(J) Relative power density, QVEZ(J, NLS1, NPL1, NFA1), at the J-th interface in stripe NLS of fuel plate NPL of assembly NFA of type I. The value of QVEZ(|NN|) must be entered. The data is normalized by the code, based on the radial power factors of fuel plates input on Card 0309, while maintaining the relative distribution of power density over all the stripes in each plate.

If NN negative:

Card (NN) 0706..... Axial shape power density for a contiguous collection of stripes (having the same power density shape) in fuel plates of assemblies of type I. Input data at heat transfer *node center*.

A contiguous collection of stripes is defined by the starting and ending stripes of the collection. Each stripe is identified by specifying its (assembly number, plate number, and stripe number), e.g., (NFA1, NPL1,

NLS1) for the starting stripe of the collection, and (NFA2, NPL2, NLS2) for the ending stripe of the collection. Use as many contiguous collections as needed to put in data for all fuel plate stripes in assemblies of type I.

I, NFA1, NFA2, NPL1, NPL2, NLS1, NLS2, (QAVEZ(J), J=1, |NN|-1)

Format (7I4, /, (6E12.5))

Use as many Cards 0706 as needed to enter |NN|-1 data values.

I, NFA1, NFA2, NPL1, NPL2, NLS1, NLS2 as defined above, and

QAVEZ(J) Relative average power density, QAVEZ(J, NLS1, NPL1, NFA1), in the J-th node of stripe NLS of fuel plate NPL of assembly NFA of type I. The value of QAVEZ(|NN|, NLS1, NPL1, NFA1) is not entered. The data is normalized by the code, based on the radial power factors of fuel plates input on Card 0309, while maintaining the relative distribution of power density over all the stripes in each plate.

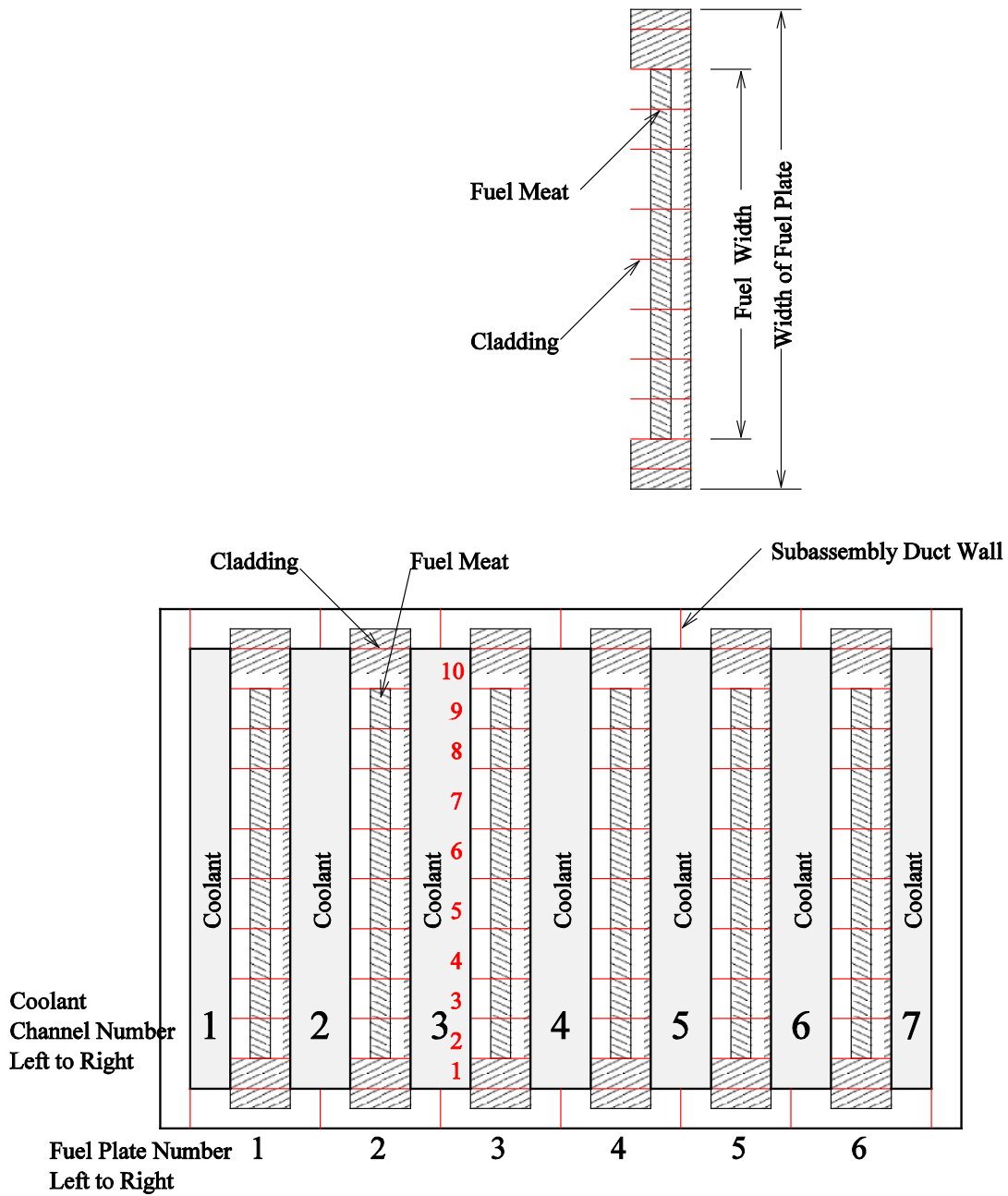


Fig. II-1. Cross Section of a Typical Fuel Assembly Having 6 Fuel Plates Modeled by Heat Transfer Option IEND=1 (A single fuel plate is shown at the top, and the longitudinal stripes, 10 shown, are numbered in red color)

APPENDIX III. HEAT CONDUCTION EQUATIONS FOR 1-D RADIAL GEOMETRY USED IN BROYDEN SOLUTION

In one-dimension radial geometry, the heat conduction equation can be written:

$$d^2t/dr^2 + (k/r)dt/dr + q'''=0$$

where k is the thermal conductivity of the medium and q''' is the volumetric heat source strength. The solution is

$$t = -q''' r^2/(4k) + C_1 \ln[r] + C_2$$

At the point of maximum temperature, r_m , the derivative of temperature with radius is zero. That is,

$$dt/dr = -q''' r/(2k) + C_1/r \rightarrow 0$$

The solution is $C_1 = q''' r_m^2/(2k)$

Assuming that the temperature is t_{out} at the outside (largest radius of curvature) of the fuel plate, then

$$t_m - t_{out} = q''' / (2k) \{ (r_{out}^2 - r_m^2)/2 - r_m^2 \ln[r_{out}/r_m] \}$$

similarly, assuming that the temperature is t_{in} at the inside (smallest radius of curvature) of the fuel plate, then

$$t_m - t_{in} = q''' / (2k) \{ -(r_m^2 - r_{in}^2)/2 + r_m^2 \ln[r_m/r_{in}] \}$$

We want to know the fraction of the heat $Q = q'''V$ generated on each side of the maximum temperature point, for use in the overall temperature solution. The fraction "on the left," outside the annulus, is obtained for an assumed flat q''' profile across the fuel meat annulus from

$$x = Q_l/Q = (r_{out}^2 - r_m^2)/(r_{out}^2 - r_{in}^2) = (r_{out} + r_m)(r_{out} - r_m)/(2 r_{mid} \delta)$$

In this equation, δ is the fuel meat thickness. Solving for r_m ,

$$r_m = r_{out} \sqrt{[1 - 2 r_{mid} \delta x / r_{out}^2]}$$

For the temperature drop across the clad of thickness ϵ , let the following radii be defined:

$$\begin{aligned} r_1 &= r_{mid} + \delta/2 + \epsilon \\ r_2 &= r_{mid} + \delta/2 \\ r_3 &= r_{mid} - \delta/2 \\ r_4 &= r_{mid} - \delta/2 - \epsilon \end{aligned}$$

Then it is necessary to determine clad effective thickness terms of the form:

$$r_1 \ln[r_1/(r_i - \varepsilon)]$$
$$r_4 \ln[(r_4 + \varepsilon)/r_4]$$

Then the temperature drop across the clad on the left or right, given heat flux J_l or J_r is:

$$t_2 - t_1 = r_1 \ln[r_1/(r_i - \varepsilon)] J_l/k_{\text{clad}}$$
$$t_4 - t_3 = r_4 \ln[(r_4 + \varepsilon)/r_4] J_r/k_{\text{clad}}$$

For comparison, the temperature drop across the clad, in slab geometry, given heat flux J is:

$$t_2 - t_1 = J \varepsilon /k_{\text{clad}}$$

APPENDIX IV. HEAT TRANSFER CORRELATIONS

1. Heat Transfer Coefficient Correlations

Carnavos Correlation for Finned Channel (See Appendix IX)

$$Nu = 0.023 Re_a^{0.8} Pr^{0.4} \left(\frac{A_{fa}}{A_{fc}} \right) \left(\frac{P_n}{P_a} \right) \sec^3 \alpha$$

where

Re_a = Actual Reynolds number of the finned channel

P_a = Actual perimeter, i.e., actual heat transfer area per unit length of the tube with fins, m^2 per meter

P_n = Nominal perimeter, i.e., nominal heat transfer area per unit length of the tube, based on tube ID as if the fins were not present, m^2 per meter

A_{fa} = Actual flow area in the tube with fins, m^2

A_{fc} = Core flow area, i.e., the flow area inside the circle touching the fin tips, (see Fig. IX-2), m^2

A_{fn} = Nominal flow area in the tube, based on tube ID as if the fins were not present, m^2

Sieder-Tate

The heat transfer coefficient can be obtained from the Nusselt number as follows:

$$Nu = 0.027 Re^{0.8} Pr^{1/3} [\mu/\mu_w]^{0.14}$$

The coolant properties used in this correlation are at the bulk temperature, except that the viscosity μ_w is at the heating wall temperature.

Dittus-Boelter

$$Nu = 0.023 Re^{0.8} Pr^{0.4}$$

The coolant properties used in this correlation are at the bulk temperature.

Dittus-Boelter Modified

$$Nu = 0.023 Re^{0.8} Pr^{0.4} [\mu/\mu_w]^{0.11}$$

The coolant properties used in this correlation are at the bulk temperature, , except that the viscosity μ_w is at the heating wall temperature.

Colburn

$$Nu = 0.023 Re^{0.8} Pr^{0.3}$$

The coolant properties used in this correlation are at the mean of bulk and wall temperatures.

Petukhov & Popov

The Darcy friction factor f_D is approximated as

$$f_D = [1.0875 - 0.1125 (b/s)] / [1.82 \log_{10} Re_b - 1.64]^2$$

Then the forced-convection heat transfer coefficient is:

$$Nu = (f_D / 8) Re_b Pr_b (\mu_b / \mu_w)^{0.11} /$$

$$[(1+3.4 f_D)+(11.7 + 1.8/Pr_b^{1/3})(f_D/8)^{1/2} (Pr_b^{2/3}-1.0)]$$

where the subscript b refers to bulk coolant, and w to coolant at the wall temperature, and

Re = Reynolds number, $\rho V D_e / \mu$

Pr = Prandtl number, $\mu C_p / k$

μ_b = Dynamic viscosity of the bulk liquid coolant, kg/(m s)

μ_w = Dynamic viscosity of the coolant at the wall temperature, kg/(m s)

k_b = Bulk coolant conductivity

D_e = Hydraulic diameter, m

b = Gap of a rectangular channel or annulus (m)

s = Span of the channel (m)

Ref: Y. A. Hassan, and L. E. Hochreiter, Nuclear reactor thermal-hydraulics, presented at the Winter Annual Meeting of the American Society of Mechanical Engineers, Atlanta, Georgia, December 1-6, 1991, American Society of Mechanical Engineers, Heat Transfer Division, New York, N.Y., p. 63.

Russian

$$Nu = 0.021 Re^{0.8} Pr^{0.43} [Pr/Pr_w]^{0.25}$$

Collier Correlation for Mixed Convection

$$Nu = \begin{cases} Nu_L \equiv \left\{ \max \left[CL1, CL2 * Re_b^{CL3} Pr_b^{CL4} \left(\frac{Pr_b}{Pr_w} \right)^{CL5} \left(\frac{g \beta \rho^2 D_e^3 (T_w - T_b)}{\mu^2} \right)^{CL6} \right] \right. & \text{if } Re < RE1 \\ Nu_T \equiv 0.023 Re_b^{0.8} Pr_b^{0.4} & \text{if } Re \geq RE2 \\ Nu_L + \frac{(Re - RE1)}{(RE2 - RE1)} (Nu_T - Nu_L) & \text{if } RE1 \leq Re < RE2 \end{cases}$$

where the suggested values are: CL1 = 4.0, CL2 = 0.17, CL3 = 0.33, CL4 = 0.43, CL5 = 0.25, CL6 = 0.1, RE1 = 2000, RE2 = 2500.

Ref: J. G. Collier and J. R. Thome, "Convective Boiling and Condensation," 3rd. Edition, p. 185, Clarendon Press, Oxford (1994).

Churchill-Chu Correlation for Free Convection from Vertical Plate

$$\overline{Nu}_L \equiv \frac{\bar{h} L}{k} = \left[0.825 + \frac{0.387 Ra^{1/6}}{\{1 + (0.492/Pr)^{9/16}\}^{8/27}} \right]^2, \text{ Rayleigh Number } Ra = \frac{g \beta (T_w - T_b) L^3}{\nu \alpha}$$

This correlation is good for both laminar and turbulent flow, and accounts for both (1) buoyancy assistance and (2) entrance effects (velocity profile and temperature profile development which is important for channels of small height). It is useful if the bulk coolant circulation velocity is small (~0.01 m/s) and the free convection-induced coolant velocity is dominant. This correlation should not be used if the boundary layers on the pair of fuel plates making the coolant channel

interfere with each other. This can be checked using the maximum thickness of the boundary layer on a plate given by [See Fig. 9.4 of Reference 41 after the main text of the Users Guide]

$$\text{Boundary Layer Thickness} \approx 3L \left(\frac{4}{\text{Gr}} \right)^{1/4} = 3L \left[\frac{4 \nu^2}{g\beta(T_w - T_b) L^3} \right]^{1/4}.$$

Ref: S. W. Churchill and H. H. S. Chu, "Correlating Equations for Laminar and Turbulent Free Convection From a Vertical Plate," Int. J. Heat Transfer Mass Transfer, Vol. 18, pp. 1323-1329 (1975).

CIAE Correlation for Natural Convection in MNSR

$$\text{Nu} = \begin{cases} 0.68 \text{Ra}^{0.25} \pm 10\% & \text{if } \text{Ra} < 6 \times 10^6 \\ 0.174 \text{Ra}^{1/3} \pm 8\% & \text{if } \text{Ra} \geq 6 \times 10^6 \end{cases}$$

where Ra = Rayleigh Number based on hydraulic diameter = $g \beta (T_w - T_b) D^3 / (\nu \alpha)$

This correlation is specific to the Miniature Neutron Source Reactor (MNSR) sold by the China Institute of Atomic Energy. The correlation is based on heat transfer measurements in a model of the MNSR.

Celata Correlation

Celata, et. al. [42] reported extensive experimental investigation of *turbulent* mixed convection heat transfer in upwards flow of water in vertical tubes. They obtained 2633 data points which are in very good agreement with results obtained by numerical methods, and cover the following ranges of parameters:

$$\begin{array}{lll} 0.038 \leq \text{Bo} \leq 12500, & 800 \leq \text{Re} \leq 23000, & 0.034 \leq V \leq 0.46 \text{ m/s}, \\ 34 \leq G \leq 460 \text{ kg/m}^2\text{-s}, & 0.1 \leq P \leq 0.55 \text{ MPa}, & 10 \leq L/D_h \leq 40, \\ 0.5 \leq L \leq 1.14 \text{ m}, & 25 \leq T_w \leq 153 \text{ }^\circ\text{C}, & 12 \leq T_b \leq 113 \text{ }^\circ\text{C}, \\ 10 \leq q_w \leq 243 \text{ kW/m}^2, & 370 \leq h \leq 4370 \text{ W/m}^2\text{-}^\circ\text{C} & \end{array}$$

Based on the data, they proposed the following Nu correlation for mixed convection in upwards flow in heated tubes, fitting most of the 2633 data points within $\pm 20\%$.

$$\frac{\text{Nu}_{\text{uf}}}{\text{Nu}_{\text{df}}} = 1 - a \exp\left\{-0.8[\log(\text{Bo}/b)]^2\right\}$$

$$\text{Bo} = \frac{8 \times 10^4 \text{Gr}^*}{\text{Re}_f^{3.425} \text{Pr}_f^{0.8}}, \quad a = 0.36 + 0.0065(L/D_h), \quad b = 869(D_h/L)^{2.16}$$

$$\text{Nu}_{\text{df}}^3 = \left[0.023 \text{Re}_b^{0.8} \text{Pr}_b^{0.4} \left(\frac{\mu_b}{\mu_w} \right)^{0.11} \right]^3 + \left[\frac{0.15(\text{Gr} \text{Pr}_w)^{1/3}}{\left\{ 1 + (0.437/\text{Pr}_w)^{9/16} \right\}^{16/27}} \right]^3$$

2. Critical Heat Flux Correlations

Mirshak-Durant-Towell (ICHF = 0)

(Based on 65 tests¹⁶ in channels of rectangular and annular cross sections, Fitting error $\pm 16\%$, Standard deviation 8%, Downward flow, Experiment range: coolant velocity 1.52 to 13.72 m/s, one of 65 tests at 1.52 m/s, pressure 1.7 to 5.8 bar, subcooling 5 to 75 °C)

$$q_c = 1.51 (1 + 0.1198 U) (1 + 0.00914 \Delta T_{\text{sub}}) (1 + 0.19 P)$$

where

- q_c = Critical heat flux (MW/m²)
- ΔT_{sub} = Coolant subcooling at the axial location of CHF (i.e., the heated length exit), °C
- U = Coolant velocity, m/s
- P = Coolant absolute pressure, bar

Bernath (ICHF = 1)

(Based on CHF data from 13 sources for water and additional data for ammonia and diphenyl; Fitting error averaged over a data source varies from 1% overprediction to 16% underprediction [Ref. 17]; Experiment range: coolant velocity 1.2 to 16.5 m/s, pressure 1.6 to 207 bar, subcooling 0 to 182 °C)

$$q_c = 3.155 \times 10^{-6} \left(\frac{10890 D}{D + \xi/\pi} + \frac{48 V}{D^{0.6}} \right) \left\{ 102.6 \ln(P) - \frac{97.2 P}{P + 15} - \frac{V}{2.22222} - 1.8 T_b \right\}$$

or,

$$q_c = 5.679 \times 10^{-6} \left(\frac{10890 D}{D + \xi/\pi} + \frac{48 V}{D^{0.6}} \right) \left\{ 57 \ln(P) - \frac{54 P}{P + 15} - \frac{V}{4} - T_b \right\}$$

where

- q_c = Critical heat transfer coefficient at burnout, MW/m²
- V = Coolant velocity, ft/s
- P = Coolant pressure, psia
- D = Hydraulic diameter, ft
- ξ = Heated perimeter, ft
- T_b = Critical bulk coolant temperature, °C

Labuntsov (ICHF = 2)

(Based on CHF data from 9 Russian sources, Fitting error $\pm 17\%$ scaled from Fig. (a) of Ref. 18, Experiment range: coolant velocity 0.7 to 45 m/s, pressure 1 to 204 bar, subcooling 0 to 240 °C)

$$q_c = 1.454 \theta(P) [1 + 2.5 U^2 / \theta(P)]^{1/4} [1 + (15.1 / P^{1/2}) (C_p \Delta T_{\text{sub}} / \lambda)],$$

where

- $\theta(P)$ = $0.99531 P^{1/3} (1 - P/P_c)^{4/3}$
- C_p = Specific heat of the coolant, kJ/kg-°C

λ	= Latent heat of vaporization, kJ/kg
P	= Pressure at the axial location of CHF, bar
P_c	= Critical pressure of the coolant, bar
ΔT_{sub}	= Coolant subcooling at the axial location of CHF (i.e., the heated length exit), °C
U	= Coolant velocity, m/s

Mishima Lower Bound (ICHF = 3)

This correlation is applicable in up-flow and down-flow at near-atmospheric pressure, for coolant inlet temperatures in the range 29 °C to 87 °C, and mass velocity less than 400 kg/m²-s.

$$q_c = q_f [1 + 2.9 \times 10^5 \{C_p (T_{sat} - T_{in})/\lambda\}^{6.5}] \quad G < 200 \text{ kg/m}^2\text{-s downflow [Eq. (10) of Ref. 19]}$$

$$q_c = 10^{-3} C_p (T_{sat} - T_{in})W/(P_h L_h) \quad 200 < G < 350 \text{ kg/m}^2\text{-s downflow [Eq. (14) of Ref. 19]}$$

$$q_c = q_f + \frac{10^{-3} C_p (T_{sat} - T_{in}) W}{P_h L_h} \quad G < 350 \text{ kg/m}^2\text{-s upflow [Eq. (18) of Ref. 19]}$$

$$q_f = \frac{0.7 \times 10^{-3} A_f \lambda \{9.80665 \rho_v (\rho_l - \rho_v) w\}^{1/2}}{P_h L_h \{1 + (\rho_v/\rho_l)^{0.25}\}^2} \quad \text{[Eq. (9) of Ref. 19]}$$

where

A_f	= Flow area, m ²
A_h	= $P_h L_h$ = Heated area, m ²
C_p	= Specific heat of the coolant, kJ/kg
G	= Mass velocity, kg/m ² -s
g	= 9.80665 m/s ² = Acceleration due to gravity, m/s ²
Δh_i	= $C_p(T_{sat} - T_{in})$ = Inlet subcooling, kJ/kg
L_h	= Heated Length, m
P	= System pressure, bar
P_h	= Heated perimeter of the channel, m
q_c	= Critical heat flux, MW/m ²
q_f	= Critical heat flux at zero mass velocity, MW/m ²
T_{in}	= Coolant inlet temperature, °C
T_{sat}	= Coolant saturation temperature, °C
W	= Mass flow rate in coolant channel, kg/s
w	= Width (larger dimension) of the channel rectangular cross section, m
λ	= Latent heat of vaporization, kJ/kg
ρ_l	= Saturated liquid density at the system pressure, kg/m ³
ρ_v	= Saturated vapor density at the system pressure, kg/m ³
$\Delta\rho$	= $\rho_l - \rho_v$ = Density difference between saturated liquid and saturated vapor, kg/m ³

Weatherhead (ICHF = 4)

Based on CHF tests for water at 200 to 2000 psia in tubes of inner diameters 0.045 to 0.436 inch, Weatherhead suggested two CHF correlations, Eqs. (8) and (9) of [Ref. 10]. A comparison of

these correlations with CHF data is shown in Figs. 16 and 17 of [Ref. 10]. One of these, Eq. (9) of [Ref. 10], was implemented in PLTEMP/ANL and is shown below. These comparisons provide the ranges of validity noted below for the correlation.

$$q_c = 1.4410 \times 10^{-4} \lambda \left(\frac{1 + 737.338 \times 10^{-6} G}{D} \right)^{0.5} \left[1 + \tanh \left(\frac{h_f - h_o}{232.60} \right) \right]$$

where

- q_c = Critical heat flux, MW/m²
- λ = Latent heat of vaporization, kJ/kg
- G = W/A_f = Mass velocity, kg/ m²-s
- D = Hydraulic diameter, m
- h_o = Coolant enthalpy at outlet, kJ/kg
- h_f = Enthalpy of saturated liquid, kJ/kg
- W = Mass flow rate in a coolant channel, kg/s
- A_f = Channel flow area in a channel, m²

The ranges of validity for the correlation are:

- 50 BTU/lb < $h_f - h_o$ < 160 BTU/lb,
- 0.9×10^6 lb/hr-ft² < G < 12×10^6 lb/hr-ft²
- 10 bar < P < 140 bar
- 3 mm < D < 12 mm

Groeneveld Lookup Table (ICHF = 5)

Lookup tables are basically normalized data banks. They eliminate the need to choose between the many different available CHF prediction methods and correlations. The 2006 Groeneveld lookup table, implemented currently in PLTEMP/ANL V4.2, contains 23x21x15 (Qualities x Mass fluxes x Pressures) CHF data points. It applies over a broad range of pressure, mass flux, quality, tube diameter, geometry, and heat flux shape. The limits of the table are: pressure P at CHF: $100 \leq P \leq 2100$ kPa; mass flux G at CHF: $0 \leq G \leq 8000$ kg/m²-s; quality range X_{cr} at CHF: $-0.5 \leq X_{cr} \leq 1$. The lookup table is valid for upflow and downflow with a correction factor used for changes in hydraulic diameter. The RMS error of the 2006 table (based on all data used in deriving the table) is quoted as 7.10 % when the table is used at constant inlet condition, or 38.93% when the table is used at constant local quality [32].

Mishima-Mirshak-Labuntsov (ICHF = 6)

To calculate CHF at near-atmospheric pressures in channels of rectangular cross section, Mishima has suggested the following equations by combining *fits to his own tests data*¹⁹ (not the lower bound of ICHF=3) at low mass velocities (i.e. ≤ 600 kg/m²-s) with the works of Mirshak¹⁶ and Labuntsov¹⁸ at higher mass velocities (i.e. ≥ 1500 kg/m²-s). In the intervening range of mass velocity (i.e. 600 to 1500 kg/m²-s), the CHF is found by interpolation between Mishima's fits at mass velocity $G=600$ kg/m²-s and the smaller of the Mirshak and Labuntsov correlations at $G=1500$ kg/m²-s, both in down-flow and up-flow.

$$q_c = \begin{cases} q_f \left[1 + 2.9 \times 10^5 \left(\frac{\Delta h_i}{\lambda} \right)^{6.5} \right] & \text{Mishima fit for } 0 \leq G \leq 200 \text{ kg/m}^2\text{-s downflow} \\ 0.001 A_f \Delta h_i G / A_h & \text{Mishima fit for } 200 \leq G \leq 600 \text{ kg/m}^2\text{-s downflow} \\ \text{Min (Mirshak correl, Labuntsov correl)} & G \geq 1500 \text{ kg/m}^2\text{-s downflow} \\ \text{Interpolate between the above if } & 600 < G < 1500 \text{ kg/m}^2\text{-s downflow} \end{cases} \quad (1)$$

$$q_c = \begin{cases} q_f + 0.00146 \lambda G & \text{Mishima fit for 1-sided heating, } G \leq 600 \text{ kg/m}^2\text{-s upflow} \\ q_f + 0.00170 \lambda G & \text{Mishima fit for 2-sided heating, } G \leq 600 \text{ kg/m}^2\text{-s upflow} \\ \text{Min(Mirshak correl, Labuntsov correl)} & G \geq 1500 \text{ kg/m}^2\text{-s upflow} \\ \text{Interpolate between the above if } & 600 < G < 1500 \text{ kg/m}^2\text{-s upflow} \end{cases} \quad (2)$$

$$q_f = \frac{0.7 \times 10^{-3} A_f \lambda (g \rho_v \Delta \rho w)^{1/2}}{A_h \left[1 + (\rho_v / \rho_l)^{1/4} \right]^2} \quad (3)$$

where

- A_f = Flow area, m^2
- A_h = $P_h L_h$ = Heated area, m^2
- C_p = Specific heat of the coolant, $\text{kJ/kg}\cdot^\circ\text{C}$
- G = Mass velocity, $\text{kg/m}^2\text{-s}$
- g = 9.80665 m/s^2 = Acceleration due to gravity, m/s^2
- Δh_i = $C_p(T_{\text{sat}} - T_{\text{in}})$ = Inlet subcooling, kJ/kg
- L_h = Heated Length, m
- P = System pressure, bar
- P_h = Heated perimeter of the channel, m
- q_c = Critical heat flux, MW/m^2
- q_f = Critical heat flux at zero mass velocity, MW/m^2
- T_{in} = Coolant inlet temperature, $^\circ\text{C}$
- T_{sat} = Coolant saturation temperature, $^\circ\text{C}$
- W = Mass flow rate in coolant channel, kg/s
- w = Width (larger dimension) of the channel rectangular cross section, m
- λ = Latent heat of vaporization, kJ/kg
- ρ_l = Saturated liquid density at the system pressure, kg/m^3
- ρ_v = Saturated vapor density at the system pressure, kg/m^3
- $\Delta \rho$ = $\rho_l - \rho_v$ = Density difference between saturated liquid and saturated vapor, kg/m^3

Shah (ICHF = 7)

Over the years 1979 to 1987, M. M. Shah³⁵ proposed a series of progressively improved correlations. Shah's most recent correlation³⁵ is really a pair of two correlations: the first [called the 'upstream conditions correlation' (UCC)] relates the CHF to the upstream conditions (namely the inlet subcooling and the distance along the tube) whereas the second [called the 'local

condition correlation' (LCC)] relates the CHF only to the local quality. The correlation was tested with CHF data from 62 sources for 23 different fluids that cover the following conditions:

- 0.315 < Diameter < 37.5 mm
- 1.3 < Length-to-Diameter ratio < 940
- 4 < Mass velocity < 29050 kg/m²-s
- 0.0014 < System pressure to Critical pressure ratio < 0.96
- 4.0 < Inlet quality < +0.85

In a comparison³⁶ with measured data, the Shah correlation was found to have an average error of -3.2% and a standard deviation of 16.9%, that was better than all other correlations included in the comparison. The UCC and LCC correlations are both given below, with the procedure for determining which one to use.

Upstream Condition Correlation (UCC):

$$\frac{q_c}{\lambda G} = 0.124 \times 10^{-3} \left(\frac{D}{L_E} \right)^{0.89} \left(\frac{10^4}{Y} \right)^n (1 - X_{iE})$$

When the inlet quality $X_i \leq 0$, $L_E = L_C$ and $X_{iE} = X_i$

When the inlet quality $X_i > 0$, $L_E = L_C + \frac{\lambda G D X_i}{4 q_{ave}}$ and $X_{iE} = 0$ (X_i is not greater than zero in the case of a nuclear reactor)

$$Y = Pe Fr^{0.4} \left(\frac{\mu_l}{\mu_v} \right)^{0.6}, \quad Pe = \frac{G D C_{pl}}{k_l}, \quad Fr = \frac{G^2}{\rho_l^2 g D}$$

$$n = \begin{cases} 0 & \text{if } Y \leq 10^4 \\ \left(\frac{D}{L_E} \right)^{0.54} & \text{if } 10^4 < Y \leq 10^6 \\ \frac{0.12}{(1 - X_{iE})^{0.5}} & \text{if } Y > 10^6 \end{cases}$$

Local Condition Correlation (LCC):

$$\frac{q_c}{\lambda G} = 10^{-3} F_x \text{Max} \left(1.0, 1.54 - \frac{0.032 L_C}{D} \right) \text{Max} \left\{ \begin{array}{l} 15 Y^{-0.612} \\ 0.082 Y^{-0.3} (1 + 1.45 P_r^{4.03}) \\ 0.0024 Y^{-0.105} (1 + 1.15 P_r^{3.39}) \end{array} \right\}$$

$$F_x = \begin{cases} F_1 \left[1 - \frac{(1-F_2)(P_r-0.6)}{0.35} \right]^b & \text{for } X_c < 0 \\ F_3 \left[1 + \frac{(F_3^{-0.29}-1)(P_r-0.6)}{0.35} \right]^{-b} & \text{for } X_c > 0 \end{cases}$$

$$b = \begin{cases} 0 & \text{if } P_r \leq 0.6 \\ 1 & \text{if } P_r > 0.6 \end{cases}$$

$$F_1 = 1 + 0.0052 (-X_c)^{0.88} \left[\text{Min}(Y, 1.4 \times 10^7) \right]^{0.41} \quad \text{for } X_c < 0$$

$$F_2 = \begin{cases} F_1^{-0.42} & \text{if } F_1 \leq 4 \\ 0.55 & \text{if } F_1 > 4 \end{cases}$$

$$F_3 = \left(\frac{1.25 \times 10^5}{Y} \right) * (0.833 X_c) \quad \text{for } X_c > 0$$

Choice between UCC and LCC: The UCC is used except when $Y > 10^6$ and $L_E > 160/P_r^{1.14}$, the smaller of the CHF's obtained from UCC and LCC is used.

where

- q_c = Critical heat flux, MW/m²
- q_{ave} = Heat flux averaged axially from the channel inlet to the CHF location, kW/m²
- λ = Latent heat of vaporization, kJ/kg
- G = Mass velocity, kg/m²-s
- C_{pl} = Specific heat of the liquid coolant, kJ/kg-°C
- D = Hydraulic diameter, m
- Fr = Froude number
- G = Mass velocity, kg/m²-s
- g = 9.80665 m/s² = Acceleration due to gravity, m/s²
- k_l = Thermal conductivity of liquid coolant, kW/m-°C
- L_B = Boiling length, i.e., the axial distance between $X=0$ and the CHF location, m
- L_C = Axial distance between channel inlet and the CHF location, m
- L_E = Effective length of channel defined by Eq. (4), m
- P = System pressure, bar
- Pe = Peclet number
- P_r = P/P_c = Reduced system pressure
- P_c = Critical pressure of the coolant, bar
- μ_l = Dynamic viscosity of liquid, Pa-s
- μ_v = Dynamic viscosity of vapor, Pa-s
- ρ_l = Saturated liquid density at the system pressure, kg/m³
- ρ_v = Saturated vapor density at the system pressure, kg/m³
- X_i = Inlet quality
- X_c = Quality at location of CHF
- Y = Shah's correlating parameter

Sudo-Kaminaga (ICHF = 8)

To calculate CHF in channels of rectangular cross section, Y. Sudo and M. Kaminaga^{37,38} improved on K. Mishima's work at low mass velocities (i.e. $\leq 600 \text{ kg/m}^2\text{-s}$) and suggested the following correlation (written with some rearrangement) covering low, medium and high mass velocities, and downflow and upflow. Note that Eqs. (6) and (7) of this correlation are similar to Mishima's Eqs. (1), (2) and (3) used in ICHF option 6. The Sudo-Kaminaga correlation was tested with 596 CHF data for water from 8 sources covering the following conditions. Note that the set of 10 tests due to Gambill (one of the 8 sources) at pressures ranging from 1.1 to 4.0 MPa are not considered thorough enough to extend the range of applicability of the Sudo-Kaminaga correlation to 4.0 MPa:

Channel gap: 2.25 to 5.0 mm

Ratio of heated length to hydraulic diameter: 8 to 240

Mass velocity: Downflow of 25,800 to stagnant flow to upflow of 6250 $\text{kg/m}^2\text{-s}$

System pressure: 0.1 to 0.72 MPa. In their 1998 paper, the authors limit the application of the correlation to a pressure of simply 1 atmosphere.

Inlet subcooling: 1 to 213 °C

Outlet condition: From subcooling of 0 to 74 °C to quality of 0 to 1.0

By comparing with the 596 CHF data, Sudo and Kaminaga³⁸ found that the measured CHF value was always greater than 67 % of the calculated CHF value (i.e., a maximum error of -33 %), and recommended that the minimum critical heat flux ratio (CHFR) should be larger than 1.5 (which is equivalent to an error of -33 %, i.e., $1/(1 - 0.33) = 1.5$). Based on a statistical analysis, Sudo and Kaminaga³⁷ also reported that the error in the correlation means that there is a 10% possibility of the occurrence of CHF condition even when the minimum CHFR is 1.5.

$$q_c = \begin{cases} \text{Max}(q_{c3}, q_{c2}) & \text{for } G < G_1 \text{ and downflow} \\ \text{Max}\left[q_{c3}, 0.005 G^* 0.611 \lambda \left\{ \sigma \rho_v^2 (\rho_l - \rho_v) g \right\}^{0.25}\right] & \text{for } G < G_1 \text{ and upflow} \\ \text{Min}(q_{c1}, q_{c2}) & \text{for } G \geq G_1, \text{ upflow or downflow} \end{cases} \quad (4)$$

$$q_{c1} = 5 \times 10^{-6} G^* 0.611 \left\{ 1 + 5000 \Delta h_o / (\lambda G^*) \right\} \lambda \left\{ \sigma \rho_v^2 (\rho_l - \rho_v) g \right\}^{0.25} \quad (5)$$

$$q_{c2} = 0.001 A_f \Delta h_i G / A_h \quad (6)$$

$$q_{c3} = \frac{0.7 \times 10^{-3} A_f \lambda \left\{ g \rho_v (\rho_l - \rho_v) w \right\}^{0.5}}{A_h \left\{ 1 + (\rho_v / \rho_l)^{0.25} \right\}^2} (1 + 3 \Delta h_i / \lambda) \quad (7)$$

$$G_1 = \left(\frac{0.005 A_h \lambda}{A_f \Delta h_i} \right)^{2.5707} \left\{ \sigma \rho_v^2 (\rho_l - \rho_v) g \right\}^{0.25} \quad (8)$$

where

A_f = Flow area, m^2

A_h = $P_h L_h$ = Heated area, m^2

- G = Mass velocity, $\text{kg/m}^2\text{-s}$
 G^* = Dimensionless mass velocity = $G / \{ \sigma \rho_v^2 (\rho_l - \rho_v) g \}^{0.25}$
 g = 9.80665 m/s^2 = Acceleration due to gravity, m/s^2
 Δh_i = Coolant subcooling at inlet, kJ/kg
 Δh_o = Coolant subcooling at outlet, kJ/kg
 L_h = Heated Length, m
 P_h = Heated perimeter of the channel, m
 q_c = Critical heat flux, MW/m^2
 w = Width (larger dimension) of the channel rectangular cross section, m
 λ = Latent heat of vaporization, kJ/kg
 ρ_l = Saturated liquid density at the system (exit) pressure, kg/m^3
 ρ_v = Saturated vapor density at the system (exit) pressure, kg/m^3
 σ = Surface tension at average temperature, N/m
 2.5707 = Exponent in Eq. (8) which is related to the exponent 0.611 of Eq. (4) = $1/(1-0.611)$

Extended Groeneveld 2006 CHF Table (ICHF = 9)

The recent subcooled critical heat flux (CHF) literature (subsequent to the Sudo-Kaminaga correlation³⁸) was searched and evaluated, and the Groeneveld 2006 CHF table³² with a new diameter correction, Eq. (9), was selected as the most reliable for predicting CHF in steady-state thermal-hydraulic analysis. The diameter correction in Eq. (9) ($n = 0.312$) was recommended by Celata (1996)⁴⁹, Hall and Mudawar (2000)⁴⁴, and finally by the exhaustive review of Tanase et al. (2009)⁵⁰ with Groeneveld as co-author. The first term in Eq. (9), $q_c(0.008, P, G, X)$, is obtained from a table of CHF for a vertical 0.008-m-diameter water-cooled tube. The 2006 table provides CHF values at 24 pressures, 20 mass fluxes, and 23 qualities, covering the ranges 1 to 210 bars pressure, 0 to 8000 $\text{kg/m}^2\text{-s}$ mass flux, and -0.5 to 1.0 critical quality. The 2006 CHF table is derived from a world-class database containing 33175 measured CHF data points, the combined database of the Atomic Energy of Canada, Limited (AECL), Canada, and the Institute of Physics and Power Engineering (IPPE), Russia. The RMS error reported by Groeneveld et al.³² for subcooled CHF is 14.7% if the 2006 table is used by the direct substitution method (DSM), and 7.1% if the table is used by the heat balance method (HBM). The factor $(G/8000)^{0.376}$ in Eq. (9) extends the application of the 2006 table to mass fluxes greater than 8000 $\text{kg/m}^2\text{-s}$, using the same mass flux-dependence of CHF as in the Hall-Mudawar subcooled correlation^{43,44}.

$$q_c(D, P, G, X_o) = q_c(0.008, P, G, X_o) \left(\frac{0.008}{D} \right)^n \left\{ \left(\frac{G}{8000} \right)^{0.376} \text{ if } G > 8000 \right\} \quad (9)$$

where

- q_c = Critical heat flux, kW/m^2
 n = 0.312
 D = Diameter of the tube, m . It is in general the heated diameter of the channel, given by (4 x flow area/heated perimeter).
 P = Coolant pressure, bar
 G = Coolant mass flux in the channel, $\text{kg/m}^2\text{-s}$
 X_o = Equilibrium quality at the CHF location (critical quality)

The Groeneveld 2006 table is currently preferred (over the next option ICHF=10) due to three considerations: (1) the ease of treating axially non-uniform heat flux and accounting for hot channel factors based on the local conditions hypothesis, (2) the fact that the Groeneveld table has been evaluated and revised three times at 10-year intervals since 1986 adds to its reliability, and (3) in addition to the subcooled CHF, the Groeneveld table also has the saturated CHF that cannot be obtained by the Hall-Mudawar correlation.

Range of application of this CHF prediction method:

Pressure: $1.0 \leq P \leq 210$ bar

Mass flux: $1000 < G < 30,000$ kg/m²-s

Quality at CHF location: $-0.5 < X_o < 1.0$

Heated diameter: $3 < D < 25$ mm

Length-to-diameter ratio: $L/D > 25$ for subcooled CHF, $L/D > 50$ for saturated CHF

Inlet temperature: $T_i > 0.01$ °C

Hall-Mudawar Subcooled CHF Inlet Conditions Correlation (ICHF = 10)

In addition to the AECL-IPPE database³², Hall and Mudawar⁴⁴ have assembled all the measured CHF data in the world literature dating back to 1949, have checked each data by heat balance for error, have independently developed another world-class database containing 32544 data points (4860 subcooled CHF data), and using the database have assessed 82 subcooled CHF correlations and ranked them in the order of reliability (ranking the Bernath correlation¹³ as 43rd). The Hall-Mudawar inlet conditions subcooled CHF correlation, Eq. (10), is derived from this database.

$$\frac{q_c(D_h, P, G, L_h, X_i^*)}{G h_{fg,o}} = \frac{C_1 \left(\frac{G^2 D_h}{\rho_f \sigma} \right)^{C_2} (\rho_f / \rho_g)^{C_3} [1 - C_4 (\rho_f / \rho_g)^{C_5} X_i^*]}{1 + 4C_1 C_4 \left(\frac{G^2 D_h}{\rho_f \sigma} \right)^{C_2} (\rho_f / \rho_g)^{C_3 + C_5} (L_h / D_h)} \quad (\text{RMS error} = 14.3\%) \quad (10)$$

where

$C_1, C_2, C_3, C_4, C_5 = 0.0722, -0.312, -0.644, 0.900, 0.724$, respectively

L_h, D_h = Heated length and heated diameter, m

$G^2 D_h / (\rho_f \sigma)$ = Weber number

$h_{fg,o}$ = Heat of vaporization at the heated length exit (CHF location), kJ/kg

$h_{f,o}$ = Saturated liquid enthalpy at the heated length exit (CHF location), kJ/kg

h_i = Inlet enthalpy, kJ/kg

X_i = Inlet quality = $(h_i - h_{f,i})/h_{fg,i}$

X_i^* = Pseudo-inlet quality = $(h_i - h_{f,o})/h_{fg,o}$

ρ_f, ρ_g = Densities of saturated liquid and saturated vapor, kg/m³

σ = Surface tension, N/m

Range of application of this correlation:

Heated diameter: $0.25 \leq D_h \leq 15$ mm

Length-to-diameter ratio: $6 \leq L_h/D_h \leq 200$

Mass flux: $300 \leq G \leq 30,000$ kg/m²-s

Pressure: $1.0 \leq P \leq 200$ bar

Inlet quality: $-2.0 \leq X_i \leq 0.0$

Exit quality (or quality at CHF location): $-1.0 \leq X_o \leq 0.0$

3. Onset-of-Nucleate Boiling Correlations

Bergles-Rohsenow

$$q_{\text{ONB}} \text{ (MW/m}^2\text{)} = 1.0829 \times 10^{-3} P^{1.156} (1.8 \Delta T_{\text{sat}})^x$$

where

P = Coolant absolute pressure, bar

ΔT_{sat} = Wall superheat temperature at ONB, $^{\circ}\text{C} = T_w - T_{\text{sat}}$

$x = 2.16/P^{0.0234}$

The experiments were conducted with water on stainless steel (SS) and nickel surfaces and covered a range of pressures from 1.02 to 138 bar.

Forster-Greif

$$\Delta T_{\text{sat}} = 0.182 q^{0.35} / P^{0.23}$$

$$T_w = T_{\text{sat}} + \Delta T_{\text{sat}}$$

where

q = Heat flux (W/m^2),

P = Pressure of the coolant (bar)

Russian-Modified Forster-Greif

$$\Delta T_{\text{sat}} = 2.04 q^{0.35} / P^{0.25}$$

$$T_w = T_{\text{sat}} + \Delta T_{\text{sat}}$$

where

q = Heat flux (kW/m^2),

P = Pressure of the coolant (bar)

The code uses a factor of $(1000)^{0.35}$ to convert q from kW/m^2 to MW/m^2 , yielding 0.181815 as the coefficient instead of 0.182 in the normal Forster-Greif correlation.

APPENDIX V. HOT CHANNEL FACTORS TREATMENT OPTION 2

(E. E. Feldman²⁴)

Summary

A conceptual overview of the method that the PLTEMP V4.2 code uses to do a nominal, or best-estimate, calculation for the margin to the Onset-of-Nucleate Boiling is provided. A new treatment of hot channel factors is recommended to incorporate the effects of manufacturing tolerances and reactor operational and modeling uncertainties in the analysis. A sample table of hot channels factors is provided and explained in detail.

With the new treatment of hot channel factors a PLTEMP solution is accomplished in three steps. The first step is the same as is done in the existing code and is a nominal, or best-estimate, calculation. The second step is a repeat of the nominal calculation with the reactor power increased and the reactor flow decreased in order to take account of uncertainties in the measurement of reactor power and flow. In this step the heat transfer coefficient is also reduced by a factor to take account of the uncertainty in the Nusselt number correlations that are used in the nominal analysis. The first two steps use the code to solve the governing equations that describe the physics of the reactor thermal-hydraulics and would require at most minimal changes to the existing code. The third step applies hot channel factors to all of the bulk coolant and film temperature rises and the clad surface heat fluxes obtained in the second step. In the third step all clad surface temperatures and heat fluxes, including the effects of hot channel factors, are obtained and compared with the limiting criteria.

A major advantage of the proposed method is that the limiting criteria for all locations in the core are obtained in a single solution. Another advantage is that the treatment of hot channel factors is relatively simple, easy to explain, and reasonably transparent.

I. The PLTEMP Code

PLTEMP is designed to do steady-state thermal-hydraulic analysis of plate type research reactor cores. A single fuel assembly, multiple assemblies, or an entire core may be represented. Although all of the assemblies can be hydraulically coupled, heat transfer from one assembly to its neighbors is not represented in the model. The core is divided into a series of axial levels. For each axial level the code determines both the bulk coolant temperature in each coolant channel and the clad surface temperatures and heat fluxes on each side of each fuel plate. All of the individual heat transfer relationships used in the code are spatially one-dimensional. Temperature variations along the width of the fuel plates are not considered. At each axial level the code determines the peak fuel meat temperature and the location of the peak temperature within the fuel meat thickness.

In addition to determining all of the needed coolant, clad, and fuel meat temperatures and fuel plate heat fluxes, the code also evaluates the limiting criteria for Onset-of-Nucleate Boiling, flow instability, and critical heat flux and compares the calculated plate temperatures and heat fluxes to them.

II. Nominal Calculations

For the typical analysis performed for research reactors with the PLTEMP/ANL V4.2 code, the most important quantity is the margin to the Onset-of-Nucleate Boiling. If nucleate boiling is avoided then flow instabilities, which could rapidly lead to fuel failure, are avoided. The margins to flow instability and to critical heat flux are also evaluated. For research reactors the margin to nucleate boiling tends to be the most limiting criterion.

Nucleate boiling is assumed to occur when the temperature anywhere on the surface of any fuel plate reaches the temperature limit, T_{onb} . This limit is always greater than the local coolant saturation temperature, T_{sat} , by an amount ΔT_{sat} . ΔT_{sat} is a function of the local water pressure and the local value of heat flux on the surface of the fuel plate and is given by one of several available correlations and is typically several degrees Centigrade.

The local value of fuel plate surface temperature, T_{surf} , is given by:

$$T_{\text{surf}} = T_{\text{in}} + \Delta T_{\text{b}} + \Delta T_{\text{h}} \quad (1)$$

where T_{in} is the inlet coolant temperature, ΔT_{b} is the bulk coolant temperature rise from the inlet of the reactor to the local plate elevation of concern, and ΔT_{h} is the local temperature rise from the bulk coolant to an immediately adjacent fuel plate surface.

ΔT_{b} and ΔT_{h} are given by:

$$\Delta T_{\text{b}} = \frac{q}{w c_p} \quad (2)$$

and

$$\Delta T_{\text{h}} = \frac{q''}{h} \quad (3)$$

where q is the power added to the coolant from the inlet to the elevation of interest, w is the flow rate in the channel, c_p is the specific heat capacity of the coolant, q'' is the local plate heat flux, and h is the local film coefficient at the surface of the fuel plate. Thus, PLTEMP calculates the fuel plate surface temperatures on all fuel plate surfaces at each axial level and compares each temperature to its allowed corresponding value of T_{onb} .

III. Limiting Calculations

A common approach in the analysis of nuclear reactors is to perform both a best-estimate calculation and a limiting calculation. For the former, all parameters, such as dimensions, power

levels, flow rates, and heat transfer coefficients are set at their nominal, or best-estimate, values. A best-estimate analysis is a good first step in understanding the behavior of a system and assessing the feasibility of a design. It is also a gage against which limiting calculations can be judged. The limiting calculation includes the effects of manufacturing tolerances and operational and modeling uncertainties in the analysis.

A best-estimate calculation would employ nominal values in the evaluation of equation 1. For a limiting calculation hot channel factors F_{bulk} and F_{film} could be incorporated into equation 1, to produce:

$$T_{\text{surf}} = T_{\text{in}} + F_{\text{bulk}} \Delta T_{\text{b}} + F_{\text{film}} \Delta T_{\text{h}} \quad (4)$$

where:

F_{bulk} is the uncertainty in bulk coolant temperature rise from reactor inlet to the local elevation of concern, and

F_{film} is the uncertainty in the local film temperature rise at the location of concern on the fuel plate surface.

The above approach differs from that taken in PLTEMP in that ΔT_{h} in equation 4 is replaced by the right side of equation 3 and this causes the PLTEMP equivalent of equation 4 to be:

$$T_{\text{surf}} = T_{\text{in}} + F_{\text{bulk}} \Delta T_{\text{b}} + F_{\text{q}} F_{\text{h}} \frac{q''}{h} = T_{\text{in}} + F_{\text{bulk}} \Delta T_{\text{b}} + F_{\text{q}} F_{\text{h}} \Delta T_{\text{h}} \quad (5)$$

where:

F_{q} is the uncertainty in heat flux at the local fuel plate surface of concern. The F_{q} factor is a multiplier on heat flux, and

F_{h} is the uncertainty in heat transfer coefficient at the location of concern on the fuel plate surface. Since a smaller value of film coefficient, h , would result in larger film temperature rise at the fuel plate surface, F_{h} is a divisor on the nominal value of h .

All hot channel factors are 1.0 for a best-estimate analysis and could be larger than 1.0 to include uncertainties in the limiting analysis. The only difference between equations 4 and 5 is that F_{film} in equation 4 is replaced by $F_{\text{q}} \times F_{\text{h}}$ in equation 5. As will be shown in the discussion of hot channel factors, below, the equation 5 approach can result in unnecessary conservatism in the PLTEMP calculations.

In the limiting calculation, nominal values of heat fluxes would be increased by a factor of F_{q} . Since ΔT_{sat} is a function of the heat flux, q'' , increasing the heat flux by a factor of F_{q} also increases T_{onb} . Since ΔT_{sat} is typically only a several degrees, the effect may be small. Hot channel factors can also affect the other limiting criteria, such as the flow stability criteria.

IV. Hot Channel Factors

Methods for determining hot channel factors for research reactors are described in References 2 and 3, which was intended for use in conjunction with earlier versions of the PLTEMP code. Some of these methods were employed in the construction of Table V-1. Two additional hot

channel factors, not included in References 2 and 3, F_{film} and F_w , have been added. The former is in equation 4 and the latter is a divisor on flow/velocity and is to account for the variation in bulk coolant flow. F_w is not used in the analysis of the Onset-of-Nucleate Boiling, but is used in some of the other limits that are evaluated by the PLTEMP code, such as those for flow instability.

Table V-1 lists random and systematic sources of uncertainty separately. The random sources can affect any fuel plate or coolant channel. However, it is unlikely that all of the sources can adversely affect the limiting location(s) in the reactor core simultaneously. The first four random sources relate to the distribution of power. The final two random sources affect channel spacing and flow distribution. The three systematic sources affect all regions of the core essentially equally.

The first two random uncertainties, which are caused by variations in the fuel meat thickness and ^{235}U homogeneity, are labeled “local” in that they are assumed to be hot-spot effects that affect the heat flux in only a local area with only minor perturbations in bulk coolant temperature. In some reactor designs, these variations can affect considerably more than a small local area. Since these sources of uncertainty affect the distribution of fuel rather than the total amount of it, the bulk coolant outlet temperature is not affected by these sources. However, the relocation of fuel so that it is closer to the coolant inlet can result in higher bulk coolant temperatures at locations upstream of the outlet. Where this is a concern, subcomponents for F_{bulk} from these sources should be included. When fuel meat thickness or the ^{235}U homogeneity subcomponents are included in F_{bulk} , it may not be appropriate to also include the ^{235}U loading per plate subcomponent in F_{bulk} .

The first four random uncertainties are assumed to affect only one of two plates that bound a coolant channel. Therefore, the effect on bulk coolant temperature rise, as represented by the corresponding F_{bulk} component, is assumed to be half as great. For example, a 3% fuel overloading in a single plate would produce a 1.030 F_q subcomponent, but only a 1.015 F_{bulk} subcomponent.

The systematic errors can be directly included in the PLTEMP calculation by increasing the reactor power, decreasing the reactor flow and decreasing the Nusselt number, which provides the film coefficient, to reflect the systematic errors. Then only the combined random errors need be modeled as direct multiplicative factors applied to calculated temperature rises and heat fluxes. This is what is being recommended. Thus, the systematic errors are directly incorporated into the physics of the problem and the random errors are largely incorporated via equation 4. Although the product of the random and systematic errors provided in the bottom row of Table V-1 represent the total combination of hot channel factors, they are not used in the proposed version of the PLTEMP code.

A line-by-line description of Table V-1 follows:

Fuel meat thickness (local)

This is a result of the manufacturing process. When the fuel plates are rolled to the desired size, the fuel meat thickness in some regions of the plate may be thicker by as much as a specified tolerance. Other regions of the fuel meat can be too thin and result in less than the nominal heat

flux. The amount of ^{235}U in each plate is assumed to be measured separately so that the fuel meat thickness only affects the distribution of power within the plate.

^{235}U homogeneity (local)

This is a tolerance on how well the ^{235}U is mixed with the other ingredients that are in the fuel meat. The amount of ^{235}U in each plate is assumed to be measured separately so that the ^{235}U homogeneity only affects the distribution of power within the plate. The 20% uncertainty shown in the table is considered to be typical for LEU fuel. For HEU fuel 3% is considered to be typical.

^{235}U loading per plate

This is a tolerance on the weight of ^{235}U that is to go into a plate.

Power density

This uncertainty is assumed to be a result of the physics calculations and can result in more power being in a particular plate than was predicted and used in the nominal thermal-hydraulic analysis.

Channel spacing, inches

This tolerance would typically be obtained by dividing the nominal channel thickness by the minimum channel thickness allowed by the dimensional tolerances. In Table V-1, 1.09 was obtained by dividing 0.124 inches by (0.124 – 0.01) inches. For plate geometry where the hydraulic diameter can be approximated as twice the channel thickness, the formulas for obtaining the F_{bulk} and F_{h} subcomponents can be found on page 5 in Reference 3. They are as follows:

$$F_{\text{bulk}} = \left(\frac{t_{\text{nc}}}{t_{\text{hc}}} \right)^{\frac{3}{2-\alpha}} \quad (6)$$

$$F_{\text{h}} = \left(\frac{t_{\text{nc}}}{t_{\text{hc}}} \right)^{\frac{0.4+\alpha}{2-\alpha}} \quad (7)$$

where t_{nc} and t_{hc} are the nominal channel thickness and the minimum (or hot) channel thickness, respectively. α is the value of the Reynolds number exponent in the friction factor relationship. In this relationship, friction factor, f , is approximated as being proportional to $\text{Re}^{-\alpha}$. For turbulent flow α is typically 0.2 or 0.25. 0.25 was used in Table V-1. For laminar flow α is 1. Thus, for laminar flow, equation 6 reduces to the following:

$$F_{\text{bulk}} = \left(\frac{t_{\text{nc}}}{t_{\text{hc}}} \right)^3 \quad (8)$$

This result is to be expected because when the flow is laminar, for a fixed pressure drop, the flow rate between two parallel plates is proportional to the cube of the channel spacing.

Equation 7 is based on the assumption that the flow is turbulent, which is the typical situation. When the flow is laminar, the Nusselt number is independent of flow rate and is a constant value. The heat transfer coefficient, h , is inversely proportional to hydraulic diameter, which is essentially equal to twice the channel thickness in plate reactors. Thus, for laminar flow, thinning the channel *increases* h . This presents a problem because thinning the channel also reduces the flow. Thus, for laminar flow, changing the channel thickness creates two opposing effects. For laminar flow, equation 7 should be replaced by:

$$F_h = \left(\frac{t_{hc}}{t_{nc}} \right) \quad (9)$$

Here the hot channel thickness, which is in the numerator, is that of the largest channel thickness allowed by the manufacturing tolerances. Obviously, the same channel cannot be both at the thinnest allowed by the manufacturing tolerances (equation 8) and at the same time also be at the thickest allowed by the manufacturing tolerance (equation 9). Employing such an assumption in the analysis would be conservative and could be used to avoid having to consider both extreme thicknesses and all thicknesses in between. For both laminar and turbulent flow the F_w subcomponent is equal to the F_{bulk} one.

Flow distribution

This uncertainty is the result of the hydraulic analysis that is used to determine the distribution of flow through the reactor. This is a local effect that does not systematically affect all coolant channels. Quantities, such as friction factors and form losses, and the influence of grid plates and fuel assembly side walls cannot be precisely predicted. Although hydraulic models often predict that channels of equal thickness have the same channel average velocity, in some plate assemblies the average velocities in the end coolant channels have been observed to be several percent less than that the average velocity of all of the coolant channels in the assembly.

Random errors combined

As suggested in the References 2 and 3, treatment of hot channel factors, it is unlikely that all of the random errors and uncertainties will occur together at the most limiting location in the reactor and that each will adversely affect reactor performance. Therefore, the random subcomponents, F^i , of each hot channel factor, F , are combined statistically, i.e.,

$$F = 1 + \sqrt{\sum_i (1 - F^i)^2} .$$

Power measurement

This is a tolerance of the meter that is used to measure power and, if present, would affect all fuel plates essentially equally.

Flow measurement

This is a tolerance of the meter that is used to measure flow and, if present, would affect the flow in all flow channels essentially equally.

Heat transfer coefficient

This is due to uncertainties in the correlations for Nusselt number that are used to determine values of heat transfer coefficient, h . If the Nusselt number correlations that are used in the analysis predict values that are too large, then the predicted temperatures on all clad surfaces will be lower than would otherwise be experienced by the reactor. This is a core-wide effect rather than one that is random in location.

Systematic errors combined

Because systematic errors, such as an error in reactor power and flow measurement, affect all locations within the reactor at the same time, it is reasonable to expect that all of them could be present at the limiting location(s). Therefore, the systematic subcomponents are combined multiplicatively, i.e., $F = \prod_i F^i$.

Product of random and systematic parts

Each of these products provides a hot channel factor, which represents the combination of all of its random and systematic subcomponents. However, these values are not directly used in the proposed modification to the PLTEMP code.

Table V-2 shows the results of two extreme methods of combining hot channel factors, a very conservative method that treats all contributors as if they were systematic and combines them multiplicatively and the opposite extreme, which is totally unacceptable and treats all contributors as if they were random and combines them statistically. Although neither of these extreme sets of results is recommended, the comparison of them with the set at the bottom of Table V-1 is informative.

V. Proposed Treatment of Hot Channel Factors in the PLTEMP Code

For the sake of transparency and simplicity it is proposed that the PLTEMP code be revised to be able to do three sets of calculations (in a single run of the code) and provide a set of results for each as described in the following three steps:

1. A nominal, or best-estimate, calculation
This would be done with all hot channel factors set to 1.0. The code already performs this calculation. Therefore, no change would be required here. If there are no systematic uncertainties, then step 2 would not be performed. If there are no random uncertainties, then step 3 would not be performed. If there are random uncertainties, but no systematic ones, then in the execution of step 3, the results of step 1 would be used in place of those of step 2.
2. A calculation that incorporates only the *systematic* uncertainties in power, flow, and heat transfer coefficient

If Table V-1 were applicable, for example, the nominal power would be multiplied by 1.05, the nominal flow would be divided by 1.10, and the nominal Nusselt numbers, which are used to evaluate h , would be divided by 1.20. The method of solution would otherwise be identical to that in the step 1 nominal, or best-estimate, calculation.

3. A final calculation that adds the effects of the *random* uncertainties to the solution obtained in step 2

When step 2 is performed, sufficient information would be stored for each location modeled in the core so that equation 4 could be evaluated at each location. The heat flux at each location on the fuel plate surfaces would also be stored. Since the results of step 2 already include the higher power, reduced flow, and reduced heat transfer coefficient caused by the systematic errors, only the hot channel factors due to random errors would be used here. These would also be used in the correlations for the limiting criteria. If Table V-1 is applicable, the hot channel factor values shown in bold for F_{bulk} and F_{film} would be used in equation 4 and the value of F_q shown in bold would be applied to all of the stored fuel plate heat fluxes. (An alternative to storing the results of step 2 is to redo step 2 and to include the hot channel factors as the step 2 results are regenerated.)

The above proposed treatment of hot channel factors enables complete results with hot channel factors included to be provided for all locations within the reactor core in a single solution of the code.

If the existing PLTEMP approach were used in step 3, equation 5 would be used in place of equation 4. The two approaches are equivalent except that in the existing PLTEMP approach, which is represented by equation 5, the F_{film} of equation 4 is replaced by the product of F_{q_q} and F_h . As Table V-1 shows, the random errors combined portion of F_{film} , F_{q_q} , and F_h , respectively are 1.29, 1.24, and 1.16. The product of the latter two values is 1.44, which is considerably larger than 1.29. This is because F_{film} statistically combines six subcomponents, but the product of F_q and F_h is the product two statistical combinations, one that combines the first four subcomponents of F_{film} to form F_q and one that combines the last two to form F_h . Thus, the existing PLTEMP approach would result in needless conservatism that is avoided in the proposed approach. The proposed use of a single hot channel factor for ΔT_h , is analogous to PLTEMP's current use of a single hot channel factor for ΔT_b , which equation 2 shows to be derived from more than one dependent variable.

The implementation of the proposed treatment of hot channel factors would require that PLTEMP be modified to accept several new inputs. These would include the following seven factors:

- Multiplier on reactor power to account for the (systematic) uncertainty in power measurement
- Divisor on reactor flow to account for the (systematic) uncertainty in flow measurement

- Divisor on heat transfer coefficient to account for the (systematic) uncertainty in Nusselt number correlation (The existing input for F_h of PLTEMP V4.2 could be renamed and redeployed here.)
- F_{bulk} (combined random components only)
- F_{film} (combined random components only)
- F_q (combined random components only)
- F_w (combined random components only)

Although one could work around having the first two factors by preparing an additional input with the power increased and the flow decreased, it would be much more convenient and could help the user avoid needless errors if the first two factors were provided as code inputs. The first three factors are used in step 2 above. The last four are used in step 3. The values of the last four are shown in bold in Table V-1. F_h is not among these four because its random subcomponents are included in F_{film} , which is a factor in equation 4, and because F_h is not used in calculating values of any of the limiting criteria. F_q is used in step 3 as a multiplier on all fuel plate heat fluxes calculated in step 2. F_w is used only in step 3 and only where flow or velocity is used in calculating values of limiting criteria.

VI. Conclusions

A new method of treating hot channel factors in the PLTEMP code has been presented. It is relatively simple, easy to explain, and reasonably transparent. Moreover, in a single PLTEMP solution it provides limiting results, including the effects of hot channel factors, for all locations represented by the PLTEMP model.

References:

1. Arne P. Olson, "A Users Guide to the PLTEMP/ANL V2.14 Code," October 14, 2005.
2. R. S. Smith and W. L. Woodruff, Argonne National Laboratory, unpublished information, 1988.
3. W. L. Woodruff, *Evaluation and Selection of Hot Channel (Peaking) Factors for Research Reactor Applications*, ANL/RERTR/TM-28, RERTR Program, Argonne National Laboratory, Argonne, Illinois, February 1997
[<http://www.rertr.anl.gov/METHODS/TM28.pdf>].

Table V-1 – Hot Channel Factors

uncertainty	type of tolerance	effect on bulk ΔT , fraction	value	tolerance	tolerance, fraction	hot channel factors				
						heat flux, F_q	channel flow rate, F_w	heat transfer coefficient, F_h	channel temperature rise, F_{bulk}	film temperature rise, F_{film}
fuel meat thickness (local)	random				0.07	1.07				1.07
U235 homogeneity (local)					0.20	1.20				1.20
U235 loading per plate		0.50			0.03	1.03			1.015	1.03
power density		0.50			0.10	1.10			1.050	1.10
channel spacing, inches	random	1.00	0.124	0.01	1.09		1.155	1.03	1.155	1.03
flow distribution		1.00			0.20		1.200	1.16	1.200	1.16
random errors combined						1.24	1.25	1.16	1.26	1.29
power measurement	systematic	1.00			0.05	1.05			1.050	1.05
flow measurement		1.00			0.10		1.100	1.08	1.100	1.08
heat transfer coefficient					0.20			1.20		1.20
systematic errors combined						1.05	1.10	1.30	1.16	1.36
product of random and systematic errors						1.30	1.38	1.50	1.45	1.75

Table V-2 – Extreme Hot Channel Factors

uncertainty extremes						F_q	F_w	F_h	F_{bulk}	F_{film}
pure multiplicative combination						1.53	1.52	1.55	1.71	2.36
pure statistical combination						1.24	1.27	1.27	1.28	1.36

APPENDIX VI. ANALYTICAL SOLUTION FOR TEMPERATURE DISTRIBUTION IN A FLAT FUEL PLATE ASSEMBLY

In a nuclear reactor, the major heat source is fuel. But some gamma radiation is deposited directly in cladding and coolant, making them minor heat sources. To model this, an analytical solution has been carried out for a flat fuel plate assembly with heat sources in all four materials, i.e., left cladding, fuel meat, right cladding and coolant. This solution was put in PLTEMP/ANL code, tested and found to work.

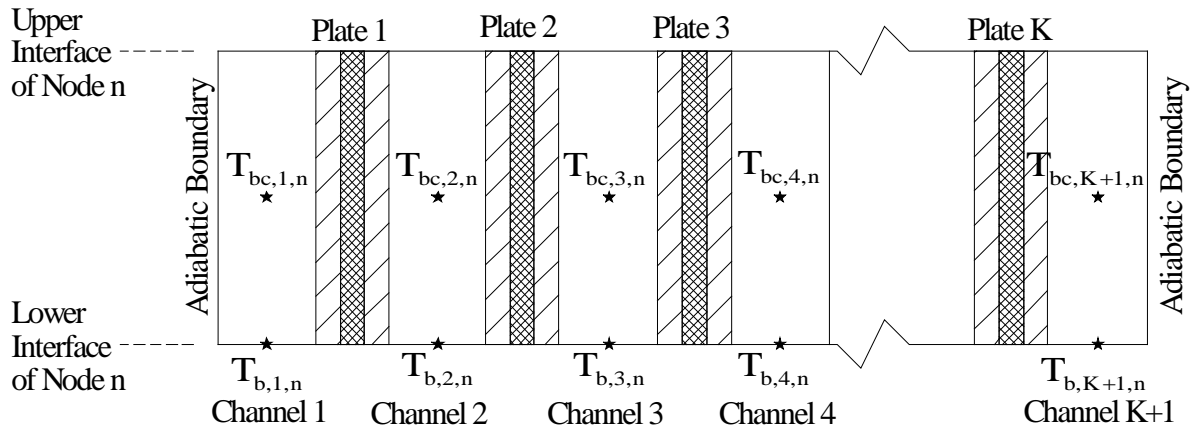


Fig.V-1. An Axial Slice of Fuel Assembly Showing a Heat Transfer Axial Node

Symbols Used:

- K = Number of fuel plates in an assembly
- $T_{bc,k,n}$ = Coolant bulk temperature in channel k at the *center* of heat transfer axial node n , (C)
- $T_{b,k,n}$ = Coolant bulk temperature in channel k at the *entry* to heat transfer axial node n , (C)
- $h_{1,k,n}$ = Convective heat transfer coefficient on the left side of fuel plate k (W/m^2-C)
- $h_{2,k,n}$ = Convective heat transfer coefficient on the right side of fuel plate k (W/m^2-C)
- $t_{a,k}$ = Thickness of cladding on the left side of fuel plate k (meter)
- $t_{b,k}$ = Fuel meat thickness in plate k (meter)
- $t_{c,k}$ = Thickness of cladding on the right side of fuel plate k (meter)
- $K_{a,k}$ = Thermal conductivity of left side cladding in fuel plate k ($W/m-C$)
- $K_{b,k}$ = Thermal conductivity of fuel meat in plate k ($W/m-C$)
- $K_{c,k}$ = Thermal conductivity of right side cladding in fuel plate k ($W/m-C$)
- $q_{a,k,n}$ = Volumetric heat source in left cladding of plate k in axial node n (W/m^3)
- $q_{b,k,n}$ = Volumetric heat source in fuel meat of plate k in axial node n (W/m^3)
- $q_{c,k,n}$ = Volumetric heat source in right cladding of plate k in axial node n (W/m^3)
- $q_{w,k,n}$ = Volumetric heat source in *coolant* (directly deposited in water) in coolant channel k in axial node n (W/m^3)
- x = Position coordinate in the direction of fuel meat thickness, with $x=0$ at the left side of fuel meat (meter)

- X_k = Position (expressed as a fraction $x/t_{b,k}$ of the meat thickness) of maximum fuel temperature in plate k in axial node n . The subscript n is dropped for brevity.
 W_k = Coolant mass flow rate in channel k (kg/sec)
 $C_{p,k,n}$ = Specific heat of coolant in channel k in axial node n , evaluated at the central bulk coolant temperature $T_{bc,k,n}$ (J/kg-C)
 $C_{T,k,n}$ = Partial derivative of coolant enthalpy with respect to pressure at constant temperature, $\left(\frac{\partial h}{\partial P}\right)_T$, in channel k in axial node n (J/kg per Pa)
 P_n = Coolant pressure in a channel at the entry to heat transfer axial node n (Pa)

Figure V-1 shows a vertical section of an experimental nuclear reactor fuel assembly consisting of several fuel plates that are cooled by coolant channels of rectangular cross section. In this formulation, each fuel plate is assumed to be different from others, and each coolant channel is assumed to have a different area and flow rate than others. The method consists of setting up $K+1$ simultaneous linear algebraic equations in $K+1$ bulk coolant temperatures $T_{bc,k,n}$ for $k = 1$ to $K+1$ in a slice of the fuel assembly shown in Fig. V-1.

The solution of heat conduction equations in the left cladding, the fuel, and the right cladding of a plate k are as follows. For brevity, the index k has been dropped in Eqs. (1) to (16).

- q_a = Volumetric heat source in the cladding on the left of fuel plate k
 q_b = Volumetric heat source in the fuel of plate k
 q_c = Volumetric heat source in the cladding on the right of fuel plate k

Temperature distribution in the cladding on left of fuel meat:

$$\begin{aligned}
 d^2T_a/dx^2 &= -q_a/K_a \\
 T_a &= -0.5q_a x^2/K_a + A_1 x + A_2 \quad (x = 0 \text{ to } x = t_a), \\
 \text{where } x = 0 &\text{ implies left surface of the left cladding.}
 \end{aligned} \tag{1}$$

Temperature distribution in the fuel meat:

$$\begin{aligned}
 d^2T_b/dx^2 &= -q_b/K_b \\
 T_b &= -0.5q_b x^2/K_b + B_1 x + B_2 \quad (x = 0 \text{ to } x = t_b), \\
 \text{where } x = 0 &\text{ implies left surface of fuel meat.}
 \end{aligned} \tag{2}$$

Temperature distribution in the cladding on right of fuel meat:

$$\begin{aligned}
 d^2T_c/dx^2 &= -q_c/K_c \\
 T_c &= -0.5q_c x^2/K_c + C_1 x + C_2 \quad (x = 0 \text{ to } x = t_c), \\
 \text{where } x = 0 &\text{ implies left surface of the right cladding.}
 \end{aligned} \tag{3}$$

The six arbitrary constants A_1 , A_2 , B_1 , B_2 , C_1 , C_2 are found using the following six boundary and interface conditions on temperature and heat flux in a fuel plate. The results are given by Eqs. (4) through (16).

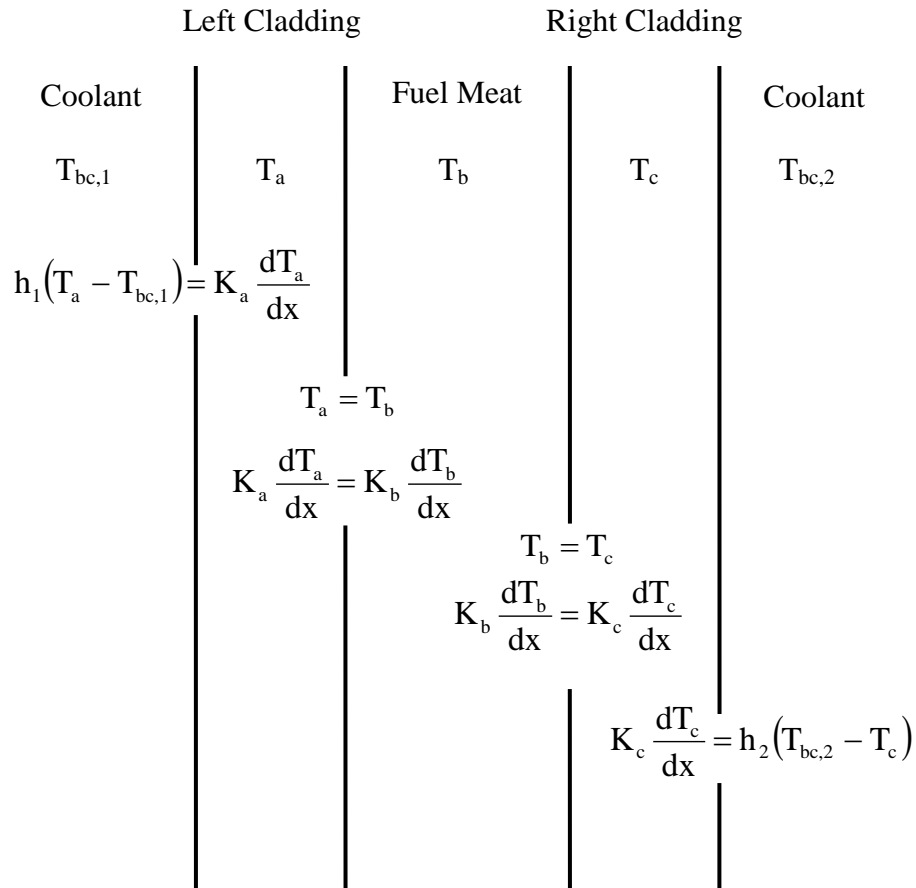


Fig. V-2. Boundary and Interface Conditions for Temperature and Heat Flux in a Plate

$$R = 1/h_1 + t_a/K_a + t_b/K_b + t_c/K_c + 1/h_2 \quad (4)$$

$$Q = q_a t_a + q_b t_b + q_c t_c \quad (5)$$

$$S_0 = q_a t_a^2/2K_a + q_b t_b^2/2K_b + q_c t_c^2/2K_c \quad (6)$$

$$\alpha = \{S_0 + Q/h_2 + q_a t_a (t_b/K_b + t_c/K_c) + q_b t_b t_c/K_c\} / R \quad (4)$$

$$A_1 = Q/(K_a h_2 R) + \{S_0 + q_a t_a (t_b/K_b + t_c/K_c) + q_b t_b t_c/K_c\}/(K_a R) + (T_{bc,2} - T_{bc,1})/(K_a R) \quad (8)$$

$$A_2 = T_{bc,1} + A_1 K_a/h_1 \quad (9)$$

$$B_1 = (A_1 K_a - q_a t_a) / K_b \quad (10)$$

$$B_2 = T_{bc,1} - q_a t_a^2 / (2K_a) + (t_a + K_a/h_1) A_1 \quad (11)$$

$$C_1 = (A_1 K_a - q_a t_a - q_b t_b) / K_c \quad (12)$$

$$C_2 = T_{bc,1} - S + A_1(t_a + K_a/h_1 + K_a t_b / K_b) \quad (13)$$

$$S = q_a t_a^2 / 2K_a + q_b t_b^2 / 2K_b + q_a t_a t_b / K_b \quad (14)$$

The symbols used in the analytical solution to find temperature profile in the thickness of a single fuel plate are defined above, and the new ones are as follows.

q''_1 = Heat flux into the coolant on the left of fuel plate $k = q''_{1,k}$

q''_2 = Heat flux into the coolant on the right of fuel plate $k = q''_{2,k}$

$$q''_1 = \alpha + (T_{bc,2} - T_{bc,1}) / R \quad (15)$$

$$q''_2 = Q - q''_1 \quad (16)$$

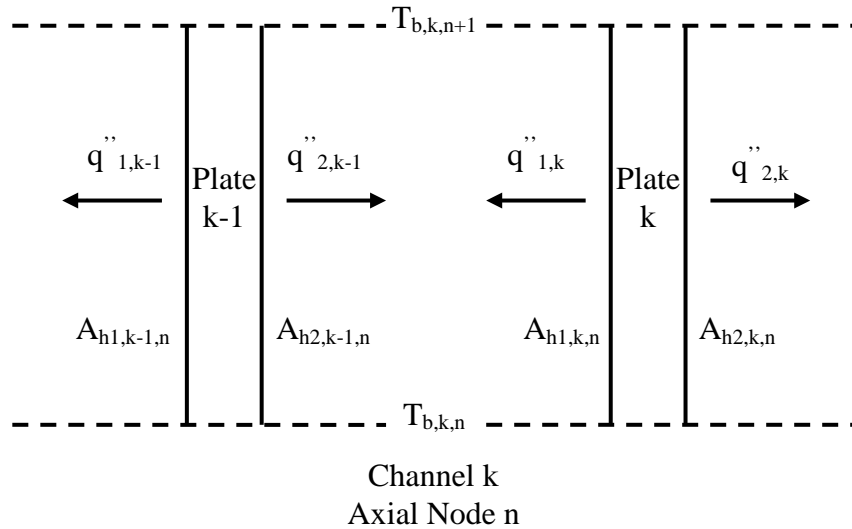


Fig. V-3. Heat Fluxes into a Coolant Heat Transfer Node

Up to this point, the equations were written without an index for identifying the fuel plate. Equations (15) and (16) can be written with an index k to identify the fuel plate, as follows:

$$q''_{1,k} = \alpha_k + (T_{bc,k+1,n} - T_{bc,k,n}) / R_k \quad (17)$$

$$q''_{2,k} = Q_k - q''_{1,k} \quad (18)$$

The heat balance for coolant axial node n of channel k (between fuel plates k-1 and k) can be written as Eq. (19) below, accounting for the coolant enthalpy dependence on both pressure and temperature. The quantity in the square parentheses on the left hand side of Eq. (19) is the change in coolant enthalpy h(P,T) from the inlet to outlet of the axial node n. Equation (20) is obtained from Eq. (19) by expressing the enthalpy change in terms of the partial derivatives of enthalpy with respect to temperature and pressure.

$$W_k [h(P_{n+1}, T_{b,k,n+1}) - h(P_n, T_{b,k,n})] = q_{w,k,n} V_{k,n} + (A_{h1,k,n} q''_{1,k} + A_{h2,k-1,n} q''_{2,k-1}) \quad (19)$$

$$W_k [(T_{b,k,n+1} - T_{b,k,n}) C_{p,k,n} + C_{T,k,n} (P_{n+1} - P_n)] = q_{w,k,n} V_{k,n} + (A_{h1,k,n} q''_{1,k} + A_{h2,k-1,n} q''_{2,k-1}) \quad (20)$$

where

$V_{k,n}$ = Volume of coolant in node n of channel k

$q_{w,k,n}$ = Volumetric heat source in water (directly deposited in coolant)

$A_{h1,k,n}$ = Surface area on the *left side* of fuel plate k for heat transfer into the coolant channel axial node n. It is the plate width times the axial height of the node.

$A_{h2,k,n}$ = Surface area on the *right side* of fuel plate k for heat transfer into the coolant channel axial node n. It is the plate width times the axial height of the node.

Using heat fluxes found from Eqs. (17) and (18), and using Eq. (21) to replace the difference between coolant node-boundary temperatures in Eq. (20), one obtains Eq.(22) for node-center coolant bulk temperatures of an assembly axial slice n.

$$T_{b,k,n+1} - T_{b,k,n} = 2 (T_{bc,k,n} - T_{b,k,n}) \quad (21)$$

The resulting final set of equations for node-center coolant bulk temperatures, $T_{bc,k,n}$, in channels (index k = 1 through K+1) in an axial slice (index n) of an assembly is given by Eq. (22)

$$-(A_{h2,k-1,n} / R_{k-1}) T_{bc,k-1,n} + (2W_k C_{p,k,n} + A_{h2,k-1,n} / R_{k-1} + A_{h1,k,n} / R_k) T_{bc,k,n} - (A_{h1,k,n} / R_k) T_{bc,k+1,n} = V_{k,n} q_{w,k,n} + A_{h2,k-1,n} (Q_{k-1} - \alpha_{k-1}) + A_{h1,k,n} \alpha_k + 2W_k C_{p,k,n} T_{b,k,n} - W_k C_{T,k,n} (P_{n+1} - P_n) \quad (22)$$

Equation (22) is a set of linear simultaneous algebraic equations for node-center coolant bulk temperatures of all channels of an axial slice n of an assembly. The coefficient matrix is tri-diagonal, and no iteration is needed in solving the equations. After solving for these coolant temperatures, the fuel meat and cladding temperatures and other quantities like heat fluxes are evaluated using the closed-form solutions given above.

APPENDIX VII. EXCURSIVE FLOW INSTABILITY PREDICTION

(A. P. Olson)

1. INTRODUCTION TO FLOW INSTABILITY MEASUREMENTS AND CALCULATIONS

PLTEMP includes two correlations for predicting the onset of excursive-flow instability that are based on the work of Whittle and Forgan (W&F) [1], and on Bowring [2]. W&F constructed a number of test sections that could be electrically heated. Table VII-1 below shows the key dimensions of these test section channels (A is the gap thickness and B is the width of the cross section). The electrical heating was applied to the two wide sides.

Table VII-1. Test Section Geometry

Test Section No.	A, in.	B, in.	Heated length, in.	Length between pressure taps, in.	L_H/D_H	P_H/P_W
1	0.127	1.0	24	24.5	94.5	0.89
2	0.090	1.0	16	19.0	83	0.91
3	0.055	1.0	16	19.0	100	0.925
4	0.055	1.0	21	21.5	191	0.95
5	Round tube 0.254 diameter		24	24.5	94.5	1.0

For each test section, a series of pressure drop vs. mass flow rate values were measured. Zero heating tests established the base conditions. Heating was applied uniformly to the sides of the channels in most of the tests. A special test section (1A) was created that had a flat heating profile axially over the inlet half, then falling linearly to 68% at the channel exit. For a given test, the flow rate was initially set higher than that for flow instability. The flow rate was reduced in steps, and the pressure drop recorded. No tests continued into the flow regime where bulk boiling could have occurred near the channel exit. A characteristic minimum in the pressure drop vs. flow curve marked the onset of flow instability. The experiments covered a useful range of parameters as shown in Table VII-2.

A total of 74 tests on rectangular channels were reported in [1]. Of these, 8 tests were illustrated graphically, showing the pressure drop minimum. Test section 1 was used for the first four shown. The axially flat heat fluxes used were: 104, 145, 184, and 250 W/cm². Test section 3 was used for the second set of four tests. The axially flat heat fluxes used were: 66, 177, 218, and 276 W/cm². All 8 of these tests have been analyzed using PLTEMP V3.0. Mass flow rates at the onset of flow instability were interpolated by hand from Figs. 4 and 5 of [1].

Table VII-2. Ranges of Experimental Parameters for the Whittle and Forgan Tests

Parameter	Minimum	Maximum
Velocity (fps)	2	30
Inlet temperature (C)	35	75
Heat flux (w/cm ²)	42	340
Exit pressure (psia)	17	25
Gap width (in.)	0.055	0.127
Heated Length (in.)	16.	24.
Geometry	Wide rectangular slot and round tube	

There is enough data provided in [1] to determine the mass flow rate at the pressure vs. flow minimum from other tabular data, for any of the other 66 tests. It is noted that Whittle and Forgan used British gallons per minute, and reported pressure drop in cm Hg. PLTEMP edits US gpm, so it is possible to supply the correct mass flow rate in kg/s. A conversion factor is needed to scale a mass flow rate into a volume measure. Similarly, one can convert pressures using 1 cm Hg = 1333.4 Pa. All outlet pressures were 17 psia (0.1172 MPa), at which $T_{sat,exit} = 104.13$ C. Inlet pressures were determined by adding the reported pressure drop to the outlet pressure. If the pressure taps extended beyond the heated length, the ΔP across the heated length was reduced in proportion. The mass flow rate m for any W&F test can be obtained from:

$$m = \text{power} \cdot \eta / [C_p \cdot (L_H/D_H) \cdot (\Delta T_c / \Delta T_{sat}) \cdot (\Delta T_{sub0} / \Delta T_c) \cdot (T_{sat,exit} - T_{in})] \quad (1)$$

where $\Delta T_c / \Delta T_{sat} = (T_{out} - T_{in}) / (T_{sat,exit} - T_{in})$; $\Delta T_{sub0} / \Delta T_c = (T_{sat,exit} - T_{out}) / (T_{out} - T_{in})$

See Table VII-3 for a comparison of graphically interpolated mass flow rate vs. Eq.(1). The average error is 2.0 %, which is quite good. But note that this calculation has numerical errors of 4-5% due to lack of precision in the tabulated temperature ratios.

Table VII-3. W & F Mass Flow Rate Graphically Interpolated vs. Calculated Using Tabulated Data (1 UK gallon = 4.5461 liters, 1 US gallon = 3.7853 liters)

Heat flux, W/cm ²	m, from graph gpm(UK)	m, from graph gpm(US)	Calc. m from Eq. (1), gpm(US)	% Difference
104	2.59	3.11	3.23	3.9
145	3.52	4.23	4.44	5.0
184	4.63	5.56	5.41	-2.7
250	5.90	7.09	7.65	8.0
66	1.05	1.26	1.36	7.9
177	3.01	3.61	3.60	-0.4
218	3.82	4.59	4.44	-3.3
276	4.79	5.75	5.61	-2.4

The PLTEMP model consisted of a single plate heated uniformly on each side. It had a half-channel on either side. Knowing the heat flux and channel dimensions, the total power is readily determined. The coolant mass flow rate was input such that the measured (graphically interpolated) gpm (US) was achieved. In each case, the input value of ETA (η) was set to the measured value determined in [1]. A second series of calculations was run using the recommended $\eta = 32.5$.

PLTEMP edits “MINIMUM FLOW INSTABILITY POWER RATIO,” FIR. This ratio would be precisely 1.0 if the experiment was exact, and if the PLTEMP model also was exact. It is based on Whittle and Forgan’s relation:

$$R = \frac{1}{1 + \eta D_H / L_H}$$

In this equation, D_H is the heated diameter of the channel and L_H is the heated length. The flow instability factor is η . Table VII-4 shows the results of the PLTEMP calculations. The average FIR is 1.10, which deviates from the expected 1.00. Why it is not closer is not clear, but there are a number of contributing factors:

1. Measurement errors in power and mass flow rate are likely to be about 5% each.
2. Some heat (about 1% estimated by W&F) is also generated in the edges of the channel, and it is not clear whether or not Ref. 1 includes that in the quoted heat flux.
3. Mass flow rate data are not directly provided. I interpolated the data from supplied graphs which should be accurate to about 1 or 2 %. The flow rates used were on average 2% larger than the W&F data directly compute, which would indicate on average a 1.02 ratio for FIR.
4. Ref. 3 concerns a similar code validation for RELAP5/3.2 against the W&F data, and against ORNL thermal-hydraulic test loop data (THTL). They also show graphically how RELAP5/3.2 compares against the W&F pressure drop vs. mass flow data, re-plotted in kPa and $\text{kg/m}^2\text{s}$ units. For the 8 cases studied with PLTEMP, the flow rate shown by Ref. 3 and accredited to their interpretation of W&F data is 5.3% high, which is consistent with my own interpretation.

Table VII-4. Computed Flow Instability Criterion at the Onset of Flow Instability

Heat Flux w/cm^2	$T_{\text{out}} \text{ C}$	$\Delta T_c / \Delta T_{\text{sat}}$	$\Delta T_{\text{sub0}} / \Delta T_c$	Flow Instability Power Ratio (using measured η)	Flow Instability Power Ratio (using $\eta=32.5$)	$\eta' \text{ min.}$
104	94.57	0.805	0.2416	1.11	1.059	24.7
145	95.59	0.826	0.2104	1.07	1.033	21.8
184	94.17	0.797	0.2543	1.13	1.070	26.2
250	97.75	0.850	0.1767	1.04	1.004	19.1
66	96.29	0.840	0.1899	1.04	1.024	21.0
177	93.64	0.786	0.2715	1.12	1.094	29.7
218	92.51	0.763	0.3099	1.16	1.127	33.5
276	92.87	0.771	0.2973	1.15	1.116	32.2

$$\Delta T_c / \Delta T_{\text{sat}} = (T_{\text{out}} - T_{\text{in}}) / (T_{\text{sat}} - T_{\text{in}}); \quad \Delta T_{\text{sub0}} / \Delta T_c = (T_{\text{sat,exit}} - T_{\text{out}}) / (T_{\text{out}} - T_{\text{in}})$$

2. STATISTICAL ANALYSIS OF W&F FLOW INSTABILITY DATA

The 74 measured values of η used by Whittle and Forgan in their flow instability correlation for rectangular channels were statistically analyzed using *Mathematica*, with the following results:

Mean value	= 24.93
Variance	=13.69
Standard Deviation	= 3.70
95% confidence interval of the mean	= (24.074, 25.788)
95% confidence interval of the variance	= (10.14, 19.49)

If there were an infinite sample of test data available, and the test data followed a normal distribution, then the probability P that η lies within a band centered on the mean value $P(a \leq X \leq b)$, is obtained from the normal distribution integrated over the interval from a to b . Using $a=-1.96$, $b=1.96$, one obtains $P(17.68 \leq X \leq 32.18) = 0.95$. But we do not have an infinite sample, and we do not know the true variance. The lack of this knowledge can be accounted for, but will broaden the result. It is necessary to switch to the Student “ t ” distribution for $N-1$ samples, where $N=74$. Then $a=-1.993$, $b=1.993$, and one obtains $P(17.56 \leq X \leq 32.30) = 0.95$. This upper bound of 32.30 is to be compared to the IAEA Generic 10 MW Reactor work prepared by INTERATOM [4] which quoted 32.5 for what appears to be the same statistical bound. INTERATOM used Safety Standards of the Nuclear Safety Standards Commission (KTA) number KTA 3101.1, “Design of Reactor Cores of Pressurized Water and Boiling Water Reactors,” Part 1: Principles of Thermo-hydraulic Design (February 1980, but reaffirmed 12/85, 6/90, 6/95, 6/00. Section 5.2 of that document states: “For operating conditions in which a critical boiling condition should be excluded, the minimum allowable margin to the critical boiling condition shall be specified in such a way that there is a 95% probability that at least 95% of the fuel rods concerned are protected from film boiling or dry-out.”

Since we are most concerned when the true η could be larger than we have estimated, rather than smaller, it is better to compute the single-sided limiting probability $P(X < 0.95)$. This is because the FIR computed by PLTEMP is smaller for larger input ETA. If the supplied ETA is too small, the computed margin of safety implied by the FIR will be non-conservative. For comparison, from the normal distribution using $a = -\infty$, $b = 1.64$ yields $P(\eta < 30.998) = 0.95$. But using the Student “ t ” distribution, using $a = -\infty$, $b = 1.666$, yields $P(\eta < 31.09) = 0.95$. This yields a 95% confidence interval that 95% of the *rectangular channel* data measured by future measurements will not exceed 31.09.

We recommend that the limiting value for ETA be 32.5, consistent with the recommendation in [4], even though it is more conservative than the value of 31.09 that is computed above.

3. WORLD DATA ON FLOW INSTABILITY

Duffy and Hughes [5] in 1991 prepared a table of world data on flow instability measurements. This information, collected from [1, 6-14], was updated by them to SI units. It includes bundle data as well as channel or tube data. Duffy and Hughes also attempted to show the parametric

dependences of flow instability measurements, and gave various predictive equations for the minimum mass flux at onset of flow instability. I have tried a number of their equations (17, 18, 26), finding very poor agreement with the W&F data. The trends look good, but the magnitudes are very far off.

Table VII-5. World Measured Data on Flow Instability

Author and Ref.	Type; flow direction	De, mm	L, m	Pressure, MPa	Heat Flux, kW/m ²	Mass flux, kg/m ² s
Costa [6]	Channel; up	38	0.6	0.17	200-4000	150-6900
Mirshak [7]	Tube; down	6.2; 9.44	4.267	0.10	195-1248; 446-1715	879-4883; 1221-4883
Whittle & Forgan [1]	Channel; up and down; tube, up	2.79-6.45	0.41; 0.61	0.12; 0.17	420-1480	917-9840
Qureshi <i>et al.</i> [8]	Annulus/tube; down	31.75; 18.8	1.83; 2.44	0.14; 0.24; 0.45	69-274; 1262-3156	2593-11161; 146-533; 1792-4992
Chen & King [9]	Annulus/tube; down	6.8; 12.7	3.57	0.19	1540-2830	4258-9712
D'Arcy [10]	Parallel/tube; up	13.26	3.05	7.0	275-893	293-1318
Massini <i>et al.</i> [11]	Parallel/annulus; up	20-30	3.00	1.0; 3.0; 5.0	30-400	180-370
Nylund <i>et al.</i> [12,13]	Tube bundle; up	36.6	4.37	5.2	480-900	570-820
Enomoto <i>et al.</i> [14]	Parallel bundle; up	20.5	3.71	6.86	366-811	278-660

4. COMPARISONS WITH THE THERMAL-HYDRAULIC TEST LOOP (THTL)

M. Siman-Tov *et al.* [15, 16] conducted experiments that were very similar to those of Whittle and Forgan. The THTL heated channel dimensions were very close to those of W&F (1.27 mm channel gap and 12.7 or 25.4 mm channel width, by 507 mm heated length), but the pressures and coolant velocities extended much higher (0.175 MPa-2.84 MPa exit pressure; 2.8-28.4 m/s exit velocity). The tests were conducted with light water in up-flow, with most cases using an inlet temperature near 45 C. The heat flux range was 0.7-18 MW/m². In addition to determining the pressure drop minimum at the onset of flow excursion, some of these tests also continued on to actual critical heat flux conditions. The axial power profile depends upon the resistivity of the aluminum heater, which varies with temperature. Consequently the axial power profile is not quite flat, but peaked toward the exit with a peak/average heat flux ratio of 1.07. The measured axial heat flux profile as shown in Fig. VII-1 was modeled in the PLTEMP calculations. Also shown in Fig. VII-1 is a highly-peaked axial profile more like a case with control rods half-inserted, having a peak/average ratio of 1.474. Results obtained using this second profile will be discussed later in this memo.

relative power density

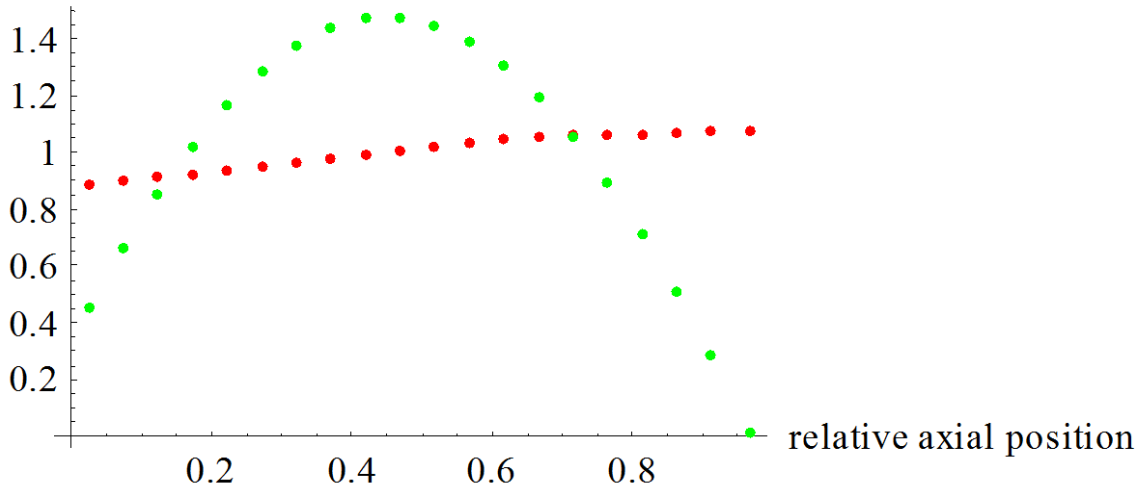


Fig. VII-1. THTL Axial Power Profile (inlet at position $x = 0$)

Table VII-1 of [15] provides sufficient information with which to model the tests in PLTEMP. The onset of significant void (OSV), i.e., onset of bubble departure from the heated wall, always occurs prior to OFI at a slightly higher flow than the OFI on the ΔP versus flow plot¹⁸ (when the flow is gradually decreased at constant heat flux). This was also tentatively pointed out earlier by Whittle and Forgan¹. As a result, an OSV correlation is used to provide a conservative estimate of OFI¹⁸. The Saha-Zuber correlation¹⁷, an OSV correlation, has been quite successful in predicting various experimental data for OSV and OFI¹⁸. The ORNL Advanced Neutron Source Reactor design team proposed the following flow instability correlation, which is a modification of the Saha-Zuber correlation [17] for onset of significant void (OSV). The flow is stable if the Stanton number is smaller than the right hand side of the correlation, and unstable if the Stanton number is greater.

$$St = q / (G C_p \Delta T_{sub0}) = 0.0065$$

$$Pe > 70,000, \text{ Saha-Zuber}$$

$$St = q / (G C_p \Delta T_{sub0}) = 0.0065 \eta_{sub}$$

$$Pe > 70,000, \text{ ORNL ANSR}$$

where $\eta_{sub} = 0.55 + 11.21/\Delta T_{sub0}$ is the proposed sub-cooling correction factor. The Stanton number is much better fitted at low exit sub-cooling (i.e. less than 20 C) by the ORNL ANSR modification. This new correlation was added to the edits from PLTEMP V3.0 as a Flow Excursion Ratio, FER. It is the minimum ratio of predicted excursion heat flux to actual flux, at all axial nodes and all heated surfaces. **The flow is stable if the ORNL FER is greater than 1.0, and unstable if FER is smaller than 1.0.**

Table VII-6 gives some results for tests carried out in the THTL that went beyond the minimum in the flow/pressure drop curve, to critical heat flux and burnout, even to melting of portions of the test section. The predictive ratios FIR and FER calculated by PLTEMP show their ability to predict these severe cases. A successful prediction of this severity requires that the FIR or FER be less than 1.

Table VII-6. THTL Critical Heat Flux Tests

Test	q, W/cm ²	ONBR	W&F FIR†	ORNL FER	Pe	q/(Tsat-Tb) kW/m ² -s	V _{exit} , m/s
CF115B	1280	0.64	0.919	0.44	232000	2248	16.65
CF328A	1260	0.64	0.918	0.43	187000	1929	13.42
CF622B	610	0.63	0.919	0.41	208000	2435	14.99
FE212A	1260	0.67	0.968	0.60	242000	1045	17.21
FE318B	214	0.74	0.972	0.74	56900	253.6	4.21
FE331A	1210	0.71	1.028	0.76	235000	615.7	17.54

† $\eta=32.5$

As can be seen in Table VII-6, the W&F prediction is correct for 5 of 6 cases, and is only off by 2.8% in the one test slightly missed. On the other hand, the ORNL FER is correct in all 6 cases.

Table VII-7 is a series of tests that looked for the pressure drop minimum to mark the onset of flow excursion. It shows that the W&F FIR averages out to 1.073. This means that it predicts onset of flow excursion at an average of 7.3% higher heat flux than actually measured. It is therefore not conservative, but only by a small margin. It is worth noting that the FIR is quite a good measure for any flow velocity in the tested range.

Table VII-7 also shows that the ORNL FER averages out to 0.936, while correctly predicting flow excursion for 8 of the 10 cases. It is worth noting that the FER does poorest at the lowest exit velocity tests with the lowest heat fluxes, where the criterion that the Peclet number should exceed 70,000 is not met. It does well for high-velocity tests of interest for the ANSR.

Table VII-7. THTL Flow Excursion Tests

	q, W/cm ²	ONBR	W&F FIR†	FER	Pe	q/(Tsat-Tb) kW/m ² -s	V _{exit} , m/s	η' minimum
CF115B	1180	0.72	1.044	0.81	232000	544.6	17.27	29.5
CF328A	1250	0.74	1.076	0.9	249000	491.6	18.6	35.3
CF622A	650	0.71	1.042	0.79	247000	601.1	18.42	28.6
FE212A	1260	0.72	1.045	0.81	248000	578.2	18.49	29.7
FE318B	220	0.8	1.062	1.01	61700	135.5	4.54	32.2
FE331A	1220	0.75	1.117	0.97	250000	446.4	18.71	39.3
FE620B	540	0.74	1.022	0.73	82000	231.4	6.12	24.7
FE713B	80	0.92	1.178	1.68	37800	49.8	2.7	53.1
FE511C	1900	0.71	1.065	0.83	328900	741.4	24.6	30.6
FE712B	190	0.8	1.075	0.83	37000	83.4	2.77	31.0

† $\eta=32.5$

Figure VII-2 shows the W&F test data and THTL test data as computed by PLTEMP. Clearly there is a smooth parametric dependence on exit coolant velocity that is not quite linear. And clearly the parameter group $q/(T_{sat}-T_b)$ in $\text{kW/m}^2\text{-s}$ captures much of the systematic effects over the computed parameter ranges.

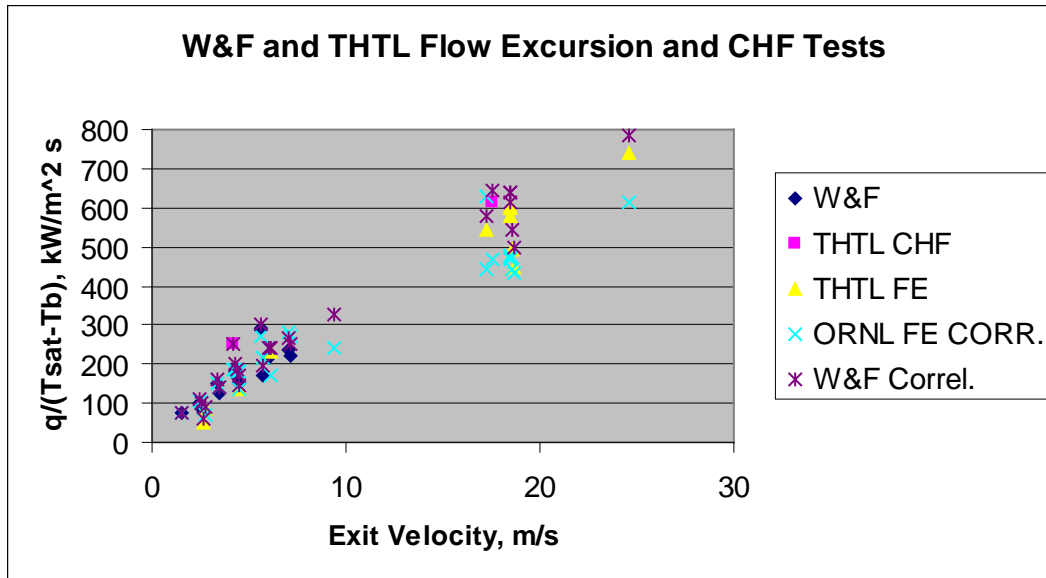


Fig. VII-2. Comparison of CHF and Flow Excursion Test Data with Correlations

The right-most column of Table VII-7 lists the minimum value of η' which was obtained by PLTEMP using the local heat flux. This value should be larger than 32.5 to be indicative of stability. One can see that test FE713B somehow is not properly predicted by any of FIR, or FER, or the η' method. The other flow excursion tests are predicted fairly well, in that 7 of 10 are predicted to be unstable and the other 3 are close to instability. The η' measure is not linear with power, so a value of 53.1 definitely cannot be interpreted as requiring 32.5/53.1 less power to achieve the edge of stability.

Effect of Axial Power Peaking on Stability Predictions

As an example, THTL case CF115B (flow excursion test) was examined for a range of powers in order to predict the precise power where a given predictor would become 1.000. Figure VII-3 shows the base condition, which uses the experimentally measured axial power profile (peak/average = 1.07).

Figure VI-4 shows the same PLTEMP case, but modified to have an axial power profile with a peak/average of 1.474, peaked toward the inlet. This case is similar to one with control rods half inserted. It was created by using a difference of $\sin(\theta)$ and $\cos(\theta)$ terms with the cosine weighted by 0.7.

It is clear that the W&F FIR is quite non-linear, and in fact yields the same predicted power ratio of 1.046. In other words, running the PLTEMP case with power scaled by a factor of 1.046 would yield FIR of 1.000. It is also clear that the ORNL FER is fairly linear, predicting a power scale factor of 0.938 for the base case and 1.028 for the peaked case. The peaked case would be permitted to run at 1.028/0.938 or 9.6% higher power than would the base case. This is because the correlation accounts for axial heat flux variation, and because the peak axial heat flux occurs well away from the channel exit. For the IAEA $\eta'/32.5$ measure, which also accounts for the local axial heat flux, the base power factor of 0.984 becomes 1.084 when highly peaked. The peaked case would be permitted to run at 1.084/0.984 or 10.2 % higher power than would the base case. Finally, one can see that the ORNL FIR and the IAEA η' measure both account for the axial power profile in quite similar ways, while the W&F FIR correlation only considers coolant channel exit conditions. It is interesting to note that accounting for a strong axial peaking by these two methods indicates a higher predicted power for onset of flow excursion than the simpler W&F method yields.

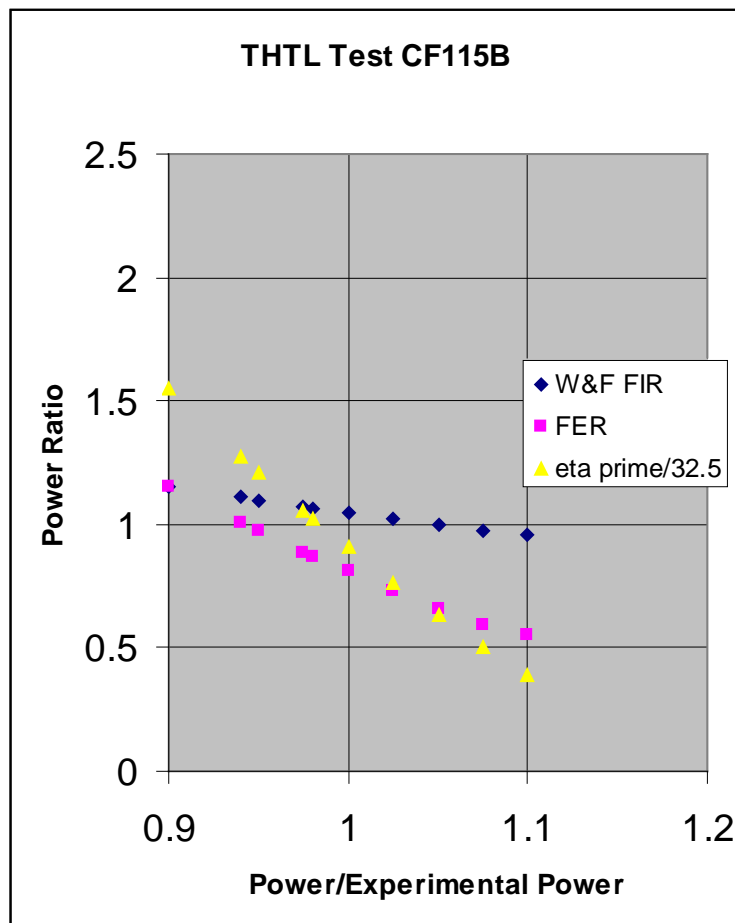


Fig. VII-3. Variation of Predictive Power Ratios FIR, FER, and $\eta'/32.5$ Near Instability: Base Axial Power Profile

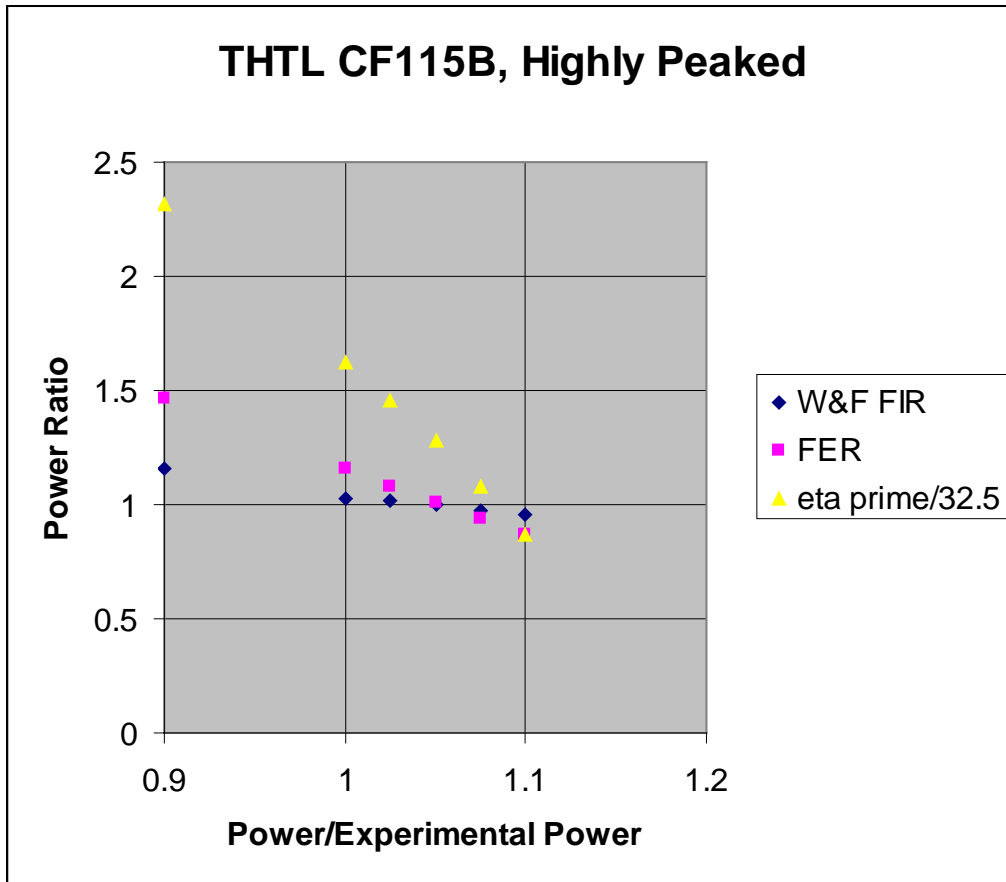


Fig. VI-4. Variation of Predictive Power Ratios FIR, FER, and $\eta'/32.5$ Near Instability: Highly Peaked Axial Power Profile

5. CONCLUSIONS

A. Whittle and Forgan Test

1. The remaining 8% error in mass flow rate falls within the measurement errors of the W&F experiments. Consequently the PLTEMP FIR for these 8 cases correctly represents the prediction of the onset of flow instability.
2. PLTEMP also computes a local value of η' on all heated surfaces. The code edits the minimum value of η' . From Table VII-4, the average minimum computed value of η' is 26.0 and an average measured value is 26.2. The very close agreement confirms that the computed η' is a valid measure of the onset of flow instability for channels with two-sided heating. As an example, Figure VI-5 shows the axial distribution of η' computed by PLTEMP for one of the cases examined. The η' appears to be of value for assessing highly peaked axial power profiles because it includes the effect of local heat flux while the W&F FIR does not.

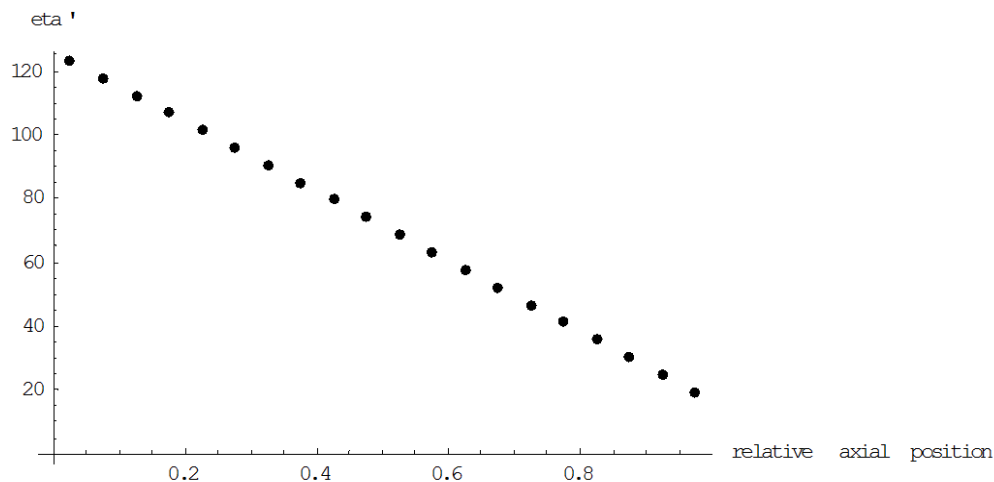


Fig. VI-5. PLTEMP Computed $\eta' = V\Delta T_{sub0}/q$ for W&F Test Section 1: 250 w/cm² Flat Power Profile

3. It is unclear at this time what validity, if any, these two measures of flow instability have for channels with heating on only one side. The theory takes into account the heated length and heated hydraulic diameter, so it in principle should be correct. The analyst must keep in mind that the W&F measurements span $83 < L_H/D_H < 191$. We have no data for one-sided heating.
4. The German (IAEA) limiting value for η of 32.5 based on W&F data is close enough to my own statistical analysis result that we can use it in RERTR for the same purpose of establishing a baseline for rectangular channels.
5. The Duffy and Hughes parametric equations show trends only. They have poor predictive value as limits on mass flux at the onset of flow instability.
6. The W&F data are mostly for a flat power profile. Some tests (in test section 1A) used a profile that was flat over the inlet half, falling linearly to 68% at the exit. This shape has an axial peak/average ratio of about 1.09. It shows onset of flow instability very similar to the flat axial profile measurements. Reactor conditions with a highly-peaked axial profile will push the simple W&F method, such that an additional measure of conservatism should be applied.

B. THTL Tests

1. The ORNL FER is excellent as a flow excursion predictor for high-velocity, high heat flux conditions as needed to design the ANSR. It should also apply well to axially peaked power profiles, as it is not a global measure like the W&F FIR.

2. The W&F FIR performs very well even for the high-velocity and high heat flux conditions examined by the THTL experiments. It seems to be more consistent than the FER as other test conditions change (geometry, pressure, sub-cooling). Using $\eta=32.5$ performs very well indeed. Unfortunately there are no measured data with a highly-peaked axial profile, which should show how the W&F FIR becomes less accurate.

6. RECOMMENDED PROCEDURE TO FIND MARGIN TO FLOW INSTABILITY

Supply η of 32.5 for the Whittle and Forgan method. Find the “MINIMUM FLOW INSTABILITY POWER RATIO.” Then search on power, by scaling the base power by the FIR. Repeat until you find FIR=1. The ratio of that power to the base power is the best estimate of the margin to flow instability. Of course, one must keep in mind that PLTEMP is a single-phase code, and calculations that exceed T_{sat} will be incorrect. There is a message produced:

“WARNING IN FINLED: NOT SUBCOOLED”

If that condition occurs, use the FIR for the highest power that does not exceed T_{sat} to extrapolate.

Also find the FER.

For the Bowring η' method, note the minimum η' for the base power. Try searching for the power at which η' becomes the value you desire (such as $32.5 \cdot 1.5$ safety factor). Then the true safety factor is the ratio of the searched power to the base power. Note that PLTEMP obtains η' at the midpoint of each axial node, for each heated plate side.

Compare key parameters such as D_e , L , L_H/D_H , system pressure, mass flux, and heat flux for your reactor conditions with the flow instability test database. If your reactor conditions are an extrapolation from this database, then a greater margin for uncertainty may be necessary. Compare the three predictions of flow instability: FER, FIR, and η' .

NOMENCLATURE

C_p	Specific heat of coolant
D_e	Equivalent diameter
D_H	Heated equivalent diameter
G	Mass flow rate per unit area, $\text{kg/m}^2\text{-s}$
L	Channel length
L_H	Channel heated length
η'	$V\Delta T_{\text{sub0}}/q$, in units of $\text{K}\cdot\text{cm}^3/\text{J}$ when V is in cm/s , temperature difference is in K , and q is in W/cm^2
Pe	Peclet number, $G C_p D_H/k$
P_H	Heated perimeter
L_H	Heated length
P_W	Wetted perimeter
q	Heat flux
St	Stanton number, $q/(G C_p \Delta T_{\text{sub0}})$
$T_{\text{sat,exit}}$	Saturation temperature at channel exit
T_{in}	Inlet temperature
T_{out}	Outlet temperature
V	Coolant velocity
ΔT_{sub0}	Exit subcooling, $T_{\text{sat,exit}} - T_{\text{out}}$
ΔT_c	Coolant temperature rise in channel, $T_{\text{out}} - T_{\text{in}}$
$\Delta T_{\text{sat,exit}}$	Inlet subcooling referred to the exit saturation temperature, $T_{\text{sat,exit}} - T_{\text{in}}$

REFERENCES

1. R. H. Whittle and R. Forgan, "A Correlation for the Minima in the Pressure Drop Versus Flow-Rate Curves for Sub-Cooled Water Flowing in Narrow Heated Channels," *Nuclear Engineering and Design* 6, pp. 89-99 (1967).
2. R. W. Bowring, "Physical Model, Based on Bubble Detachment and Calculation of Voidage in the Sub-cooled Region of a Heated Channel." OECD Halden Reactor Project Report. HPR-10 (1962).
3. Tewfik Hamidouche and Anis Bousbia-salah, "RELAP5/3.2 Assessment Against Low Pressure Onset of Flow Instability in Parallel Heated Channels," *Annals of Nuclear Energy* 33, pp. 510-520 (2006).
4. INTERATOM, on behalf of the Minister of Research and Technology of the Federal Republic of Germany, Appendix A-1 of IAEA-TECDOC-643, "Research Reactor Core Conversion Guidebook," Vol. 2: Analysis (Appendices A-F), International Atomic Energy Agency, Vienna, (April 1992).
5. R. B. Duffey and E. D. Hughes, "Static Flow Instability Onset in Tubes, Channels, Annuli, and Rod Bundles," *Int. J. Heat Mass Transfer* Vol. 34, No. 10, pp. 2483-2496 (1991).
6. J. Costa, M. Courtaud, S. Elberg and J. Lafay, "La redistribution de débit dans les réacteurs de recherche," *Bull. Inform. Sci. Tech. Commissariat à l'Energie Atomique*, No. 117, 89-103 (1967).
7. S. Mirshak, "Transient Flow of Boiling Water in Heated Tubes," DOE Report DP-301TL (1958).
8. Z. H. Qureshi, B. S. Johnson and K. Chen, "Flow Instability in Vertical Heated Tubes under Down-flow Conditions," *Proc. ANS Workshop on Safety of Uranium-Aluminum Fueled Reactors*, Idaho Falls, Idaho, 14-16 March (1989).
9. K. F. Chen and J. F. King, "FLOWTRAN Benchmarking with Onset of Flow Instability Data from 1963 Columbia University Experiments," DOE Report DPST-88-666 (1989).
10. D. F. D'Arcy, An Experimental Investigation of Boiling Channel Flow Instability, *Proc. Symp. on Two-phase Flow Dynamics*, EUR 4288e, Vol. II, pp 1173-1223 (1967).
11. G. Masini, G. Possa and F. A. Tacconi, Flow Instability Thresholds in Parallel Heated Channels, *Energ. Nucl.* **15**, 777-786 (1968).

12. O. Nylund, K. M. Becker, R. Eklund, O. Gelius, A. Jensen, D. Malnes, A. Olsen, Z. Rouhani, J. Skaug and F. Akerhielm, Hydrodynamic and Heat Transfer Measurements on a Full-scale Simulated 36-rod Marviken Fuel Element with Non-uniform Radial Heat Flux Distribution, AB-Atomenergi ASEA-ATOM Report FRIGG-4, R4-502/R1-1253 (1970).
13. O. Nylund, K. M. Becker, R. Eklund, O. Gelius, I. Haga, A. Jensen, D. Malnes, A. Olsen, Z. Rouhani, J. Skaug and F. Akerhielm, Hydrodynamic and Heat Transfer Measurements on a Full-scale Simulated 36-rod Marviken Fuel Element with Non-uniform Radial Heat Flux Distribution, AB-Atomenergi ASEA-ATOM Report FRIGG-3, R4-494/R1-1154 (1969).
14. T. Enomoto, S. Muto, T. Ishizuka, A. Tanabe, T. Mitsutake and M. Sakurai, Thermal hydraulic stability experiments in rod bundle, Proc. Third Int. Topical Meeting on Reactor Thermal hydraulics, 9.B, Newport, Rhode Island (1985).
15. M. Siman-Tov, D. K. Felde, G. Farquharson, J. L. McDuffee, M. T. McFee, A. E. Ruggles, M. W. Wendel, and G. L. Yoder, FY 1995 Progress Report on the ANS Thermal-Hydraulic Test Loop Operation and Results, ORNL/TM-12972, Oak Ridge National Laboratory (July 1997).
16. M. Siman-Tov, D. K. Felde, J. L. McDuffee, and G. L. Yoder, Experimental Study of Static Flow Instability in Sub-cooled Flow Boiling in Parallel Channels, 4th ASME/JSME Thermal Engineers Joint Conference, Maui, Hawaii, CONF-950113-1, Oak Ridge National Laboratory (January 1995).
17. P. Saha and N. Zuber, Point of Net Vapor Generation and Vapor Void Fraction in Subcooled Boiling, *Proceedings of the 5th International Heat Transfer Conference*, Tokyo, IV, 175-179 (1974).
18. J. E. Kennedy, G. M. Roach, Jr., M. F. Dowling, S. I. Abdel-Khalik, S. M. Ghiaasiaan, S. M. Jeter, and Z. H. Qureshi, "The Onset of Flow Instability in Uniformly Heated Horizontal Microchannels," *Transactions of the ASME*, Vol. 122, pp. 118-125 (2000).

APPENDIX VIII. ANALYTICAL SOLUTION FOR RADIAL TEMPERATURE DISTRIBUTION IN A MULTI-TUBE FUEL ASSEMBLY

(M. Kalimullah, E. E. Feldman, and A. P. Olson)

1. Description of the Analytical Solution

In a nuclear reactor, the major heat source is fuel. But some gamma radiation is deposited directly in cladding and coolant, making them minor heat sources. To model this, an analytical solution has been obtained using *Mathematica* in radial geometry for a multi-tube fuel assembly with heat sources in all four materials, i.e., inner cladding, fuel meat, outer cladding, and coolant. The gap resistances at (1) the meat-inner cladding interface and (2) the meat-outer cladding interface of each fuel tube are also included in the solution. This solution is being implemented in the PLTEMP/ANL code, tested, and verified for some sample problems.

Figure VIII-1 shows a vertical section of an experimental nuclear reactor fuel assembly consisting of several coaxial fuel tubes that are cooled by coolant channels of annular cross section. In this formulation, each fuel tube is assumed to be different from the others, and each coolant channel is assumed to have a different area and flow rate than the others. The gap resistances at the fuel meat interface with the inner and outer claddings are included. The method consists of setting up $K+1$ simultaneous linear algebraic equations in $K+1$ bulk coolant temperatures, $T_{bc,k,n}$, for $k = 1$ to $K+1$ in a slice of the fuel assembly shown in Fig. VIII-1.

Symbols Used:

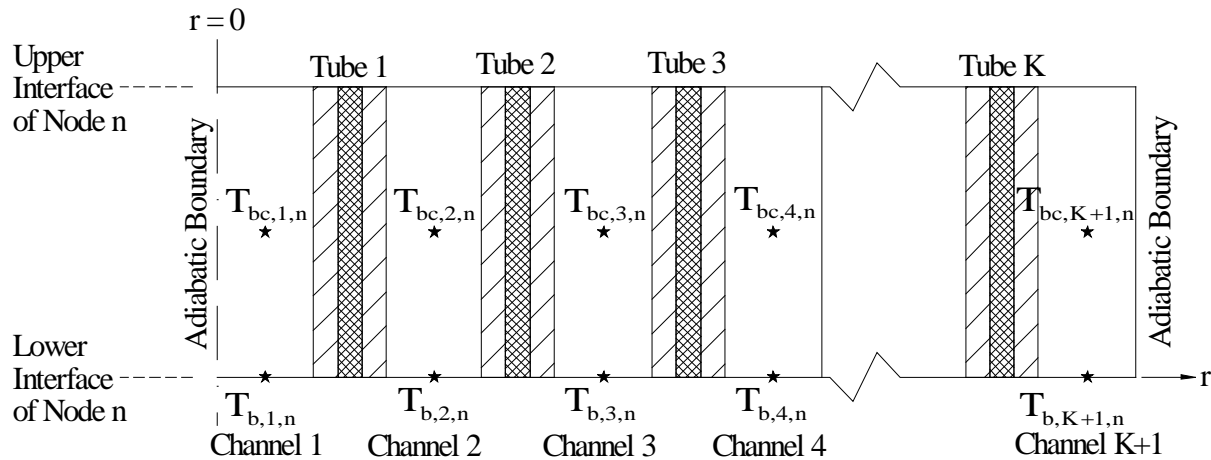


Fig. VIII-1. An Axial Slice of Fuel Assembly Showing a Heat Transfer Axial Node

- K = Number of fuel tubes in an assembly
- $T_{bc,k,n}$ = Coolant bulk temperature in channel k at the *center* of heat transfer axial node n , (C)
- $T_{b,k,n}$ = Coolant bulk temperature in channel k at the *entry* to heat transfer axial node n , (C)
- $h_{g1,k}$ = Gap conductance at the fuel meat and inner cladding interface, ($W/m^2 \cdot ^\circ C$)
- $h_{g2,k}$ = Gap conductance at the fuel meat and outer cladding interface, ($W/m^2 \cdot ^\circ C$)

- $h_{1,k,n}$ = Convective heat transfer coefficient on the inside of fuel tube k (W/m²-C)
 $h_{2,k,n}$ = Convective heat transfer coefficient on the outside of fuel tube k (W/m²-C)
 $K_{a,k}$ = Thermal conductivity of inner cladding of fuel tube k (W/m-C)
 $K_{b,k}$ = Thermal conductivity of fuel meat in tube k (W/m-C)
 $K_{c,k}$ = Thermal conductivity of outer cladding of fuel tube k (W/m-C)
 P_n = Coolant pressure in a channel at the entry to heat transfer axial node n (Pa)
 $q_{a,k,n}$ = Volumetric heat source in inner cladding of tube k in axial node n (W/m³)
 $q_{b,k,n}$ = Volumetric heat source in fuel meat of tube k in axial node n (W/m³)
 $q_{c,k,n}$ = Volumetric heat source in outer cladding of tube k in axial node n (W/m³)
 $q_{w,k,n}$ = Volumetric heat source in *coolant* (directly deposited in water) in coolant channel k in axial node n (W/m³)
 r = Radial position coordinate with $r = 0$ at the common axis of fuel tubes (meter)
 $r_{a,k}$ = Inner radius of fuel tube k, (m)
 $r_{b,k}$ = Inner radius of meat in fuel tube k, (m)
 $r_{c,k}$ = Outer radius of meat in fuel tube k, (m)
 $r_{d,k}$ = Outer radius of fuel tube k, (m)
 $r_{max,k}$ = Radial position of maximum fuel temperature in tube k, (m)
 $R_{g1,k}$ = $1/h_{g1,k}$ = Gap resistance at the fuel meat and inner cladding interface, (m²-°C/W).
It is *zero for good meat-cladding contact* present in research reactor fuels.
 $R_{g2,k}$ = $1/h_{g2,k}$ = Gap resistance at the fuel meat and outer cladding interface, (m²-°C/W).
It is *zero for good meat-cladding contact* present in research reactor fuels.
 $t_{a,k}$ = Thickness of inner cladding of fuel tube k (meter)
 $t_{b,k}$ = Fuel meat thickness in tube k (meter)
 $t_{c,k}$ = Thickness of outer cladding of fuel tube k (meter)
 W_k = Coolant mass flow rate in channel k (kg/sec)
 X_k = Maximum fuel temperature's radial position expressed as the areal fraction $\frac{(r_{max,k}^2 - r_{b,k}^2)}{(r_{c,k}^2 - r_{b,k}^2)}$
of the meat cross-sectional area. The subscript n is dropped for brevity.

The solution of heat conduction equations in the inner cladding, the fuel meat, and the outer cladding of a tube k are given below. For brevity, the index k has been dropped in Eqs. (1) to (20).

Temperature distribution in the inner cladding of fuel tube:

$$\frac{d}{dr} \left(r \frac{dT_a}{dr} \right) + \frac{q_a r}{K_a} = 0 \quad (1)$$

$$T_a(r) = A_2 + A_1 \text{Log}(r/r_b) - \frac{q_a r^2}{4K_a} \quad (r = r_a \text{ to } r = r_b = r_a + t_a), \quad (2)$$

Temperature distribution in the fuel meat:

$$\frac{d}{dr} \left(r \frac{dT_b}{dr} \right) + \frac{q_b r}{K_b} = 0 \quad (3)$$

$$T_b(r) = A_4 + A_3 \text{Log}(r/r_c) - \frac{q_b r^2}{4K_b} \quad (r = r_b \text{ to } r = r_c = r_b + t_b), \quad (4)$$

Temperature distribution in the outer cladding of fuel tube:

$$\frac{d}{dr} \left(r \frac{dT_c}{dr} \right) + \frac{q_c r}{K_c} = 0 \quad (5)$$

$$T_c(r) = A_6 + A_5 \text{Log}(r/r_d) - \frac{q_c r^2}{4K_c} \quad (r = r_c \text{ to } r = r_d = r_c + t_c), \quad (6)$$

The six arbitrary constants $A_1, A_2, A_3, A_4, A_5,$ and A_6 are determined by six boundary and interface conditions as follows: a convective boundary condition at the tube inner radius, a convective boundary condition at the tube outer radius, and two matching conditions (equal temperatures and equal heat fluxes) at each of the two meat-cladding interfaces. The interface conditions account for the temperature jump due to the gap resistances R_{g1} at the fuel meat interface with the inner cladding, and the jump due to the gap resistance R_{g2} at the fuel meat interface with the outer cladding. These boundary/interface conditions are shown in Fig. VIII- 2 with their equality signs aligned with the corresponding boundary or interface.

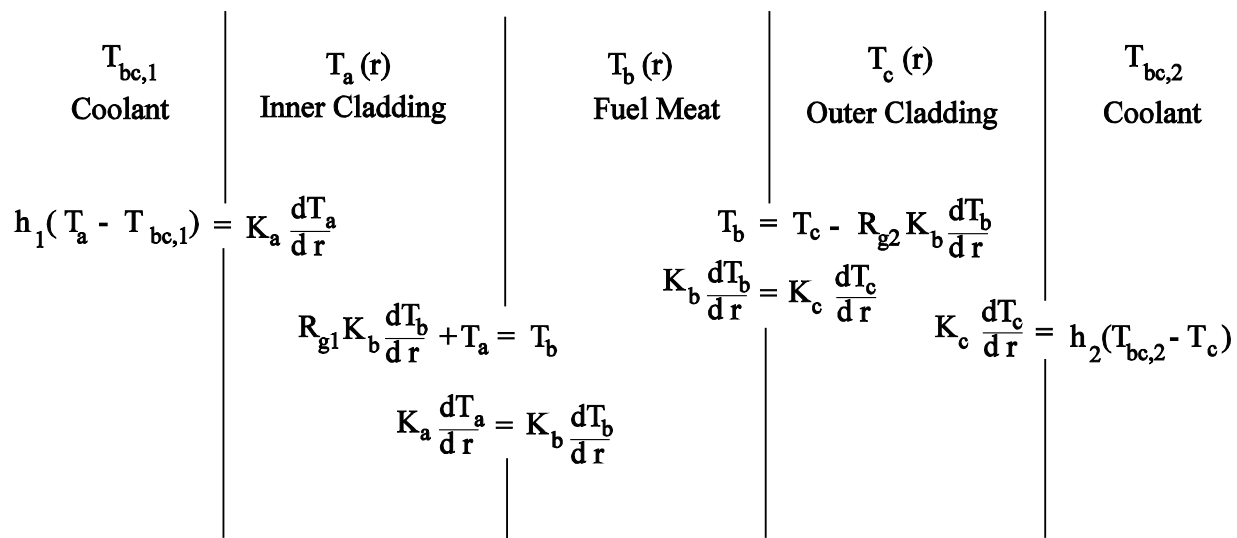


Fig. VIII-2. Boundary/Interface Conditions for Temperature and Heat Flux in a Fuel Tube

For a *single fuel tube*, the inner radius and the film coefficients at the inner and outer surfaces, i.e., parameters r_a, h_1 and h_2 , could be greater than zero or equal to zero. This leads mathematically to a total of 6 cases (types of boundary conditions) tabulated below.

Case	r_a	h_1	h_2	Physically Possible?
1	$r_a > 0$	$h_1 > 0$	$h_2 > 0$	Yes
2	$r_a > 0$	$h_1 = 0$	$h_2 > 0$	Yes
3	$r_a = 0$	h_1 irrelevant	$h_2 > 0$	Yes
4	$r_a > 0$	$h_1 > 0$	$h_2 = 0$	Yes
5	$r_a > 0$	$h_1 = 0$	$h_2 = 0$	Not Possible
6	$r_a = 0$	h_1 irrelevant	$h_2 = 0$	Not Possible

Out of these 6 cases, only the first four are physically possible because of two reasons: (1) Both heat transfer coefficients h_1 and h_2 cannot be zero together in a steady-state problem with heat source. If one of them is zero, then the other must be non-zero. (2) If r_a is zero, i.e., the innermost fuel tube is solid, then the outer heat transfer coefficients h_2 must be non-zero. It is because there is no material (contacting the inner radius r_a) to transfer the heat to.

The six arbitrary constants $A_1, A_2, A_3, A_4, A_5,$ and A_6 were found by *Mathematica* for the four possible cases, and are given by Eqs. (7) through (15).

$$A_1 = \frac{r_a R}{K_a} \left[\frac{q_a r_a}{2 h_1} + \frac{S}{4} + \frac{1}{2 h_2 r_c r_d} \left\{ q_a r_b (r_b r_c + R_{g1} h_2 r_c r_d + R_{g2} h_2 r_b r_d) \right. \right. \\ \left. \left. + q_b (r_c^2 - r_b^2) (r_c + R_{g2} h_2 r_d) + q_c r_c (r_d^2 - r_c^2) \right\} \right. \\ \left. + (T_{bc,2} - T_{bc,1}) + \frac{1}{2 K_b K_c} \left\{ K_b (q_b - q_c) r_c^2 \text{Log}(r_d/r_c) \right. \right. \\ \left. \left. - K_c (q_b - q_a) r_b^2 \text{Log}(r_c/r_b) - K_b (q_b - q_a) r_b^2 \text{Log}(r_d/r_c) \right\} \right] \quad (\text{for case 1}) \quad (7a)$$

$$A_1 = \frac{q_a r_a^2}{2 K_a} \quad (\text{for cases 2 and 3}) \quad (7b)$$

$$A_1 = \frac{(q_a - q_b) r_b^2 + (q_b - q_c) r_c^2 + q_c r_d^2}{2 K_a} \quad (\text{for case 4}) \quad (7c)$$

The quantities R and s used in case 1 are given by Eqs. (8) and (9). In the other three physically possible cases (cases 2, 3, and 4), the quantity R is not used, and hence it is set to zero. Note that Log is the natural logarithm.

$$R = \frac{h_1 h_2 r_d}{h_1 r_a + h_2 r_d + h_1 h_2 r_a r_d} \left\{ \frac{\text{Log}(r_b/r_a)}{K_a} + \frac{\text{Log}(r_c/r_b)}{K_b} + \frac{\text{Log}(r_d/r_c)}{K_c} + \frac{R_{g1}}{r_b} + \frac{R_{g2}}{r_c} \right\} \quad (\text{for case 1}) \quad (8a)$$

$$R = 0 \quad (\text{for cases 2, 3, and 4}) \quad (8b)$$

$$S = \frac{q_a(r_b^2 - r_a^2)}{K_a} + \frac{q_b(r_c^2 - r_b^2)}{K_b} + \frac{q_c(r_d^2 - r_c^2)}{K_c} \quad (9)$$

$$A_3 = \frac{(q_b - q_a)r_b^2 + 2K_a A_1}{2K_b} \quad (10)$$

$$A_5 = \frac{(q_b - q_a)r_b^2 - (q_b - q_c)r_c^2 + 2K_a A_1}{2K_c} \quad (11)$$

$$A_6 = T_{bc,2} + \frac{q_c r_d^2}{4K_c} + \frac{1}{h_2} \left(\frac{q_c r_d}{2} - \frac{K_c A_5}{r_d} \right) \quad (\text{for cases 1, 2 and 3}) \quad (12a)$$

$$A_6 = T_{bc,1} - \frac{S}{4} + \frac{q_c r_d^2}{4K_c} + \frac{1}{h_1} \left(\frac{K_a A_1}{r_a} - \frac{q_a r_a}{2} \right) \\ + A_1 \text{Log}(r_b/r_a) + A_3 \text{Log}(r_c/r_b) + A_5 \text{Log}(r_d/r_c) \quad (\text{for case 4}) \quad (12b) \\ + R_{g1} \left(\frac{K_b A_3}{r_b} - \frac{q_b r_b}{2} \right) + R_{g2} \left(\frac{K_b A_3}{r_c} - \frac{q_b r_c}{2} \right)$$

$$A_4 = \frac{q_b r_c^2}{4K_b} - \frac{q_c r_c^2}{4K_c} + A_6 - A_5 \text{Log}(r_d/r_c) + R_{g2} \left(\frac{q_b r_c}{2} - \frac{K_b A_3}{r_c} \right) \quad (13)$$

$$A_2 = T_{bc,1} + \frac{q_a r_a^2}{4K_a} + A_1 \text{Log}(r_b/r_a) + \frac{1}{h_1} \left(\frac{K_a A_1}{r_a} - \frac{q_a r_a}{2} \right) \quad (\text{for cases 1 and 4}) \quad (14a)$$

$$A_2 = \frac{q_a r_b^2}{4K_a} - \frac{q_b r_b^2}{4K_b} + A_4 - A_3 \text{Log}(r_c/r_b) + R_{g1} \left(\frac{q_b r_b}{2} - \frac{K_b A_3}{r_b} \right) \quad (\text{for cases 2 and 3}) \quad (14b)$$

The following mathematically equivalent equation for A_4 is used only for testing purposes.

$$A_4 = \frac{q_b r_b^2}{4K_b} - \frac{q_a r_b^2}{4K_a} + A_2 + A_3 \text{Log}(r_c/r_b) + R_{g1} \left(\frac{K_b A_3}{r_b} - \frac{q_b r_b}{2} \right) \quad (\text{for testing}) \quad (15)$$

For simplicity and brevity, the tube index k and the level index n have been omitted from the symbols used above in the analytical solution to find temperature profile in the thickness of a single fuel tube. As shown in Fig. VIII-3 for an axial slice n of the assembly, the heat fluxes from a tube k to its inner and outer adjacent coolant channels are defined as $q_{1,k,n}''$ and $q_{2,k,n}''$ respectively, and have corresponding heat transfer areas $A_{h1,k,n}$ and $A_{h2,k,n}$ where

$$q_1'' = h_1 \{ T_a(r_a) - T_{bc,1} \} = \text{Heat flux into the coolant on the inside of fuel tube } k = q_{1,k,n}''$$

- $q_2'' = h_2 \{ T_c(r_d) - T_{bc,2} \} = \text{Heat flux into the coolant on the outside of fuel tube } k = q_{2,k,n}''$
 $A_{h1,k,n} = \text{Surface area on the } \textit{inside} \text{ of fuel tube } k \text{ for heat transfer into the coolant channel axial node } n. \text{ It is the tube circumference (based on radius } r_{a,k}) \text{ times the axial height of the node.}$
 $A_{h2,k,n} = \text{Surface area on the } \textit{outside} \text{ of fuel tube } k \text{ for heat transfer into the coolant channel axial node } n. \text{ It is the tube circumference (based on radius } r_{d,k}) \text{ times the axial height of the node.}$

With the aid of Mathematica, these two heat fluxes can be expressed as

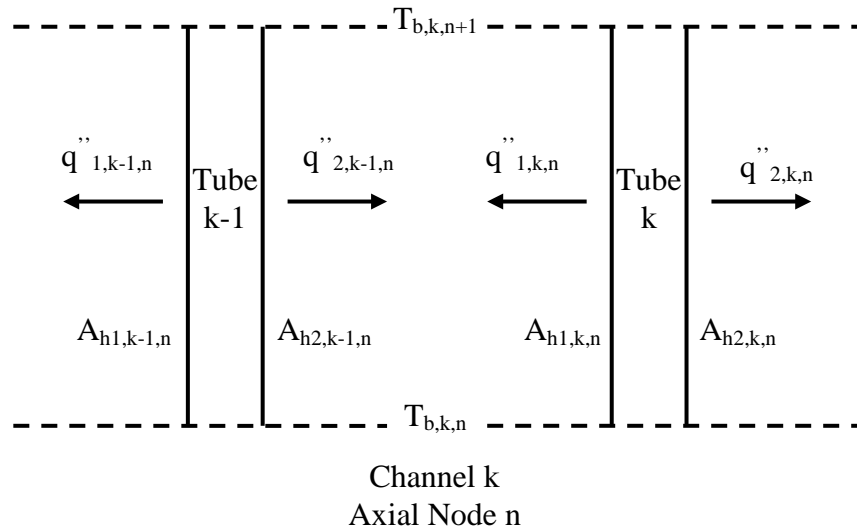


Fig. VIII-3. Heat Fluxes into a Coolant Heat Transfer Node

$$q_1'' = \alpha + R(T_{bc,2} - T_{bc,1}) \quad (16)$$

$$q_2'' = Q - (r_a/r_d)q_1'' \quad (17)$$

where Q and α are given by

$$Q = \frac{q_a(r_b^2 - r_a^2) + q_b(r_c^2 - r_b^2) + q_c(r_d^2 - r_c^2)}{2r_d} \quad (18)$$

$$\alpha = R \left(\frac{Q}{h_2} + \frac{B}{2} + \frac{S}{4} \right) \quad (\text{for case 1}) \quad (19a)$$

$$\alpha = Q(r_d/r_a) \quad (\text{for case 4}) \quad (19b)$$

$$\alpha = 0 \quad (\text{for cases 2 and 3}) \quad (19c)$$

The quantity B used in Eq. (19a) to find the quantity α which is used in Eqs. (16) and (17) for the heat flux q_1'' is given by Eq. (20a). If $r_a = 0$, the quantity B is not required because R and q_1'' are then zero. Hence the quantity B is set to zero if $r_a = 0$.

$$B = -\frac{\text{Log}(r_b/r_a)}{K_a} q_a r_a^2 + \frac{\text{Log}(r_c/r_b)}{K_b} (q_a r_b^2 - q_a r_a^2 - q_b r_b^2) + \frac{\text{Log}(r_d/r_c)}{K_c} (q_a r_b^2 - q_a r_a^2 + q_b r_c^2 - q_b r_b^2 - q_c r_c^2) \quad (\text{for case 1}) \quad (20a)$$

$$+ \frac{R_{g1} q_a (r_b^2 - r_a^2)}{r_b} + \frac{R_{g2} \{q_a (r_b^2 - r_a^2) + q_b (r_c^2 - r_b^2)\}}{r_c} \quad (\text{for cases 2, 3, and 4}) \quad (20b)$$

Up to this point, the equations were written without an index for identifying the fuel tube and axial level. When the tube index k and the axial level index n are included, Eqs. (16) and (17) can be rewritten as follows:

$$q_{1,k,n}'' = \alpha_{k,n} + R_{k,n} (T_{bc,k+1,n} - T_{bc,k,n}) \quad (21)$$

$$q_{2,k,n}'' = Q_{k,n} - (r_{a,k}/r_{d,k}) q_{1,k,n}'' \quad (22)$$

The heat balance for coolant axial node n of channel k (between fuel tubes k-1 and k) can be written as Eq. (23) below, accounting for the coolant enthalpy dependence on both pressure and temperature. The quantity in the square parentheses on the left hand side of Eq. (23) is the change in coolant enthalpy $h(P,T)$ from the inlet to outlet of the axial node n. Equation (24) is obtained from Eq. (23) by expressing the enthalpy change in terms of the partial derivatives of enthalpy with respect to temperature and pressure.

$$W_k [h(P_{n+1}, T_{b,k,n+1}) - h(P_n, T_{b,k,n})] = q_{w,k,n} V_{k,n} + A_{h1,k,n} q_{1,k,n}'' + A_{h2,k-1,n} q_{2,k-1,n}'' \quad (23)$$

$$W_k [(T_{b,k,n+1} - T_{b,k,n}) C_{p,k,n} + C_{T,k,n} (P_{n+1} - P_n)] = q_{w,k,n} V_{k,n} + A_{h1,k,n} q_{1,k,n}'' + A_{h2,k-1,n} q_{2,k-1,n}'' \quad (24)$$

where

$C_{p,k,n}$ = Specific heat of coolant in channel k in axial node n, evaluated at the central bulk coolant temperature $T_{bc,k,n}$ (J/kg-C)

$C_{T,k,n}$ = Partial derivative of coolant enthalpy with respect to pressure at constant temperature, $\left(\frac{\partial h}{\partial P}\right)_T$, in channel k in axial node n (J/kg per Pa)

$V_{k,n}$ = Volume of coolant in node n of channel k

Using the heat fluxes found from Eqs. (21) and (22), and using Eq. (25) to replace the difference between coolant node-boundary temperatures in Eq. (24), one obtains Eq.(26) for node-center coolant bulk temperatures of an assembly axial slice n.

$$T_{b,k,n+1} - T_{b,k,n} = 2 (T_{bc,k,n} - T_{b,k,n}) \quad (25)$$

The resulting final set of equations for node-center coolant bulk temperatures, $T_{bc,k,n}$, in channels (index $k = 1$ through $K+1$) in an axial slice (index n) of an assembly is given by Eq. (26). These equations are of the form shown by the set of equations (26a) in which the coefficients a_k , b_k , c_k and d_k are known.

$$a_k T_{bc,k-1,n} + b_k T_{bc,k,n} + c_k T_{bc,k+1,n} = d_k \quad (\text{for channels } k = 1 \text{ through } K+1) \quad (26a)$$

where

$$a_k = -\frac{r_{a,k-1} R_{k-1} A_{h2,k-1,n}}{r_{d,k-1}}$$

$$b_k = 2 W_k C_{p,k,n} + \frac{r_{a,k-1} R_{k-1} A_{h2,k-1,n}}{r_{d,k-1}} + R_k A_{h1,k,n} \quad (26b)$$

$$c_k = -R_k A_{h1,k,n}$$

$$d_k = V_{k,n} q_{w,k,n} + A_{h2,k-1,n} \left(Q_{k-1} - \frac{r_{a,k-1}}{r_{d,k-1}} \alpha_{k-1} \right) + A_{h1,k,n} \alpha_k + 2 W_k C_{p,k,n} T_{b,k,n} - W_k C_{T,k,n} (P_{n+1} - P_n)$$

Equation (26) is a set of linear simultaneous algebraic equations for node-center coolant bulk temperatures $T_{bc,k,n}$ of all channels in an axial slice n of the fuel assembly. The coefficients a_k , b_k , c_k and d_k are known. The coefficient matrix of the set of equations is tri-diagonal. A very simple and fast method employing Gaussian elimination is used to directly solve for the unknown temperatures $T_{bc,k,n}$. Once the node-center temperatures are obtained for the level n , Eq. (25) is used to obtain the node outlet temperatures $T_{b,k,n+1}$ which are the node inlet temperatures for the next axial slice, or the channel outlet temperatures of the assembly if level n is the last axial slice.

For a *fuel assembly consisting of two or more tubes*, it is possible in steady-state heat transfer to simultaneously have zero film coefficients on the inner surface of the innermost tube and the outer surface of the outermost tube. Therefore, the following six types of boundary conditions are physically possible for a fuel assembly of two or more tubes, and are handled in the PLTEMP code.

Case	r_a	h_1 of the Innermost Fuel Tube	h_2 of the Outermost Fuel Tube	Number of Effective Channels
1	$r_a > 0$	$h_1 > 0$	$h_2 > 0$	$K+1$
2	$r_a > 0$	$h_1 = 0$	$h_2 > 0$	K
3	$r_a = 0$	$h_1 = 0$	$h_2 > 0$	K
4	$r_a > 0$	$h_1 > 0$	$h_2 = 0$	K
5	$r_a > 0$	$h_1 = 0$	$h_2 = 0$	$K-1$
6	$r_a = 0$	$h_1 = 0$	$h_2 = 0$	$K-1$

If the film coefficient on the inner surface of the innermost fuel tube is zero, then the first coolant channel is thermally disconnected from the rest of the assembly, thus reducing the number of effective (i.e., heat removing) channels by 1, as shown in the above table. Similarly, if the film coefficient on the outer surface of the outermost tube is zero, then the last coolant channel is thermally disconnected from the rest of the assembly, thus reducing the number of effective channels by 1. These conditions are accounted for in the PLTEMP code.

After solving for these coolant temperatures, the fuel meat and cladding temperatures and other quantities like heat fluxes are evaluated using the closed-form solutions given above by Eqs. (2), (4), and (6). The radial location of the maximum fuel temperature is found by setting the derivative of $T_b(r)$, given by Eq. (4), equal to zero.

$$r_{\max,k} = \sqrt{\frac{2 A_3 K_{b,k}}{q_{b,k}}} \quad (27)$$

The radial location found by Eq. (27) may or may not be in the fuel meat thickness, i.e., may or may not satisfy the condition $r_b \leq r_{\max} \leq r_c$. If r_{\max} is in the fuel meat thickness, the maximum fuel temperature is found by setting $r = r_{\max}$ in Eq. (4). If r_{\max} is *not* in the fuel meat thickness, the maximum fuel temperature is found by choosing the greater of the two fuel interface temperatures $T_b(r_b)$ and $T_b(r_c)$. Accordingly, r_{\max} is also redefined as r_b or r_c in this case. The fractional fuel meat cross sectional area, X_{\max} , inside the radial location of the maximum fuel temperature is given by

$$X_k = \frac{r_{\max,k}^2 - r_{b,k}^2}{r_{c,k}^2 - r_{b,k}^2} \quad (28)$$

2. Technique Used if Input Data Has the Outermost Tube First

The method in Section 1 assumes that the fuel tubes are numbered from the innermost to the outermost (see Fig. VIII-1). In order to handle an input data file having the outermost tube numbered as 1, the code internally rearranges the input data that depend on the *numbering* of fuel tubes and coolant channels, then solves the problem using the method of Section 1, and finally rearranges the solution. The input data card types 307, 308, 308A, 309 and 310 contain all the tube-numbering-dependent input data. The calculated data that are saved in the direct access file written on logical units 19 and 20 are rearranged after the solution. All rearranging is done in the subroutine SLICE1, using variables with the suffix *_R* (for example, AFF_R, DFF_R). It is noted that the input data arrays read from the input file are never changed during this whole technique.

The verification of the implementation of the method described in Sections 1 and 2 is reported in two memoranda [1, 2].

REFERENCES

1. Kalimullah, A. P. Olson, and E. E. Feldman, "Verification of the Radial Geometry Analytical Solution Method in PLTEMP/ANL Version 3.2," Intra-Laboratory Memorandum to J. E. Matos, Reduced Enrichment for Research and Test Reactor (RERTR) Program, Nuclear Engineering Division, Argonne National Laboratory, IL, USA (March 16, 2007).
2. M. Kalimullah, and A. P. Olson, "Numbering the Outermost Fuel Tube as the First in the Radial Geometry Exact Method in PLTEMP Code - Implementation and Verification," Intra-Laboratory Memorandum to J. E. Matos, Reduced Enrichment for Research and Test Reactor (RERTR) Program, Nuclear Engineering Division, Argonne National Laboratory, IL, USA (September 25, 2007).

APPENDIX IX. HEAT TRANSFER COEFFICIENT AND FRICTION FACTOR IN CHANNELS HAVING LONGITUDINAL INNER FINS

1. Introduction

The MIT Reactor coolant channels have straight longitudinal internal fins of rectangular cross section. In preparation for the thermal-hydraulic analysis of this reactor, the PLTEMP/ANL code has been improved to handle heat transfer coefficient and friction factor in finned channels. Fins of different cross sections (triangular and rectangular), with the fin axis parallel to the channel axis or making an angle (called helix angle) with the channel axis, are used in heat exchangers. The fins of trapezoidal cross section (that covers both triangular and rectangular cross sections) at a user-input helix angle (0 to 30°) were recently modeled in PLTEMP/ANL V3.3.

Figure IX-1 shows reactor coolant channels with straight longitudinal inner fins of trapezoidal cross section. Channels of two cross-sectional shapes are shown: (i) the circular tube, and (ii) the channel between parallel plates. The detailed geometry of the fins used in calculating the heat transfer area and the coolant flow area is shown in Fig. IX-2. The Carnavos correlations [1, 2] for heat transfer coefficient and friction factor in a tube having internal longitudinal fins (straight or helical) were implemented in the PLTEMP/ANL V3.3 code, as described below. Although developed based on measured data for tubes, the correlations are used for rectangular cross-section channels also, based on hydraulic diameter, flow area, and heated perimeter.

A verification of the implemented fin model by hand calculation is presented here. The friction factor, coolant flow rate, heat transfer coefficient, Groeneveld critical heat flux calculations were verified with and without fins. The method and the new input card required are also described. The older input decks should work without any change. The Onset-of-Nucleate Boiling (ONB) temperatures are also now printed in the main output. PLTEMP/ANL V3.3 code was also verified for a standard set of 14 test problems without fins, and found to reproduce the results saved earlier from the V3.2 of the code. The flow instability edits are revised to include the effect of fins.

2. Carnavos Correlation and its Implementation

Based on his experimental data for 14 tubes with and without fins, Carnavos obtained the following correlations for heat transfer coefficient and Darcy-Weisbach friction factor, each representing the data to within $\pm 10\%$. The heat transfer coefficient correlation is basically the Dittus-Boelter correlation multiplied by a factor that is a function of the fin geometry. The friction factor correlation is basically the McAdams correlation multiplied by a factor that is a function of the fin geometry. Equations (1) and (2) give these correlations, assuming the fins to be of a trapezoidal cross section as shown in Fig. IX-2.

$$\text{Nu} = 0.023 \text{Re}_a^{0.8} \text{Pr}^{0.4} \left(\frac{A_{fa}}{A_{fc}} \right)^{0.1} \left(\frac{P_n}{P_a} \right)^{0.5} \text{sec}^3 \alpha \quad (1)$$

$$f_a = \frac{0.184}{\text{Re}_a^{0.2}} \left(\frac{A_{fn}}{A_{fa}} \right)^{0.5} (\cos\alpha)^{0.75} \quad (2)$$

Where the subscript a = actual, n = nominal (see nomenclature at the end).

Here, the actual and nominal heat transfer areas, the actual and nominal coolant flow areas, and the actual and nominal hydraulic diameters are given by the following equations based on the trapezoidal cross section of the fins. The equations for a rectangular channel are a theoretical extension of the experimental data for tubes. It should be noted that, in the implementation, the *nominal perimeters and flow areas input on Card type 0307 are used* rather than the values obtained from Eq. (3), Eq. (5), and the input channel width and thickness.

$$P_n = \begin{cases} \pi D_i & \text{for tube} \\ 2(W_{ch} + T_{ch}) & \text{for rectangular channel} \end{cases} \quad (3)$$

$$P_a = P_n + n P_{fin} \sec \alpha \quad (4)$$

$$A_{fn} = \begin{cases} \frac{\pi D_i^2}{4} & \text{for tube} \\ W_{ch} T_{ch} & \text{for rectangular channel} \end{cases} \quad (5)$$

$$A_{fa} = A_{fn} - n A_{fin} \sec \alpha \quad (6)$$

$$A_{fc} = \begin{cases} \frac{\pi (D_i - 2e - 2\delta)^2}{4} & \text{for tube} \\ W_{ch} (T_{ch} - 2e) & \text{for rectangular channel} \end{cases} \quad (7)$$

P_{fin} = Sides EB+ BC+ CF– Arc length EF (in Fig. VIII– 2)

$$= \begin{cases} t + 2\sqrt{e^2 + \{(b-t)/2\}^2} - \beta D_i/2 & \text{for tube} \\ t + 2\sqrt{e^2 + \{(b-t)/2\}^2} - b & \text{for rectangular channel} \end{cases} \quad (8)$$

$$A_{fin} = \begin{cases} \frac{e(b+t)}{2} + \frac{\beta D_i^2}{8} - \frac{b\sqrt{D_i^2 - b^2}}{4} & \text{for tube} \\ \frac{e(b+t)}{2} & \text{for rectangular channel} \end{cases} \quad (9)$$

$$D_{ha} = \frac{4 A_{fa}}{P_a}, \quad D_{hn} = \frac{4 A_{fn}}{P_n} \quad (10)$$

$$\text{Re}_a = \frac{W D_{ha}}{A_{fa} \mu}, \quad \text{Re}_n = \frac{W D_{hn}}{A_{fn} \mu} \quad (11)$$

$$\text{Pr} = \frac{\mu C_p}{K} \quad (12)$$

$$D_c = D_i - 2(e + \delta) \quad (13)$$

$$\delta = \frac{D_i - \sqrt{D_i^2 - b^2}}{2} \quad (14)$$

$$\beta = 2 \sin^{-1}(b/D_i) \quad (15)$$

$$A_\delta = \frac{\beta D_i^2}{8} - \frac{b \sqrt{D_i^2 - b^2}}{4} \quad (16)$$

The range of applicability of correlations in Eqs. (1) and (2) is given below [1,2]. The last three restrictions on fin geometry are given in Refs. [3, 4].

Helix angle range:	$0 < \alpha < 30^\circ$
Reynolds number range:	$10,000 < \text{Re} < 100,000$
Prandtl number range:	$0.7 < \text{Pr} < 30$
Fin pitch:	$3.3 < p/e < 5.6$
Fin height:	$e/D_i < 0.29$
Fin aspect ratio:	$\frac{e}{0.5(b+t)} < 3.5$

The Reynolds number and the other five above problem parameters are checked against their range. If the Reynolds number or any parameter is found to be out of range, then a warning message is printed, identifying the parameter which was found to be out of range. A maximum of 12 messages is printed. The solution is not stopped due to any number of warnings.

Equation (1) results in Eq. (17) below for the finned tube heat transfer coefficient h_a that is based on the *actual* heat transfer area (P_a). For use in the PLTEMP/ANL code, one needs to express the coefficient h_a given by Eq. (17) as a heat transfer coefficient h_{a_n} based on the *nominal* heat transfer area P_n , preserving the heat transfer rate as done by Eq. (18).

$$h_a = \frac{\text{Nu} K}{D_{ha}} \quad (17)$$

$$h_{a,n} = \frac{P_a h_a}{P_n} \quad (18)$$

Equation (2) gives the finned tube friction factor f_a that is based on the *actual* hydraulic diameter D_{ha} . For use in PLTEMP/ANL, one needs to express the friction factor f_a as a friction factor $f_{a,n}$ based on the *nominal* hydraulic diameter (D_{hn}). To do this, one must equate the pressure drop due to friction. For a given flow rate W in the channel, the pressure drop due to the finned tube friction factor f_a over a length L of the channel can be written as Eq. (19). The first factor on the right hand side of Eq. (19) must be preserved because the second factor is the same whether the nominal or the actual hydraulic diameter is used. Equating the first factor on the right hand side of Eq. (19) results in Eq. (20), which is rewritten as Eq. (21) below.

$$\Delta p_a = \left(\frac{f_a}{A_{fa}^2 D_{ha}} \right) \left(\frac{LW^2}{2\rho} \right) \quad (19)$$

$$\frac{f_{a,n}}{A_{fn}^2 D_{hn}} = \frac{f_a}{A_{fa}^2 D_{ha}} \quad (20)$$

$$f_{a,n} = \frac{A_{fn}^2 D_{hn} f_a}{A_{fa}^2 D_{ha}} \quad (21)$$

A subroutine CARNAVOS was developed to calculate the results of Eqs. (18) and (21). The subroutine has been implemented into the PLTEMP/ANL V3.3. The subroutine CARNAVOS is called by the existing multi-option heat transfer subroutine HCOEF1 of the code.

3. Verification of Carnavos Correlation Implemented in PLTEMP/ANL

The purpose here is to verify the heat transfer coefficient, friction factor, and coolant flow rate calculated by PLTEMP/ANL V3.3 for a sample problem with finned coolant channels. Figure IX-3 shows a sample input deck (Test Problem 16) to model the coolant channels of the MIT Reactor. The sample problem has two assemblies of a single type, each having 9 fuel plates and 10 coolant channels. The reactor core axial region (region 2) of each assembly has the fin geometry of the MIT Reactor. The first and third axial regions (the inlet and exit regions) are each made artificially short (0.01 mm), and the minor loss coefficients are set to zero, so that the coolant flow rate in a channel could be hand-calculated. The power produced is set artificially small so that there is a negligible coolant temperature rise in channels and the coolant properties only at the inlet temperature are required in the hand calculation of friction factor, flow rate and heat transfer coefficient.

The newly developed PLTEMP/ANL V3.3 code was run for this sample deck, *with the fins* (Run 1), for an input frictional pressure drop of 0.1 MPa. The code was also run *without the fins* (Run 2), by modifying the input cards 200 and 202 of the deck (i.e., setting option IH=1 and fin height to zero). Table IX-1 provides the geometry of the finned channel, the needed coolant properties,

and some data from the debug outputs printed by the code (using input KPRINT = 2). The columns 1 and 2 of Table IX-1 show selected results from the run with fins, and the column 3 shows results from the run without fins.

3.1. Verification of Friction Factor and Flow Rate in Finned Coolant Channels

In the first run, the code calculated a flow rate of 0.58046 kg/s per coolant channel with fins. This flow rate is established by a frictional pressure drop of 0.1 MPa. In the second run, it calculated a flow rate of 1.11814 kg/s per coolant channel without fins, at the same frictional pressure drop (0.1 MPa). The actual Reynolds number and friction factor, f_a in the finned channel (column 1 of Table IX-1) were hand-calculated as follows. The value of f_a at the flow rate of 0.58046 kg/s per coolant channel is found using the Carnavos correlation, i.e., Eq. (2).

$$Re_a = \frac{D_{ha} W}{\mu A_{fa}} = \frac{0.0021817 \times 0.58046}{5.9309 \times 10^{-4} \times 1.13548 \times 10^{-4}} = 18805.2$$

$$f_a = \frac{0.184}{(18805.2)^{0.2}} \left(\frac{1.26451}{1.13548} \right)^{0.5} \times 1.0 = 0.027123$$

The frictional pressure drop in the finned channel can be hand-calculated as follows.

$$\begin{aligned} \Delta p_a &= \left(\frac{f_a L}{D_{ha}} \right) \left(\frac{W^2}{2 \rho A_{fa}^2} \right) \\ &= \frac{0.027123 \times 0.61}{0.0021817} \times \frac{(0.58046)^2}{2 \times 991.148 \times (1.13548 \times 10^{-4})^2} = 0.099975 \text{ MPa} \end{aligned}$$

The above values of actual Reynolds number, friction factor, and pressure drop agree with those printed by the code and shown in column 1 of Table IX-1.

The Reynolds number Re_n and friction factor, f_n in the un-finned channel at the same flow rate, 0.58046 kg/s, were hand-calculated using $Re_n = D_{hn} W / (\mu A_{fn})$ and $f_n = 0.184 / Re_n^{0.2}$.

$$Re_n = \frac{D_{hn} W}{\mu A_{fn}} = \frac{0.0047459 \times 0.58046}{5.9309 \times 10^{-4} \times 1.26451 \times 10^{-4}} = 36732.0$$

$$f_n = \frac{0.184}{(36732.0)^{0.2}} = 0.022481$$

These nominal values are shown in columns 2 of Table IX-1, and agree with those printed by the code. The frictional pressure drop, Δp_n in the un-finned channel at this flow rate (0.58046 kg/s) can be hand-calculated as follows.

$$\begin{aligned}\Delta p_n &= \left(\frac{f_n L}{D_{hn}} \right) \left(\frac{W^2}{2 \rho A_{fn}^2} \right) \\ &= \frac{0.022481 \times 0.61}{0.0047459} \times \frac{(0.58046)^2}{2 \times 991.148 \times (1.26451 \times 10^{-4})^2} = 0.0307156 \text{ MPa}\end{aligned}$$

At the flow rate 0.58046 kg/s, the ratio of pressure drop in the finned channel to that in the un-finned channel is hand-calculated to be 3.25487, which agrees with the ratio printed by the code.

$$\frac{\Delta p_a}{\Delta p_n} = \frac{0.099975}{0.0307156} = 3.25487$$

The flow rate W_3 in the un-finned channel at the input pressure drop of 0.1 MPa (Run 2) should be about $\sqrt{3.25487}$ times 0.58046 kg/s = 1.04722 kg/s. Actually it will be more than this value because the un-finned friction factor will be lower than 0.022481, because of the increase in Reynolds number at the increased flow rate. The code-calculated W_3 is 1.11814 kg/s as shown in column 3 of Table IX-1. This flow rate is verified by hand-calculating the corresponding Reynolds number, friction factor, and pressure drop, as follows.

$$Re_3 = \frac{D_{hn} W_3}{\mu A_{fn}} = \frac{0.0047459 \times 1.11814}{5.9341 \times 10^{-4} \times 1.26451 \times 10^{-4}} = 70719.2$$

$$f_3 = \frac{0.184}{(70719.2)^{0.2}} = 0.019720$$

$$\begin{aligned}\Delta p_3 &= \left(\frac{f_3 L}{D_{hn}} \right) \left(\frac{W_3^2}{2 \rho A_{fn}^2} \right) \\ &= \frac{0.019720 \times 0.61}{0.0047459} \times \frac{(1.11814)^2}{2 \times 991.223 \times (1.26451 \times 10^{-4})^2} = 0.099968 \text{ MPa}\end{aligned}$$

The value of Δp_3 agrees with the input pressure drop of 0.1 MPa, and this agreement verifies the code calculated results shown in column 3 of Table IX-1. In summary, the hand-calculated values of friction factor and coolant flow rate in the three cases are found to agree with the code-calculated values shown in Table IX-1. This verifies the implementation of the Carnavos correlation for friction factor.

3.2. Verification of Heat Transfer Coefficient

The actual heat transfer coefficient in the finned channel (column 1 of Table IX-1) was hand-calculated as follows, using the Carnavos correlation, i.e., Eq. (1).

$$\frac{h_a D_{ha}}{K} = 0.023 \times (18805.2)^{0.8} (3.86247)^{0.4} \left(\frac{1.13548}{1.00645}\right)^{0.1} \left(\frac{0.10658}{0.20818}\right)^{0.5} \times 1.0 = 75.11963$$

$$h_a = \frac{75.11963 \times 0.64130}{0.0021817} = 22081.0 \text{ W/m}^2 - ^\circ\text{C} \text{ (based on actual heat transfer area)}$$

The above actual heat transfer coefficient (22081.0) is based on the heat transfer area with fins. This value agrees with the value (22080.4) printed by the code. Since the code has all along used un-finned coolant channels, the heat transfer coefficients and heat transfer areas used throughout the code are those of the un-finned coolant channel. Therefore, the above heat transfer coefficient must be expressed as an equivalent heat transfer coefficient, h_{a_n} that is based on the heat transfer area of the un-finned coolant channel (nominal heat transfer area), such that the heat transfer rate and the temperature difference between the bulk coolant and cladding surface remain unchanged. The equivalent heat transfer coefficient is found using Eq. (18), as follows.

$$h_{a_n} = \frac{h_a P_a}{P_n} = \frac{22081.0 \times 0.20818}{0.10658} = 43130.3 \text{ W/m}^2 - ^\circ\text{C} \text{ (based on nominal heat transfer area)}$$

This is the value that is printed in the main temperature edits of PLTEMP/ANL V3.3. To evaluate the heat transfer enhancement caused by the fins, the actual heat transfer rate is compared below with the heat transfer rate without fins at the same coolant flow rate (0.58046 kg/s). The heat transfer coefficient, h_n in the un-finned channel is given by

$$\frac{h_n D_{hn}}{K} = 0.023 \times (36732.0)^{0.8} \times (3.86247)^{0.4} = 177.2187$$

$$h_n = \frac{177.2187 \times 0.64130}{0.0047459} = 23947.1 \text{ W/m}^2 - ^\circ\text{C} \text{ (based on nominal heat transfer area)}$$

This value of the nominal heat transfer coefficient (23947.1) agrees with the value printed by the code (shown in column 2). The heat transfer enhancement factor provided by the fins is given by

$$\text{Enhancement factor} = \frac{h_{a_n}}{h_n} = \frac{43130.3}{23947.1} = 1.8010$$

This value of the heat transfer enhancement factor agrees with the value printed by the code.

3.3 Comparison of Zero-Height Fin Option with No Fin Option

The output obtained by running the code with fins of zero height (using option IH = -1 on input card 200, and fin height EFIN = 0.0 on input card 202), and that obtained by running the code without fins (using option IH = 1 without providing the input card 202) were compared to verify that the code gave the same results in both cases. It was found that the code does give the same results. A previously-developed PLTEMP/ANL output comparing utility program *differ.x* was

used to compare the two cases. The maximum temperature difference for coolant, cladding, and fuel peak was found to be 0.001 °C. Two points of detail are noted here:

- (1) In the latter case (without fins), the selected coolant flow friction factor uses input values of FCOEF, FEXPF, and ROUGH (0.184, 0.2, and 0.0) on the card 305. This was done because the finned friction factor correlation (Carnavos correlation) implemented in the code, is based on the McAdams correlation ($f = 0.184/Re^{0.2}$) and reduces to it in the absence of fins.
- (2) In the latter case (without fins), IH is selected to be 1, implying the Dittus-Boelter correlation (not one of the other correlations available in the code). The reason for this is that the finned heat transfer correlation (Carnavos correlation) implemented in the code, is based on the Dittus-Boelter correlation and reduces to it in the absence of fins.

Without these two input choices, the code may not give the same results in the two cases discussed above.

The case without fins of this problem (Test Problem 16) was also run using the older version of PLTEMP/ANL (V3.2), and the results were compared with that obtained by V3.3. This comparison was performed at two power levels: 0.0024 MW and 0.24 MW. Using the utility program *differ.x*, the maximum temperature difference for coolant, cladding, and fuel peak was found to be zero, in the comparison at each power level. This verifies the implementation of Carnavos correlations in the coolant flow rate and temperature calculations in the code.

4. Code Output for Finned Coolant Channels

The following should be accounted for in using the code output. The flow instability edits are revised to include the effect of fins.

- (1) The heat transfer area (when using the fin option $IH = -1$) in the code are left unchanged as the *nominal* area without fins (just as it was calculated before implementing the fin option). The code performs the temperature calculation using the enhanced heat transfer coefficients expressed based on the nominal heat transfer area, $2(W_{ch} + T_{ch})$ m² per meter, of the coolant channel. The calculated heat fluxes are therefore based on the nominal heat transfer area. The heat transfer coefficients printed in the temperature table of code output (see part of output in Table IX-2) are based on the nominal heat transfer area in the channel without fins.
- (2) The heat fluxes printed by the code in the table of heat fluxes are based on the *nominal* heat transfer area, $2(W_{ch} + T_{ch})$ m² per meter, in the coolant channel without fins.
- (3) The *actual* heat flux (not the *nominal* heat flux) is used in finding the ONB temperature used to calculate the ONB ratio in subroutines FINLED, FINLED6, FINLEDIT, and FINLEDIT6. The actual heat flux q_a equals the nominal heat flux q_n divided by the actual-to-nominal perimeter ratio (P_a / P_n). The ratio P_a/P_n is stored in the COMMON block FINGEOM.

$$q_a = \frac{q_n}{(P_a/P_n)}$$

- (4) The *actual* heat flux is used in calculating the DNB ratio. All six critical heat flux correlations in the code (i.e., Mirshak-Durant-Towell, Bernath, Labuntsov, Mishima, and Weatherhead correlations, and the Groeneveld table) in the subroutines DNB and DNB2 were revised to use the actual (with fins) flow area, perimeter, hydraulic diameter, and

Quality →	CHF, kW/m ² At 1000 kPa		CHF, kW/m ² At 3000 kPa		CHF, kW/m ² At Outlet Pressure of 1300 kPa		
	-0.4	-0.3	-0.4	-0.3	-0.4	-0.3	-0.3173
Mass Flux, kg/m ² -s ↓							
5000.0	14574	12447	14778	13200	14604.6	12560.0	12913.7
5500.0	15273	13033	15454	13765	15300.2	13142.8	13516.0
5112.1							13048.7

coolant velocity. A hand calculation (shown below) of the Groeneveld critical heat flux (code input option ICHF = 5) was done to verify the code calculated value with fins. The code had the 1995 version of the Groeneveld critical heat flux table. The needed parts of the table [5] at pressures of 1000 kPa and 3000 kPa (that bracket the coolant outlet pressure of 1300 kPa in Test Problem 16) are given below. All interpolations are also shown.

As mentioned above, the coolant temperature rise is small (only 0.06 °C) (see the code output shown in Table IX-2), the coolant outlet temperature is 45.06 °C, and outlet pressure is 1300 kPa (=1.4 MPa inlet pressure – 0.1 MPa pressure drop). Using these values, the exit quality is found as follows:

$$h_{f,sat} = \text{Saturated liquid enthalpy at 1300 kPa} = 814.70 \text{ kJ/kg}$$

$$h_{g,sat} = \text{Saturated vapor enthalpy at 1300 kPa} = 2785.43 \text{ kJ/kg}$$

$$h_f = \text{Liquid enthalpy at 45.06 °C (from ASME Steam Table)} = 189.48 \text{ kJ/kg}$$

$$\text{Quality of the sub-cooled liquid, } x = \frac{189.48 - 814.70}{2785.42 - 814.70} = -0.3173$$

Using the coolant flow rate and actual flow area in a channel (shown in Table IX-1), the coolant mass flux *with fins* is found to be $(0.58046/1.13548 \times 10^{-4}) = 5112.1 \text{ kg/m}^2\text{-s}$. The critical heat flux for the reference 8-mm diameter tube, and that for the finned channel are shown below.

$$\text{CHF}(1300 \text{ kPa}, 5112.1 \text{ kg/m}^2\text{-s}, -0.3171) \text{ for diameter } 8 \text{ mm} = 13048.7 \text{ kW/m}^2$$

$$\text{CHF}(1300 \text{ kPa}, 5112.1 \text{ kg/m}^2\text{-s}, -0.3171) \text{ for hydraulic diameter } 2.1817 \text{ mm}$$

$$= 13048.7 \left(\frac{8}{2.1817} \right)^{0.3333} = 20121.8 \text{ kW/m}^2$$

The above hand-calculated critical heat flux of 20121.8 kW/m² is in agreement with the code-calculated value of 20241 kW/m² (see part of code output in Table IX-2).

NOMENCLATURE

- P_a = Actual perimeter, i.e., actual heat transfer area per unit length of the tube with fins, m² per meter
- P_n = Nominal perimeter, i.e., nominal heat transfer area per unit length of the tube, based on tube ID as if the fins were not present, m² per meter
- P_{fin} = *Additional* heated perimeter provided by a single fin. It is the additional is over the tube perimeter covered by the fin, m
- A_{fa} = Actual flow area in the tube with fins, m²
- A_{fc} = Core flow area, i.e., the flow area inside the circle touching the fin tips, (see Fig. IX-2), m²
- A_{fn} = Nominal flow area in the tube, based on tube ID as if the fins were not present, m²
- b = Fin thickness at the bottom, m
- A_{fin} = Cross sectional area of a single fin, m²
- C_p = Specific heat of the coolant, J/kg-°C
- D_c = Core diameter of a channel, i.e., diameter inside the fin tips, m
- D_i = Inner diameter of the tube, m
- D_{ha} = Actual hydraulic diameter of the finned channel, m
- D_{hn} = Nominal hydraulic diameter of the channel without fins, m
- e = Height of fins, m
- f_a = Finned tube Darcy-Weisbach friction factor based on the *actual* hydraulic diameter D_{ha}
- $f_{a,n}$ = Finned tube Darcy-Weisbach friction factor expressed as a friction factor based on the *nominal* flow area A_{fn} and hydraulic diameter D_{hn}
- h_a = Finned tube heat transfer coefficient based on the *actual* heat transfer area, W/m²-°C
- $h_{a,n}$ = Finned tube heat transfer coefficient expressed as a coefficient based on the *nominal* heat transfer area, W/m²-°C
- K = Thermal conductivity of the coolant, W/m-°C
- L = Channel length, m
- n = Number of fins in a channel
- Nu = $\frac{h_a D_{ha}}{K}$ = Nusselt number based on P_a and A_{fa} (i.e., actual perimeter and actual flow area)
- p = Circumferential pitch of fins = $\pi D_i / n$ for tube = $2W_{ch} / n$ for rectangular channel
- Pr = Prandtl number of the coolant
- Δp_a = Actual pressure drop due to friction in the finned channel, N/m²
- Re_a = $\frac{W D_{ha}}{\mu A_{fa}}$ = Reynolds number based on P_a and A_{fa} (i.e., actual perimeter and actual

- flow area)
- $Re_n = \frac{W D_{hn}}{\mu A_{fn}}$ = Reynolds number based on P_n and A_{fn} (i.e., nominal perimeter and nominal flow area)
- t = Fin thickness at the tip, m
- T_{ch} = Channel thickness between the parallel plates, m
- W_{ch} = Channel width of the channel between the parallel plates, m
- W = Coolant flow rate in the channel, kg/s
- α = Angle between the spiral fin's longitudinal axis and the tube axis (called helix angle)
- ρ = Density of the coolant, kg/m³
- μ = Dynamic viscosity of the coolant, N-s/m²

REFERENCES

1. T. C. Carnavos, "Heat Transfer Performance of Internally Finned Tubes in Turbulent Flow," AIChE Paper presented at the 18th National Heat Transfer Conference, San Diego, CA (Aug. 1979).
2. T. C. Carnavos, "Heat Transfer Performance of Internally Finned Tubes in Turbulent Flow," Heat Transfer Eng., Vol. 1, No. 4, pp. 32-37 (Apr-June 1980).
3. R. L. Webb and M. J. Scott, "A Parametric Analysis of the Performance of Internally Finned Tubes for Heat Exchanger Application," J. of Heat Transfer, Trans. of the ASME, Vol. 102, pp. 38-43 (Feb. 1980).
4. N. H. Kim and R. L. Web, "Analytic Prediction of the Friction and Heat Transfer for Turbulent Flow in Axial Internal Fin Tubes," J. of Heat Transfer, Trans. of the ASME, Vol. 115, pp. 553-559 (Aug. 1993).
5. D. C. Groeneveld, et. al., "The 1995 Look-up Table for Critical Heat Flux in Tubes," Nuclear Eng. Design, Vol. 163, pp. 1-28 (1996).

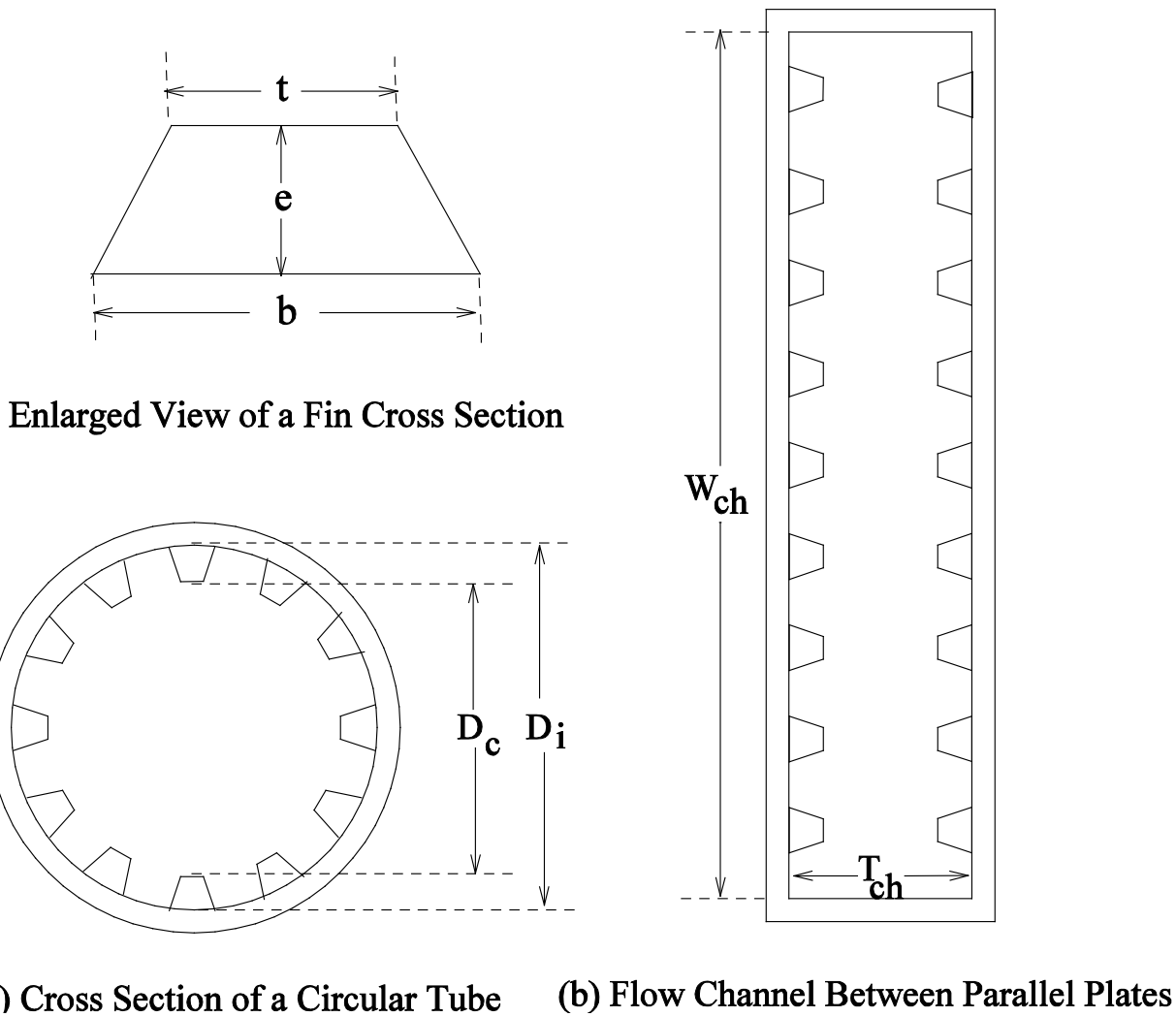


Fig. IX-1. Reactor Coolant Channels with Longitudinal Inner Fins:
(a) Circular Tube, and (b) Channel between Parallel Plates

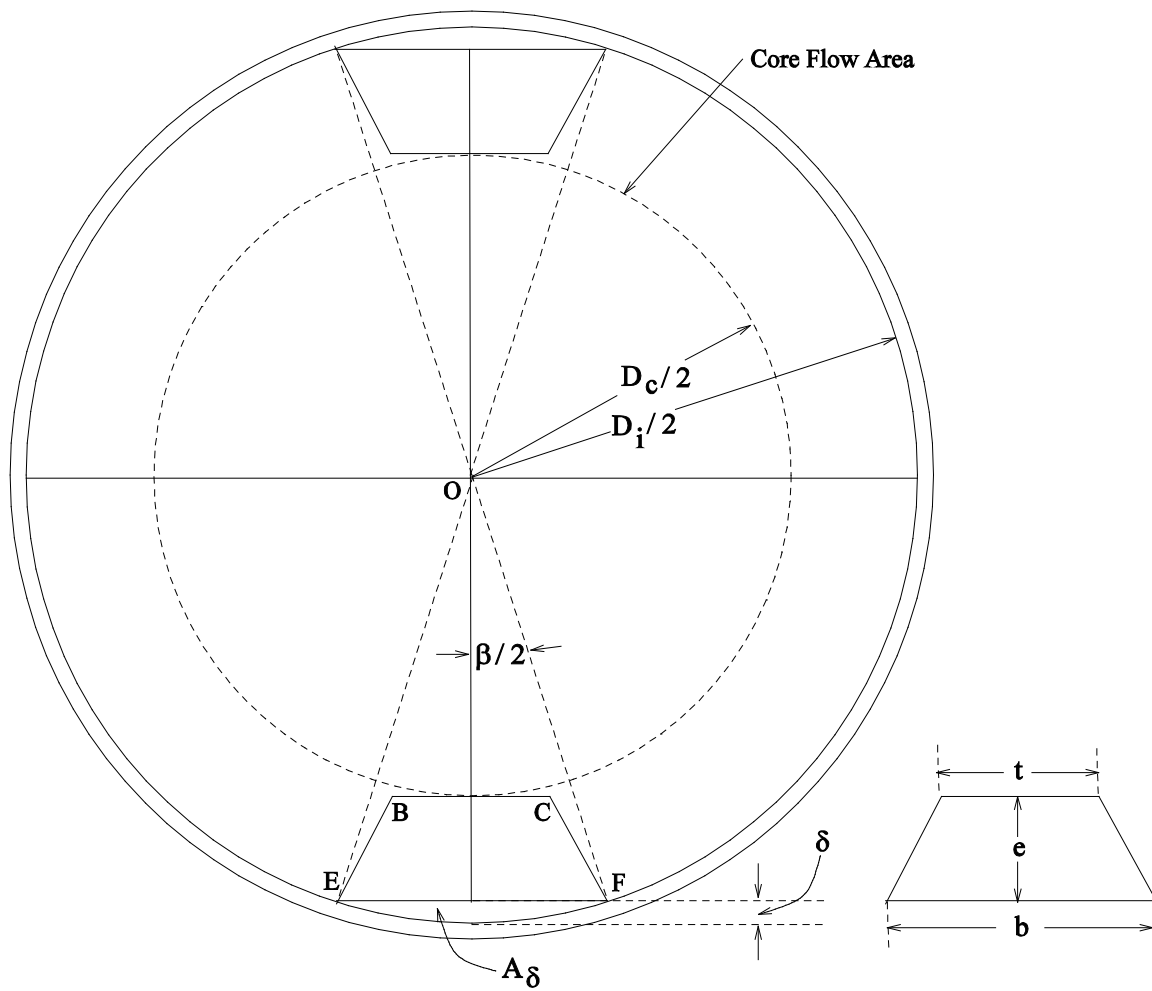


Fig. IX-2. Fin Geometry Used in Calculating Coolant Flow Area in a Circular Tube Having Longitudinal Internal Fins

Fig. IX-3. Input Data for Test Problem 16 Having MITR-Type Finned Coolant Channels

```

Test Problem 16: MITR with fins
! 2 assemblies of one type, each producing 1.2 kWt
! Each assembly has 9 fuel plates and 10 coolant channels
! H2O coolant, Flow is calculated from input pressure drop
! All hot channel factors = 1.0
! No bypass flow, NCTYP=0
! 10 axial heat transfer nodes in the heated length of fuel plates
! 1 2 3 4 5 6 7 8 9 10 11 12 13 14 15 16 17 18 Indices
-1 0 5 1 0 1 1 1 0 0 0 0 0 1 2 00 Card(1)0200
0.000254 0.000254 0.000254 0.0 200 Card(1)0202
2 3 5.00 1.00 1.00 1.00 3 Card(1)0300
! Using pressure driven mode
1 20 1.00 Card(1)0301
1 1 1 Card(1)0302
1.20 1.20 Card(2)0303
12.645E-04 4.74585E-03 0.00001 0.00 0.0508 2.4892E-03 Card(3)0304
12.645E-04 4.74585E-03 0.61 0.00 0.0508 2.4892E-03 Card(3)0304
12.645E-04 4.74585E-03 0.00001 0.00 0.0508 2.4892E-03 Card(3)0304
! Use the code's built-in correlation for friction factor
0.184 0.20 0.00 Card(1)0305
10 3 0.00 0.61 0.25E-03 0.00 0.55E-03 100.00 Card(1)0306
1.2645E-04 4.74585E-03 0.106578 0.0508 0.0508 2.4892E-03 Card(5)0307
1.2645E-04 4.74585E-03 0.106578 0.1016 0.0508 2.4892E-03 Card(5)0307
1.2645E-04 4.74585E-03 0.106578 0.0508 0.0508 2.4892E-03 Card(5)0307
0.0508 0.0508 0.0508 0.0508 0.0508 0.0508 Card(1)0308
0.0508 0.0508 0.0508 Card(1)0308
! Card 0308A not required in slab geometry
! Radial power peaking factor data by fuel plate for each subassembly. Input flow data by
! channel for each subassembly on Cards 0310 not required because WFGES(1) is non-zero
0.800 0.850 0.900 0.950 1.000 1.050 Card(2)0309
1.100 1.150 1.200 Card(2)0309
0.801 0.851 0.901 0.951 1.001 1.051 Card(2)0309
1.101 1.151 1.201 Card(2)0309
! DPO DDP DPMAX POWER TIN PIN
0.10 0.04 0.10 2.4E-03 45.0 1.40 Card(1)0500
0.00 0.00 Card(2)0500
50 0.0001 25.0 0.50 2.0E-03 Card(1)0600
11 Card(1)0700
0.00 0.80 Card(11)0701
0.10 0.88 Card(11)0701
0.20 0.96 Card(11)0701
0.30 1.04 Card(11)0701
0.40 1.12 Card(11)0701
0.50 1.20 Card(11)0701
0.60 1.12 Card(11)0701
0.70 1.04 Card(11)0701
0.80 0.96 Card(11)0701
0.90 0.88 Card(11)0701
1.00 0.80 Card(11)0701
0 Card(11)0702

```

Table IX-1. Comparison of PLTEMP Calculations With and Without Fins in Internal Coolant Channels of Test Problem 16

Parameter	With Fins at 0.1 MPa Pressure Drop (Run 1)	Without Fins at Finned Channel Flow Rate (Run 1)	Without Fins at 0.1 MPa Pressure Drop (Run 2)
Column Number	1	2	3
PLTEMP/ANL Input			
Nominal thickness of channel, mm	2.4892		
Nominal width of channel, mm	50.8		
Channel Length, m	0.61		
Number of fins in a channel	200		
Fin height, mm	0.254		
Fin thickness (uniform), mm	0.254		
PLTEMP/ANL Output			
Core flow area (within fin tips), A_{fc} , m^2	1.00645×10^{-4}		
Flow area (A_{fa} and A_{fn}), m^2	1.13548×10^{-4}	1.26451×10^{-4}	
Perimeter (P_a and P_n), m	0.20818	0.10658	
Hydraulic diameter (D_{ha} and D_{hn}), m	0.0021817	0.0047459	
Coolant density, kg/m^3	991.148		991.223
Coolant specific heat, $J/kg \cdot ^\circ C$	4176.421		
Coolant dynamic viscosity, $N \cdot s/m^2$	5.9309×10^{-4}		5.9341×10^{-4}
Coolant thermal conductivity, $W/m \cdot ^\circ C$	0.64130		
Prandtl number	3.86247		
Flow rate in a channel, kg/s	0.58046		1.11814
Reynolds number	18805.2	36732.0	70719.2
Darcy-Weisbach Friction Factor	0.027123	0.022481	0.019720
Pressure drop increase factor $\Delta p_a / \Delta p_n$	3.2548		
Actual heat transfer coefficient, $W/m^2 \cdot ^\circ C$	22080.4	23947.2	
Enhancement factor $h_a P_a / (h_n P_n)$	1.8010		
Hand Calculation			
Pressure Drop (Δp), MPa	0.099975	0.030716	0.099968

Table IX-2. Portion of PLTEMP/ANL V3.3 Output for Test Problem 16 Having MITR-Type Finned Coolant Channels

FUEL PLATE	2 (ExactSoln)												
NODE	COOLANTl	CladSl	FUEL PEAK	CladSr	COOLANTr	HCOFl	HCOFr	ONBRl	ONBRr	ETA'l	ETA'r	ONB Temp	ONB Temp
	(C)	(C)	(C)	(C)	(C)	W/C-m ²	W/C-m ²	[F Note 1]		K-cm ³ /J	K-cm ³ /J	left(C)	right(C)
						[F Note 2]	[F Note 2]						
	45.000				45.000								
1	45.003	45.039	45.043	45.039	45.003	4.3130E+04	4.3130E+044.E+034.E+03	5.037E+05	5.034E+05			194.966	194.966
2	45.010	45.049	45.054	45.049	45.010	4.3132E+04	4.3132E+043.E+033.E+03	4.569E+05	4.604E+05			194.616	194.616
3	45.016	45.059	45.065	45.060	45.018	4.3134E+04	4.3135E+043.E+033.E+03	4.156E+05	4.264E+05			194.264	194.263
4	45.022	45.069	45.075	45.069	45.025	4.3137E+04	4.3138E+042.E+032.E+03	3.776E+05	4.007E+05			193.911	193.907
5	45.027	45.079	45.085	45.080	45.033	4.3138E+04	4.3140E+042.E+032.E+03	3.440E+05	3.799E+05			193.555	193.549
6	45.033	45.086	45.092	45.087	45.041	4.3140E+04	4.3143E+042.E+032.E+03	3.378E+05	3.857E+05			193.193	193.184
7	45.040	45.089	45.095	45.090	45.048	4.3143E+04	4.3146E+042.E+032.E+03	3.583E+05	4.181E+05			192.823	192.814
8	45.047	45.093	45.098	45.094	45.055	4.3145E+04	4.3149E+042.E+032.E+03	3.838E+05	4.534E+05			192.450	192.441
9	45.053	45.096	45.102	45.098	45.063	4.3148E+04	4.3151E+042.E+032.E+03	4.092E+05	5.016E+05			192.076	192.064
10	45.059	45.099	45.104	45.100	45.069	4.3150E+04	4.3153E+041.E+031.E+03	4.392E+05	5.602E+05			191.699	191.686
	45.061				45.071								

- [1] The ONB ratio is here defined as $(T_{onb} - T_{inlet}) / (T_{surf} - T_{inlet})$. If the heat flux is negative (the coolant is hotter than the adjacent cladding surface), then the ONB ratio is arbitrarily set to 99.99 .
- [2] The finned heat transfer coeff is here expressed as an average over the nominal heat transfer area in the unfinned coolant channel. It equals $(\text{actual finned surface heat transfer coeff}) \times (1.9533 \text{ finned-to-unfinned heat transfer area ratio})$.

Departure from Nucleate Boiling Ratio (DNBR) (ExactSoln)
Using Groeneveld Tables for CHF(Pressure, MassFlux, Quality)

NOTE: The coolant channel has fins. The CHF and peak heat flux are here based on the actual (not nominal) flow area, perimeter, and hydraulic diameter.

FUEL PLATE	1	LEFT SIDE:	DNBR = 9.2017E+03, CHF = 2.0309E+01 MW/m**2, PEAK HEAT FLUX= 1.4947E-03 MW/m**2 of finned surface
FUEL PLATE	1	RIGHT SIDE:	DNBR = 1.1195E+04, CHF = 2.0242E+01 MW/m**2, PEAK HEAT FLUX= 9.2567E-04 MW/m**2 of finned surface
FUEL PLATE	2	LEFT SIDE:	DNBR = 8.9538E+03, CHF = 2.0242E+01 MW/m**2, PEAK HEAT FLUX= 1.1574E-03 MW/m**2 of finned surface
FUEL PLATE	2	RIGHT SIDE:	DNBR = 1.0046E+04, CHF = 2.0241E+01 MW/m**2, PEAK HEAT FLUX= 1.0316E-03 MW/m**2 of finned surface
FUEL PLATE	3	LEFT SIDE:	DNBR = 9.0431E+03, CHF = 2.0241E+01 MW/m**2, PEAK HEAT FLUX= 1.1459E-03 MW/m**2 of finned surface
FUEL PLATE	3	RIGHT SIDE:	DNBR = 8.9510E+03, CHF = 2.0241E+01 MW/m**2, PEAK HEAT FLUX= 1.1577E-03 MW/m**2 of finned surface
FUEL PLATE	4	LEFT SIDE:	DNBR = 8.4010E+03, CHF = 2.0241E+01 MW/m**2, PEAK HEAT FLUX= 1.2335E-03 MW/m**2 of finned surface
FUEL PLATE	4	RIGHT SIDE:	DNBR = 8.6062E+03, CHF = 2.0241E+01 MW/m**2, PEAK HEAT FLUX= 1.2041E-03 MW/m**2 of finned surface
FUEL PLATE	5	LEFT SIDE:	DNBR = 8.0426E+03, CHF = 2.0241E+01 MW/m**2, PEAK HEAT FLUX= 1.2885E-03 MW/m**2 of finned surface
FUEL PLATE	5	RIGHT SIDE:	DNBR = 8.1786E+03, CHF = 2.0241E+01 MW/m**2, PEAK HEAT FLUX= 1.2670E-03 MW/m**2 of finned surface
FUEL PLATE	6	LEFT SIDE:	DNBR = 7.5341E+03, CHF = 2.0241E+01 MW/m**2, PEAK HEAT FLUX= 1.3754E-03 MW/m**2 of finned surface
FUEL PLATE	6	RIGHT SIDE:	DNBR = 7.8488E+03, CHF = 2.0241E+01 MW/m**2, PEAK HEAT FLUX= 1.3202E-03 MW/m**2 of finned surface
FUEL PLATE	7	LEFT SIDE:	DNBR = 7.4072E+03, CHF = 2.0241E+01 MW/m**2, PEAK HEAT FLUX= 1.3990E-03 MW/m**2 of finned surface
FUEL PLATE	7	RIGHT SIDE:	DNBR = 7.3034E+03, CHF = 2.0241E+01 MW/m**2, PEAK HEAT FLUX= 1.4188E-03 MW/m**2 of finned surface
FUEL PLATE	8	LEFT SIDE:	DNBR = 6.9616E+03, CHF = 2.0241E+01 MW/m**2, PEAK HEAT FLUX= 1.4885E-03 MW/m**2 of finned surface
FUEL PLATE	8	RIGHT SIDE:	DNBR = 7.1311E+03, CHF = 2.0241E+01 MW/m**2, PEAK HEAT FLUX= 1.4531E-03 MW/m**2 of finned surface
FUEL PLATE	9	LEFT SIDE:	DNBR = 7.4507E+03, CHF = 2.0241E+01 MW/m**2, PEAK HEAT FLUX= 1.3908E-03 MW/m**2 of finned surface
FUEL PLATE	9	RIGHT SIDE:	DNBR = 6.1030E+03, CHF = 2.0308E+01 MW/m**2, PEAK HEAT FLUX= 2.2535E-03 MW/m**2 of finned surface

APPENDIX X. COMPARISON OF BABELLI-ISHII FLOW INSTABILITY CRITERION WITH 75 TESTS DONE BY WHITTLE AND FORGAN

Executive Summary

The Babelli-Ishii flow instability criterion based on the Subcooling number and the Zuber number is tested and verified. A utility program has been developed to apply the Babelli-Ishii flow instability criterion of Eq. (1) or the simple criterion of Eq. (5) to 75 tests (using uniform heat flux) reported by Whittle and Forgan. The comparison of the measured and calculated (using either criterion) coolant inlet velocities at the onset of flow instability in these tests shows that both criteria are conservative. Based on this work, the following three improvements were made to the PLTEMP/ANL code.

- (i) The older versions of the code (V3.3 and older) printed the results of the simplified Babelli-Ishii flow instability criterion of Eq. (5). Now, the code V3.4 and newer also print the results of the main Babelli-Ishii flow instability criterion of Eq. (1).
- (ii) An error in the implementation of the simplified Babelli-Ishii flow instability criterion was corrected. The error was related to the adjustment (to account for axially non-uniform heat flux) of the dimensionless non-boiling length. To adjust the uniform-heat-flux-based non-boiling length for heat flux non-uniformity, it may be divided by the peak/average heat flux ratio in the channel, but it was incorrectly divided by the peak heat flux. This has been corrected.
- (iii) The coding in the newer versions of the code (V3.4 and newer) of the Babelli-Ishii criteria, both the main criterion and the simplified criterion, was improved to account for fuel plates with fins (i.e., if the input option IH = -1). Along with this, the coding of the other two flow instability criteria available in PLTEMP/ANL (i.e., the Whittle and Forgan criterion, and the ORNL criterion) was also improved to account for the presence of fins.

1. Babelli-Ishii Criterion for Flow Instability

This section summarizes the Babelli-Ishii criterion [1] for excursive flow instability after boiling inception. Figure 1 shows a coolant channel with downward flow. The results are applicable to upward flow also. Babelli and Ishii obtained Eq. (1) given below as a criterion for excursive flow instability due to boiling inception in a coolant channel heated by a *uniform* wall heat flux, based on their theoretical and experimental work and the experimental data of Dougherty [2]. This equation is Eq. (5) of Babelli and Ishii [1], after substituting the value of $\rho_{in} V_{in} \Delta h_{nvg} / q_w''$ from Eq. (6) of Babelli and Ishii [1] which is basically the Saha-Zuber correlation [3] for net vapor generation. The channel flow is *stable* if the ratio N_{sub}/N_{zu} on the left hand side of Eq. (1) is greater than the quantity on the right hand side, and *unstable* if the ratio N_{sub}/N_{zu} is smaller.

$$\frac{N_{sub}}{N_{zu}} = \left(\frac{L_{nvg}}{L} \right)_{critical} + \frac{A_F}{\zeta_H L} \begin{cases} 0.0022 Pe & \text{if } Pe < 70000 \\ 154 & \text{if } Pe > 70000 \end{cases} \quad (1)$$

where

$$N_{\text{sub}} = \text{Subcooling number} = \frac{\Delta h_{\text{in}} (\rho_{\text{f,nvg}} - \rho_{\text{g,nvg}})}{h_{\text{fg}} \rho_{\text{g,nvg}}} \quad (2)$$

$$N_{\text{Zu}} = \text{Zuber number} = \frac{q_w'' \zeta_H L (\rho_{\text{f,nvg}} - \rho_{\text{g,nvg}})}{\rho_{\text{in}} V_{\text{in}} A_F h_{\text{fg}} \rho_{\text{g,nvg}}} \quad (3)$$

$$N_{\text{sub}}/N_{\text{Zu}} = \text{Ratio of Subcooling number to Zuber number} = \frac{\rho_{\text{in}} V_{\text{in}} A_F \Delta h_{\text{in}}}{q_w'' \zeta_H L} \quad (4)$$

Δh_{in} = Subcooling at the start of heated length, J/kg = $h_{\text{f}}(P_{\text{in}}) - h_{\text{in}} \approx h_{\text{f}}(P_{\text{nvg}}) - h_{\text{in}}$

Δh_{nvg} = Subcooling at the NVG position, J/kg = $h_{\text{f}}(P_{\text{in}}) - h_{\text{nvg}} \approx h_{\text{f}}(P_{\text{nvg}}) - h_{\text{nvg}}$

L = Channel heated length, m

L_{nvg} = Non-boiling length, i.e., the distance from the start of heated length of channel to the position of net vapor generation, m

L_{nvg}/L = Dimensionless non-boiling length

$(L_{\text{nvg}}/L)_{\text{critical}}$ = Critical value of the dimensionless non-boiling length. Based on experimental data for freon-113 and water, it is plotted in Fig. 4 of Ref. [1] as function of the Subcooling number, and the same data is tabulated here in Table X-1.

A_F = Flow area of channel, m^2

ζ_H = Heated perimeter of channel, m

ρ_{in} = Coolant density at inlet, kg/m^3

V_{in} = Coolant velocity at inlet, m/s

q_w'' = Wall heat flux, W/m^2

Pe = Peclet number = $\rho_{\text{in}} C_p V_{\text{in}} D_h / K$

The Peclet number dependent quantity inside the curly brackets on the right hand side of Eq. (1) can also be found in Ref. [4]. In the case of *upward flow*, the quantity is calculated as shown in Eq. (1) given above. However, in the case of *downward flow*, Babelli and Ishii suggest (based on the experimental data of Johnston [5]) that the quantity is always 154. Saha and Zuber [3] have discussed two regions, i.e., the region $Pe < 70,000$ and the region $Pe > 70,000$, as follows:

In the region $Pe < 70,000$ (i.e., at low mass flow rates), bubbles form attached to the wall downstream of the position at which the condition for the onset of nucleate boiling is satisfied, the local subcooling is still high, the bubbles that detach and move to the liquid core get immediately condensed, and the detached bubbles are forced to stay near the wall. The bubbles flow downstream while remaining close to the wall, until the local subcooling is low enough to initiate a rapid increase in void fraction. This is the position of net vapor generation. The region $Pe < 70,000$ is called the thermally controlled region.

In the region $Pe > 70,000$ (i.e., at high mass flow rates), the Stanton number $q_w'' / \rho_{\text{in}} V_{\text{in}} \Delta h_{\text{nvg}}$ reaches the value of 0.0065, the bubbles attached to the wall grow in size acting like wall surface roughness, the bubbles detach due to hydrodynamic forces at the point where the surface roughness reaches a characteristic value of 0.02, the detached bubbles can move to the liquid core without being rapidly condensed, and this results in a rapid increase in vapor void fraction at the point of bubble detachment. The region $Pe > 70,000$ is called the hydrodynamically controlled region.

Table X-1. Critical Value of Dimensionless Non-boiling Length (L_{nvg}/L)_{critical} as Function of Subcooling Number

Subcooling Number, N_{sub}	Experimental Value of (L_{nvg}/L) _{critical}	
	Lower Limit	Upper Limit
2.69	0.0232	0.0232
5.38	0.0684	0.414
8.07	0.141	0.594
10.76	0.256	0.756
21.51	0.440	1.083
32.27	0.527	1.222
43.03	0.594	1.297
53.78	0.711	1.222
64.54	0.905	1.083
69.92	1.00	1.00
160.00	1.00	1.00

To calculate the Subcooling number using Eq. (2), the system reference pressure could be assumed equal to P_{in} or P_{nvg} , i.e., the coolant pressure at the start of the heated section or the pressure at the NVG position. The latter value is preferred as discussed in Appendix X.A.

A simpler criterion for flow instability due to boiling inception may also be inferred from Fig. 5 of Ref. [1] which is a plot on the N_{sub} - N_{zu} plane of several flow instability test data for Freon-113 and water. The plot suggests the following simple criterion for flow instability.

$$\frac{N_{sub}}{N_{zu}} = \begin{cases} > 1.36 & \text{clearly stable} \\ < 1.36 \text{ to } 1.0 & \text{may be stable or unstable} \\ < 1.0 & \text{clearly unstable} \end{cases} \quad (5)$$

To calculate the quantities in Eq. (1) for evaluating flow instability, one needs the channel exit temperature and pressure. The *first estimates* of the exit enthalpy h_{out} , and total pressure drop ΔP are calculated using Eqs. (6) and (7) where the thermally-induced change in coolant density is calculated using Eq. (8). The exit temperature T_{out} is estimated for use in Eq. (7), from h_{out} by assuming the exit pressure $P_{out} = P_{in}$. These estimates are improved by iteration.

$$h_{out} = h_{in} + \frac{q_w \zeta_H L}{\rho_{in} V_{in} A_F} \quad (6)$$

$$\Delta P = \left\{ K_{orifice} + \frac{f L}{D_h} \right\} \frac{W^2}{2 \rho_{ave} A_F^2} \pm \left(\rho_{in} - \frac{\Delta \rho}{2} \right) g L + \rho_{in} V_{in}^2 (\rho_{in} / \rho_{out} - 1), \quad (7)$$

use + for upflow, and – for downflow

$$\Delta \rho = \rho_{in} - \rho_{out} = \frac{\beta_{ave} Q}{C_{p,in} V_{in} A_F} \quad (8)$$

In Eq. (7), the terms in the curly brackets are the orifice loss and frictional pressure drop, the terms (having \pm sign) in the parentheses are the gravitational pressure drop, and the last term is the pressure drop due to velocity increase at exit caused by the coolant density decrease. In the absence of boiling at higher flow rates, the last term is negligible. ΔP decreases with decreasing inlet velocity V_{in} because the frictional pressure drop (the terms in the curly brackets of Eq. (7)) are then dominant, and these terms decrease with V_{in} . The term $\Delta\rho gL/2$ increases in magnitude with decreasing inlet velocity, and it is positive in downflow. Therefore, in the absence of boiling in downflow, there is a *minimum* in the ΔP versus V_{in} plot, i.e., $\partial(\Delta P)/\partial V_{in} = 0$ at a certain inlet velocity. At this minimum, the flow in the channel is unstable. In the absence of boiling in upflow, there is no such *minimum* in the ΔP versus V_{in} plot.

In the case of boiling and voiding, the last term may become as large as ~ 1000 times the inlet velocity head, and the frictional drop from the ONB position to the channel exit also becomes much greater than its liquid-phase value, thus increasing ΔP at low inlet velocities. This results in a *minimum* in the ΔP versus V_{in} plot, in both downflow and upflow.

2. Application of Babelli-Ishii Flow Instability Criterion to Whittle and Forgan Tests

The Babelli-Ishii criterion for the onset of flow instability (OFI) was applied to all 75 tests performed by Whittle and Forgan at a uniform heat flux [6]. The geometry data used in the present calculation of these 75 tests are listed in Table X-2. The last column of Table X-2 is an operating data, i.e., the measured ratio $\Delta T_{sub,o}/\Delta T_c$ at OFI, which is used for comparison with the present calculation. Eight tests (Test Numbers 17 to 24) performed in test section 1A using non-uniform heat fluxes were not analyzed. A program *Babelli.WFtests.f* was developed to calculate for each test, the coolant exit temperature, single-phase pressure drop, Subcooling number, Zuber number, and other needed quantities, for an *assumed* coolant inlet velocity.

2.1. Application of Flow Instability Criterion of Equation (1)

The coolant inlet velocity was varied in steps of 0.001 m/s from a suitable low value to a higher value, in search of the inlet velocity at which the ratio N_{sub}/N_{zub} , the left hand side of Eq. (1) becomes higher than the right hand side, i.e., the flow becomes stable. The inlet velocity just before the flow becomes stable is the inlet velocity at OFI. Table X-3 shows the exit coolant temperatures and pressure drops at different inlet velocities calculated for the application of the flow instability criterion of Eq. (1) to a typical Whittle and Forgan test (Test Number 1 for example). Using the data of Table X-3, the application of Babelli and Ishii flow instability criterion of Eq. (1) to Test Number 1 is shown in Table X-4. The data line shown in bold letters in Table X-4, at the inlet velocity of 2.712 m/s, marks the onset of flow instability.

The inlet velocity at OFI was calculated for each test listed in Table X-2, and the results are shown in Table X-5. The results for all 75 tests remain unchanged irrespective of whether the upper or the lower limit of $(L_{nvg} / L)_{critical}$ (given in Table X-1) is used in the calculation. This is because the upper and lower limits of $(L_{nvg} / L)_{critical}$, i.e., two limits exist only if the Subcooling number is less than 69.92. However, in all the 75 tests the Subcooling number is greater than 69.92, as shown in Table X-5.

The measured coolant inlet velocity and flow rate at OFI are also shown in Table X-5. The measured flow rate (W) and inlet velocity at OFI (V_{in}) were calculated from the measured exit coolant temperature using Eq. (7). This equation is obtained by equating the total power to the coolant enthalpy change times flow rate.

$$\rho_{in} V_{in} A_F = W = \frac{Q}{h(P_{out}, T_{out}) - h(P_{in}, T_{in})} \quad (7)$$

The measured exit temperature was itself calculated from the measured ratio $\Delta T_{sat,out}/\Delta T_c$ reported by Whittle and Forgan [6], using Eq. (8). To derive this equation, one substitutes the definitions $\Delta T_{sat,out} = T_{sat,out} - T_{out}$ and $\Delta T_c = T_{out} - T_{in}$ into the definition $\Delta T_{sat,out}/\Delta T_c = r$, obtains the relationship $(T_{sat,out} - T_{out})/(T_{out} - T_{in}) = r$, and then solves for T_{out} .

$$T_{out} = \frac{T_{sat,out} + r T_{in}}{1 + r} \quad (8)$$

where $r =$ the measured ratio $\Delta T_{sat,out}/\Delta T_c$ at OFI reported by Whittle and Forgan, and shown in Table X-2. See nomenclature for the other symbols.

The measured flow rates at OFI thus obtained were found to be in agreement with those obtained by A. P. Olson using a different approach during an earlier analysis of these tests [7]. The difference between the measured and calculated inlet velocities at OFI in a test determines the error in the Babelli and Ishii flow instability criterion. A statistical analysis was done to find the mean and the standard deviation of the difference between the calculated and measured inlet velocities (calculated – measured), and the results are shown below and in Table X-5.

Mean error in the calculated inlet velocity at OFI	= 0.384 m/s
Standard deviation of the error in the calculated inlet velocity at OFI	= 0.242 m/s

The mean error is positive, implying that the criterion predicts flow instability at a higher inlet velocity (and hence higher flow rate) than that measured experimentally. Figure 4 shows a comparison of the calculated versus the measured coolant inlet velocity at OFI. The data points are generally above the line of slope 1, indicating that the criterion is conservative. The mean value of the Whittle and Forgan parameter η at OFI is found to be 37.55 with a standard deviation of 3.16.

In these tests, Table X-5 shows that the calculated ratio $\Delta T_c/\Delta T_{sat}$ at OFI, i.e., coolant temperature change divided by the difference between the saturation temperature at exit and the inlet temperature, has a mean value of 0.7314 which is smaller than the measured value of about 0.8 reported by Whittle and Forgan. This implies that the Babelli-Ishii criterion predicts flow instability earlier than it should, i.e., at a smaller coolant temperature rise than that measured experimentally. This also indicates that the criterion is conservative.

2.2. Application of Flow Instability Criterion of Eq. (5)

The simple flow instability criterion of Eq. (5) was also applied to the above 75 tests reported by Whittle and Forgan. The coolant inlet velocity was varied in steps of 0.001 m/s from a suitable low value to a higher value, in search of the inlet velocity at which the ratio $N_{\text{sub}}/N_{\text{zub}}$ becomes greater than 1.36, i.e., the flow becomes stable according to Eq. (5). The inlet velocity just before the ratio $N_{\text{sub}}/N_{\text{zub}}$ becomes greater than 1.36 is the inlet velocity at OFI. Table X-3 is independent of the flow instability criterion used, i.e., whether Eq. (1) or Eq. (5) is used. This table shows the exit coolant temperatures and pressure drops at different inlet velocities calculated for the application of the flow instability criterion of Eq. (5) to a typical Whittle and Forgan test (e.g., Test Number 1). Using the data of Table X-3, the application of the flow instability criterion of Eq. (5) to Test Number 1 is shown by an underlined line in Table X-4. The data in the underlined line in Table X-4, at the inlet velocity of 2.620 m/s, marks the onset of flow instability.

The inlet velocity at OFI was calculated for each test listed in Table X-2, and the results are shown in Table X-6. The last column of Table X-6 gives the ratio $N_{\text{sub}}/N_{\text{zub}}$ calculated at OFI and is 1.36 for all tests as required by the criterion. The difference between the measured and calculated inlet velocities at OFI in a test determines the error in this flow instability criterion. A statistical analysis was done to find the mean and the standard deviation of the difference between the calculated and measured inlet velocities (calculated – measured), and the results are shown below and in Table X-6.

Mean error in the calculated inlet velocity at OFI	= 0.363 m/s
Standard deviation of the error in the calculated inlet velocity at OFI	= 0.319 m/s

Again, the mean error is positive, implying that the criterion predicts instability at a higher inlet velocity (and hence flow rate) than that measured experimentally. It is noted that the mean error for the criterion of Eq. (5) is somewhat smaller than that for the criterion of Eq. (1), and the standard deviation for the criterion of Eq. (5) is greater than that for the criterion of Eq. (1). Figure 5 shows a comparison of the calculated versus the measured coolant inlet velocity at OFI. The data points in Fig. 5 are generally above the line of slope 1, indicating that the criterion is conservative.

A comparison of the scatter of data points in Figs. 4 and 5 also shows that the standard deviation in Fig. 5 is greater than that in Fig. 4. For the 12 tests done by Whittle and Forgan in their test section number 3 (having a $L/D_H = 190.9$), the simple criterion finds the parameter η at OFI to be about 68.2 which is about two times the values of η at OFI found for all other tests. This happens because the parameter η at OFI *calculated based on Eq. (5)* equals $0.36(L/D_H)$, as explained in Section 3 below.

The average value of the calculated ratio $\Delta T_c/\Delta T_{\text{sat}}$ at OFI determined by the simple criterion is 0.7367 which is closer (compared to the former criterion) to the measured value of about 0.8 reported by Whittle and Forgan. This implies that the simple criterion also predicts flow instability earlier than it should, i.e., at a smaller coolant temperature rise than that measured experimentally. This criterion also is conservative.

2.3. Approach to Flow Instability

To understand how a research reactor approaches the flow instability condition in a typical channel, seven important quantities tabulated in Table X-4 for Whittle and Forgan Test Number 1 are plotted in Fig. 6 as functions of the inlet velocity. These quantities include the left and right hand sides of Babelli-Ishii criterion given by Eq. (1). The program *Babelli.WFtests.f* developed to apply the flow instability criteria of Eq. (1) and Eq. (5) to Whittle and Forgan tests saves the data shown in Table X-4 and Fig. 6 in an output file named *flow.instability.unit9*. If Eq. (1) is used to find flow instability as the coolant inlet velocity decreases from 7.5 m/s, the ratio $(L_{nv}/L)_{critical}$ on the right hand side (RHS) of Eq. (1) is always 1.0 because the Subcooling number, 129.41, remains greater than 69.92 (see Table X-1). Furthermore, the Peclet number is always greater than 70,000, thus making the quantity in the curly brackets on the RHS of Eq. (1) constant at 154. Therefore, using the channel thickness, width, and heated length given in Table X-2, the RHS of Eq. (1) becomes constant at $1.407 \left(= 1.0 + \frac{0.127}{2 \times 24.0} \times 154 \right)$ as shown in Fig. 6.

The ratio N_{sub}/N_{zub} on the left hand side of Eq. (1) decreases linearly with the coolant inlet velocity (from 3.891 at $V_{in} = 7.5$ m/s to 0.830 at $V_{in} = 1.6$ m/s). The ratio N_{sub}/N_{zub} at inlet velocity V_{in} is $3.891 * V_{in} / 7.5$. Therefore, the inlet velocity at which the ratio N_{sub}/N_{zub} equals 1.407 is $1.407 \times 7.5 / 3.891 = 2.712$ m/s. This is the calculated inlet velocity at OFI in Test Number 1, according to the Babelli-Ishii criterion of Eq. (1).

It is noted that the ratio N_{sub}/N_{zub} at OFI is 1.407, and not 1.36 as required by the simple instability criterion given by Eq. (5). From the above description it is seen that the ratio N_{sub}/N_{zub} at OFI equals $1.0 + 77 \times (\text{channel thickness} / \text{heated length})$ for channels of rectangular cross section. The ratio N_{sub}/N_{zub} at OFI is therefore not constant. It depends on the channel thickness and length. The values of this ratio for the 75 tests are given in the last column of Table X-5. They vary from 1.107 to 1.462.

3. Value of Parameter η According to the Instability Criterion of Equation (5)

It is shown in this section that the simple flow instability criterion of Eq. (5) implies that the parameter η at OFI is about $0.36(L / D_H)$. This explains why in Table X-6 the values of parameter η at OFI for Test Numbers 63 to 74 are about twice the values of η at OFI found for all other tests. The reason is that Test Numbers 63 to 74 were performed in a test section having an L/D_H nearly twice the L/D_H in all other tests (see L/D_H of all tests in Table X-2).

To show that the parameter η at OFI based on Eq. (5) is about $0.36(L / D_H)$, it is noted that the ratio N_{sub}/N_{zub} at OFI equals 1.36 according to this criterion. The ratio N_{sub}/N_{zub} is defined above by Eq. (4). The numerator of Eq. (4) can be written as Eq. (9), and the denominator of Eq. (4) is simply the total heat transferred, Q , to the coolant in the channel. Thus the ratio N_{sub}/N_{zub} equals $W\Delta h_{in}/Q$ as shown in Eq. (10). Noting that Q/W equals Δh_c (the coolant enthalpy rise in the channel), the ratio N_{sub}/N_{zub} is given by $\Delta h_{in}/\Delta h_c$ as shown in Eq. (10). Therefore, at OFI, the criterion of Eq. (5) implies Eq. (11).

$$\rho_{in} V_{in} A_F \Delta h_{in} = W \Delta h_{in} \quad (9)$$

$$\frac{N_{\text{sub}}}{N_{\text{zub}}} = \frac{W \Delta h_{\text{in}}}{Q} = \frac{\Delta h_{\text{in}}}{\Delta h_{\text{c}}} \quad (10)$$

$$\Delta h_{\text{in}} = 1.36 \Delta h_{\text{c}} \quad \text{at OFI} \quad (11)$$

Noting that $\Delta h_{\text{in}} = \Delta h_{\text{out}} + \Delta h_{\text{c}}$, Eq. (11) gives Δh_{out} at the onset of flow instability.

$$\Delta h_{\text{out}} = 0.36 \Delta h_{\text{c}} \quad \text{at OFI} \quad (12)$$

The purpose here is to find the value of the Whittle and Forgan parameter η at OFI which is defined by Eq. (13). In Eq. (13), the ratio of temperature differences, $\Delta T_{\text{sub,o}}/\Delta T_{\text{c}}$, can be estimated by the ratio of the corresponding enthalpy differences, as written below in Eq. (14).

$$\eta = \frac{\Delta T_{\text{sub,o}}}{\Delta T_{\text{c}}} \frac{L}{D_{\text{H}}} \quad \text{at OFI} \quad (13)$$

$$\frac{\Delta T_{\text{sub,o}}}{\Delta T_{\text{c}}} = \frac{T_{\text{sat,out}} - T_{\text{out}}}{T_{\text{out}} - T_{\text{in}}} = \frac{(h_{\text{f}} - h_{\text{out}})/C_{\text{p}}}{(h_{\text{out}} - h_{\text{in}})/C_{\text{p}}} = \frac{\Delta h_{\text{out}}}{\Delta h_{\text{c}}} \quad \text{at OFI} \quad (14)$$

Using Eq. (14) in Eq. (13), the parameter η can be approximated by Eq. (15).

$$\eta = \frac{\Delta h_{\text{out}}}{\Delta h_{\text{c}}} \frac{L}{D_{\text{H}}} \quad \text{at OFI} \quad (15)$$

Using the value of Δh_{out} at OFI obtained in Eq. (12), one gets from Eq. (15) the value of parameter η at OFI.

$$\eta = \frac{0.36 \Delta h_{\text{c}}}{\Delta h_{\text{c}}} \frac{L}{D_{\text{H}}} = 0.36 \frac{L}{D_{\text{H}}} \quad \text{at OFI} \quad (16)$$

Equation (16) is the desired result of this section. It means that the Whittle and Forgan parameter η at OFI based on the simple flow instability criterion of Eq. (5) is not constant. It varies linearly with the heated length-to-hydraulic diameter ratio. That is why the parameter η at OFI calculated based on Eq. (5) is about 68.2 in Test Numbers 63 to 74 (having $L/D_{\text{H}} = 190.9$).

4. A Program for Applying the Instability Criteria to Whittle and Forgan Tests

A program *Babelli.WFtests.f* was developed to apply the flow instability criteria of Eq. (1) and Eq. (5) to the 75 tests reported by Whittle and Forgan. It reads an input file containing the geometry and operating data of the tests. The input data are shown in Table X-2. It saves the output results shown in Tables X-3, X-4, and X-5 (or X-6 depending upon the criterion chosen) in three output files as listed below.

(1) Input file	Babelli.WFtests.Input.Data	contains the data shown in Table X-2.
(2) Output file	flow.instability.unit6	contains the results shown in Table X-3.
(3) Output file	flow.instability.unit9	contains the results shown in Table X-4.
(4) Output file	flow.instability.summary	contains the results shown in Table X-5 or Table X-6.

There is an internally set input variable IEQ to choose one of the two instability criteria, as defined below, and there is an internally set input variable DELVIN to define the step size for coolant inlet velocity (usually DELVIN = 0.001 m/s).

IEQ = 1, use Babelli-Ishii Eq. (1) to predict flow instability
 = 2, use $N_{sub}/N_{zu} > 1.36$ for stability

5. Conclusions

A program has been developed to apply the Babelli-Ishii flow instability criterion of Eq. (1) or the simple criterion of Eq. (5) to 75 tests reported by Whittle and Forgan. The comparison of the calculated (using either criterion) and measured coolant inlet velocities at OFI in these tests shows that both criteria are conservative. Both criteria, Eqs. (1) and (5), are implemented in the PLTEMP/ANL V3.4 code [7].

NOMENCLATURE

Symbols

A_F	= Flow area of channel, m^2
C_p	= Specific heat of the coolant, $J/kg\text{-}^\circ C$
D_h	= Hydraulic diameter based on the <i>wetted</i> perimeter of the channel, m
D_H	= Hydraulic diameter based on the <i>heated</i> perimeter of the channel, m
$h(P,T)$	= Liquid coolant enthalpy as a function of coolant pressure P and temperature T, J/kg
h_{in}	= Coolant enthalpy at the heated length inlet = $h(P_{in}, T_{in})$, J/kg
h_{out}	= Coolant enthalpy at the heated length exit = $h(P_{out}, T_{out})$, J/kg
$h_{f,in}$	= Saturated liquid enthalpy at the heated length inlet pressure = $h(P_{in})$, J/kg
$h_{f,out}$	= Saturated liquid enthalpy at the heated length exit pressure = $h(P_{out})$, J/kg
$h_{fg}(P)$	= Latent heat of vaporization as a function of coolant pressure P
Δh_c	= $h_{out} - h_{in}$ = Coolant enthalpy rise in the channel, J/kg
Δh_{in}	= $h_{f,out} - h_{in}$ = Inlet subcooling in terms of enthalpy, J/kg
Δh_{out}	= $h_{f,out} - h_{out}$ = Exit subcooling in terms of enthalpy, J/kg
K	= Coolant thermal conductivity, $W/m\text{-}^\circ C$
L	= Channel heated length, m
L_{nvg}	= Non-boiling length, i.e., the distance from start of heated length of channel to the position of net vapor generation, m
N_{zu}	= Zuber number
N_{sub}	= Subcooling number

P	= Coolant pressure, Pa
Pe	= Peclet number = $Re Pr = \rho_{in} C_p V_{in} D_h / K$
Pr	= Prandtl number = $\mu C_p / K$
P _{in}	= Channel inlet pressure, Pa
P _{out}	= Channel outlet pressure, Pa
q _w "	= Wall heat flux (assumed uniform over the channel length), W/m ²
Q	= q _w " ζ _H L = Total power input to the coolant, W
Re	= Reynolds number = $\rho_{in} V_{in} D_h / \mu$
ρ	= Coolant density, kg/m ³
T	= Coolant temperature, °C
T _{in}	= Coolant temperature at the channel inlet, °C
T _{out}	= Coolant temperature at the channel outlet, °C
T _{sat} (P)	= Coolant saturation temperature at a specific pressure P, °C
T _{sat,in}	= Coolant saturation temperature at channel inlet, °C
T _{sat,out}	= Coolant saturation temperature at channel outlet, °C
ΔT _c	= T _{out} - T _{in} = Coolant temperature rise at OFI, °C
ΔT _{sat}	= T _{sat,out} - T _{in} = Saturation temperature at exit minus inlet temperature at OFI, °C
ΔT _{sub,o}	= T _{sat,out} - T _{out} = Exit subcooling at the onset of flow instability, °C
η	= $\frac{T_{sat,out} - T_{out}}{T_{out} - T_{in}} \frac{L}{D_H}$ = A parameter used by Whittle and Forgan in their analysis of the flow instability tests
μ	= Absolute viscosity of the coolant, Pa-s
V	= Coolant velocity, m/s
W	= $\rho_{in} V_{in} A_F$ = Coolant flow rate, kg/s
ζ _H	= Heated perimeter, m

Subscripts

c	= coolant
F	= flow
f	= saturated liquid
g	= saturated vapor
fg	= liquid to vapor phase change
H	= heated
h	= hydraulic
in	= channel heated length inlet
nvg	= position of net vapor generation
out	= channel heated length outlet
sat	= saturated

REFERENCES

- (1) I. Babelli and M. Ishii, "Flow Excursion Instability in Downward Flow Systems, Part II: Two-Phase Instability," *Nuclear Engineering and Design*, Vol. 206, pp. 97-104 (2001).
- (2) T. Dougherty, C. Fighetti, G. Reddy, B. Yang, E. McAssey Jr., and Z. Qureshi, "Flow Instability in Vertical Channels," *ASME Heat Transfer Division, HTD-Vol. 159*, pp. 177-186 (1991).
- (3) P. Saha and N. Zuber, "Point of Net Vapor Generation and Vapor Void Fraction in Subcooled Boiling," *Proc. Fifth International Heat Transfer Conf.*, Vol. 4, pp. 175-179 (1974).
- (4) W. M. Rohsenow, J. P. Hartnett, and Y. I. Cho, "Handbook of Heat Transfer," McGraw-Hill, Washington D.C., Third Edition, p. 15.92, (1998).
- (5) B. S. Johnston, "Subcooled Boiling of Downward Flow in a Vertical Annulus," *ASME Heat Transfer Division, HTD-Vol. 109*, pp. 149-156 (1989).
- (6) W. H. Whittle and R. Forgan, "A Correlation for the Minima in the Pressure Drop Versus Flow-Rate Curves for Sub-cooled Water Flowing in Narrow Heated Channels," *Nuclear Engineering and Design*, Vol. 6, pp. 89-99 (1967).
- (7) A. P. Olson and M. Kalimullah, Argonne National Laboratory, unpublished information, 2008.

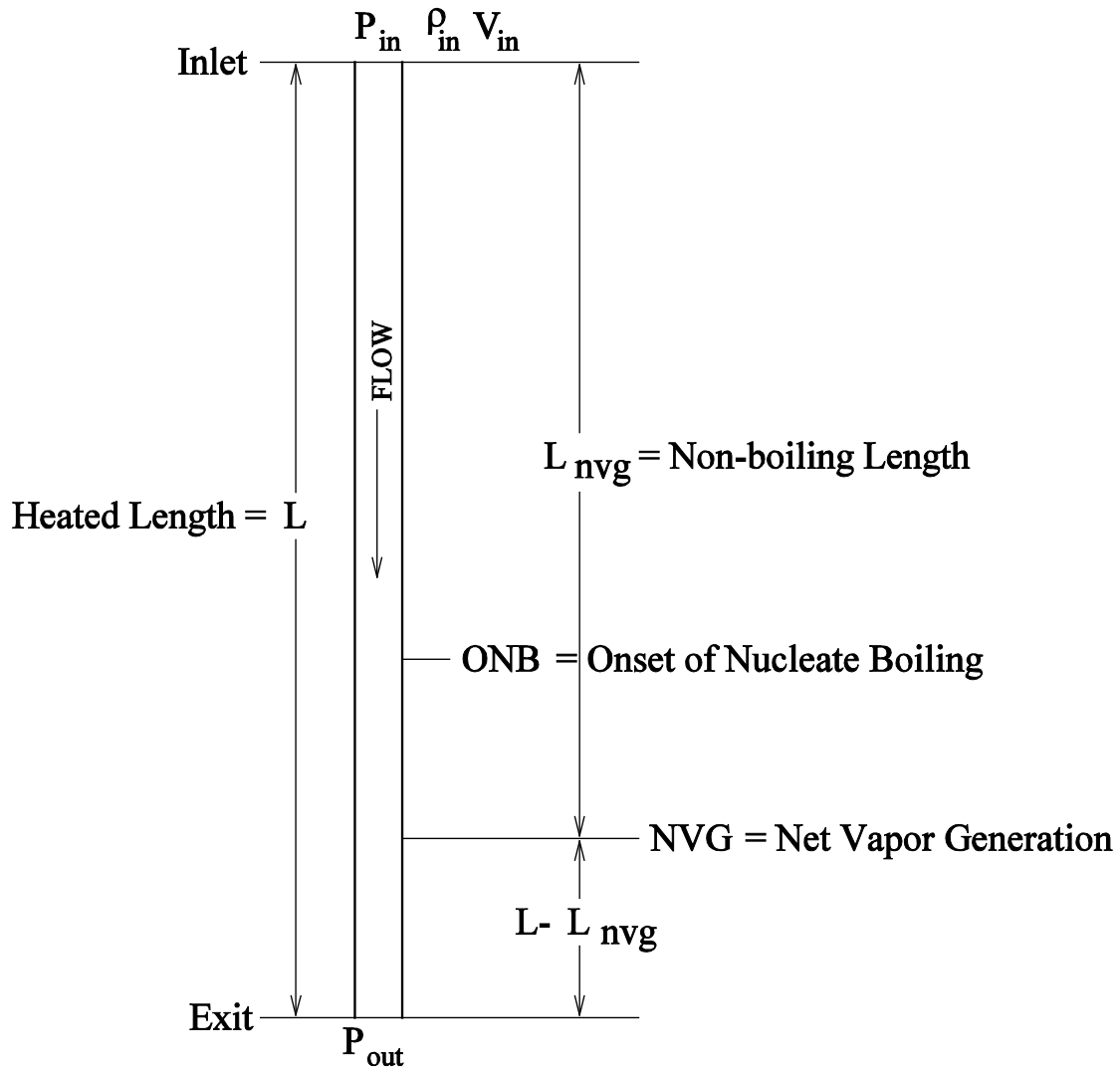


Fig. 1. Schematic Diagram of a Heated Coolant Channel with Downward Flow

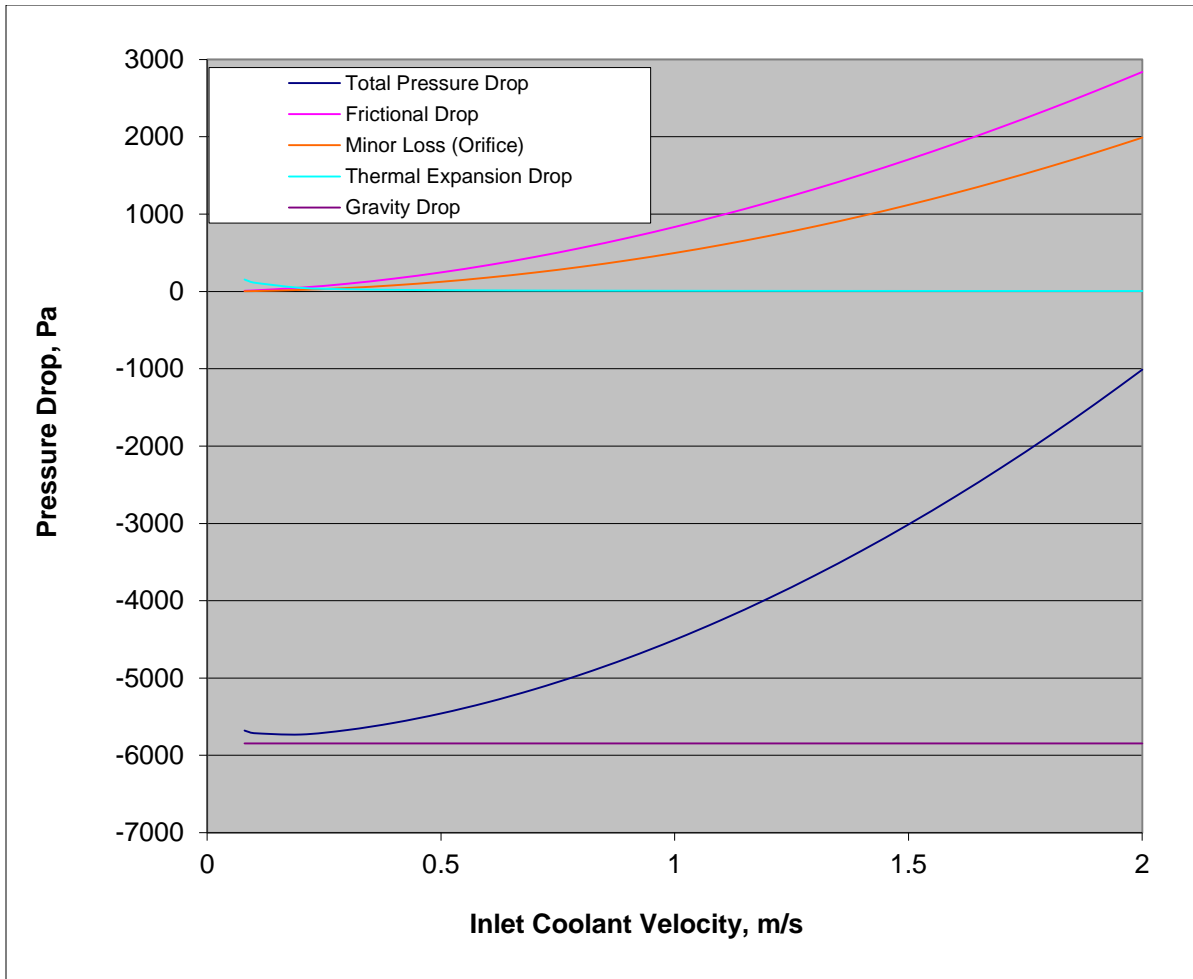


Fig. 2. Dependence of Total Pressure Drop on Inlet Velocity for a Coolant Channel with Downflow of Water at a Given Power of 7 kW

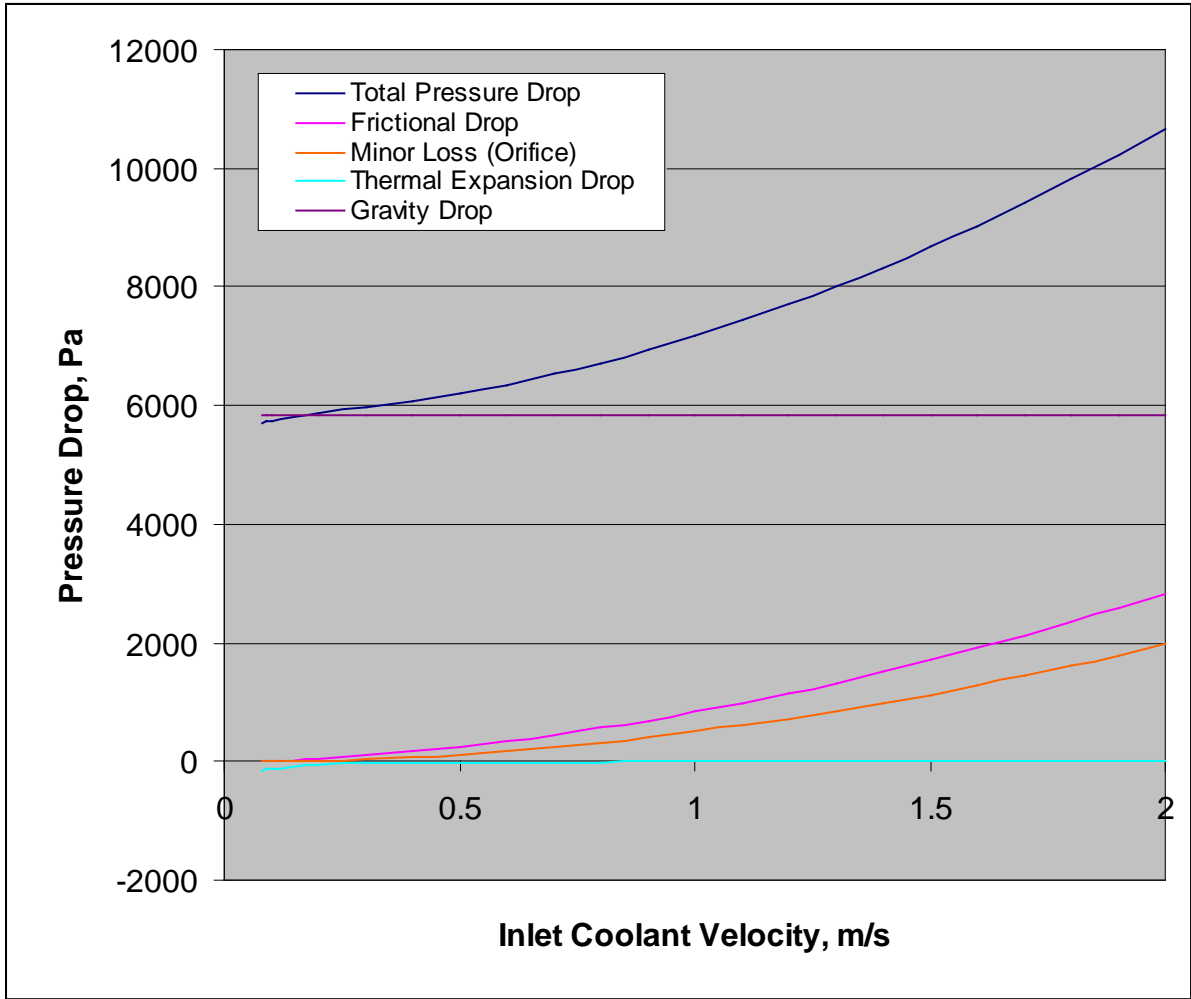


Fig. 3. Dependence of Total Pressure Drop on Inlet Velocity for a Coolant Channel with Upflow of Water at a Given Power of 7 kW

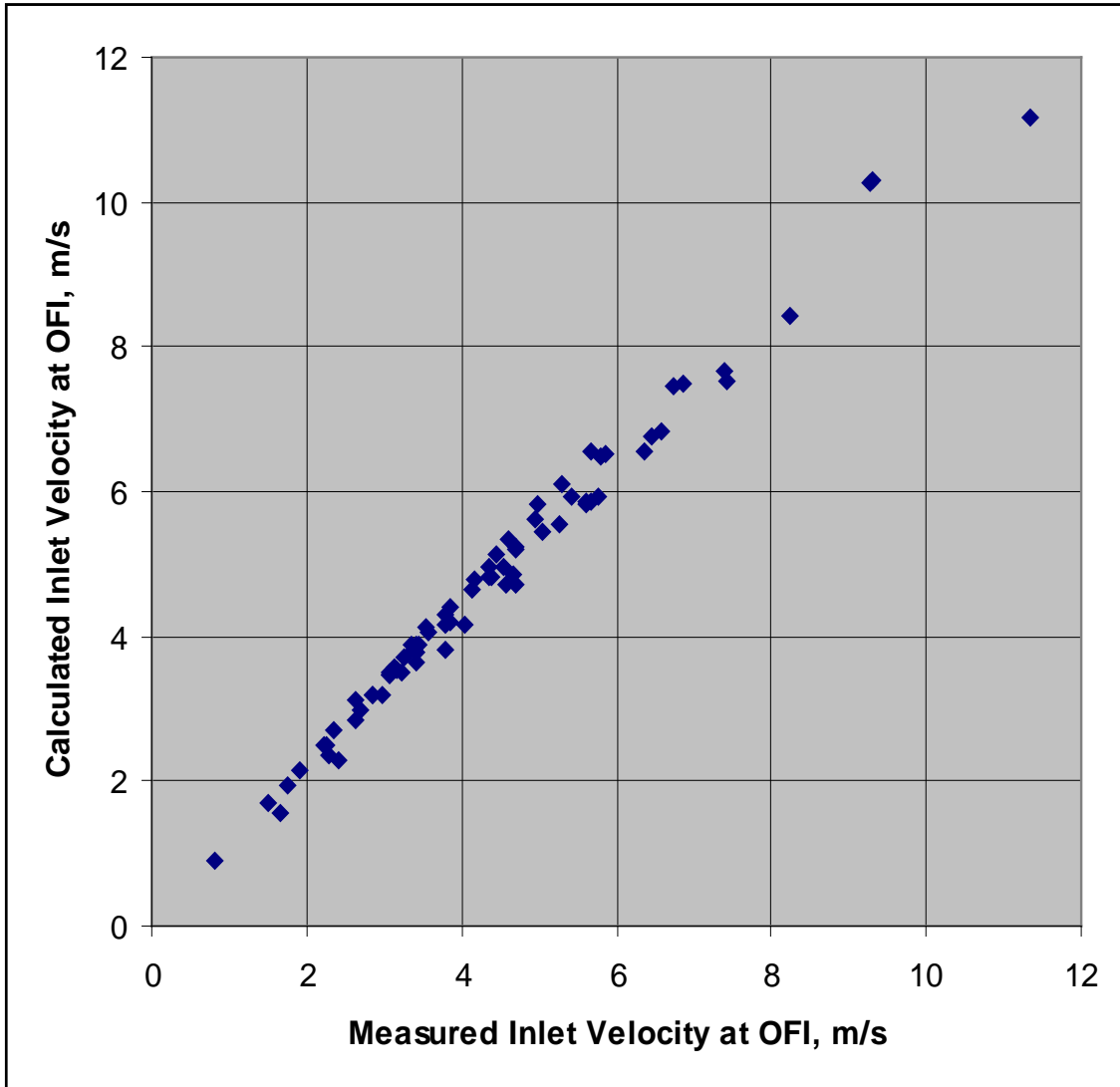


Fig. 4. Comparison of Coolant Inlet Velocity at OFI Calculated Using Eq. (1) Versus its Measured Value in 75 Tests Reported by Whittle and Forgan

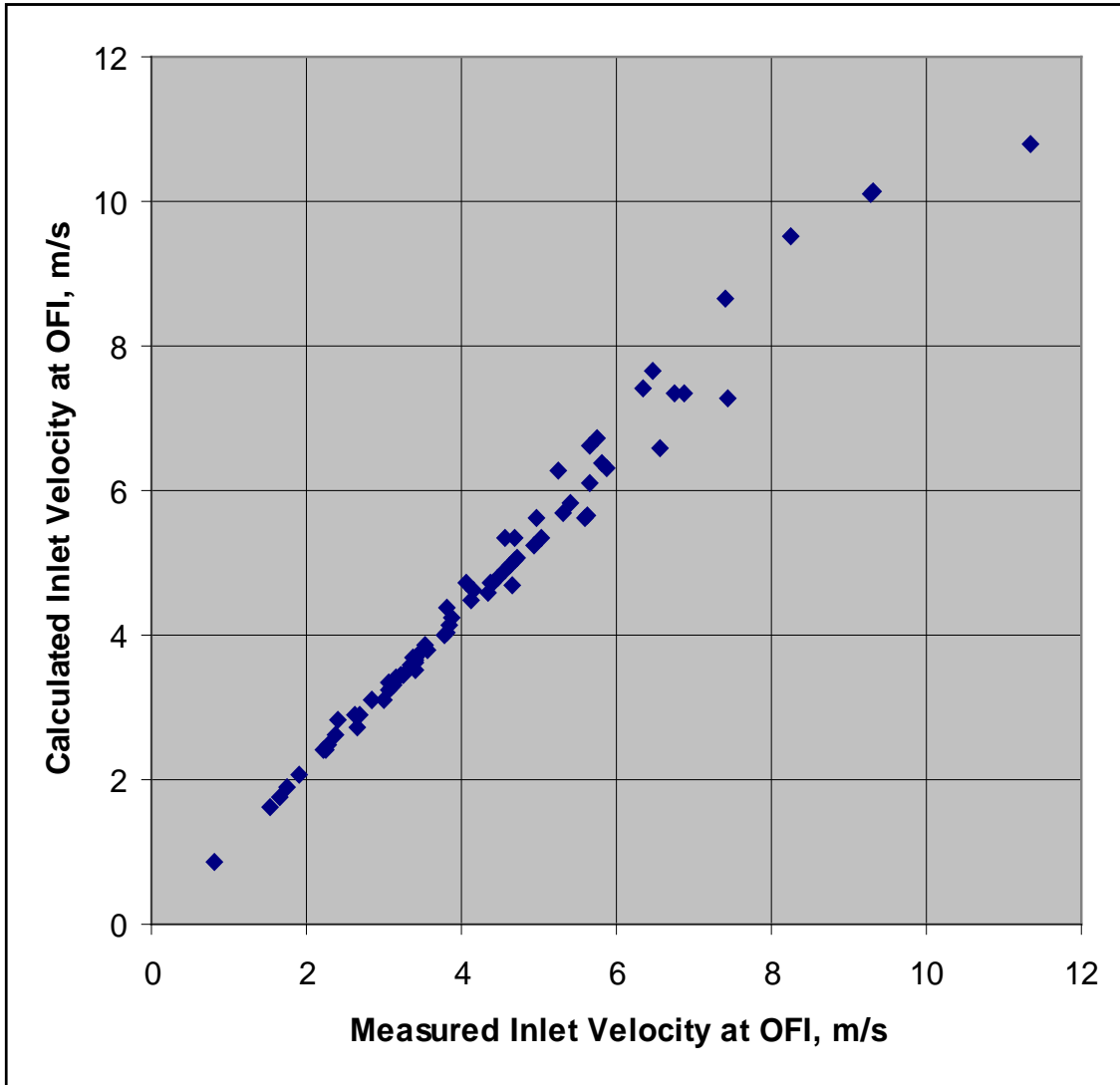


Fig. 5. Comparison of Coolant Inlet Velocity at OFI Calculated Using Eq. (5) Versus its Measured Value in 75 Tests Reported by Whittle and Forgan

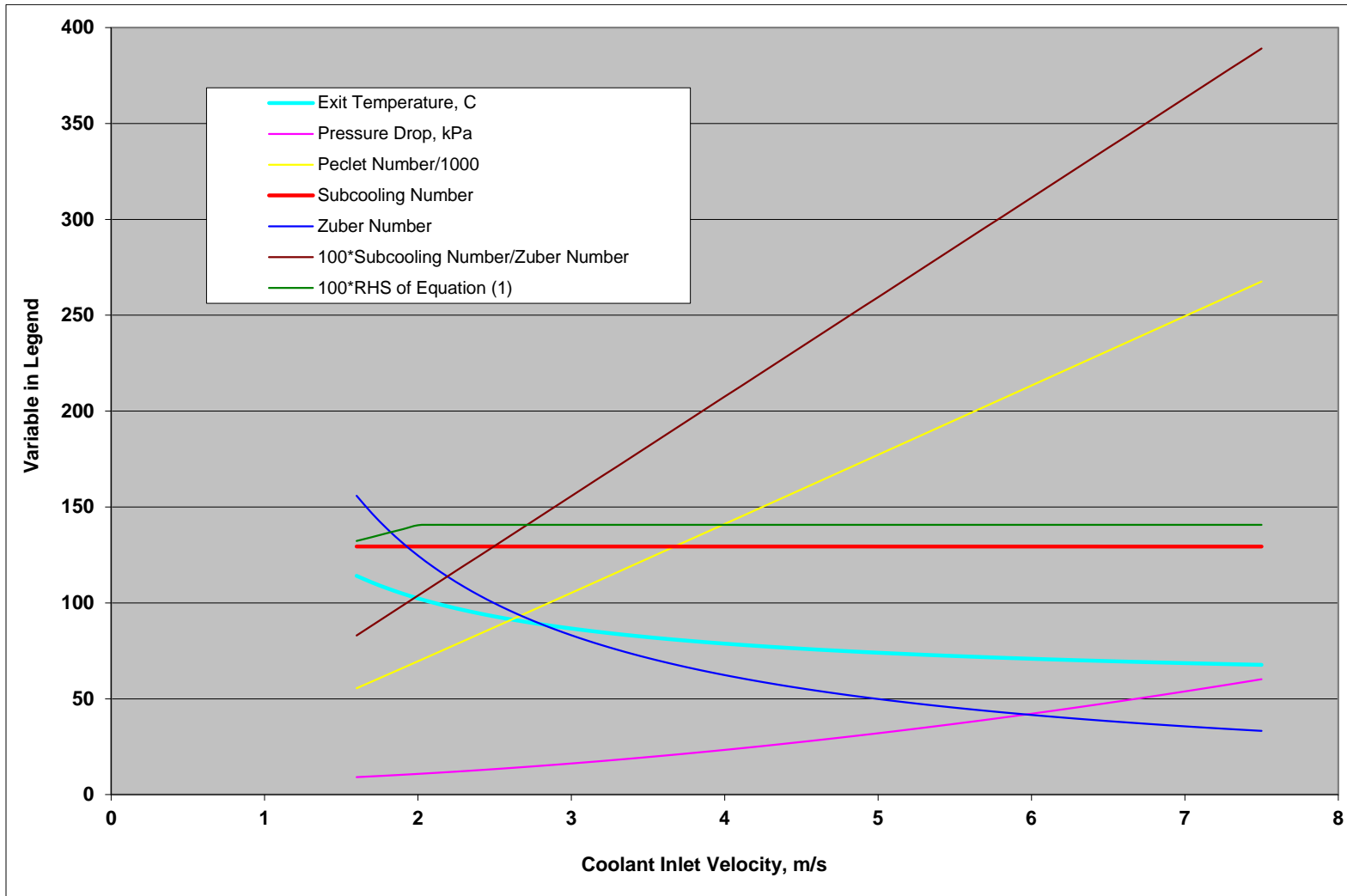


Fig. 6. Variation of Ratio N_{sub}/N_{zub} and Right Hand Side of Eq. (1) Over the Heated Length of Channel in Whittle and Forgan Test 1.

Table X-2. Geometry and Operating Data for 75 Flow Instability Tests Performed by Whittle and Forgan

Test No.	Flow Direction*	Inlet Temp °C	Heat Flux W/cm ²	Channel Thickness inch	Channel Width inch	Heated Length inch	Minor Loss Coeff	Exit Pressure psia	$\Delta T_{sub,o} / \Delta T_c$
1	1	55.0	104.0	0.127	1.0	24.0	0.0	17.0	0.224
2	1	55.0	145.0	0.127	1.0	24.0	0.0	17.0	0.266
3	1	55.0	184.0	0.127	1.0	24.0	0.0	17.0	0.220
4	1	55.0	250.0	0.127	1.0	24.0	0.0	17.0	0.266
5	1	55.0	82.0	0.127	1.0	24.0	0.0	17.0	0.250
6	1	55.0	136.0	0.127	1.0	24.0	0.0	17.0	0.250
7	1	55.0	160.0	0.127	1.0	24.0	0.0	17.0	0.282
8	1	55.0	200.0	0.127	1.0	24.0	0.0	17.0	0.266
9	1	45.0	160.0	0.127	1.0	24.0	0.0	17.0	0.250
10	1	45.0	180.0	0.127	1.0	24.0	0.0	17.0	0.250
11	1	45.0	204.0	0.127	1.0	24.0	0.0	17.0	0.234
12	1	60.0	110.0	0.127	1.0	24.0	0.0	17.0	0.250
13	1	60.0	160.0	0.127	1.0	24.0	0.0	17.0	0.250
14	1	60.0	180.0	0.127	1.0	24.0	0.0	17.0	0.266
15	1	60.0	200.0	0.127	1.0	24.0	0.0	17.0	0.204
16	1	35.0	136.0	0.127	1.0	24.0	0.0	17.0	0.250
25	0	45.0	78.0	0.127	1.0	24.0	0.0	17.0	0.266
26	0	45.0	116.0	0.127	1.0	24.0	0.0	17.0	0.266
27	0	45.0	148.0	0.127	1.0	24.0	0.0	17.0	0.250
28	0	55.0	115.0	0.127	1.0	24.0	0.0	17.0	0.266
29	0	55.0	75.0	0.127	1.0	24.0	0.0	17.0	0.266
30	0	55.0	146.0	0.127	1.0	24.0	0.0	17.0	0.250
31	0	45.0	42.0	0.127	1.0	24.0	0.0	17.0	0.282
32	1	55.0	147.0	0.096	1.0	16.0	0.0	17.0	0.282
33	1	55.0	170.0	0.096	1.0	16.0	0.0	17.0	0.282
34	1	55.0	180.0	0.096	1.0	16.0	0.0	17.0	0.282
35	1	55.0	215.0	0.096	1.0	16.0	0.0	17.0	0.266
36	1	45.0	196.0	0.096	1.0	16.0	0.0	17.0	0.282
37	1	45.0	250.0	0.096	1.0	16.0	0.0	17.0	0.282
38	1	45.0	180.0	0.096	1.0	16.0	0.0	17.0	0.282
39	1	65.0	177.0	0.096	1.0	16.0	0.0	17.0	0.266
40	1	65.0	203.0	0.096	1.0	16.0	0.0	17.0	0.266
41	1	65.0	218.0	0.096	1.0	16.0	0.0	17.0	0.261
42	1	65.0	123.0	0.096	1.0	16.0	0.0	17.0	0.282
43	1	45.0	250.0	0.096	1.0	16.0	0.0	25.0	0.250
44	1	65.0	242.0	0.096	1.0	16.0	0.0	25.0	0.282
45	1	65.0	134.0	0.096	1.0	16.0	0.0	25.0	0.234

Table X-2. Cont'd.

Test No.	Flow Direction	Inlet Temp °C	Heat Flux W/cm ²	Channel Thickness inch	Channel Width inch	Heated Length inch	Minor Loss Coeff	Exit Pressure psia	$\Delta T_{sub,o} / \Delta T_c$
46	1	55.0	200.0	0.096	1.0	16.0	0.0	25.0	0.266
47	1	55.0	180.0	0.096	1.0	16.0	0.0	25.0	0.282
48	1	55.0	177.0	0.080	1.0	16.0	0.0	17.0	0.266
49	1	55.0	218.0	0.080	1.0	16.0	0.0	17.0	0.266
50	1	55.0	276.0	0.080	1.0	16.0	0.0	17.0	0.266
51	1	65.0	141.0	0.080	1.0	16.0	0.0	17.0	0.250
52	1	65.0	218.0	0.080	1.0	16.0	0.0	17.0	0.250
53	1	65.0	300.0	0.080	1.0	16.0	0.0	17.0	0.250
54	1	65.0	110.0	0.080	1.0	16.0	0.0	17.0	0.250
55	1	45.0	221.0	0.080	1.0	16.0	0.0	17.0	0.266
56	1	45.0	289.0	0.080	1.0	16.0	0.0	17.0	0.234
57	1	35.0	283.0	0.080	1.0	16.0	0.0	17.0	0.282
58	1	35.0	219.0	0.080	1.0	16.0	0.0	17.0	0.266
59	1	35.0	183.0	0.080	1.0	16.0	0.0	17.0	0.266
60	1	55.0	93.0	0.080	1.0	16.0	0.0	17.0	0.250
61	1	75.0	223.0	0.080	1.0	16.0	0.0	17.0	0.250
62	1	55.0	66.0	0.080	1.0	16.0	0.0	17.0	0.282
63	1	55.0	170.0	0.055	1.0	21.0	0.0	17.0	0.163
64	1	55.0	93.0	0.055	1.0	21.0	0.0	17.0	0.163
65	1	55.0	130.0	0.055	1.0	21.0	0.0	17.0	0.163
66	1	45.0	127.0	0.055	1.0	21.0	0.0	17.0	0.190
67	1	45.0	176.0	0.055	1.0	21.0	0.0	17.0	0.163
68	1	45.0	67.0	0.055	1.0	21.0	0.0	17.0	0.163
69	1	45.0	226.0	0.055	1.0	21.0	0.0	17.0	0.177
70	1	35.0	122.0	0.055	1.0	21.0	0.0	17.0	0.177
71	1	65.0	119.0	0.055	1.0	21.0	0.0	17.0	0.149
72	1	65.0	98.0	0.055	1.0	21.0	0.0	17.0	0.136
73	1	65.0	83.0	0.055	1.0	21.0	0.0	17.0	0.163
74	1	35.0	187.0	0.055	1.0	21.0	0.0	17.0	0.163
75	1	55.0	186.0	0.127	0.399	24.0	0.0	17.0	0.351
76	1	55.0	262.0	0.127	0.399	24.0	0.0	17.0	0.351
77	1	55.0	140.0	0.127	0.399	24.0	0.0	17.0	0.315
78	1	45.0	148.0	0.127	0.399	24.0	0.0	17.0	0.315
79	1	45.0	270.0	0.127	0.399	24.0	0.0	17.0	0.351
80	1	45.0	348.0	0.127	0.399	24.0	0.0	17.0	0.389
81	1	65.0	86.0	0.127	0.399	24.0	0.0	17.0	0.315
82	1	65.0	178.0	0.127	0.399	24.0	0.0	17.0	0.351
83	1	65.0	340.0	0.127	0.399	24.0	0.0	17.0	0.428

* 1 implies upward flow, 0 implies downward flow.

Table X-3. Exit Temperature and Pressure Drop at Different Inlet Velocities Calculated in the Application of Babelli and Ishii Flow Instability Criterion to a Typical Whittle and Forgan Test (Number 1)

Whittle & Forgan Test Numner	=	1
Hydraulic diameter (heated), m	=	0.00645
Hydraulic diameter (wetted), m	=	0.00572
Channel heated length, m	=	0.6096
Total minor loss coefficient	=	0.0000
Inlet temperature, C	=	55.000
Power removed by the channel, W	=	3.22064E+04
Pressure at heated section exit, Pa	=	1.17211E+05
Saturation temperature at exit, C	=	104.131
Channel flow area, m**2	=	8.19353E-05
Heated perimeter, m	=	0.05080
Measured ratio of exit subcooling-to-coolant temp rise, at flow instability	=	0.224
Measured coolant velocity at OFI, m/s	=	2.361
Measured flow rate at OFI, kg/s	=	0.191

Inlet Vel, m/s	Inlet Temp, C	Exit Temp, C	Friction Factor	Beta per C	Total Press Drop, Pa	Friction Drop, Pa	Orifice Drop, Pa	Mom Change Drop, Pa	Gravity Drop, Pa	Reynolds Number	Inlet Press, Pa
2.500	55.00	92.92	0.0224	6.10E-04	13394.79	7423.94	0.00	146.79	5824.05	36997.61	130605.45
2.510	55.00	92.77	0.0224	6.09E-04	13449.43	7477.80	0.00	147.25	5824.37	37111.60	130660.09
2.520	55.00	92.62	0.0224	6.09E-04	13504.25	7531.84	0.00	147.71	5824.69	37225.56	130714.91
2.530	55.00	92.48	0.0223	6.08E-04	13559.23	7586.05	0.00	148.17	5825.01	37339.53	130769.90
2.540	55.00	92.33	0.0223	6.08E-04	13614.39	7640.44	0.00	148.63	5825.32	37453.46	130825.05
2.550	55.00	92.18	0.0223	6.08E-04	13669.72	7695.00	0.00	149.09	5825.63	37567.41	130880.38
2.560	55.00	92.04	0.0223	6.07E-04	13725.22	7749.73	0.00	149.55	5825.94	37681.32	130935.88
2.570	55.00	91.89	0.0223	6.07E-04	13780.88	7804.63	0.00	150.01	5826.25	37795.24	130991.55
2.580	55.00	91.75	0.0223	6.06E-04	13836.72	7859.70	0.00	150.47	5826.55	37909.12	131047.38
2.590	55.00	91.61	0.0222	6.06E-04	13892.73	7914.95	0.00	150.93	5826.85	38023.02	131103.39
2.600	55.00	91.47	0.0222	6.06E-04	13948.90	7970.38	0.00	151.38	5827.14	38136.90	131159.56
2.610	55.00	91.33	0.0222	6.05E-04	14005.25	8025.97	0.00	151.84	5827.44	38250.74	131215.91
2.620	55.00	91.19	0.0222	6.05E-04	14061.76	8081.73	0.00	152.30	5827.73	38364.60	131272.42
2.630	55.00	91.06	0.0222	6.04E-04	14118.53	8137.75	0.00	152.76	5828.02	38478.44	131329.19
2.640	55.00	90.92	0.0222	6.04E-04	14175.39	8193.86	0.00	153.22	5828.31	38592.26	131386.05
2.650	55.00	90.79	0.0222	6.04E-04	14232.41	8250.15	0.00	153.68	5828.59	38706.09	131443.08
2.660	55.00	90.65	0.0221	6.03E-04	14289.60	8306.60	0.00	154.13	5828.87	38819.89	131500.27
2.670	55.00	90.52	0.0221	6.03E-04	14346.97	8363.22	0.00	154.59	5829.15	38933.69	131557.62
2.680	55.00	90.39	0.0221	6.02E-04	14404.50	8420.02	0.00	155.05	5829.43	39047.47	131615.16
2.690	55.00	90.26	0.0221	6.02E-04	14462.20	8476.99	0.00	155.51	5829.70	39161.25	131672.86
2.700	55.00	90.13	0.0221	6.02E-04	14520.07	8534.13	0.00	155.97	5829.98	39275.00	131730.73
2.710	55.00	90.00	0.0221	6.01E-04	14578.11	8591.44	0.00	156.42	5830.25	39388.77	131788.78
2.711	55.00	89.98	0.0221	6.01E-04	14583.92	8597.18	0.00	156.47	5830.27	39400.14	131794.58
2.712	55.00	89.97	0.0221	6.01E-04	14589.74	8602.92	0.00	156.52	5830.30	39411.52	131800.41
2.713	55.00	89.96	0.0221	6.01E-04	14595.55	8608.67	0.00	156.56	5830.33	39422.89	131806.22
2.714	55.00	89.95	0.0221	6.01E-04	14601.37	8614.41	0.00	156.61	5830.35	39434.27	131812.03
2.715	55.00	89.93	0.0221	6.01E-04	14607.19	8620.16	0.00	156.65	5830.38	39445.64	131817.86

Table X-3. Cont'd.

Inlet Vel, m/s	Inlet Temp, C	Exit Temp, C	Friction Factor	Beta per C	Total Press Drop, Pa	Friction Drop, Pa	Orifice Drop, Pa	Mom Change Drop, Pa	Gravity Drop, Pa	Reynolds Number	Inlet Press, Pa
2.716	55.00	89.92	0.0221	6.01E-04	14613.01	8625.91	0.00	156.70	5830.41	39457.02	131823.67
2.717	55.00	89.91	0.0221	6.01E-04	14618.84	8631.66	0.00	156.75	5830.43	39468.39	131829.50
2.718	55.00	89.89	0.0221	6.01E-04	14624.66	8637.41	0.00	156.79	5830.46	39479.77	131835.33
2.719	55.00	89.88	0.0221	6.01E-04	14630.49	8643.17	0.00	156.84	5830.49	39491.13	131841.16
2.720	55.00	89.87	0.0220	6.01E-04	14636.31	8648.92	0.00	156.88	5830.51	39502.51	131846.98
2.730	55.00	89.74	0.0220	6.00E-04	14694.69	8706.57	0.00	157.34	5830.78	39616.23	131905.36
2.740	55.00	89.62	0.0220	6.00E-04	14753.23	8764.39	0.00	157.80	5831.04	39729.97	131963.89
2.750	55.00	89.49	0.0220	6.00E-04	14811.95	8822.39	0.00	158.25	5831.30	39843.68	132022.61
2.760	55.00	89.37	0.0220	5.99E-04	14870.82	8880.55	0.00	158.71	5831.56	39957.39	132081.48
2.770	55.00	89.24	0.0220	5.99E-04	14929.87	8938.88	0.00	159.17	5831.82	40071.08	132140.53
2.780	55.00	89.12	0.0220	5.99E-04	14989.09	8997.38	0.00	159.63	5832.08	40184.77	132199.75
2.790	55.00	89.00	0.0219	5.98E-04	15048.47	9056.06	0.00	160.08	5832.33	40298.44	132259.12
2.800	55.00	88.88	0.0219	5.98E-04	15108.02	9114.90	0.00	160.54	5832.58	40412.11	132318.69
2.810	55.00	88.76	0.0219	5.98E-04	15167.74	9173.91	0.00	161.00	5832.83	40525.75	132378.41
2.820	55.00	88.64	0.0219	5.97E-04	15227.62	9233.09	0.00	161.46	5833.08	40639.43	132438.28
2.830	55.00	88.52	0.0219	5.97E-04	15287.68	9292.44	0.00	161.91	5833.32	40753.07	132498.34
2.840	55.00	88.40	0.0219	5.96E-04	15347.90	9351.96	0.00	162.37	5833.56	40866.69	132558.56
2.850	55.00	88.28	0.0219	5.96E-04	15408.28	9411.65	0.00	162.83	5833.80	40980.31	132618.95

Table X-4. Application of Babelli and Ishii Flow Instability Criterion to a Typical Whittle and Forgan Test (Number 1)

Inlet Vel, m/s	Exit Temp, C	Tot Press Drop, Pa	Exit Press Pa	Pecllet Number	Inlet Subc J/kg	Subcool Number	Zuber Number	Nsub/Nzu	RHS of Eq. (1)	Stable?	Critical Lnv/L	0.0022Pe or 154.0
2.500	92.92	13394.79	117210.66	87332.46	206803.64	129.41	99.75	1.297	1.407	unstable	1.000	154.000
2.510	92.77	13449.43	117210.66	87689.20	206803.64	129.41	99.35	1.303	1.407	unstable	1.000	154.000
2.520	92.62	13504.25	117210.66	88046.04	206803.64	129.41	98.96	1.308	1.407	unstable	1.000	154.000
2.530	92.48	13559.23	117210.66	88402.89	206803.64	129.41	98.57	1.313	1.407	unstable	1.000	154.000
2.540	92.33	13614.39	117210.66	88759.84	206803.64	129.41	98.18	1.318	1.407	unstable	1.000	154.000
2.550	92.18	13669.72	117210.66	89116.76	206803.64	129.41	97.79	1.323	1.407	unstable	1.000	154.000
2.560	92.04	13725.22	117210.66	89473.73	206803.64	129.41	97.41	1.328	1.407	unstable	1.000	154.000
2.570	91.89	13780.88	117210.66	89830.73	206803.64	129.41	97.03	1.334	1.407	unstable	1.000	154.000
2.580	91.75	13836.72	117210.66	90187.84	206803.64	129.41	96.65	1.339	1.407	unstable	1.000	154.000
2.590	91.61	13892.73	117210.66	90544.95	206803.64	129.41	96.28	1.344	1.407	unstable	1.000	154.000
2.600	91.47	13948.90	117210.66	90902.08	206803.64	129.41	95.91	1.349	1.407	unstable	1.000	154.000
2.610	91.33	14005.25	117210.66	91259.28	206803.64	129.41	95.54	1.354	1.407	unstable	1.000	154.000
2.620	91.19	14061.76	117210.66	91616.52	206803.64	129.41	95.18	1.360	1.407	unstable	1.000	154.000
2.630	91.06	14118.53	117210.66	91973.76	206803.64	129.41	94.82	1.365	1.407	unstable	1.000	154.000
2.640	90.92	14175.39	117210.66	92331.06	206803.64	129.41	94.46	1.370	1.407	unstable	1.000	154.000
2.650	90.79	14232.41	117210.66	92688.41	206803.64	129.41	94.10	1.375	1.407	unstable	1.000	154.000
2.660	90.65	14289.60	117210.66	93045.74	206803.64	129.41	93.75	1.380	1.407	unstable	1.000	154.000
2.670	90.52	14346.97	117210.66	93403.16	206803.64	129.41	93.40	1.386	1.407	unstable	1.000	154.000
2.680	90.39	14404.50	117210.66	93760.57	206803.64	129.41	93.05	1.391	1.407	unstable	1.000	154.000
2.690	90.26	14462.20	117210.66	94118.10	206803.64	129.41	92.70	1.396	1.407	unstable	1.000	154.000
2.700	90.13	14520.07	117210.66	94475.60	206803.64	129.41	92.36	1.401	1.407	unstable	1.000	154.000
2.710	90.00	14578.11	117210.66	94833.12	206803.64	129.41	92.02	1.406	1.407	unstable	1.000	154.000
2.710	90.00	14578.11	117210.66	94833.12	206803.64	129.41	92.02	1.406	1.407	unstable	1.000	154.000
2.711	89.98	14583.92	117210.66	94868.88	206803.64	129.41	91.98	1.407	1.407	unstable	1.000	154.000
2.712	89.97	14589.74	117210.66	94904.67	206803.64	129.41	91.95	1.407	1.407	unstable	1.000	154.000
2.713	89.96	14595.55	117210.66	94940.33	206803.64	129.41	91.92	1.408	1.407	stable	1.000	154.000
2.714	89.95	14601.37	117210.66	94976.14	206803.64	129.41	91.88	1.408	1.407	stable	1.000	154.000
2.715	89.93	14607.19	117210.66	95011.90	206803.64	129.41	91.85	1.409	1.407	stable	1.000	154.000
2.716	89.92	14613.01	117210.66	95047.68	206803.64	129.41	91.82	1.409	1.407	stable	1.000	154.000
2.717	89.91	14618.84	117210.66	95083.46	206803.64	129.41	91.78	1.410	1.407	stable	1.000	154.000
2.718	89.89	14624.66	117210.66	95119.23	206803.64	129.41	91.75	1.410	1.407	stable	1.000	154.000
2.719	89.88	14630.49	117210.66	95154.93	206803.64	129.41	91.71	1.411	1.407	stable	1.000	154.000
2.720	89.87	14636.32	117210.66	95190.72	206803.64	129.41	91.68	1.412	1.407	stable	1.000	154.000
2.720	89.87	14636.31	117210.66	95190.69	206803.64	129.41	91.68	1.412	1.407	stable	1.000	154.000
2.730	89.74	14694.69	117210.66	95548.28	206803.64	129.41	91.34	1.417	1.407	stable	1.000	154.000
2.740	89.62	14753.23	117210.66	95905.96	206803.64	129.41	91.01	1.422	1.407	stable	1.000	154.000
2.750	89.49	14811.95	117210.66	96263.64	206803.64	129.41	90.68	1.427	1.407	stable	1.000	154.000
2.760	89.37	14870.82	117210.66	96621.38	206803.64	129.41	90.35	1.432	1.407	stable	1.000	154.000
2.770	89.24	14929.87	117210.66	96979.12	206803.64	129.41	90.03	1.437	1.407	stable	1.000	154.000
2.780	89.12	14989.09	117210.66	97336.86	206803.64	129.41	89.70	1.443	1.407	stable	1.000	154.000
2.790	89.00	15048.47	117210.66	97694.67	206803.64	129.41	89.38	1.448	1.407	stable	1.000	154.000
2.800	88.88	15108.02	117210.66	98052.58	206803.64	129.41	89.06	1.453	1.407	stable	1.000	154.000
2.810	88.76	15167.74	117210.66	98410.45	206803.64	129.41	88.74	1.458	1.407	stable	1.000	154.000
2.820	88.64	15227.62	117210.66	98768.30	206803.64	129.41	88.43	1.463	1.407	stable	1.000	154.000
2.830	88.52	15287.68	117210.66	99126.25	206803.64	129.41	88.12	1.469	1.407	stable	1.000	154.000
2.840	88.40	15347.90	117210.66	99484.29	206803.64	129.41	87.81	1.474	1.407	stable	1.000	154.000
2.850	88.28	15408.28	117210.66	99842.28	206803.64	129.41	87.50	1.479	1.407	stable	1.000	154.000

The underlined line marks the flow instability predicted by the simple criterion of Eq. (5).

Table X-5. Comparison of Coolant Inlet Velocity at OFI Calculated Using Eq. (1) Versus its Measured Value in 75 Tests Reported by Whittle and Forgan

Test No.	Calc. Inlet Vel, m/s	Inlet Temp C	Heat Flux W/cm ²	L/D _H Ratio	Exit Press psia	Exit Temp C	Ratio $\Delta T_c / \Delta T_{sat}$	η W&F	Measured at OFI		Peclet Number	Subcool Number	Zuber Number	Ratio N_{sub} / N_{zuber}
									Inlet Vel, m/s	Flow kg/s				
1	2.712	55.000	104.000	94.488	17.000	89.971	0.712	38.260	2.361	0.1908	94905.	129.406	91.950	1.407
2	3.781	55.000	145.000	94.488	17.000	89.974	0.712	38.248	3.406	0.2752	132314.	129.402	91.954	1.407
3	4.798	55.000	184.000	94.488	17.000	89.975	0.712	38.244	4.164	0.3365	167903.	129.397	91.953	1.407
4	6.520	55.000	250.000	94.488	17.000	89.975	0.712	38.246	5.872	0.4745	228166.	129.384	91.938	1.407
5	2.138	55.000	82.000	94.488	17.000	89.976	0.712	38.240	1.902	0.1537	74818.	129.406	91.964	1.407
6	3.546	55.000	136.000	94.488	17.000	89.977	0.712	38.236	3.154	0.2549	124090.	129.402	91.962	1.407
7	4.172	55.000	160.000	94.488	17.000	89.977	0.712	38.238	3.806	0.3075	145996.	129.397	91.957	1.407
8	5.216	55.000	200.000	94.488	17.000	89.972	0.712	38.257	4.697	0.3796	182532.	129.393	91.939	1.407
9	3.455	45.000	160.000	94.488	17.000	87.105	0.712	38.210	3.073	0.2494	121664.	155.577	110.556	1.407
10	3.887	45.000	180.000	94.488	17.000	87.103	0.712	38.214	3.457	0.2806	136876.	155.577	110.552	1.407
11	4.405	45.000	204.000	94.488	17.000	87.107	0.712	38.201	3.868	0.3139	155117.	155.572	110.559	1.407
12	3.200	60.000	110.000	94.488	17.000	91.406	0.712	38.284	2.845	0.2293	111606.	116.295	82.629	1.407
13	4.654	60.000	160.000	94.488	17.000	91.412	0.712	38.262	4.138	0.3336	162317.	116.290	82.638	1.407
14	5.236	60.000	180.000	94.488	17.000	91.412	0.712	38.261	4.715	0.3801	182616.	116.286	82.634	1.407
15	5.818	60.000	200.000	94.488	17.000	91.410	0.712	38.267	4.982	0.4016	202915.	116.286	82.631	1.407
16	2.505	35.000	136.000	94.488	17.000	84.247	0.712	38.152	2.229	0.1816	88704.	181.713	129.155	1.407
25	1.684	45.000	78.000	94.488	17.000	87.108	0.712	38.200	1.517	0.1232	59299.	155.590	110.578	1.407
26	2.505	45.000	116.000	94.488	17.000	87.100	0.712	38.226	2.257	0.1832	88210.	155.585	110.551	1.407
27	3.196	45.000	148.000	94.488	17.000	87.100	0.712	38.225	2.843	0.2307	112543.	155.585	110.552	1.407
28	2.998	55.000	115.000	94.488	17.000	89.979	0.712	38.228	2.701	0.2183	104912.	129.410	91.977	1.407
29	1.955	55.000	75.000	94.488	17.000	89.982	0.712	38.219	1.762	0.1424	68413.	129.415	91.987	1.407
30	3.807	55.000	146.000	94.488	17.000	89.973	0.712	38.251	3.386	0.2736	133223.	129.406	91.956	1.407
31	0.907	45.000	42.000	94.488	17.000	87.097	0.712	38.233	0.827	0.0672	31939.	155.590	110.550	1.407
32	3.512	55.000	147.000	83.333	17.000	88.671	0.685	38.263	3.084	0.1884	95608.	129.402	88.514	1.462
33	4.061	55.000	170.000	83.333	17.000	88.675	0.685	38.249	3.566	0.2178	110553.	129.402	88.525	1.462
34	4.300	55.000	180.000	83.333	17.000	88.674	0.685	38.252	3.776	0.2307	117060.	129.402	88.522	1.462
35	5.136	55.000	215.000	83.333	17.000	88.676	0.685	38.244	4.454	0.2721	139819.	129.397	88.524	1.462
36	3.878	45.000	196.000	83.333	17.000	85.534	0.685	38.233	3.406	0.2090	106263.	155.577	106.414	1.462
37	4.946	45.000	250.000	83.333	17.000	85.539	0.686	38.218	4.344	0.2665	135528.	155.572	106.423	1.462
38	3.561	45.000	180.000	83.333	17.000	85.539	0.686	38.218	3.128	0.1919	97576.	155.577	106.427	1.462
39	5.331	65.000	177.000	83.333	17.000	91.812	0.685	38.288	4.621	0.2808	144098.	103.170	70.576	1.462
40	6.115	65.000	203.000	83.333	17.000	91.810	0.685	38.299	5.300	0.3221	165290.	103.166	70.566	1.462
41	6.566	65.000	218.000	83.333	17.000	91.813	0.685	38.284	5.669	0.3445	177481.	103.166	70.575	1.462
42	3.704	65.000	123.000	83.333	17.000	91.813	0.685	38.283	3.252	0.1976	100119.	103.179	70.588	1.462
43	4.137	45.000	250.000	83.333	25.000	93.422	0.686	38.159	3.543	0.2174	112790.	130.125	89.009	1.462
44	5.629	65.000	242.000	83.333	25.000	99.683	0.686	38.231	4.943	0.3004	151549.	93.463	63.930	1.462
45	3.116	65.000	134.000	83.333	25.000	99.690	0.686	38.207	2.634	0.1601	83891.	93.469	63.949	1.462

Table X-5. Cont'd.

Test No.	Calc.	Inlet	Heat	L/D _H Ratio	Exit	Exit	Ratio $\Delta T_c / \Delta T_{sat}$	η W&F	Measured at OFI		Peclet Number	Subcool Number	Zuber Number	Ratio N_{sub} / N_{zub}
	Inlet	Temp	Flux		Press	Temp			Inlet	Flow				
	Vel, m/s	C	W/cm ²		psia	C			Vel, m/s	kg/s				
46	3.868	55.000	200.000	83.333	25.000	96.556	0.686	38.180	3.355	0.2050	104826.	111.814	76.493	1.462
47	3.481	55.000	180.000	83.333	25.000	96.558	0.686	38.173	3.058	0.1868	94338.	111.814	76.497	1.462
48	4.807	55.000	177.000	100.000	17.000	90.538	0.723	38.249	4.400	0.2240	110537.	129.397	93.439	1.385
49	5.921	55.000	218.000	100.000	17.000	90.538	0.723	38.249	5.419	0.2759	136154.	129.389	93.430	1.385
50	7.497	55.000	276.000	100.000	17.000	90.540	0.723	38.244	6.861	0.3493	172396.	129.376	93.421	1.385
51	4.828	65.000	141.000	100.000	17.000	93.296	0.723	38.295	4.361	0.2209	110269.	103.170	74.495	1.385
52	7.466	65.000	218.000	100.000	17.000	93.296	0.723	38.291	6.743	0.3415	170522.	103.153	74.480	1.385
53	10.276	65.000	300.000	100.000	17.000	93.299	0.723	38.276	9.279	0.4699	234706.	103.131	74.466	1.385
54	3.766	65.000	110.000	100.000	17.000	93.298	0.723	38.283	3.402	0.1723	86013.	103.175	74.506	1.385
55	4.971	45.000	221.000	100.000	17.000	87.779	0.723	38.226	4.550	0.2327	115013.	155.568	112.326	1.385
56	6.500	45.000	289.000	100.000	17.000	87.785	0.724	38.205	5.799	0.2965	150390.	155.559	112.334	1.385
57	5.430	35.000	283.000	100.000	17.000	85.033	0.724	38.172	5.035	0.2584	126321.	181.699	131.215	1.385
58	4.202	35.000	219.000	100.000	17.000	85.032	0.724	38.175	3.848	0.1974	97753.	181.704	131.216	1.385
59	3.511	35.000	183.000	100.000	17.000	85.034	0.724	38.169	3.215	0.1650	81677.	181.708	131.226	1.385
60	2.369	55.000	93.000	100.000	17.000	92.875	0.771	29.718	2.282	0.1162	54400.	129.406	99.621	1.299
61	10.311	75.000	223.000	100.000	17.000	96.062	0.723	38.311	9.308	0.4686	233771.	76.856	55.494	1.385
62	1.546	55.000	66.000	100.000	17.000	96.172	0.838	19.331	1.661	0.0846	35439.	129.406	108.335	1.195
63	7.651	55.000	170.000	190.909	17.000	95.934	0.833	38.233	7.408	0.2593	123456.	129.341	107.638	1.202
64	4.154	55.000	93.000	190.909	17.000	96.226	0.839	36.608	4.053	0.1418	67016.	129.389	108.460	1.193
65	5.849	55.000	130.000	190.909	17.000	95.937	0.833	38.215	5.665	0.1983	94377.	129.367	107.673	1.201
66	4.732	45.000	127.000	190.909	17.000	94.269	0.833	38.214	4.691	0.1649	76753.	155.555	129.453	1.202
67	6.558	45.000	176.000	190.909	17.000	94.275	0.833	38.189	6.352	0.2233	106373.	155.533	129.445	1.202
68	2.300	45.000	67.000	190.909	17.000	98.442	0.904	20.323	2.418	0.0850	37229.	155.577	140.510	1.107
69	8.423	45.000	226.000	190.909	17.000	94.274	0.833	38.193	8.255	0.2902	136627.	155.503	129.412	1.202
70	3.803	35.000	122.000	190.909	17.000	93.738	0.850	33.779	3.803	0.1341	61920.	181.695	154.190	1.178
71	6.751	65.000	119.000	190.909	17.000	97.600	0.833	38.249	6.457	0.2248	108283.	103.131	85.836	1.201
72	5.559	65.000	98.000	190.909	17.000	97.597	0.833	38.266	5.257	0.1830	89163.	103.149	85.847	1.202
73	4.708	65.000	83.000	190.909	17.000	97.595	0.833	38.281	4.559	0.1587	75513.	103.157	85.850	1.202
74	5.945	35.000	187.000	190.909	17.000	92.610	0.833	38.178	5.759	0.2032	96859.	181.669	151.183	1.202
75	4.851	55.000	186.000	94.488	17.000	89.971	0.712	38.261	4.663	0.1504	145126.	129.393	91.936	1.407
76	6.833	55.000	262.000	94.488	17.000	89.976	0.712	38.241	6.569	0.2118	204422.	129.380	91.937	1.407
77	3.651	55.000	140.000	94.488	17.000	89.972	0.712	38.256	3.416	0.1102	109225.	129.397	91.944	1.407
78	3.196	45.000	148.000	94.488	17.000	87.103	0.712	38.215	2.991	0.0969	96212.	155.577	110.552	1.407
79	5.831	45.000	270.000	94.488	17.000	87.106	0.712	38.206	5.607	0.1816	175538.	155.559	110.542	1.407
80	7.517	45.000	348.000	94.488	17.000	87.102	0.712	38.218	7.431	0.2407	226297.	155.546	110.519	1.407
81	2.827	65.000	86.000	94.488	17.000	92.848	0.712	38.284	2.645	0.0848	83993.	103.179	73.321	1.407
82	5.853	65.000	178.000	94.488	17.000	92.846	0.712	38.295	5.624	0.1804	173901.	103.162	73.298	1.407
83	11.184	65.000	340.000	94.488	17.000	92.853	0.712	38.262	11.357	0.3643	332305.	103.114	73.268	1.407

Mean error in calculated inlet velocity at OFI, m/s = 0.384
Standard deviation of the error in calculated inlet velocity at OFI, m/s = 0.242

Table X-6. Comparison of Coolant Inlet Velocity at OFI Calculated Using Eq. (5) Versus its Measured Value in 75 Tests Reported by Whittle and Forgan

Test No.	Calc.	Inlet	Heat	L/D _H Ratio	Exit	Exit	Ratio $\Delta T_c / \Delta T_{sat}$	η W&F	Measured at OFI		Peclet Number	Subcool Number	Zuber Number	Ratio N_{sub} / N_{zuber}
	Inlet Vel, m/s	Temp C	Flux W/cm ²		Press psia	Temp C			Inlet Vel, m/s	Flow kg/s				
1	2.620	55.000	104.000	94.488	17.000	91.194	0.737	33.775	2.361	0.1908	91617.	129.406	95.179	1.360
2	3.654	55.000	145.000	94.488	17.000	91.184	0.736	33.808	3.406	0.2752	127775.	129.402	95.150	1.360
3	4.637	55.000	184.000	94.488	17.000	91.184	0.736	33.808	4.164	0.3365	162149.	129.397	95.145	1.360
4	6.300	55.000	250.000	94.488	17.000	91.189	0.737	33.792	5.872	0.4745	220303.	129.389	95.149	1.360
5	2.066	55.000	82.000	94.488	17.000	91.190	0.737	33.789	1.902	0.1537	72244.	129.406	95.169	1.360
6	3.427	55.000	136.000	94.488	17.000	91.187	0.737	33.801	3.154	0.2549	119837.	129.402	95.155	1.360
7	4.032	55.000	160.000	94.488	17.000	91.186	0.737	33.802	3.806	0.3075	140993.	129.397	95.150	1.360
8	5.040	55.000	200.000	94.488	17.000	91.188	0.737	33.797	4.697	0.3796	176241.	129.393	95.149	1.360
9	3.339	45.000	160.000	94.488	17.000	88.560	0.737	33.776	3.073	0.2494	117464.	155.577	114.397	1.360
10	3.756	45.000	180.000	94.488	17.000	88.565	0.737	33.763	3.457	0.2806	132134.	155.577	114.408	1.360
11	4.257	45.000	204.000	94.488	17.000	88.562	0.737	33.769	3.868	0.3139	149759.	155.577	114.403	1.360
12	3.092	60.000	110.000	94.488	17.000	92.499	0.736	33.820	2.845	0.2293	107770.	116.295	85.515	1.360
13	4.497	60.000	160.000	94.488	17.000	92.504	0.737	33.801	4.138	0.3336	156741.	116.290	85.523	1.360
14	5.060	60.000	180.000	94.488	17.000	92.500	0.736	33.817	4.715	0.3801	176365.	116.286	85.508	1.360
15	5.622	60.000	200.000	94.488	17.000	92.501	0.736	33.812	4.982	0.4016	195954.	116.286	85.512	1.360
16	2.421	35.000	136.000	94.488	17.000	85.946	0.737	33.728	2.229	0.1816	85623.	181.713	133.636	1.360
25	1.627	45.000	78.000	94.488	17.000	88.576	0.737	33.729	1.517	0.1232	57236.	155.590	114.452	1.359
26	2.420	45.000	116.000	94.488	17.000	88.570	0.737	33.748	2.257	0.1832	85133.	155.590	114.434	1.360
27	3.088	45.000	148.000	94.488	17.000	88.565	0.737	33.761	2.843	0.2307	108633.	155.585	114.419	1.360
28	2.897	55.000	115.000	94.488	17.000	91.194	0.737	33.775	2.701	0.2183	101302.	129.410	95.183	1.360
29	1.889	55.000	75.000	94.488	17.000	91.199	0.737	33.757	1.762	0.1424	66054.	129.415	95.201	1.359
30	3.679	55.000	146.000	94.488	17.000	91.185	0.736	33.806	3.386	0.2736	128648.	129.406	95.155	1.360
31	0.876	45.000	42.000	94.488	17.000	88.578	0.737	33.723	0.827	0.0672	30816.	155.594	114.462	1.359
32	3.267	55.000	147.000	83.333	17.000	91.184	0.736	29.819	3.084	0.1884	88798.	129.406	95.152	1.360
33	3.778	55.000	170.000	83.333	17.000	91.187	0.737	29.809	3.566	0.2178	102688.	129.402	95.156	1.360
34	4.000	55.000	180.000	83.333	17.000	91.189	0.737	29.803	3.776	0.2307	108721.	129.402	95.162	1.360
35	4.778	55.000	215.000	83.333	17.000	91.189	0.737	29.803	4.454	0.2721	129868.	129.397	95.157	1.360
36	3.607	45.000	196.000	83.333	17.000	88.565	0.737	29.776	3.406	0.2090	98631.	155.577	114.410	1.360
37	4.601	45.000	250.000	83.333	17.000	88.563	0.737	29.782	4.344	0.2665	125812.	155.577	114.403	1.360
38	3.312	45.000	180.000	83.333	17.000	88.571	0.737	29.761	3.128	0.1919	90564.	155.581	114.429	1.360
39	4.959	65.000	177.000	83.333	17.000	93.815	0.736	29.837	4.621	0.2808	133891.	103.175	75.871	1.360
40	5.688	65.000	203.000	83.333	17.000	93.813	0.736	29.842	5.300	0.3221	153574.	103.170	75.863	1.360
41	6.108	65.000	218.000	83.333	17.000	93.816	0.736	29.830	5.669	0.3445	164914.	103.166	75.867	1.360
42	3.446	65.000	123.000	83.333	17.000	93.814	0.736	29.840	3.252	0.1976	93040.	103.179	75.873	1.360
43	3.848	45.000	250.000	83.333	25.000	97.037	0.737	29.720	3.543	0.2174	104716.	130.125	95.694	1.360
44	5.236	65.000	242.000	83.333	25.000	102.274	0.737	29.782	4.943	0.3004	140825.	93.463	68.729	1.360
45	2.899	65.000	134.000	83.333	25.000	102.274	0.737	29.781	2.634	0.1601	77969.	93.469	68.736	1.360

Table X-6. Cont'd.

Test No.	Calc. Inlet	Inlet Temp	Heat Flux	L/D _H Ratio	Exit Press	Exit Temp	Ratio $\Delta T_c / \Delta T_{sat}$	η W&F	Measured at OFI		Peclet Number	Subcool Number	Zuber Number	Ratio N_{sub} / N_{zuber}
	Vel, m/s	C	W/cm ²		psia	C			Inlet Vel, m/s	Flow kg/s				
46	3.598	55.000	200.000	83.333	25.000	99.657	0.737	29.741	3.355	0.2050	97372.	111.814	82.233	1.360
47	3.238	55.000	180.000	83.333	25.000	99.660	0.737	29.734	3.058	0.1868	87629.	111.814	82.238	1.360
48	4.720	55.000	177.000	100.000	17.000	91.190	0.737	35.758	4.400	0.2240	108494.	129.397	95.161	1.360
49	5.814	55.000	218.000	100.000	17.000	91.189	0.737	35.762	5.419	0.2759	133641.	129.389	95.150	1.360
50	7.362	55.000	276.000	100.000	17.000	91.187	0.737	35.772	6.861	0.3493	169225.	129.380	95.134	1.360
51	4.741	65.000	141.000	100.000	17.000	93.813	0.736	35.812	4.361	0.2209	108251.	103.170	75.862	1.360
52	7.331	65.000	218.000	100.000	17.000	93.814	0.736	35.808	6.743	0.3415	167391.	103.157	75.851	1.360
53	10.090	65.000	300.000	100.000	17.000	93.819	0.736	35.783	9.279	0.4699	230392.	103.131	75.839	1.360
54	3.698	65.000	110.000	100.000	17.000	93.816	0.736	35.795	3.402	0.1723	84436.	103.175	75.876	1.360
55	4.881	45.000	221.000	100.000	17.000	88.562	0.737	35.741	4.550	0.2327	112872.	155.572	114.397	1.360
56	6.383	45.000	289.000	100.000	17.000	88.565	0.737	35.730	5.799	0.2965	147606.	155.559	114.393	1.360
57	5.332	35.000	283.000	100.000	17.000	85.947	0.737	35.691	5.035	0.2584	123959.	181.699	133.627	1.360
58	4.126	35.000	219.000	100.000	17.000	85.948	0.737	35.689	3.848	0.1974	95921.	181.704	133.633	1.360
59	3.448	35.000	183.000	100.000	17.000	85.943	0.737	35.703	3.215	0.1650	80159.	181.708	133.624	1.360
60	2.480	55.000	93.000	100.000	17.000	91.187	0.737	35.769	2.282	0.1162	57005.	129.406	95.162	1.360
61	10.125	75.000	223.000	100.000	17.000	96.448	0.736	35.825	9.308	0.4686	229510.	76.856	56.514	1.360
62	1.760	55.000	66.000	100.000	17.000	91.187	0.737	35.769	1.661	0.0846	40455.	129.406	95.162	1.360
63	8.660	55.000	170.000	190.909	17.000	91.194	0.737	68.241	7.408	0.2593	140103.	129.324	95.096	1.360
64	4.735	55.000	93.000	190.909	17.000	91.193	0.737	68.245	4.053	0.1418	76600.	129.380	95.151	1.360
65	6.621	55.000	130.000	190.909	17.000	91.189	0.737	68.276	5.665	0.1983	107113.	129.358	95.118	1.360
66	5.355	45.000	127.000	190.909	17.000	88.568	0.737	68.195	4.691	0.1649	87154.	155.551	114.392	1.360
67	7.423	45.000	176.000	190.909	17.000	88.568	0.737	68.199	6.352	0.2233	120814.	155.520	114.360	1.360
68	2.825	45.000	67.000	190.909	17.000	88.562	0.737	68.232	2.418	0.0850	45977.	155.572	114.397	1.360
69	9.534	45.000	226.000	190.909	17.000	88.571	0.737	68.177	8.255	0.2902	155176.	155.481	114.330	1.360
70	4.389	35.000	122.000	190.909	17.000	85.942	0.737	68.168	3.803	0.1341	71813.	181.691	133.602	1.360
71	7.642	65.000	119.000	190.909	17.000	93.819	0.736	68.309	6.457	0.2248	122809.	103.118	75.827	1.360
72	6.292	65.000	98.000	190.909	17.000	93.818	0.736	68.322	5.257	0.1830	101113.	103.140	75.845	1.360
73	5.329	65.000	83.000	190.909	17.000	93.815	0.736	68.352	4.559	0.1587	85637.	103.149	75.845	1.360
74	6.728	35.000	187.000	190.909	17.000	85.947	0.737	68.138	5.759	0.2032	110086.	181.660	133.587	1.360
75	4.687	55.000	186.000	94.488	17.000	91.189	0.737	33.792	4.663	0.1504	140114.	129.393	95.153	1.360
76	6.603	55.000	262.000	94.488	17.000	91.189	0.737	33.793	6.569	0.2118	197394.	129.380	95.140	1.360
77	3.528	55.000	140.000	94.488	17.000	91.186	0.737	33.802	3.416	0.1102	105467.	129.397	95.150	1.360
78	3.088	45.000	148.000	94.488	17.000	88.568	0.737	33.752	2.991	0.0969	92870.	155.577	114.418	1.360
79	5.635	45.000	270.000	94.488	17.000	88.561	0.737	33.772	5.607	0.1816	169472.	155.564	114.387	1.360
80	7.263	45.000	348.000	94.488	17.000	88.565	0.737	33.761	7.431	0.2407	218436.	155.551	114.384	1.360
81	2.732	65.000	86.000	94.488	17.000	93.813	0.736	33.838	2.645	0.0848	81127.	103.179	75.871	1.360
82	5.655	65.000	178.000	94.488	17.000	93.817	0.736	33.819	5.624	0.1804	167928.	103.162	75.865	1.360
83	10.807	65.000	340.000	94.488	17.000	93.818	0.736	33.814	11.357	0.3643	320930.	103.118	75.824	1.360

Mean error in calculated inlet velocity at OFI, m/s = 0.363
 Standard deviation of the error in calculated inlet velocity at OFI, m/s = 0.319

APPENDIX X.A. Derivation of Flow Instability Equation in Reference [1]

Equation (2) of Ref. [1] is the starting point of Babelli and Ishii in obtaining the flow instability criterion. The purpose of this Appendix is to point out an inherent assumption or approximation in the derivation that affects the calculation of Subcooling number.

The coolant flow rate times the enthalpy change from channel inlet to the NVG position is related to the power generated in the fuel and transferred to the coolant over the non-boiling length, $q_w'' \zeta_H L_{\text{nvsg}}$.

$$(h_{\text{nvsg}} - h_{\text{in}}) = \frac{q_w'' \zeta_H L_{\text{nvsg}}}{\rho_{\text{in}} V_{\text{in}} A_F} \quad (\text{A-1})$$

Assume the coolant pressure P_{in} at the start of the heated section to be a *reference pressure* for calculating coolant subcooling at inlet and at the NVG position. Then the enthalpy difference between any pair of axial positions exactly equals the corresponding subcooling difference. The inlet subcooling $\Delta h_{\text{in}} = h_f(P_{\text{in}}) - h_{\text{in}}$, the subcooling at the NVG position $\Delta h_{\text{nvsg}} = h_f(P_{\text{in}}) - h_{\text{nvsg}}$, and the left hand side of Eq. (A-1) is

$$(h_{\text{nvsg}} - h_{\text{in}}) = \Delta h_{\text{in}} - \Delta h_{\text{nvsg}} \quad (\text{A-2})$$

If the coolant pressure at the NVG position (instead of the pressure P_{in} at the start of the heated section) were used as the system *reference pressure*, then inlet subcooling $\Delta h_{\text{in}} = h_f(P_{\text{nvsg}}) - h_{\text{in}}$, the subcooling at the NVG position $\Delta h_{\text{nvsg}} = h_f(P_{\text{nvsg}}) - h_{\text{nvsg}}$, and Eq. (A-2) remains unchanged. With this assumption the subcooling at the NVG position is accurate and the subcooling at inlet is approximate, whereas with the former assumption, the subcooling at the NVG position is approximate and the subcooling at inlet is accurate (the reverse is true).

Substituting Eq. (A-2) into Eq. (A-1), and solving for the non-boiling length L_{nvsg} , one gets

$$\frac{L_{\text{nvsg}}}{L} = \frac{\rho_{\text{in}} V_{\text{in}} A_F (\Delta h_{\text{in}} - \Delta h_{\text{nvsg}})}{q_w'' \zeta_H L} \quad (\text{A-3})$$

Equation (A-3) is the desired Eq. (2) of Ref. [1]. Using the Subcooling number and Zuber number defined above by Eqs. (2) and (3), Babelli and Ishii recast Eq. (A-3) as

$$\frac{N_{\text{sub}}}{N_{\text{zu}}} = \frac{L_{\text{nvsg}}}{L} + \frac{A_F}{\zeta_H L} \left\{ \frac{\rho_{\text{in}} V_{\text{in}} \Delta h_{\text{nvsg}}}{q_w''} \right\} \quad (\text{A-4})$$

The ratio inside the curly brackets on the right hand side of Eq. (A-4) is obtained from the Zuber correlation for the net vapor generation. For an accurate application of the Zuber correlation, it is preferred that the system *reference pressure* is assumed equal to the coolant pressure at the NVG position (rather than the pressure P_{in} at the start of the heated section), making the value of the subcooling at the NVG position accurate.

APPENDIX XI. CALCULATION OF NATURAL CIRCULATION FLOW RATE

Executive Summary

A method of calculating natural circulation flow, up through the fuel assemblies into a chimney and down through the flow area in the reactor pool/vessel outside the fuel assemblies, is described in Sections 2. The solution strategy described in Section 3 uses (i) inner iterations to find channel flow rates for a given set of coolant channel temperature profiles, and (ii) outer iterations to make the hydraulic calculation and the heat transfer calculation consistent with each other. In computing the buoyancy head and frictional pressure drop, the method accounts for (i) the channel-to-channel variation of coolant temperature profiles, and (ii) the axial variation of coolant temperature, density, viscosity, Reynolds number, and friction factor. Section 4 describes the approximation involved in defining an equivalent hydraulic resistance of the multiple parallel coolant channels in a reactor fuel assembly. Section 5 describes an approximation of the method of Sections 2 and 3 that easily fits in the older PLTEMP/ANL V3.4 code structure.

The general method of Sections 2 and 3 has been implemented in PLTEMP/ANL, with the approximate method of Section 5 implemented as the first outer iteration. In the first outer iteration, the flow rates are calculated using coolant density and viscosity at only three coolant temperatures, i.e., the assembly inlet and outlet temperatures and their arithmetic mean. A summary of the changes made to implement the methods is given in Section 6.

The results obtained by the new code for a natural circulation test problem (Sample Problem 20 for a fuel assembly with each fuel plate producing equal power) are shown in Table XI-7 and discussed in Section 7. The natural circulation flow rate of 0.1093 kg/s in a channel compares well with 0.1086 kg/s calculated earlier by a hand calculation using *Mathematica* and confirmed by the NATCON and RELAP5-3D codes (see Table XI-1). This provides a verification of the implementation of the method in the code. A test problem (Sample Problem 21) for an assembly with fuel plates producing unequal power is also solved.

1. Introduction

Some research reactors are cooled during steady-state operation by the natural circulation of the coolant (water), without a pump forcing the coolant flow. The coolant flows up through the fuel assemblies due to buoyancy (see Fig. 1), and down through the flow area in the reactor pool/vessel outside the fuel assemblies. The flow area outside the fuel assemblies is usually large, and the *frictional* pressure drop in the down-flow part of the flow circuit can be ignored. The bypass assemblies (that do not generate any power) play a minor role of simply providing an additional path of downward coolant flow. A method of calculating the flow rate in this circuit, described below, was implemented in the PLTEMP/ANL code, resulting in its V4.2.

The NATCON code¹ is capable of doing a similar calculation for a single coolant channel in a fuel assembly. When using NATCON, one selects the hottest coolant channel in the reactor core, and then *assumes that half* of the power generated by the two fuel plates that are adjacent to the selected hottest channel goes into the channel. This assumption is avoided when using the PLTEMP/ANL code to calculate the natural circulation flow rate in a fuel assembly. This is because PLTEMP/ANL performs a multi-fuel-plate heat transfer calculation to find the coolant temperature profiles in all coolant channels of a fuel assembly. The fraction of each fuel plate

power that goes into an adjacent coolant channel is determined by the multi-fuel-plate heat transfer calculation, and hence need not be assumed to be half.

PLTEMP/ANL V4.2 accounts for the effect of the shape of fuel plate power axial distribution (for the same plate power). In computing the buoyancy head and frictional pressure drop, the code accounts for (i) the channel-to-channel variation of coolant temperature profiles, and (ii) the axial variation of coolant temperature, density, viscosity, Reynolds number, friction factor.

2. Hydraulic Equations for Modeling Natural Circulation

The hydraulic equations implemented in PLTEMP/ANL to calculate the natural circulation flow rate in a fuel assembly are derived below, based on the modified Bernoulli equation, Eq. (10-25) in Shames². Figure 1 shows the coolant flow paths and flow resistances in a fuel assembly as modeled in PLTEMP/ANL. Each fuel assembly consists of an unheated axial region (region 1) below the heated section (axial region 2) consisting of multiple parallel coolant channels, above which are several unheated axial regions (regions 3 to $N_f - 2$). In Fig. 1, point 1' is located inside the flow area at the assembly inlet; point 2 is located *just before the inlet* to the heated section and is common to all coolant channels of the assembly; point 3 is located *just after the exit* from the heated section and is common to all coolant channels; and point 4' is located inside the flow area at the assembly exit. Figure 2 shows the details of coolant pressures in the pool and inside the assembly flow area at the inlet and exit.

The modified Bernoulli equation between points 1 and 5 in Fig. 1, for the flow path passing through coolant channel 1 of a fuel assembly j (index j not shown for clarity), can be written as:

$$\begin{aligned}
 P_1 = P_5 + & \overset{3^{\text{rd}} \text{ term}}{g \rho_1 L_1} + \overset{4^{\text{th}} \text{ term}}{\left(K_1 + \frac{f_1 L_1}{D_{h,1}} \right)} \overset{5^{\text{th}} \text{ term}}{\frac{W^2}{2 \rho_1 A_1^2}} \\
 & + g \int_{\text{Channel 1}} \rho_{c,1}(z) dz + \frac{K_2 W_{c,1}^2}{2 \rho_{c,1} A_{c,1}^2} + \frac{W_{c,1}^2}{2 D_{hc,1} A_{c,1}^2} \int_{\text{Channel 1}} \frac{f_{c,1} dz}{\rho_{c,1}(z)} \\
 & + g \rho_3 L_3 + \left(K_3 + \frac{f_3 L_3}{D_{h,3}} \right) \frac{W^2}{2 \rho_3 A_3^2} + g \rho_{ch} L_{ch}
 \end{aligned} \tag{1}$$

All symbols are defined in the nomenclature at the end. In Eq. (1), the third, fourth, and fifth terms on the right hand side are the gravity head, minor loss, and pressure drop due to wall shear for axial region 1. The three terms in the second line of Eq. (1) are the gravity head, minor loss, and pressure drop due to wall shear for axial region 2. The first three terms in the third line of Eq. (1) are the gravity head, minor loss, and pressure drop due to wall shear for axial region 3. The last term in the third line of Eq. (1) is the gravity head for the chimney.

The pressure of the creeping coolant at point 1 in the reactor pool at the assembly inlet level (see Fig. 2) is related by the Bernoulli equation, Eq. (2), to the coolant pressure at point 1' inside the flow area at the assembly inlet. The pressure of the creeping coolant at point 5 in the reactor pool at the chimney exit level is related by the Bernoulli equation, Eq. (3), to the coolant pressure at

point 5' inside the flow area at the chimney exit. Equation (3) assumes that the velocity head exiting from the chimney is fully converted into pressure head (not lost into heat).

$$P_1 = P_1' + \frac{W^2}{2 \rho_1 A_1^2} \quad (2)$$

$$P_5 = P_5' + \frac{\left(\sum_j W^{(j)} \right)^2}{2 \rho_{ch} A_{ch}^2} \quad (3)$$

The mixed mean coolant enthalpy h_{ch} in the chimney is calculated using Eq. (4), ignoring any heat transfer from the coolant in the chimney to the coolant in the pool. The coolant temperature and density in the chimney are obtained from the enthalpy h_{ch} .

$$h_{ch} = \frac{\sum_j \sum_k W_{c,k}^{(j)} h(T_{ex,k}^{(j)})}{\sum_j \sum_k W_{c,k}^{(j)}} \quad (4)$$

In the steady-state natural circulation, the difference between the pressures at points 1 and 5 equals the static head of the coolant in the pool, as shown by Eq. (5). The difference between the pressure at point 5 and that at the bottom of the chimney (point 4 in Fig. 2) equals the static head of the coolant in the chimney, also shown by Eq. (5). This assumes that the frictional pressure drop due to the creeping flow of coolant in the pool is negligible, and that the coolant temperature in the pool is uniformly equal to the inlet temperature over the fuel assembly plus chimney height.

$$P_1 - P_5 = g \rho_1 (L_1 + L_2 + L_3 + L_{ch}) \quad ; \quad P_4 - P_5 = g \rho_{ch} L_{ch} \quad (5)$$

Combining Eqs. (1) and (5), the following equation is obtained for the flow rate in a fuel assembly in steady-state natural circulation.

$$\begin{aligned} g \rho_1 (L_2 + L_3) + g L_{ch} (\rho_1 - \rho_{ch}) = & \left(K_1 + \frac{f_1 L_1}{D_{h,1}} \right) \frac{W^2}{2 \rho_1 A_1^2} \\ & + g \int_{\text{Channel 1}} \rho_{c,1}(z) dz + \frac{K_2 W_{c,1}^2}{2 \rho_{c,1} A_{c,1}^2} + \frac{W_{c,1}^2}{2 D_{hc,1} A_{c,1}^2} \int_{\text{Channel 1}} \frac{f_{c,1} dz}{\rho_{c,1}(z)} \\ & + g \rho_3 L_3 + \left(K_3 + \frac{f_3 L_3}{D_{h,3}} \right) \frac{W^2}{2 \rho_3 A_3^2} \end{aligned} \quad (6)$$

It is noted that Eq. (6) accounts for the difference between the coolant temperature axial profiles of different channels in the heated section. Basically, the equation states that the gravity head difference between the reactor pool and the assembly, summed up for axial regions 2, 3, and the chimney (the sum is called the buoyancy head), equals the frictional pressure drop (minor loss +

wall shear) summed up for all three axial regions in the assembly. The frictional pressure drop in the chimney is ignored.

Equation (6) uses the flow path through coolant channel 1 but any other channel could be used in place of channel 1. This fact is expressed mathematically by writing the modified Bernoulli equation between points 2 and 3, for the flow path through the k^{th} coolant channel in Fig. 1.

$$P_2 + \frac{W^2}{2\rho_1 A_1^2} = P_3 + \frac{W^2}{2\rho_3 A_3^2} + g \int_{\text{Channel } k} \rho_{c,k}(z) dz + \frac{K_2 W_{c,k}^2}{2\rho_{c,k} A_{c,k}^2} + \frac{W_{c,k}^2}{2D_{hc,k} A_{c,k}^2} \int_{\text{Channel } k} \frac{f_{c,k} dz}{\rho_{c,k}(z)} \quad (7)$$

In Eq. (7), the point 2 is located in axial region 1 just before the entry to all the channels, and is common to all channels of the heated section. The point 3 is located in axial region 3 just after the exit from all the channels, and is common to all channels. The second term on the left hand side of the equation is the velocity head at point 2, and the second term on the right hand side is the velocity head at point 3.

The third, fourth, and fifth terms on the right hand side of Eq. (7) are the gravity head, the minor loss, and the pressure drop due to wall shear for the k^{th} coolant channel. The gravity head is found by integrating the coolant density over the channel height because the density varies with coolant temperature in the channel. The gravity head varies from channel to channel in an assembly (because the coolant temperature profile varies from channel to channel). The channel-to-channel variation of gravity head must be included in the model in order to calculate the channel-to-channel variation of the natural circulation flow rate, since the gravity head determines the buoyancy head that drives the natural circulation.

The mean coolant density of the channel, $\overline{\rho_{c,k}} = [\rho_1 + \rho(T_{ex,k})]/2$, is used in the minor loss term because the coefficient K_2 for the channel is the sum of the losses at the channel entrance and exit. The frictional pressure drop due to wall shear needs to be calculated by integration over the channel length because the coolant (water) viscosity, density, Reynolds number, and Darcy-Weisbach friction factor all vary with temperature.

Collecting the channel-independent terms in Eq. (7) on the left hand side, we get Eq. (8) for any coolant channel k in the heated section of the assembly.

$$P_2 - P_3 + \frac{W^2}{2\rho_1 A_1^2} - \frac{W^2}{2\rho_3 A_3^2} = g \int_{\text{Channel } k} \rho_{c,k}(z) dz + \frac{K_2 W_{c,k}^2}{2\rho_{c,k} A_{c,k}^2} + \frac{W_{c,k}^2}{2D_{hc,k} A_{c,k}^2} \int_{\text{Channel } k} \frac{f_{c,k} dz}{\rho_{c,k}(z)} \quad (k = 1, 2, \dots, N_c) \quad (8)^*$$

Equation set (8) shows that the sum of the gravity head and the frictional pressure drop due to minor loss and wall shear is the same for each coolant channel. The frictional pressure drop

alone is *not the same* for each channel. (But it is assumed to be the same in PLTEMP/ANL forced flow calculation. This assumption is reasonable only if the frictional drop is much larger than the gravity head differences among channels). Equation (8) is a set of equations for the channel flow rates $W_{c,k}$. The assembly flow rate W is the sum of all the channel flow rates $W_{c,k}$ in the heated section.

$$W = \sum_{k=1}^{N_c} W_{c,k} \quad (9)^*$$

The modified Bernoulli equation between points 1 and 2 can be written as

$$P_1 = P_2 + \frac{W^2}{2 \rho_1 A_1^2} + g \rho_1 L_1 + \left(K_1 + \frac{f_1 L_1}{D_{h,1}} \right) \frac{W^2}{2 \rho_1 A_1^2} \quad (10)$$

The absolute pressure P_2 obtained from this Bernoulli equation is

$$P_2 = P_1 - \frac{W^2}{2 \rho_1 A_1^2} - g \rho_1 L_1 - \left(K_1 + \frac{f_1 L_1}{D_{h,1}} \right) \frac{W^2}{2 \rho_1 A_1^2} \quad (11)^*$$

The modified Bernoulli equation between points 3 and 5' (see Fig. 2) can be written as

$$P_3 + \frac{W^2}{2 \rho_3 A_3^2} = P_5 + \frac{\left(\sum_j W^{(j)} \right)^2}{2 \rho_{ch} A_{ch}^2} + g \rho_{ch} L_{ch} + g \rho_3 L_3 + \left(K_3 + \frac{f_3 L_3}{D_{h,3}} \right) \frac{W^2}{2 \rho_3 A_3^2} \quad (12)$$

Note that the first two terms on the right hand side of Eq. (12) equal P_5 according to Eq. (3), and $(P_5 + g \rho_{ch} L_{ch})$ equals P_4 according to Eq. (5). Using these equations in Eq. (12), the absolute pressure P_3 is given by Eq. (13).

$$P_3 = P_4 - \frac{W^2}{2 \rho_3 A_3^2} + g \rho_3 L_3 + \left(K_3 + \frac{f_3 L_3}{D_{h,3}} \right) \frac{W^2}{2 \rho_3 A_3^2} \quad (13)^*$$

Taken together, Equations (8), (9), (11), and (13) form a set of N_c+3 simultaneous equations in N_c+3 unknown variables P_2 , P_3 , W and $W_{c,k}$. The pressure P_1 in the pool at the assembly inlet level is an input datum, and acts as the system reference pressure. The following solution strategy is used in PLTEMP/ANL to solve these equations to find the flow rates.

3. Solution Strategy to Find Natural Circulation Flow Rates

The hydraulic equations are solved using two kinds of iteration, inner iteration and outer iteration, using the logical flow diagram shown in Fig. 3. The inner iteration is that which is

performed at a fixed set of coolant channel temperature profiles, to find a consistent set of channel flow rates $W_{c,k}$ and assembly flow rate W that satisfy the hydraulic requirements, i.e., Eqs. (8), (9), (11), and (13). The outer iteration is that in which a *new multi-fuel-plate heat transfer calculation* is done, using an available set of channel flow rates. After each heat transfer calculation, the inner iteration is performed again, using a new set of coolant channel temperature profiles, to satisfy the hydraulic equations, obtaining another consistent set of channel flow rates $W_{c,k}$ and assembly flow rate W . The problem is solved when the consistent set of channel flow rates and assembly flow rate change by a negligible amount, from an outer iteration to the next.

In the first outer iteration, the inner iteration is performed (in subroutine RESIST_NC) by using coolant density, viscosity, and friction factor at only three temperatures, T_{in} , $(T_{in}+T_{out})/2$, and T_{out} . It is noted that this calculation requires the total assembly flow rate but not the channel flow rates. In outer iterations 2 and later (performed in subroutine NATCIRC), in order to assure convergence, only a fraction ε (e.g., 0.6) of the coolant temperature change from the previous outer iteration is used to find the temperature-dependent coolant properties and friction factor during the inner iterations. The coolant properties and friction factor used in evaluating the integrals in Eq. (8), are evaluated at the temperature $T_{c,k,used}(z)$ defined by Eq. (14).

$$T_{c,k,used}(z) = T_{c,k,L-1}(z) + \varepsilon [T_{c,k,L}(z) - T_{c,k,L-1}(z)] \quad (14)$$

where

L = Outer iteration counter

$T_{c,k,L}(z)$ = Coolant temperature profile obtained by the multi-fuel-plate heat transfer calculation done *just before* outer iteration L

Two sets of coolant channel temperature profiles, $T_{c,k,L-1}(z)$ and $T_{c,k,L}(z)$, are needed in each outer iteration. The following steps are used to find the solution to the set of equations.

1. Start with $W = W_{guess}$, a guessed flow rate in the assembly. Initialize an outer iteration counter to 1.
2. The power Q generated in each assembly is given by the input data. Using the assembly power and the flow rate W , find the assembly mixed mean temperature T_{out} .
3. Find the coolant density and viscosity at the temperatures T_{in} and T_{out} . Find the Reynolds number and friction factor in axial regions 1, 3. Thus ρ_1 , ρ_3 , f_1 , and f_3 are known for the guessed flow rate. Set P_1 equal to the input inlet pressure (read from the input card 0500). Calculate the absolute pressures P_2 , P_3 , and P_4 using Eqs. (11), (13), and (5) respectively.
4. In outer iteration 2, the coolant temperature temperatures $T_{c,k,2}(z)$ and $T_{c,k,1}(z)$ are both needed in Eq. (14). Since $T_{c,k,1}(z)$ calculated by the multi-fuel-plate heat transfer calculation is not available, assume that the coolant temperature $T_{c,k,1}(z)$ in each channel of the heated section varies linearly from T_{in} to T_{out} (assembly outlet temperature). In the third outer iteration and onwards ($L \geq 3$), the coolant temperature profiles $T_{c,k,L-1}(z)$ and

$T_{c,k,L}(z)$, both calculated by the multi-fuel-plate heat transfer calculation, are available. Find temperature-dependent coolant density and viscosity by heat transfer node, for the coolant temperature $T_{c,k,used}(z)$ in each channel. Find the Reynolds number and friction factor by heat transfer node at the temperature $T_{c,k,used}(z)$, and evaluate the integrals in Eq. (8). These integrals are defined by Eqs. (15) and (16) below. Find the mean coolant density $\overline{\rho_{c,k}}$ used in minor loss calculation using Eq. (17).

$$I_{g,k} = g \int_{\text{Channel } k} \rho_{c,k}(z) dz \quad (15)$$

$$I_{f,k} = \int_{\text{Channel } k} \frac{f_{c,k} dz}{\rho_{c,k}(z)} \quad (16)$$

$$\overline{\rho_{c,k}} = \frac{\rho_1 + \rho(T_{ex,k})}{2} \quad (17)$$

- Equation (8) has only one unknown variable $W_{c,k}$, the flow rate in the k^{th} coolant channel. Solve it to find the flow rate in each coolant channel.

$$W_{c,k} = \left[\frac{P_2 - P_3 + \frac{W^2}{2 \rho_1 A_1^2} - \frac{W^2}{2 \rho_3 A_3^2} - I_{g,k}}{\frac{K_2}{2 \overline{\rho_{c,k}} A_{c,k}^2} + \frac{I_{f,k}}{2 D_{hc,k} A_{c,k}^2}} \right]^{0.5} \quad (18)$$

- Find the sum of coolant channel flow rates, $\sum_{k=1}^{N_c} W_{c,k}$. This sum will not be equal to the assembly flow rate W with which the calculation steps 2 through 5 were carried out. Define a new guess for the assembly flow rate by re-setting $W = F_{\text{inner}} \left(W_{\text{guess}} + \sum_{k=1}^{N_c} W_{c,k} \right)$. For $F_{\text{inner}} = 0.5$, the code converges in most cases. Go to step 2 and repeat the steps 2 through 5 until the assembly flow rate W converges. These inner iterations will yield a converged set of coolant channel flow rates $W_{c,k}$ such that $W = \sum_{k=1}^{N_c} W_{c,k}$. These are not the final solution to the problem because a multi-fuel-plate heat transfer calculation is not yet done. This completes the first outer iteration only. Store these flow rates for checking the convergence of outer iterations in the second outer iteration (and later).
- Perform a multi-fuel-plate heat transfer calculation using the flow rates found in step 6. Increment the outer iteration counter by one. If the outer iteration counter is 1, then go to step 2, and repeat the steps 2 to 7. If the outer iteration counter is 2 or more, then check the outer iteration convergence. If the channel flow rates are *not converged* from an

outer iteration to the next, then repeat the steps 2 to 7. If the channel flow rates are *converged* from an outer iteration to the next, then go to step 8.

8. The multi-fuel-plate heat transfer calculation and the hydraulic calculation are consistent. The natural circulation problem is solved.

4. Equivalent Hydraulic Resistance of the Heated Section

The purpose of this section is to find an equivalent hydraulic resistance of all the parallel coolant channels in the heated section. An equivalent hydraulic resistance of the parallel channels in the heated section is needed for checking the FORTRAN coding for it (equivalent resistance) in the older PLTEMP/ANL V3.4 code. For this purpose, Eq. (8) needs to be written as a pressure drop equal to $(W_{c,k})^2$ times a coefficient, *with the same pressure drop being common to each channel*. The need for the italicized condition will become obvious below when Eq. (25) is obtained from Eq. (24). To achieve the italicized condition, the gravity head in Eq. (8) must be assumed to be the same for all channels, and hence the gravity head is approximated below by Eq. (19). It is noted that this assumption is *not reasonable* in the calculation of natural circulation because:

- (i) The gravity head determines the buoyancy head which causes natural circulation, and
- (ii) The gravity head varies from channel to channel as shown by the variation of channel exit temperatures in a research reactor.

$$g \int_{\text{Channel } k} \rho_{c,k}(z) dz = g L_2 \frac{\rho_1 + \rho(T_{\text{out}})}{2} \quad (\text{an approximation}) \quad (19)$$

Using Eq. (19), Eq. (8) can be written as Eq. (20), with the channel resistance $R_{c,k}$ and the approximate frictional pressure drop $\Delta P_{f,2,\text{app}}$ defined as follows.

$$\Delta P_{f,2,\text{app}} = R_{c,k} W_{c,k}^2 \quad (k = 1, 2, \dots N_c) \quad (20)$$

$$\Delta P_{f,2,\text{app}} = P_2 - P_3 - 0.5 g L_2 [\rho_1 + \rho(T_{\text{out}})] \quad (21)$$

$$R_{c,k} = \frac{K_2}{2 \rho_{c,k} A_{c,k}^2} + \frac{1}{2 D_{hc,k} A_{c,k}^2} \int_{\text{Channel } k} \frac{f_{c,k} dz}{\rho_{c,k}(z)} \quad (22)$$

Using Eq. (20), the flow rate in each coolant channel can be written as follows.

$$W_{c,k} = \left(\frac{\Delta P_{f,2,\text{app}}}{R_{c,k}} \right)^{0.5} \quad (k = 1, 2, \dots N_c) \quad (23)$$

Summing Eq. (23) for all coolant channels, the assembly flow rate W is given by Eq. (24) which is re-written as Eq. (25). The re-writing of Eq. (24) as Eq. (25) requires that $\Delta P_{f,2,\text{app}}$ be independent of channel, as pointed out above.

$$W = \sum_{k=1}^{N_c} W_{c,k} = \sum_{k=1}^{N_c} \frac{(\Delta P_{f,2,app})^{0.5}}{R_{c,k}^{0.5}} \quad (24)$$

$$W = (\Delta P_{f,2,app})^{0.5} \sum_{k=1}^{N_c} \frac{1}{R_{c,k}^{0.5}} \quad (25)$$

By definition, the equivalent resistance R_{eqv} of the heated section is related to the assembly flow rate as follows.

$$W = \left(\frac{\Delta P_{f,2,app}}{R_{eqv}} \right)^{0.5} \quad (26)$$

Equating the right hand side of Eq. (25) with that of Eq. (26), the equivalent resistance of the heated section is given by

$$\frac{1}{R_{eqv}^{0.5}} = \sum_{k=1}^{N_c} \frac{1}{R_{c,k}^{0.5}} \quad (27)$$

Inserting the value of channel resistance $R_{c,k}$ from Eq. (22), Eq. (27) gives the following desired relationship.

$$\frac{1}{R_{eqv}^{0.5}} = \sum_{k=1}^{N_c} \frac{A_{c,k}}{\left(\frac{K_2}{2 \rho_{c,k}} + \frac{1}{2 D_{hc,k}} \int_{Channel\ k} \frac{f_{c,k}}{\rho_{c,k}(z)} dz \right)^{0.5}} \quad (28)^*$$

The coefficient $DENOF_2$ used in the PLTEMP/ANL code can be approximately calculated using Eq. (26). Equation (26) can be written as

$$\Delta P_{f,2,app} = DENOF_2 \frac{W^2}{2 \rho_a}, \quad DENOF_2 = 2 \rho_a R_{eqv} \quad (29)$$

Equations (28) and (29) are derived for comparison with the coding in PLTEMP/ANL V3.4.

5. An Approximation of Hydraulic Equations for Natural Circulation

The hydraulic equations and a method of solution for calculating the natural circulation flow, without any approximation about the coolant density and viscosity, are given in Sections 2 to 3. This section describes an approximation of those general hydraulic equations that will easily fit in the older PLTEMP/ANL V3.4 code structure. In this approximation, it is assumed that the coolant density and viscosity are uniform over each axial region in a fuel assembly. The coolant properties are evaluated (i) at the inlet temperature in axial region 1 ($n = 1$), (ii) at the mean temperature $0.5(T_{in} + T_{out})$ in the heated section ($n = 2$), and (iii) at the assembly exit temperature

in all axial regions downstream ($n \geq 3$) of the heated section. Then the general hydraulic equation, Eq. (6), simplifies to Eq. (30) below. The gravity head terms are collected on the left hand side of this equation.

$$g L_2 (\rho_1 - \rho_a) + g L_3 (\rho_1 - \rho_3) + g L_{ch} (\rho_1 - \rho_{ch}) = \left(K_1 + \frac{f_1 L_1}{D_{h,1}} \right) \frac{W^2}{2 \rho_1 A_1^2} + \left(K_2 + \frac{f_{c,1} L_2}{D_{hc,1}} \right) \frac{W_{c,1}^2}{2 \rho_a A_{c,1}^2} + \left(K_3 + \frac{f_3 L_3}{D_{h,3}} \right) \frac{W^2}{2 \rho_3 A_3^2} \quad (30)$$

where

ρ_1, μ_1 = Coolant density and dynamic viscosity in axial region 1

ρ_a, μ_a = Coolant density and dynamic viscosity in the heated section (axial region 2)

ρ_3, μ_3 = Coolant density and dynamic viscosity in axial region 3 and others downstream of the heated section

The middle term on the right hand side of Eq. (30) is the frictional pressure drop over the heated section. It is written in terms of the flow rate in the coolant channel 1. In what follows, this term is expressed in terms of the assembly flow rate W . Under the assumptions made in this section, Eqs. (20) and (22) for coolant channel 1 ($k = 1$) give

$$\Delta P_{f,2,app} = R_{c,1} W_{c,1}^2 \quad (31)$$

$$R_{c,1} = \left(K_2 + \frac{f_{c,1} L_2}{D_{hc,1}} \right) \frac{1}{2 \rho_a A_{c,1}^2} \quad (32)$$

Equation (26) can be written in the form

$$\Delta P_{f,2,app} = R_{eqv} W^2 \quad (33)$$

Combining Eqs. (31) and (33), one gets

$$R_{c,1} W_{c,1}^2 = R_{eqv} W^2 \quad (34)$$

The middle term on the right hand side of Eq. (30) can be written as follows by using Eqs. (32) and Eq. (34).

$$\left(K_2 + \frac{f_{c,1} L_2}{D_{hc,1}} \right) \frac{W_{c,1}^2}{2 \rho_a A_{c,1}^2} = R_{c,1} W_{c,1}^2 = R_{eqv} W^2 \quad (35)$$

Equation (35) relates the flow rate in a single channel to the assembly flow rate. The hydraulic equation, Eq. (30), can be written as follows when the middle term on its right hand side is replaced using Eq. (35).

$$\begin{aligned}
& gL_2(\rho_1 - \rho_a) + gL_3(\rho_1 - \rho_3) + gL_{ch}(\rho_1 - \rho_{ch}) \\
& = \left[\left(K_1 + \frac{f_1 L_1}{D_{h,1}} \right) \frac{\rho_a}{\rho_1 A_1^2} + 2 \rho_a R_{eq} + \left(K_3 + \frac{f_3 L_3}{D_{h,3}} \right) \frac{\rho_a}{\rho_3 A_3^2} \right] \frac{W^2}{2 \rho_a} \quad (36a)
\end{aligned}$$

$$= \left[\text{DENO}F_1 + \text{DENO}F_2 + \text{DENO}F_3 \right] \frac{W^2}{2 \rho_a} \quad (36b)$$

Equation (36a) is the approximate hydraulic equation for calculating the assembly flow rate W due to natural circulation, under the assumptions made in this section. Equation (36b) is shown here simply to associate the three terms in the square brackets of Eq. (36a) with three FORTRAN variables used in the older PLTEMP/ANL V3.4 code. The equivalent hydraulic resistance R_{eq} is given by Eq. (28) without any assumption about coolant properties. Under the assumptions made in this section, Eq. (28) simplifies to

$$\frac{1}{2 \rho_a R_{eq}} = \left[\sum_{k=1}^{N_c} \frac{A_{c,k}}{\left(K_2 + \frac{f_{c,k} L_2}{D_{hc,k}} \right)^{0.5}} \right]^2 \equiv \frac{1}{\text{DENO}F_2} \quad (37)$$

Equation (36) is simpler to implement but has some drawbacks. It does not include the coolant temperature *axial profile's* effect on the gravity head and frictional pressure drop of the heated section. Hence, the channel-to-channel variation of the buoyancy head and frictional pressure drop, and their effect on the induced flow rate, are ignored.

6. Changes Made to PLTEMP/ANL V3.4 to Obtain V4.2

Two groups of changes are described, one to implement the approximate method of Section 5, and the other to implement the general method described in Sections 2 and 3 which has inner and outer iterations.

6.1 Changes Made to Implement the Approximate Method

The following changes were made to PLTEMP/ANL V3.4 to implement the method of Section 5 to calculate the natural circulation flow, obtaining the new developmental V4.2. The changes were made in steps, tabulating and checking detailed debug output of the code at each step. The last change was to set the driving pressure drop equal to the buoyancy head on the left hand side of Eq. (36). The debug outputs of the last two steps are discussed in Section 7.

1. PLTEMP/ANL V3.4 used a single set of coolant density and viscosity in flow calculation. As described in Section 5, three sets of coolant density and viscosity are used in PLTEMP/ANL V4.2 in flow calculation in both natural circulation and forced flow. This is required in calculating natural circulation.

2. In natural circulation, the flow (although usually laminar) could be turbulent in some axial regions and laminar in others. Hence, a single routine for getting friction factor is needed. Therefore, the two routines GETF and FFCON for friction factor were combined. GETF covers all three flow regimes (laminar, critical, and turbulent) but calculated the laminar friction factor as $f_{lam} = C/Re$ (with $C = 96$) without varying C with the aspect ratio of the rectangular duct. FFCON did provide the dependence of C on the aspect ratio, but it is limited to only laminar flow regime. So, the routine GETF was improved to account for the dependence of the numerator C ($f_{lam} = C/Re$) on the duct aspect ratio, using the Shah and London correlation³ for C as documented in Section 8. The value of C from subroutine FFCON is not used in PLTEMP/ANL V4.2. PLTEMP/ANL V3.4 uses the infinitely narrow channel approximation $C = 96$, irrespective of the input channel cross section.
3. The subroutine RESIST_NC was changed to calculate flow resistance using Eq. (37). The coolant density ratios ρ_a/ρ_1 and ρ_a/ρ_3 appearing in Eq. (37) are included in calculating DENO in the new RESIST_NC.
4. In PLTEMP/ANL V4.2, the flow rate in each coolant channel is calculated in the subroutine WORK, just after finishing the assembly flow rate calculation. It is done using Eq. (23) or Eq. (31) from the values of the heated section frictional pressure drop DPF(I,J,2) and channel resistance $R_{c,k}$ already calculated and saved in the subroutine RESIST_NC. The channel flow rates are calculated or refined later by the subroutine CNLFLO_NC. The channel-wise flow rates calculated by the subroutines WORK and CNLFLO_NC are the same. Therefore, the subroutine CNLFLO_NC seems unnecessary.
5. During the assembly flow rate calculation in subroutine WORK, the driving pressure drop DP (which is set by input data in forced flow), is set equal to the left hand side of Eq. (36) in the case of natural circulation. This is done in subroutine WORK.

The outer iteration described in the solution strategy of Section 3 is not yet implemented. The outer iterations are required in a problem if the gravity head integrated over a coolant channel varies from channel to channel. The outer iterations are not important if all coolant channels have the same integrated gravity head.

6.2 Changes Made to Implement the General Method

1. The driver subroutine WORK was changed to perform the outer iterations between the heat transfer calculation and the hydraulic calculation, as a preparation for implementing the general method of Sections 2 and 3. No such outer iteration was done in PLTEMP/ANL V3.4 and earlier versions.
2. A subroutine NATCIRC was developed to implement the general method described in Sections 2 and 3. The subroutine was implemented in PLTEMP/ANL. It is called from the driver routine WORK (near the initial flow calculation in WORK) to calculate flow rates in the 2nd and later outer iterations. NATCIRC iteratively calculates the flow rates in

coolant channels, using a *given* set of channel coolant temperature axial profiles (resulting from a heat transfer calculation by the Analytical Method).

3. The subroutine CNLFLO_NC was commented out as it was unnecessary, and it is not used now. It was excluded because it modified the flow rates in the 4th significant digit. This disturbed the outer iterations mentioned above in item 1. With this change, the subroutine FINLED5 for printing the natural circulation output was also commented out because it printed some intermediate results of A. P. Olson's natural circulation coding (which are not calculated now). The subroutine FINLED5 may be included later after it is modified to print what is calculated by the general method of Sections 2 and 3.
4. The convergence of inner iterations (done in the subroutine NATCIRC) was checked by using different values for the allowed fraction (F_{inner}) of the calculated flow change due to an inner iteration. The number of inner iterations, N_{inner} , required for the convergence of all channel flow rates to a fractional error less than CONV2 (called the convergence criterion) is shown below. The routine was tested by varying F_{inner} from 0.1 to 1.0, and the convergence criterion CONV2 from 10^{-4} to 10^{-12} .

Convergence Behavior of Inner Iterations in Calculating Natural Circulation

CONV2→	1.0×10^{-4}	1.0×10^{-6}	1.0×10^{-8}	1.0×10^{-10}	1.0×10^{-12}
F_{inner}	N_{inner}	N_{inner}	N_{inner}	N_{inner}	N_{inner}
0.1	60	109	159	208	259
0.2	29				124
0.3	19				79
0.4	14				56
0.5	11	19	26	34	42
0.6	9				33
0.7	7				26
0.8	6				21
0.9	5	6	11	13	16
1.0	4	6	8	10	12

5. During the above testing of subroutine NATCIRC, it was noted that the initial flow calculation in the subroutine WORK does not converge for tighter convergence criteria, e.g., less than 10^{-5} . This should be investigated.
6. The subroutine WORK was changed to call the output printing subroutines *only once for a fuel assembly* when its outer iteration has converged.

7. PLTEMP/ANL V4.2 Testing and Verification

The code was tested by running a number of cases for two natural circulation problems, Sample Problem 20 and Sample Problem 21. The results are summarized here. These results provide a verification of the code. Further verification by comparing the code calculation with experimental data may be useful.

7.1 Results for Natural Circulation Sample Problem 20

Two solutions of this problem are reported here: (i) the solution obtained by the approximate method of Section 5, which forms the first iteration of the general method of Sections 2 and 3, and (ii) the solution obtained by the general method of Sections 2 and 3.

7.1.1 Sample Problem 20 Results after the First Outer Iteration

The following natural circulation test problem (Sample Problem 20) was defined and solved earlier by hand calculation⁴, by the NATCON code¹, and by the RELAP5-3D code⁵. The three solutions are given in Table XI-1. The PLTEMP/ANL input data for this natural circulation test problem is shown in Table XI-2.

Problem Definition: Calculate the coolant flow rate caused by natural circulation in a 1.05 m long vertical coolant channel with a 0.75 m long heated length (the lower unheated length being 0.15 m, and the upper unheated length 0.15 m). The heated length has a power of 25 kW distributed uniformly over the 0.75 m length, with an inlet temperature of 25 °C. The channel has a rectangular cross section of thickness 3 mm, width 0.3 m, inlet pressure loss coefficient 0.5, and exit pressure loss coefficient 1.0. The absolute pressure at the channel inlet is 5 bar, corresponding to the channel inlet being 40.81 m below the free surface of water in the pool.

After making all the changes but the last, listed above in Section 6.1, (setting the driving pressure drop to the buoyancy head), PLTEMP/ANL was run for the input data given in Table XI-2. Basically, this run is a forced flow calculation for a driving pressure drop of 327.5 Pa (input on card type 0500). The results are shown in Table XI-3. The density, viscosity, Reynolds number, friction factor, and flow resistance of each axial region, shown in Table XI-3, were all checked by hand calculation. The frictional pressure drops of the three axial regions add up to 327.57 Pa, compared to the input value of 327.5 Pa. The channel-wise flow rates (0.1178 kg/s in the first and last channels, and 0.2356 kg/s in inner channels) calculated by the subroutines WORK and CNLFLO_NC are the same. Therefore, CNLFLO_NC is redundant, as mentioned earlier.

After making the last change, the code (referred to as PLTEMP/ANL V4.2) uses the buoyancy head given in Eq. (36) as the driving head in natural circulation. Table XI-4 shows the results of running this code for the same input data of Table XI-2. This is a solution to the natural circulation problem. The frictional pressure drops of the three axial regions add up to 105.33 Pa, compared to the buoyancy head of 105.32 Pa. Again, the channel-wise flow rates calculated by the subroutines WORK and CNLFLO_NC are the same. The inner channel flow rate of 0.10811 kg/s calculated by PLTEMP/ANL V4.2 compares well with 0.1086 kg/s calculated earlier by hand calculation using *Mathematica*, and confirmed by the NATCON and RELAP5-3D codes. These results are compared in Table XI-1.

7.1.2 Sample Problem 20 Results after the Convergence of Outer Iteration

The results given in this section for Sample Problem 20 were obtained after implementing the general method of Sections 2 and 3. The results were obtained after outer iteration convergence.

The convergence of outer iteration (done in subroutine WORK) was checked by running Sample Problem 20. Each fuel plate has a radial power peaking factor of 1.0 in this problem. The outer iteration converged in 17 iterations, and Table XI-7 summarizes the outer iteration history of channel flow rates, buoyancy head of the fuel assembly, and coolant channel exit temperatures. The converged flow rate is not very different from that shown in Table XI-4 which was calculated in one outer iteration by the approximate method of Section 5.

7.3 Results for Sample Problem 20 Run as a Forced Flow Problem

The purpose here to assess the effect of the present changes to the code (for implementing a natural circulation calculation method) on the forced flow calculation. To do this, the above test problem (i.e., Sample Problem 20 with input data given in Table XI-2) was changed into a forced flow problem by setting the input option IH = 0 instead of 6. Two solutions of the resulting forced flow problem were obtained, using the code before and after making the changes, i.e., using the V3.4 and V4.2 of PLTEMP/ANL. The input DP0 (the frictional pressure drop from assembly inlet to outlet) is 327.5 Pa in this problem. The results of the two calculations are given in Tables XI-5 and XI-6.

The assembly flow rate calculated by the subroutines WORK and RESIST is the same as that calculated by the subroutine CNLFLO, in each of Tables XI-5 and XI-6. This indicates that the subroutine CNLFLO is redundant. The three frictional pressure drops over the axial regions 1, 2, and 3 add up to about 327.5 Pa, the input driving pressure drop, in each of Tables XI-5 and XI-6.

Three solutions to the forced flow problem (i.e., Sample Problem 20 driven by an input pressure drop of 327.5 Pa) are given in Table XI-3, Table XI-5, and Table XI-6. The two calculations by V4.2 (Tables XI-3 and XI-6) give the same assembly flow rate (0.94225 kg/s) which is slightly different from the flow rate 0.95191 kg/s calculated by V3.4. It should be noted that all flow-related variables are equal in these two calculations (see Tables XI-3 and XI-6). This implies that it makes no difference (in the solution of this problem) whether the natural circulation subroutines RESIST_NC and CNLFLO_NC are exercised in the calculation, or the forced flow subroutines RESIST and CNLFLO are exercised.

The assembly flow rate (of Table XI-5) calculated by PLTEMP/ANL V3.4 is 0.95191 kg/s ($T_{out} = 50.171$ °C) compared to 0.94225 kg/s ($T_{out} = 50.428$ °C) calculated by PLTEMP/ANL V4.2 (given in Table XI-6). This is due to two reasons: (i) V3.4 uses a single set of coolant density and viscosity in all axial regions of the assembly in calculating frictional pressure drops whereas V4.2 uses three sets of coolant density and viscosity (at temperatures T_{in} , $(T_{in}+T_{out})/2$, and T_{out}) in different axial regions of the assembly, and (ii) V3.4 finds the heated section flow resistance using Eq. (38) whereas V4.2 uses Eq. (37). These modeling differences are tabulated below.

$$DENO_{f_n} = \frac{1}{A_n^2} \left(K_n + \frac{f_n L_n}{D_{h,n}} \right) \quad (\text{for heated or unheated sections}) \quad (38)$$

Comparison of the Three Results for the Forced Flow Sample Problem 20

Output	PLTEMP/ ANL Code Version	Subroutines Used	Number of Coolant Densities Used in Hydraulic Equations	Heated Section Flow Resistance	Flow Rate in Assembly, kg/s
Table XI-3	Version 4.2	RESIST_NC, CNLFLO_NC	Three Density	Eq. (37)	0.94225
Table XI-6	Version 4.2	RESIST, CNLFLO	Three Density	Eq. (38)	0.94225
Table XI-5	Version 3.4	RESIST, CNLFLO	One Density	Eq. (38)	0.95191

7.4 Results for Natural Circulation Sample Problem 21

The input data for Sample Problem 21 is shown in Table XI-8. This problem is a variation of Sample Problem 20. Each of these problems has two fuel assemblies. In Sample Problem 21, the radial power peaking factors of the four fuel plates of assembly 2 are changed to 0.6, 1.4, 1.4, and 0.6 (unequal) instead of 1.0 for each plate in Sample Problem 20. The radial power peaking factors of the four fuel plates of assembly 1 in Sample Problem 21 are kept unchanged, i.e., equal to 1.0 for each plate, as in Sample Problem 20. The results given in this section for Sample Problem 21 were obtained after implementing the general method of Sections 2 and 3. These results were obtained after the outer iterations have converged.

The convergence of outer iteration (done in subroutine WORK) was checked by running Sample Problem 21. The outer iteration converged in 19 iterations, and Table XI-9 summarizes the outer iteration history of channel flow rates, buoyancy head of the fuel assembly, and coolant channel exit temperatures. The *converged* coolant exit temperature in channel 3 (having the hottest coolant) is 86.18 °C compared to 98.64 °C calculated after the *first outer iteration*. This happens because (i) in the first outer iteration, each coolant channel is assumed to have the *same* buoyancy head driving its flow, whereas in reality (ii) the hottest channel develops the largest buoyancy head resulting in the largest coolant flow in the channel and a moderation of its coolant temperature.

Another reason for the moderation of coolant temperature in channel 3 is the decrease of the fraction of power generated in fuel plates 2 and 3 (surrounding channel 3) that is transferred into channel 3. This happens because channel 3 runs hotter than the surrounding channels 2 and 4, and hence the power of plates 2 and 3 are split unequally, more into the cooler channel 2 (or channel 4) and less into the hotter channel 3. The calculated split fractions are shown below.

Fuel Plate Power Split Fractions between Adjacent Channels in Sample Problem 20 and 22

Test Problem	Plate 1 Power Fractions Transferred to Adjacent Channels		Plate 2 Power Fractions Transferred to Adjacent Channels		Plate 3 Power Fractions Transferred to Adjacent Channels		Plate 4 Power Fractions Transferred to Adjacent Channels	
	Chan 1	Chan 2	Chan 2	Chan 3	Chan 3	Chan 4	Chan 4	Chan 5
Assembly 2 of Sample Problem 21	0.5000	0.5000	0.5000	0.5000	0.5000	0.5000	0.5000	0.5000
Assembly 1 of Sample Problem 21	0.5444	0.4556	0.5161	0.4839	0.4839	0.5161	0.4556	0.5444

Only a fraction 0.4839 of the power of plates 2 and 3 goes to channel 3 in fuel assembly 2 of Sample Problem 21, compared to a fraction 0.5 in fuel assembly 1 of the same problem. These power fractions in fuel assembly 2 vary with the axial position over the heated length, and the values tabulated above are those at the channel exit.

The flow rate in assembly 2 is 0.43420 kg/s, not very different (the difference is 0.4 %) from 0.43244 kg/s calculated after the first outer iteration (see Table XI-9).

To test the code for more than three axial regions, the *input data* shown in Table XI-8 for Sample Problem 21 was rerun with the axial region 3 above the heated section split into two regions of length 0.05 m and 0.10 m. Although the input data is changed, the problem remains unchanged physically. Exactly the same flow rates and temperatures, as shown in Table XI-9, were obtained by running the code for the changed input data.

7.5 Dependence of Outer Iteration Convergence on Parameter ϵ of Equation (14)

The parameter ϵ of Eq. (14) is the fraction of coolant temperature change (from the previous heat transfer calculation to the current heat transfer calculation) that is used in the current outer iteration. Due the importance of ϵ in outer iteration convergence, a parametric study was done by varying it from 0.3 to 0.9 in steps of 0.05 in Sample Problem 21. The code converged for values of ϵ from 0.45 to 0.80. Table XI-10 summarizes the converged cases. The assembly buoyancy head, the channel flow rates, and the channel exit temperatures are practically the same for all these converged cases. A value of 0.60 is currently used in PLTEMP/ANL V4.2.

8. Friction Factor in Rectangular Channels

The Darcy-Weisbach friction factor in PLTEMP/ANL is calculated by the function subprogram GETF using the following correlations. The correlations cover all three flow regimes (laminar, critical, and turbulent) in smooth and rough ducts. The fully-developed laminar friction factor is calculated using the Shah and London correlation³, given by Eq. (40).

$$f = \begin{cases} f_{\text{lam}}(\text{Re}, a) & \text{if } \text{Re} \leq 2200 \\ \left(3.75 - \frac{8250}{\text{Re}}\right)(f_a - f_{2200}) + f_{2200} & \text{if } 2200 < \text{Re} < 3000 \\ 4 \text{ Solve} \left[f = \frac{6.25002}{1 - 8.68591 \ln(\text{Re} \sqrt{f}) + 18.8612 \left\{ \ln(\text{Re} \sqrt{f}) \right\}^2} \right] & \text{if } \text{Re} \geq 3000, \quad E_{\text{rel}} = 0 \\ 4 \text{ Solve} \left[f = 0.331369 / \left\{ \ln \left(0.27027 E_{\text{rel}} + \frac{1.255}{\text{Re} \sqrt{f}} \right) \right\}^2 \right] & \text{if } \text{Re} \geq 3000, \quad E_{\text{rel}} \geq 10^{-8} \end{cases} \quad (39)$$

where

- a = Channel aspect ratio = Channel thickness/width ratio, always ≤ 1.0
- E_{rel} = Relative roughness ROUGH = e/D_e input on Card 0305

$$f_{\text{lam}}(\text{Re}, a) = \frac{96(1 - 1.3553a + 1.9467a^2 - 1.7012a^3 + 0.9564a^4 - 0.2537a^5)}{\text{Re}} \quad (40)$$

$$f_{2200} = f_{\text{lam}}(2200, a) \quad (41)$$

$$f_a = \left[-2 \text{Log}_{10} \left\{ \frac{E_{\text{rel}}}{3.7} + \frac{2.51}{\text{Re}} \left\{ 1.14 - 2 \text{Log}_{10} (E_{\text{rel}} + 21.25 \text{Re}^{-0.9}) \right\} \right\} \right]^{-2} \quad (42)$$

NOMENCLATURE

- a = Aspect ratio of a rectangular channel, i.e., thickness/width (the ratio must be ≤ 1.0).
 A_n = Flow area of the n^{th} axial region of the assembly, m^2 .
 A_{ch} = Flow area in the chimney, m^2 .
 $A_{\text{c},k}$ = Flow area of coolant channel k in the heated section (axial region 2) of the assembly, m^2 .
 $A_2 = \sum_{k=1}^{N_c} A_{\text{c},k}$ = Total flow area of the heated section (axial region 2) of the assembly, m^2 .
 CONV2 = Maximum fractional error allowed for the convergence of each channel flow rate during inner iteration (called the convergence criterion).
 $\text{DENO}F_n$ = Flow resistance of the n^{th} axial region, defined by Eqs. (36), m^{-2} .
 $\text{DENO}F = \sum_{n=1}^{N_c} \text{DENO}F_n$ = Variable in PLTEMP/ANL for the flow resistance of all axial regions of an assembly, m^{-2} .
 $D_{\text{h},n}$ = Hydraulic diameter of the n^{th} axial region, m. It is an input data.
 $D_{\text{hc},k}$ = Hydraulic diameter of the k^{th} coolant channel in the heated section, m. It is an input datum.
 F_{inner} = Fraction of the calculated flow rate change due to an inner iteration, that is allowed to find the next guess for flow rate.
 $f(z)$ = Darcy-Weisbach friction factor as a function of axial position z .
 f_n = Darcy-Weisbach friction factor in the n^{th} axial region. It is calculated by subroutine RESIST for a *guessed* flow rate in the assembly, coolant kinematic viscosity ν_a , density ρ_a , and an input pipe roughness. Only the turbulent correlation is currently coded in subroutine RESIST.
 h_{ch} = Enthalpy of coolant in the chimney, J/kg.
 K_n = Sum of minor loss coefficients at inlet and exit of the n^{th} axial region n . It is an input datum.
 L_{ch} = Effective chimney length (at the mixed mean temperature of all fuel assemblies), m.
 L_n = Length of the n^{th} axial region, m. It is an input datum.
 n = Axial region index, where $n = 2$ is the heated section, $n = 1$ is the region upstream of the heated section, and $n = 3$ to N_f are regions downstream of the heated section.
 N_{inner} = Number of inner iterations required for the convergence of all channel flow rates to a fractional error less than CONV2 (called the convergence criterion).
 N_c = Number of coolant channels in the assembly.
 N_f = Total number of axial regions in the assembly.

- ΔP_f = Frictional pressure drop (minor loss + wall shear) from the inlet to exit of the assembly J of type I, Pa. The assembly indices (I, J) are dropped from the equations in this document for brevity.
- P_1 = Absolute pressure of the creeping coolant in the pool at the assembly inlet level, Pa.
- P_1' = Absolute pressure of the coolant moving inside the flow area at the assembly inlet, Pa.
- P_2 = Absolute coolant pressure just before the inlet to the heated section, Pa.
- P_3 = Absolute coolant pressure just after the exit from the heated section, Pa.
- P_4 = Absolute coolant pressure in the chimney at the bottom, Pa.
- P_5' = Absolute coolant pressure in the chimney at the top, Pa.
- P_5 = Absolute pressure of the creeping coolant in the pool at the chimney top level, Pa.
- $\Delta P_{f,n}$ = Frictional pressure drop (minor loss + wall shear) in the n^{th} axial region of the assembly J of type I, Pa.
- $\Delta P_{f,2,\text{app}}$ = Approximate frictional pressure drop (minor loss + wall shear) in a coolant channel of the heated section (axial region 2) of the assembly J of type I, defined by Eq. (21), Pa.
- ΔP_n = Absolute pressure drop in the n^{th} axial region of the assembly J of type I, Pa;
= $(P_1 - P_2)$ for axial region 1;
= $(P_2 - P_3)$ for axial region 2;
= $(P_3 - P_4)$ for axial region 3.
- Q = Power produced in the assembly, W.
- T_{ch} = Coolant temperature in the chimney, °C.
- $T_{c,k}(z)$ = Coolant temperature in channel k, °C.
- T_{in} = Coolant temperature at the assembly inlet, °C.
- T_{out} = Coolant temperature at the assembly outlet, °C.
- $T_{\text{ex},k}$ = Coolant temperature at the exit of the k^{th} channel, °C.
- W = $W^{(i)}$ = Flow rate in assembly J (total flow in all coolant channels), kg/s.
- $W_{c,k}$ = $W_{c,k}^{(j)}$ = Flow rate in the k^{th} coolant channel of assembly J, kg/s.
- ε = Fraction of coolant temperature change (from the previous heat transfer calculation) that is used in the current outer iteration; see Eq. (14).
- $\rho(z)$ = Coolant density as a function of axial position z, kg/m^3 .
- ρ_a = $\rho(0.5(T_{\text{in}} + T_{\text{out}}))$ = Average coolant density for the assembly, kg/m^3 . It is calculated at the mean of the assembly inlet and exit temperatures. The pressure used in getting ρ_a is the input inlet pressure plus half of the input frictional pressure drop DP_0 . Although the pressure used is not strictly correct because the gravity head is not accounted, it is accurate enough for calculating water density and viscosity because these properties have negligible variation with pressure.
- ρ_{ch} = Coolant density in the chimney, kg/m^3 .
- $\mu(z)$ = Coolant dynamic viscosity as a function of axial position z, Pa-s.
- μ_a = Average dynamic coolant viscosity for the assembly, Pa-s. It is calculated at the same temperature and pressure as those used in ρ_a .

REFERENCES

- (1) R. S. Smith and W. L. Woodruff, "A Computer Code, NATCON, for the Analysis of Steady-State Thermal-Hydraulics and Safety Margins in Plate-Type Research Reactors Cooled by Natural Convection", ANL/RERTR/TM-12, Argonne National Laboratory, Argonne, IL (December 1988).
- (2) I. H. Shames, "Mechanics of Fluids," International Student Edition, McGraw-Hill Book Company, Tokyo, Japan, p. 287 (1962).
- (3) R. K. Shah and A. L. London, "Laminar Flow Forced Convection in Ducts," Advances in Heat Transfer, Supplement 1, Academic Press, New York (1978).
- (4) M. Kalimullah, A. P. Olson, and E. E. Feldman, "Solution of a Natural Circulation Sample Problem for Use in Verification of the PLTEMP/ANL Code," Intra-Laboratory Memorandum to J. E. Matos, RERTR Program, Nuclear Engineering Division, Argonne National Laboratory, IL (DRAFT of March 31, 2008).
- (5) The RELAP5-3D Code Development Team, RELAP5-3D Code Manual, Version 2.3, INEEL-EXT-98-00834, Idaho National Engineering Laboratory (April 2005).

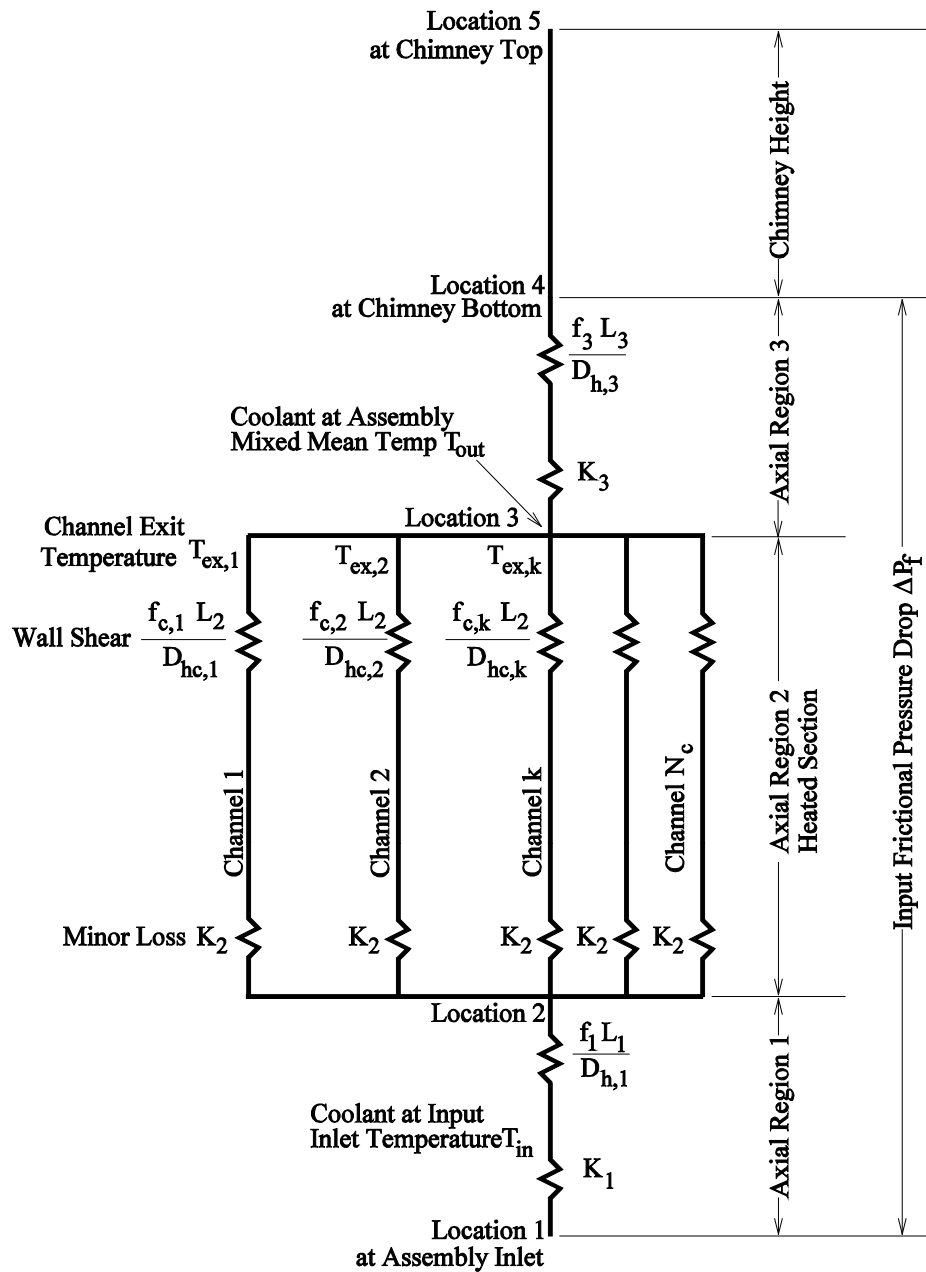


Fig. 1. Coolant Flow Path in a Fuel Assembly and Chimney Modeled in PLTEMP/ANL (Multiple Axial Regions Downstream of the Heated Section Are Allowed)

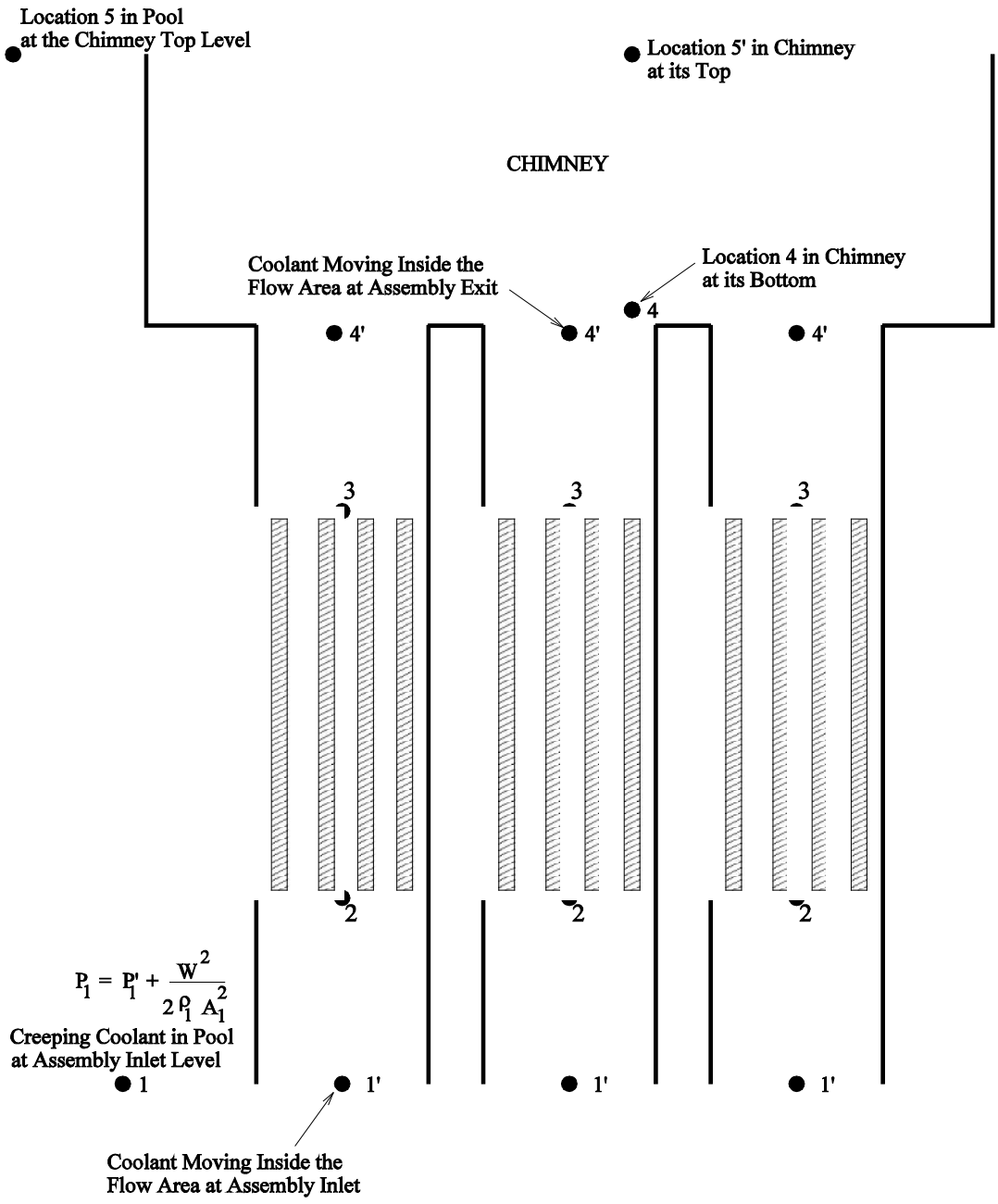


Fig. 2. Locations of Coolant Pressure in a Group of Fuel Assemblies Exiting into a Common Chimney

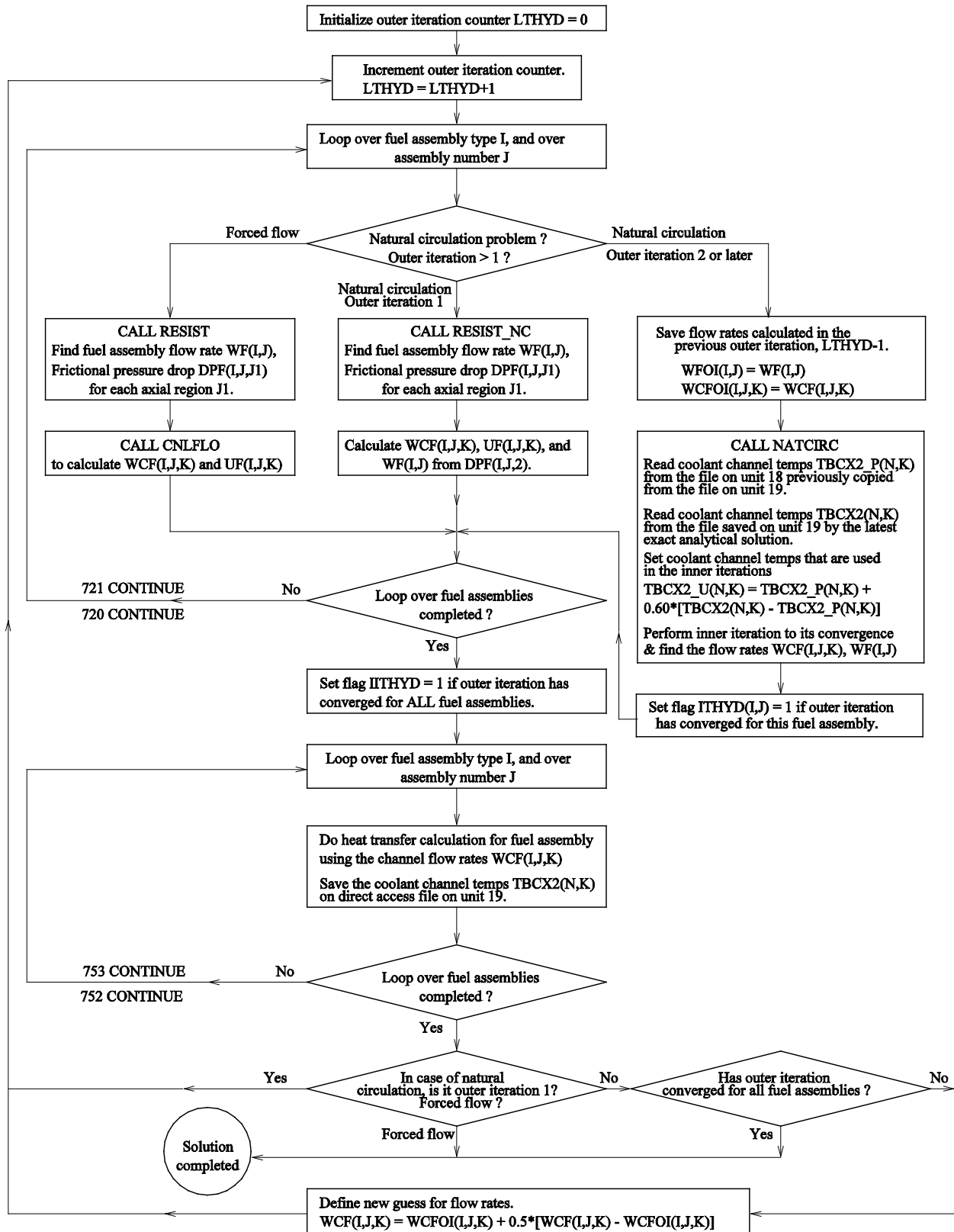


Fig. 3. Logic Flow Diagram for Outer Iteration in Natural Circulation Calculation in PLTEMP/ANL V4.2 Code

Table XI-1. Flow Rate Calculation for the Natural Circulation Problem by 3 Methods

Input or Calculated Quantity	Hand Calculation Using 5 Segments in Heated Length	NATCON Code Calculation	RELAP5-3D Code Calculation	PLTEMP/ANL Code Calculation	
				Approximate Method of Section 5	General Method of Sect. 2 and 3
Inlet Temperature, °C	25	25	25	25	25
Power per Channel, W	25000	25000	25000	25000	25000
Loss Coeff. at Inlet	0.5	0.5	0.5	0.5	0.5
Loss Coeff. At Exit	1.0	1.0	1.0	1.0	1.0
Calculated Quantities					
Flow per Channel, kg/s	0.1086	0.1087	0.1141	0.1081	0.1093
Exit Temperature, C	79.967	79.970	77.44	80.249	79.647
Buoyancy Head ΔP_{buoy}, Pa					
Axial Region 1	0.0	0.0	0.0	0.0	0.0
Heated Section (Axial Region 2)	75.716	75.783		68.99	75.33
Axial Region 3	36.040	36.034		36.33	35.79
Total ΔP_{buoy}	111.756	111.817	117.80	105.32	111.12
Frictional Pressure Drop ΔP_{fric}, Pa					
Inlet Loss	3.652	3.659		25.48	25.80
Axial Region 1	22.268	22.348			
Sub-section 1 of Heated Length	19.672	19.791			
Sub-section 2 of Heated Length	15.729	15.803			
Sub-section 3 of Heated Length	12.988	13.034			
Sub-section 4 of Heated Length	11.010	11.046			
Sub-section 5 of Heated Length	9.571	9.601			
Heated Length	68.970 [Note 1]	69.275		63.60	68.75
Axial Region 3	9.015	9.033		16.25	16.57
Exit Loss	7.487	7.503			
Pressure Drop due to Momentum Flux	0.368	0.0		0.0	0.0
Total ΔP_{fric}	111.760	111.817		105.33	111.12

Note 1. The frictional pressure drop in the heated section, calculated using coolant properties at the mean temperature, using one instead of 5 sub-sections is 64.938 Pa.

Table XI-2. PLTEMP/ANL Input Data for Natural Circulation Sample Problem 20

```

Test Problem 20: Flow is calculated by natural circulation
! 2 assemblies, Total power = 0.20 MWT, Axially uniform power profile
! Each assembly has 4 fuel plates and 5 coolant channels
! H2O coolant, All hot channel factors = 1.0, No bypass flow, NCTYP=0
! 14 axial heat transfer nodes in the heated length of fuel plates
! 1 2 3 4 5 6 7 8 9 10 11 12 13 14 15 16 17 18 Indices Card 200
  5 0 0 1 0 1 1 1 0 0 0 0 0 0 1 0 0 0 Card(1)0200
  2 3 0.50 1.00 1.00 1.00 0 Card(1)0300
! Using pressure driven mode
  1 1 1.00 Card(1)0301
  1 1 1 Card(1)0302
1.00 1.00 Card(2)0303
36.0E-04 5.94059E-03 0.15 0.50 0.30 3.00E-03 Card(3)0304
0.00 5.94059E-03 0.75 0.00 0.30 3.00E-03 Card(3)0304
36.0E-04 5.94059E-03 0.15 1.00 0.30 3.00E-03 Card(3)0304
! Use the code's built-in correlation for friction factor
0.00 0.00 0.00 Card(1)0305
  5 3 0.00 0.75 0.50E-03 180.00 1.00E-03 100.00 Card(1)0306
4.50E-04 5.94059E-03 0.3030 0.30 0.30 3.00E-03 Card(5)0307
9.00E-04 5.94059E-03 0.6060 0.60 0.30 3.00E-03 Card(5)0307
9.00E-04 5.94059E-03 0.6060 0.60 0.30 3.00E-03 Card(5)0307
9.00E-04 5.94059E-03 0.6060 0.60 0.30 3.00E-03 Card(5)0307
4.50E-04 5.94059E-03 0.3030 0.30 0.30 3.00E-03 Card(5)0307
0.30 0.30 0.30 0.30 Card(1)0308
! Card 0308A not required
! Radial power peaking factor data by fuel plate for each subassembly. Input flow data by
! channel for each subassembly on Cards 0310 not required because WFGES(1) is non-zero
1.000 1.000 1.000 1.000 Card(2)0309
1.000 1.000 1.000 1.000 Card(2)0309
! DPO DDP DPMAX POWER TIN PIN
0.0003275 0.04 0.00 0.200 25.0 0.50 Card(1)0500
0.00 0.00 Card(2)0500
  50 0.0001 25.0 0.00 0.00 Card(1)0600
  15 Card(1)0700
0.0 1.000 Card(11)0701
0.100 1.000 Card(11)0701
0.167 1.000 Card(11)0701
0.233 1.000 Card(11)0701
0.300 1.000 Card(11)0701
0.367 1.000 Card(11)0701
0.433 1.000 Card(11)0701
0.5 1.000 Card(11)0701
0.567 1.000 Card(11)0701
0.633 1.000 Card(11)0701
0.700 1.000 Card(11)0701
0.767 1.000 Card(11)0701
0.833 1.000 Card(11)0701
0.900 1.000 Card(11)0701
1.0 1.000 Card(11)0701
  0 Card(11)0702

```

**Table XI-3. Debug Output of Natural Circulation Subroutines in PLTEMP/ANL V4.2
For Sample Problem 20 Driven by Input Pressure Drop, not Buoyancy [1]**

Quantity	Axial Region 1	Axial Region 2	Axial Region 3	Total
Assembly Flow Rate WF, kg/s	0.94225	0.94225	0.94225	
Mean Temperature, °C	25.000	37.714	50.428	T _{out} = 50.428
Length, m	0.15	0.75	0.15	
Flow Area m ²	3.6x10 ⁻³	3.6x10 ⁻³	3.6x10 ⁻³	
Hydraulic Diameter D _h , m	5.9406x10 ⁻³	5.9406x10 ⁻³	5.9406x10 ⁻³	
Coolant Density, kg/m ³	996.87	993.36	988.50	
Dynamic Viscosity, Pa-s	9.0121x10 ⁻⁴	6.8349x10 ⁻⁴	5.3961x10 ⁻⁴	
Reynolds Number, Re	1725.32	2274.91	2881.47	
Friction Factor (from new GETF [2])	0.0548986	0.0435656	0.0437941	
Minor Loss Coeff., K	0.5	0.0	1.0	
Flow Resistance, R = K+fL/D _h	1.88619	5.50016	2.10580	
DENOF from RESIST_NC	145026.5	424394.8	163283.7	732705.0
DPF, Press Drop, Pa	64.81	189.66	72.97	327.44
DENOF from First Principles, Using Eq. (36)	145026.9	424395.1	163283.4	732705.4

Channel-wise flow rates calculated by subroutine CNLFLO_NC given below.

Channel	Channel Flow, kg/s
1	0.117774
2	0.235549
3	0.235549
4	0.235549
5	0.117774
Total	0.94220 kg/s as compared to 0.94225 kg/s calculated by subroutine WORK.

Notes:

- [1] PLTEMP/ANL V4.2 was run using the input option IH = 6, exercising the natural circulation subroutines RESIST_NC and CNLFLO_NC. But the forced flow problem was solved because this calculation was done before implementing the buoyancy as the driving pressure drop.
- [2] New subroutine GETF has all flow regimes, with $f_{lam} = C/Re$, $C = 94.7174$ for the channel aspect ratio = 0.01

**Table XI-4. Debug Output of Natural Circulation Subroutines in PLTEMP/ANL V4.2
For Sample Problem 20 Driven by Buoyancy [1]**

Quantity	Axial Region 1	Axial Region 2	Axial Region 3	Total
Assembly Flow Rate WF, kg/s	0.43244	0.43244	0.43244	
Mean Temperature, °C	25.000	52.625	80.249	T _{out} = 80.249
Length, m	0.15	0.75	0.15	
Flow Area m ²	3.6x10 ⁻³	3.6x10 ⁻³	3.6x10 ⁻³	
Hydraulic Diameter D _h , m	5.9406x10 ⁻³	5.9406x10 ⁻³	5.9406x10 ⁻³	
Coolant Density, kg/m ³	996.87	987.49	972.17	
Dynamic Viscosity, Pa-s	9.0121x10 ⁻⁴	5.1951x10 ⁻⁴	3.5509x10 ⁻⁴	
Reynolds Number, Re	791.82	1373.6	2009.6	
Friction Factor (from new GETF [2])	0.11962	0.068956	0.047132	
Minor Loss Coeff., K	0.5	0.0	1.0	
Flow Resistance, R = K+fL/D _h	3.52040	8.70571	2.19009	
DENOF from RESIST_NC	269079.6	671737.1	171650.3	1112467.0
DPF, Press Drop, Pa	25.48	63.60	16.25	105.33 [3]
DENOF from First Principles, Using Eq. (36)	269079.7	671731.1	171651.7	1112462.5

Channel-wise flow rates calculated by subroutine CNLFLO_NC given below.

Channel	Channel Flow, kg/s
1	0.054063
2	0.108126
3	0.108126
4	0.108126
5	0.054063
Total	0.43250 kg/s as compared to 0.43244 kg/s calculated by subroutine WORK.

Notes:

[1] PLTEMP/ANL V4.2 was run using the input option IH = 6, exercising the natural circulation subroutines RESIST_NC and CNLFLO_NC. This calculation is a solution of the natural circulation problem because it was done after implementing the buoyancy as the driving pressure drop.

[2] New subroutine GETF has all flow regimes, with $f_{\text{laminar}} = C/Re$, $C = 94.7174$ for the channel aspect ratio = 0.01

[3] Buoyancy head = $gL_2(\rho_1 - \rho_a) + gL_3(\rho_1 - \rho_3) = 105.32$ Pa

Table XI-5. Debug Output of Forced Flow Subroutines in PLTEMP/ANL V3.4 for Sample Problem 20 Driven by an Input Pressure Drop of 327.5 Pa [1]

Quantity	Axial Region 1	Axial Region 2	Axial Region 3	Total
Assembly Flow Rate WF, kg/s	0.95191	0.95191	0.95191	
Mean Temperature, °C	37.586	37.586	37.586	T _{out} = 50.171
Length, m	0.15	0.75	0.15	
Flow Area m ²	3.6x10 ⁻³	3.6x10 ⁻³	3.6x10 ⁻³	
Hydraulic Diameter D _h , m	5.9406x10 ⁻³	5.9406x10 ⁻³	5.9406x10 ⁻³	
Coolant Density, kg/m ³	993.40	993.40	993.40	
Dynamic Viscosity, Pa-s	6.8527x10 ⁻⁴	6.8527x10 ⁻⁴	6.8527x10 ⁻⁴	
Reynolds Number, Re	2292.3	2292.3	2292.3	
Friction Factor (from old GETF [2])	0.044158	0.044158	0.044158	
Minor Loss Coeff., K	0.5	0.0	1.0	
Flow Resistance, R = K+fL/D _h	1.61498	5.57489	2.11498	
DENOF from RESIST_NC	124613.0	430161.0	163193.0	717967.0
DPF, Press Drop, Pa	56.83	196.19	74.43	327.45
DENOF from First Principles	124612.7	430165.3	163192.9	717970.9

Channel-wise flow rates calculated by subroutine CNLFLO given below.

Channel	Channel Flow, kg/s
1	0.118985
2	0.237969
3	0.237969
4	0.237969
5	0.118985
Total	0.95188 kg/s as compared to 0.95191 kg/s calculated by subroutine WORK.

Notes:

- [1] PLTEMP/ANL V3.4 was run using the input option IH = 0, exercising the forced flow subroutines RESIST and CNLFLO. This is a solution of the forced flow problem by V3.4.
- [2] Old subroutine GETF has all flow regimes, but $f_{\text{laminar}} = C/Re$ with $C = 96$, ignoring its variation with the duct aspect ratio.

Table XI-6. Debug Output of Forced Flow Subroutines in PLTEMP/ANL V4.2 for Sample Problem 20 Driven by an Input Pressure Drop of 327.5 Pa [1]

Quantity	Axial Region 1	Axial Region 2	Axial Region 3	Total
Assembly Flow Rate WF, kg/s	0.94225	0.94225	0.94225	
Mean Temperature, °C	25.000	37.714	50.428	T _{out} = 50.428
Length, m	0.15	0.75	0.15	
Flow Area m ²	3.6x10 ⁻³	3.6x10 ⁻³	3.6x10 ⁻³	
Hydraulic Diameter D _h , m	5.9406x10 ⁻³	5.9406x10 ⁻³	5.9406x10 ⁻³	
Coolant Density, kg/m ³	996.87	993.36	988.50	
Dynamic Viscosity, Pa-s	9.0121x10 ⁻⁴	6.8349x10 ⁻⁴	5.3961x10 ⁻⁴	
Reynolds Number, Re	1725.32	2274.91	2881.47	
Friction Factor (from new GETF [2])	0.0548986	0.0435656	0.0437941	
Minor Loss Coeff., K	0.5	0.0	1.0	
Flow Resistance, R = K+fL/D _h	1.88619	5.50015	2.10580	
DENOF from RESIST_NC	145026.5	424394.5	163283.7	732704.7
DPF, Press Drop, Pa	64.81	189.66	72.97	327.44
DENOF from First Principles, Using Eq. (36)	145026.9	424394.3	163283.4	732704.6

Channel-wise flow rates calculated by subroutine CNLFLO given below.

Channel	Channel Flow, kg/s
1	0.117774
2	0.235549
3	0.235549
4	0.235549
5	0.117774
Total	0.94220 kg/s as compared to 0.94225 kg/s calculated by subroutine WORK.

Notes:

[1] PLTEMP/ANL V4.2 was run using the input option IH = 0, exercising the forced flow subroutines RESIST and CNLFLO. This is a solution of the forced flow problem by V4.2.

[2] The new subroutine GETF has all flow regimes, with $f_{lam} = C/Re$, $C = 94.7174$ for the channel aspect ratio = 0.01

Table XI-7. PLTEMP/ANL Outer Iteration History for Running Sample Problem 20
 (The outer iteration convergence criterion was applied only to the assembly flow rate. Outer iteration ϵ of Eq. (14) = 1.0)

Outer Iteration	Quantity	Assembly Flow Rate, kg/s	Coolant Channels				
			1	2	3	4	5
1	Buoyancy, Pa		105.32	105.32	105.32	105.32	105.32
	Flow, kg/s	0.43244	0.0541	0.1081	0.1081	0.1081	0.0541
	Exit Temp, C		80.26	80.26	80.26	80.26	80.26
2	Buoyancy, Pa		111.87	111.87	111.87	111.87	111.87
	Flow, kg/s	0.44075	0.0551	0.1102	0.1102	0.1102	0.0551
	Exit Temp, C		79.22	79.22	79.22	79.22	79.22
3	Buoyancy, Pa		110.60	110.60	110.60	110.60	110.60
	Flow, kg/s	0.43481	0.0544	0.1087	0.1087	0.1087	0.0544
	Exit Temp, C		79.96	79.96	79.96	79.96	79.96
	Iterations 4 to 15 are not tabulated						
16	Buoyancy, Pa		111.13	111.13	111.13	111.13	111.13
	Flow, kg/s	0.43732	0.0547	0.1093	0.1093	0.1093	0.0547
	Exit Temp, C		79.642	79.642	79.642	79.642	79.642
17 Converged	Buoyancy, Pa		111.12	111.12	111.12	111.12	111.12
	Flow, kg/s	0.43724	0.0547	0.1093	0.1093	0.1093	0.0547
	Exit Temp, C		79.647	79.647	79.647	79.647	79.647

Table XI-8. PLTEMP/ANL Input Data for Natural Circulation Sample Problem 21

```

Test Problem 21: Flow is calculated by natural circulation
! 2 assemblies, Total power = 0.20 MWt, Axially uniform power profile
! Each assembly has 4 fuel plates and 5 coolant channels
! H2O coolant, All hot channel factors = 1.0, No bypass flow, NCTYP=0
! 14 axial heat transfer nodes in the heated length of fuel plates
! 1 2 3 4 5 6 7 8 9 10 11 12 13 14 15 16 17 18 19 # Card 200
  5 0 0 1 0 1 1 1 0 0 0 0 0 0 1 0 0 0 1 Card(1)0200
  2 3 0.50 1.00 1.00 1.00 0 Card(1)0300
! Using pressure driven mode
  1 1 1.00 Card(1)0301
  1 1 1 Card(1)0302
1.00 1.00 Card(2)0303
36.0E-04 5.94059E-03 0.15 0.50 0.30 3.00E-03 Card(3)0304
0.00 5.94059E-03 0.75 0.00 0.30 3.00E-03 Card(3)0304
36.0E-04 5.94059E-03 0.15 1.00 0.30 3.00E-03 Card(3)0304
! Use the code's built-in correlation for friction factor
0.00 0.00 0.00 Card(1)0305
! Use laminar friction factor
!94.7174 1.00 0.00 Card(1)0305
  5 3 0.00 0.75 0.50E-03 180.00 1.00E-03 100.00 Card(1)0306
4.50E-04 5.94059E-03 0.3030 0.30 0.30 3.00E-03 Card(5)0307
9.00E-04 5.94059E-03 0.6060 0.60 0.30 3.00E-03 Card(5)0307
9.00E-04 5.94059E-03 0.6060 0.60 0.30 3.00E-03 Card(5)0307
9.00E-04 5.94059E-03 0.6060 0.60 0.30 3.00E-03 Card(5)0307
4.50E-04 5.94059E-03 0.3030 0.30 0.30 3.00E-03 Card(5)0307
0.30 0.30 0.30 0.30 Card(1)0308
! Card 0308A not required
! Radial power peaking factor data by fuel plate for each subassembly. Input flow data by
! channel for each subassembly on Cards 0310 not required because WFGES(1) is non-zero
1.000 1.000 1.000 1.000 Card(2)0309
0.600 1.400 1.400 0.600 Card(2)0309
! DP0 DDP DPMAX POWER TIN PIN
0.0000 0.04 0.00 0.200 25.0 0.50 Card(1)0500
0.00 0.00 Card(2)0500
  50 1.E-04 25.0 0.00 0.00 Card(1)0600
  15 Card(1)0700
0.0 1.000 Card(11)0701
0.100 1.000 Card(11)0701
0.167 1.000 Card(11)0701
0.233 1.000 Card(11)0701
0.300 1.000 Card(11)0701
0.367 1.000 Card(11)0701
0.433 1.000 Card(11)0701
0.5 1.000 Card(11)0701
0.567 1.000 Card(11)0701
0.633 1.000 Card(11)0701
0.700 1.000 Card(11)0701
0.767 1.000 Card(11)0701
0.833 1.000 Card(11)0701
0.900 1.000 Card(11)0701
1.0 1.000 Card(11)0701
  0 Card(11)0702

```

Table XI-9. PLTEMP/ANL Outer Iteration History in Natural Circulation Calculation for Fuel Assembly 2 in Sample Problem 21

(The outer iteration convergence criteria are applied to the assembly flow rate and to each channel flow rate. Outer iteration ϵ of Eq. (14) = 0.6)

Outer Iteration	Quantity	Assembly Flow Rate, kg/s	Coolant Channels				
			1	2	3	4	5
1	Buoyancy, Pa		105.32	105.32	105.32	105.32	105.32
	Flow, kg/s	0.43244	0.0541	0.1081	0.1081	0.1081	0.0541
	Exit Temp, C		61.93	80.19	98.64	80.19	61.93
2	Buoyancy, Pa		90.88	111.83	135.38	111.83	90.88
	Flow, kg/s	0.43980	0.0355	0.1103	0.1484	0.1103	0.0355
	Exit Temp, C		76.42	79.09	81.09	79.09	76.42
3	Buoyancy, Pa		93.87	111.07	128.97	111.07	93.87
	Flow, kg/s	0.43594	0.0385	0.1095	0.1401	0.1095	0.0385
	Exit Temp, C		73.42	79.38	83.99	79.38	73.42
4	Buoyancy, Pa		101.52	110.90	118.01	110.90	101.52
	Flow, kg/s	0.43362	0.0457	0.1095	0.1232	0.1095	0.0457
	Exit Temp, C		67.25	79.40	90.88	79.40	67.25
Iterations 5 to 15 are not tabulated							
16	Buoyancy, Pa		95.85	111.01	124.79	111.01	95.85
	Flow, kg/s	0.43424	0.0404	0.1096	0.1343	0.1096	0.0404
	Exit Temp, C		71.60	79.34	86.22	79.34	71.60
17	Buoyancy, Pa		95.62	111.00	125.00	111.00	95.62
	Flow, kg/s	0.43416	0.0402	0.1096	0.1346	0.1096	0.0402
	Exit Temp, C		71.79	79.34	86.09	79.34	71.79
18	Buoyancy, Pa		95.91	110.95	124.83	110.95	95.91
	Flow, kg/s	0.43421	0.0404	0.1095	0.1343	0.1095	0.0404
	Exit Temp, C		71.56	79.37	86.20	79.37	71.56
19 Converged	Buoyancy, Pa		95.79	111.00	124.85	111.00	95.79
	Flow, kg/s	0.43420	0.0403	0.1096	0.1344	0.1096	0.0403
	Exit Temp, C		71.65	79.34	86.18	79.34	71.65

Table XI-10. Dependence of Outer Iteration Convergence on Parameter ϵ in Natural Circulation Calculation for Fuel Assembly 2 in Sample Problem 21
 (The outer iteration convergence criteria are applied to the assembly flow and to *each channel* flow rate.)

ϵ of Eq. (14) [1]	Number of Outer Iteration Required	Quantity	Assembly Flow Rate, kg/s	Converged Solution by Coolant Channel				
				1	2	3	4	5
0.45	39	Buoyancy, Pa		95.76	110.98	124.90	110.98	95.76
		Flow, kg/s	0.43418	0.0403	0.1096	0.1344	0.1096	0.0403
		Exit Temp, C		71.67	79.35	86.16	79.35	71.67
0.50	30	Buoyancy, Pa		95.79	110.99	124.86	110.99	95.79
		Flow, kg/s	0.43419	0.0403	0.1096	0.1344	0.1096	0.0403
		Exit Temp, C		71.64	79.34	86.17	79.34	71.64
0.55	26	Buoyancy, Pa		95.78	110.99	124.88	110.99	95.78
		Flow, kg/s	0.43420	0.0403	0.1096	0.1344	0.1096	0.0403
		Exit Temp, C		71.65	79.35	86.16	79.35	71.65
0.60	19	Buoyancy, Pa		95.79	111.00	124.85	111.00	95.79
		Flow, kg/s	0.43420	0.0403	0.1096	0.1344	0.1096	0.0403
		Exit Temp, C		71.65	79.34	86.18	79.34	71.65
0.60 [2]	20	Buoyancy, Pa		95.78	110.97	123.91	110.97	95.78
		Flow, kg/s	0.43491	0.0403	0.1094	0.1355	0.1094	0.0403
		Exit Temp, C		71.71	79.38	85.74	79.38	71.71
0.65	18	Buoyancy, Pa		95.80	110.99	124.86	110.99	95.80
		Flow, kg/s	0.43420	0.0403	0.1096	0.1344	0.1096	0.0403
		Exit Temp, C		71.64	79.35	86.17	79.35	71.64
0.70	13	Buoyancy, Pa		95.79	110.97	124.91	110.97	95.79
		Flow, kg/s	0.43419	0.0403	0.1095	0.1344	0.1095	0.0403
		Exit Temp, C		71.65	79.36	86.15	79.36	71.65
0.75	13	Buoyancy, Pa		95.78	111.00	124.87	111.00	95.78
		Flow, kg/s	0.43421	0.0403	0.1096	0.1344	0.1096	0.0403
		Exit Temp, C		71.66	79.34	86.18	79.34	71.66
0.80	31	Buoyancy, Pa		95.82	110.97	124.87	110.97	95.82
		Flow, kg/s	0.43420	0.0404	0.1096	0.1344	0.1096	0.0404
		Exit Temp, C		71.63	79.35	86.17	79.35	71.63

- Notes: 1. ϵ = Fraction of coolant temperature change (from the previous heat transfer calculation) that is used in the current outer iteration
 2. Using laminar friction factor $f = 94.7174/Re$ instead of the laminar, transition, or turbulent value calculated by routine GETF

APPENDIX XII. VERIFICATION AND APPLICATION OF SEARCH CAPABILITY

1. Introduction

To save the reactor analyst's time, a general search capability (input option ISRCH = 1) has been implemented in the version V4.2 of the code to get a user-specified target value for a specified code output variable (e.g., reactor coolant flow rate) by adjusting a specified input datum (e.g., applied pressure drop). Two basic types of search are implemented: (1) Single search in which *one* input datum is adjusted to achieve a target value for *one* output variable; and (2) Double search in which *two* input data are adjusted to achieve target values for *two* output variables. Figure 5 (in the main body of this Users Guide) shows the logic flow diagram of performing a search using the *interval-halving technique*.

Currently, 11 single searches and 5 double searches are available in the code, as listed in the input description in Appendix I. These searches adjust the input applied pressure drop or/and reactor power to get target values of any one or any two of these calculated quantities: core flow rate, minimum onset of nucleate boiling ratio (ONBR), minimum departure from nucleate boiling ratio (DNBR), minimum flow instability power ratio FIR, maximum cladding surface temperature ($T_{cs,max}$), and maximum coolant exit temperature ($T_{ex,max}$). The search capability is implemented such that new searches can be easily added.

The search capability also works for reactor problems using the hot channel factors option 2 (input IHCF = 2). When the option IHCF is 2, an input datum (depending on the search type) is adjusted so that the value of a code output quantity with *both* global and local hot channel factors applied equals an input target value. Using the search capability, a single run of the code generates all the data needed to plot a reactor operation diagram showing the relationship among three reactor parameters, e.g., nominal or true reactor power, nominal or true core flow, and the global minimum ONBR or minimum DNBR with all hot channel factors applied.

2. History Data and Search Capability

At the end of the output file on unit 6, the code prints one line of history data (a summary of the key results of the run) for a problem that does not use the hot channel factors option 2, and two lines of history data for a problem that uses the hot channel factors option 2. The first line is for the nominal case (without applying any hot channel factors), and the second line is for the case with global and local hot channel factors applied.

The history data is useful in plotting the results obtained by the search capability, as demonstrated herein. In a single run of the code, one can make a diagram plotting the *nominal reactor power versus the nominal core flow* at a constant value of the minimum ONBR with global and local hot channel factors applied, parametrically varying the constant value of the minimum ONBR. Using the results of the same run, one can also make some another diagram plotting the *true reactor power versus the true core flow* at constant values of the minimum ONBR with global and local hot channel factors applied.

3. Verification for a Test Problem without Hot Channel Factors

In order to verify the code for problems not using hot channel factors, Table XII-1 shows an input data file for a test problem (Test Problem 27) having 2 fuel assemblies of identical geometry, without any bypass channel. Each fuel assembly has 4 fuel plates and 5 coolant channels. The geometry and power distribution in the fuel assemblies are specified in the input data file. The flow through the coolant channels is determined by a pressure drop applied on the fuel assemblies. As specified on input cards 0203 and 0204 in Table XII-1, this problem exercises the double search type 21 with the objective of verifying the implementation of this search type. The input cards 0203 and 0204 specify that the applied pressure drop be adjusted in the range 0.1 to 0.5 MPa, and the nominal reactor power be adjusted in the range 0.5 to 2.5 MW so that the reactor achieves a core flow of 35.0 kg/s with a minimum ONBR of 5.0. The following steps were taken in the verification of the code:

- (1) The code was run for Test Problem 27 (input file in Table XII-1). The code writes and saves the input data file (named *input.modified* and shown in Table XII-2) used in the last iteration of the search which has the converged values of the two input data that are adjusted during the search, i.e., the applied pressure drop (0.32109375 MPa) and the nominal reactor power (1.4580078 MW, both shown in boldface on the card 0500 in Table XII-2). The output file and the converged input data file were saved.
- (2) The converged input data file saved in step 1 was converted into an input data file *without any search* for an older pre-search version (V3.6) of the code, simply by commenting out the input cards 0203 and 0204, and by setting the search option ISRCH to zero on the input card 0200. Table XII-2 shows the converged input data file thus obtained. Then the older version of the code was run for the converged input data file obtained, and the resulting output file was saved.
- (3) The implementation of the search option 21 is verified if the two codes give the same results. The output files obtained by running the current code and the older version of the code were compared. Table XII-3 shows a comparison of the key results. The older version of the code gives a core flow of 35.0 kg/s and a minimum ONBR of 5.0, the same results as the current code. This provides a verification of the implementation of the search option 21.

The history data written by the older version of the code does not have three key results: the minimum flow instability power ratio FIR_{min} , the maximum cladding surface temperature $T_{cs,max}$, and the maximum coolant temperature $T_{ex,max}$. This is because the older code calculates FIR_{min} , and prints it in the body of the output file but does not include it in the history data. Its value printed in the body of the output file is 9.1616, identical to that in the output of the current code. Furthermore, the older version of the code does not calculate the other two key data ($T_{cs,max}$ and $T_{ex,max}$) and hence they are not present in its history data. These two data were added in the current version of the code in the course of adding the search capability.

4. Verification for a Test Problem Using Hot Channel Factors

The same approach as used in Section 4 (for problems without hot channel factors) is used again to verify the implementation of the search type 21 for a problem with hot channel factors. To verify the code for problems using the option 2 of hot channel factors, Table XII-4 shows the input data file for a test problem (Test Problem 28) having 2 fuel assemblies of identical geometry, without any bypass channel. Each fuel assembly has 4 fuel plates and 5 coolant channels. The geometry and power distribution in the fuel assemblies are specified in the input data file. The six hot channel factors that are used in the option 2 are defined in Section 3.5.2 of the main body of this Users Guide. Their values, shown in boldface in Table XII-4, are:

Global Factors: FPOWER = 1.18, FFLOW = 1.25, FNUSLT = 1.20
Local Factors: FBULK = 1.05, FFILM = 1.06, FFLUX = 1.07

The flow through the coolant channels is determined by a pressure drop applied on the fuel assemblies. As specified on input cards 0203 and 0204 in Table XII-4, this problem exercises the double search type 21 with the objective of verifying the implementation of this search type. The input cards 0203 and 0204 specify that the applied pressure drop be adjusted in the range 0.1 to 0.5 MPa, and the nominal reactor power be adjusted in the range 0.5 to 3.0 MW so that the reactor achieves, with all hot channel factors applied, a core flow of 6.0 kg/s with a minimum ONBR of 1.2. The following steps were taken to verify the code:

- (1) The code was run for Test Problem 28 (input file in Table XII-4). The code writes and saves the input data file (named *input.modified* and shown in Table XII-5) used in the last iteration of the search which has the converged values of the two input data that are adjusted during the search, i.e., the applied pressure drop (0.11537476 MPa) and the nominal reactor power (0.95423889 MW, both shown in boldface on the card 0500 in Table XII-5). The output file and the converged input data file were saved.
- (2) The converged input data file saved in step 1 was converted into an input data file *without any search* for the older version of the code, simply by commenting out the input cards 0203 and 0204, and by setting the search option ISRCH to zero on the input card 0200. Table XII-5 shows the converged input data file thus obtained. Then the older version of the code was run for the converged input data file obtained, and the resulting output file was saved.
- (3) The implementation of the search option 21 is verified if the two codes give the same results. The output files obtained by running the current code and the older version of the code were compared. Table XII-6 shows a comparison of the key results printed as the history data at the end of the output file. *As discussed below*, the older version of the code gives a core flow of 6.000 kg/s and a minimum ONBR of 1.200 with both global and local hot channel factors, the same results as the current code. This provides a verification of the implementation of the search option 21 for problems using hot channel factors.

Discussion of ONBR with Hot Channel Factors: When using the hot channel factors option 2, the older versions of the code calculate (i) the minimum ONBR with only global hot channel

factors, and also (ii) the minimum ONBR with both global and local hot channel factors. Both minima are printed in the main body of the output file. However, the history data printed at the end of the older code output file contains the former, not the latter. This discrepancy is removed in the current code, and the history data printed at the end of its output file contains the minimum ONBR with both global and local hot channel factors. As shown in Table XII-6, both code versions calculate a minimum ONBR of 1.268 with only global hot channel factors. Both code versions calculate a minimum ONBR of 1.200 with both global and local hot channel factors.

Discussion of DNBR with Hot Channel Factors: Regarding the DNBR using the hot channel factors option 2, the older versions of the code calculate the minimum DNBR with only global hot channel factors. The older and the current code versions calculate a minimum DNBR of 14.092 with only global hot channel factors. The minimum DNBR with both global and local hot channel factors is not calculated by the older versions of the code. This discrepancy is removed in the current code. The minimum DNBR of 12.934 with both global and local hot channel factors is printed in the main body of the current code output file, and also in the pass 2 of the history data.

Flow Instability Power Ratio (FIR) with Hot Channel Factors: Regarding the FIR using the hot channel factors option 2, the older versions of the code calculate the minimum FIR with only global hot channel factors. The older and the current code versions calculate a minimum FIR of 1.807 with only global hot channel factors. The minimum FIR with both global and local hot channel factors is not calculated by the older versions of the code. This discrepancy is removed in the current code. The minimum FIR of 1.721 with both global and local hot channel factors is printed in the main body of the current code output file, and also in the pass 2 of the history data.

5. Plotting Reactor Operation Diagrams Using the Search Capability

We now demonstrate how to use the search capability to get, in one run of the code, all the data needed to plot a three-parameter reactor operation diagram, e.g., to plot multiple power versus flow curves, each at a constant value of minimum ONBR, varying the ONBR parametrically. The power and flow could be nominal or true. The value of minimum ONBR could be with or without the global and local hot channel factors applied when the hot channel factors option 2 is used. Instead of the minimum ONBR, the parameter could be (i) the minimum DNBR, (ii) the maximum cladding surface temperature, or (iii) the maximum coolant temperature.

Table XII-7 shows an input data file (Test Problem 29) for the current code that uses the search type 21 to get all the data needed (in a single code run) for plotting a diagram of the nominal power versus the nominal core flow, parametrically varying the minimum ONBR. This problem uses the hot channel factors option 2 (global and local hot channel factors). Therefore, the minimum ONBR mentioned here is its value with all six hot channel factors applied. The search data is provided on input cards 0203 and 0204. The card 0203 specifies that the fuel assembly applied pressure drop be adjusted between 0.1 and 0.5 MPa to achieve a target core flow rate of 6.0 kg/s (the first of the 10 target flow rates 6.0, 6.5, 7.0, 7.5, 8.0, 9.0, 10.0, 11.0, 12.0, and 12.5 kg/s input on card 0203). These flow rates are with all hot channel factors applied. The card 0204 specifies that the reactor power be adjusted between 0.2 and 3.0 MW to achieve a target

minimum ONBR of 1.2 (the first of the 4 target ONBR minima 1.2, 1.5, 2.0, and 2.5 input on card 0204). These ONBR minima are with all the hot channel factors applied.

Using 10 target values for the core flow and 4 target values for the minimum ONBR, it is noted that Test Problem 29 has 40 double searches. Each double search involves about 300 to 400 iterations (or runs of the pre-search code). This problem made a total of 13737 iterations, requiring on the average about 343 iterations per double search, and used an elapsed time of 2.6 hours. An output file *output.srch* newly added to current code contains a summary of the iterations. The converged results for each double search are saved in the output file on unit 6, as usual. In addition, a summary of the key results for all searches (history data) are saved at the end of the output file on unit 6.

Table XII-8 shows the summary of the history data calculated for this problem. In the history data, the code writes, for each search with hot channel factors option 2, two lines containing 17 key results per line. Of these 17 results, only 13 are shown in Table XII-8 for brevity. The first column shows the pass number for each search. It is noted that the data in pass 1 ($I = 1$) is the nominal case without any hot channel factors whereas the data in pass 2 ($I = 2$) has all the hot channel factors applied. Thus the summary of the key results for all 40 searches *printed by the code* is a table of 80 rows and 17 columns, whereas the summary shown in Table XII-8 is a table of 80 rows and 13 columns.

The reactor power in column 2 of pass 1 (Table XII-8), the core flow in column 4 of pass 1, and the minimum ONBR in column 7 of pass 2 were plotted (on a Microsoft Spreadsheet) to obtain the reactor operation diagram shown in Fig. 1. This is a three-parameter reactor operation diagram, showing the relationship among the nominal reactor power, the nominal core flow, and the minimum ONBR with all six hot channel factors applied.

It is noted that the power and flow data in pass 2 ($I = 2$) are with the hot channel factors applied, and hence are true reactor power and true flow rate. The reactor power in column 2 of pass 2, the core flow in column 4 of pass 2, and the minimum ONBR in column 7 of pass 2 were plotted to obtain the diagram shown in Fig. 2. This is a three-parameter reactor operation diagram, showing the relationship among the true reactor power, the true core flow, and the minimum ONBR with all six hot channel factors applied.

6. Conclusions

A general search capability implemented in the code has been verified for problems with or without hot channel factors. The utility of the search capability has been demonstrated by plotting some reactor operation diagrams involving three reactor parameters, using data obtained by a single run of the code. This greatly reduces the reactor analyst's effort. In the course of implementing the search capability, the calculation of minimum DNBR and minimum flow instability power ratio (FIR), with both global and local hot channel factors applied, were added to the code when using the hot channel factors option 2 (input IHCF = 2). The newly calculated ratios are used as target values in some searches available in the code.

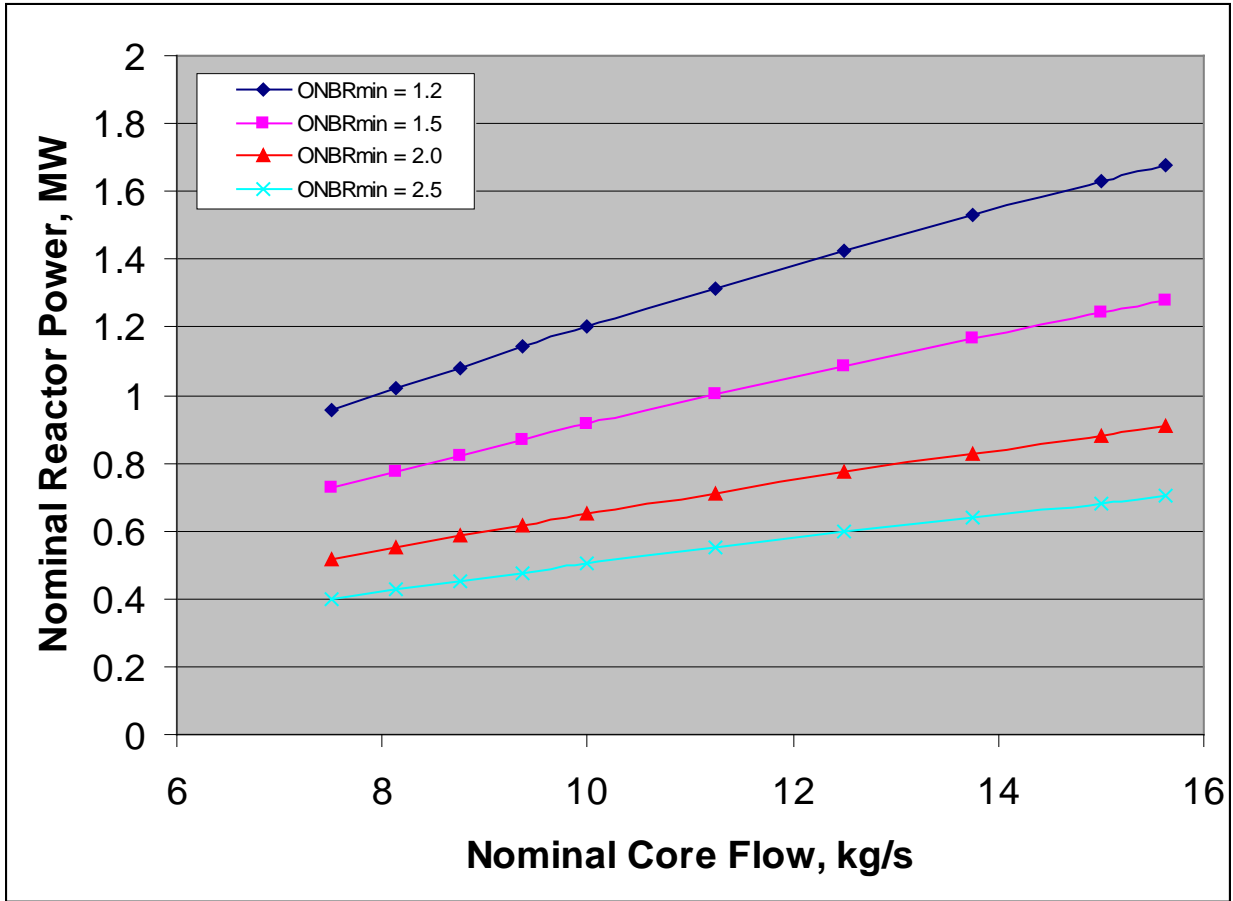


Fig. 1. Reactor Operation Diagram Showing the Relationship among Nominal Reactor Power, Nominal Core Flow, and the Minimum ONBR with Global and Local Hot Channel Factors

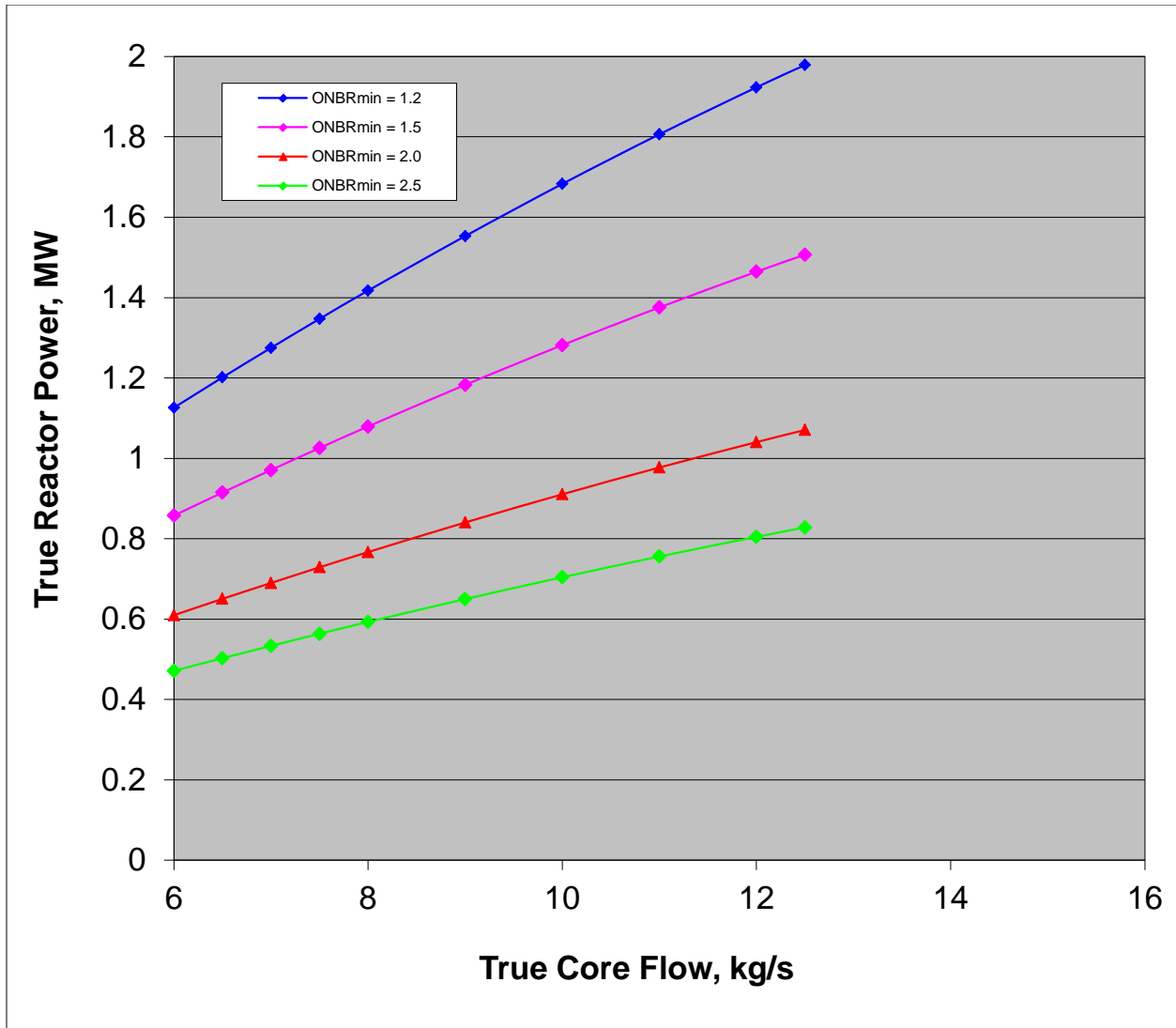


Fig. 2. Reactor Operation Diagram Showing the Relationship among True Reactor Power, True Core Flow, and the Minimum ONBR with Global and Local Hot Channel Factors Applied

TABLE XII-1. Input File for Test Problem 27 without Hot Channel Factors That Uses Double Search Type 21

```

Test Problem: Using Search Option, 2 assy (of identical geometry) producing 1 MWT
! Each assembly has 4 fuel plates and 5 coolant channels
! H2O coolant, Flow is calculated from input pressure drop
! All hot channel factors = 1.0
! No bypass flow, NCTYP=0
! 10 axial heat transfer nodes in the heated length of fuel plates
! 1 2 3 4 5 6 7 8 9 10 11 12 13 14 15 16 17 18 19 # Card 0200
  0 0 0 1 0 1 1 1 0 0 0 0 0 0 0 0 1 0 Card(1)0200
  21 0.1 0.5 1 35.0 Card(1)0203
  0.5 2.5 1 5.00 Card(1)0204
  2 3 0.50 1.00 1.00 1.00 3 Card(1)0300
! Using pressure driven mode
  1 20 1.00 Card(1)0301
  1 1 1 Card(1)0302
1.20 1.20 Card(2)0303
30.0E-04 0.02955665 0.15 8.00 0.20 15.0E-03 Card(3)0304
30.0E-04 5.91133E-03 0.75 0.00 0.20 3.00E-03 Card(3)0304
30.0E-04 0.02955665 0.15 8.00 0.20 15.0E-03 Card(3)0304
! Use the code's built-in correlation for friction factor
0.00 0.00 0.00 Card(1)0305
  5 3 0.00 0.75 0.50E-03 0.00 1.00E-03 100.00 Card(1)0306
6.00E-04 5.91133E-03 0.4060 0.20 0.20 3.00E-03 Card(5)0307
6.00E-04 5.91133E-03 0.4060 0.40 0.20 3.00E-03 Card(5)0307
6.00E-04 5.91133E-03 0.4060 0.40 0.20 3.00E-03 Card(5)0307
6.00E-04 5.91133E-03 0.4060 0.40 0.20 3.00E-03 Card(5)0307
6.00E-04 5.91133E-03 0.4060 0.20 0.20 3.00E-03 Card(5)0307
0.20 0.20 0.20 0.20 Card(1)0308
! Card 0308a not required
! Radial power peaking factor data by fuel plate for each assembly. Input flow data by
! channel for each assembly on Cards 0310 not required because WFGES(1) is non-zero
0.900 0.950 1.050 1.100 Card(2)0309
0.901 0.951 1.049 1.099 Card(2)0309
! DP0 DDP DPMAX POWER TIN PIN
0.10 0.04 0.10 1.00 45.0 1.40 Card(1)0500
Card(2)0500
  50 0.0001 25.0 0.00 1.00 Card(1)0600
  11 Card(1)0700
0.00 0.80 Card(11)0701
0.10 0.88 Card(11)0701
0.20 0.96 Card(11)0701
0.30 1.04 Card(11)0701
0.40 1.12 Card(11)0701
0.50 1.20 Card(11)0701
0.60 1.12 Card(11)0701
0.70 1.04 Card(11)0701
0.80 0.96 Card(11)0701
0.90 0.88 Card(11)0701
1.00 0.80 Card(11)0701
  0 Card(11)0702

```


TABLE XII-3. Comparison of Key Results for Test Problem 27 Obtained by PLTEMP/ANL V4.2 and V3.6

Pass No.	Power MW	Delta P MPa	Core Flow kg/s	Bypass kg/s	Total kg/s	ONBR Min	DNBR Min	Total m ³ /hr	Total gpm	FIR Min	Max Clad Surf T(C)	Max Cool Temp(C)
History Data for Test Problem 27 Calculated by PLTEMP/ANL V4.2 Using Input File of Table 1												
1	1.45801	0.32109375	35.0000	0.0000	35.0000	5.000	23.799	127.11796	559.68352	9.162	74.489	58.035
History Data for Test Problem 27 Calculated by PLTEMP/ANL V3.6 Using Converged Input File of Table 2												
1	1.45801	0.32109375	35.0000	0.0000	35.0000	5.000	23.799	127.11796	559.68352			

TABLE XII-6. Comparison of Key Results for Test Problem 28 Calculated by PLTEMP/ANL V4.2 and V3.6

Pass No.	Power MW	Delta P MPa	Core Flow kg/s	Bypass kg/s	Total kg/s	ONBR Min	DNBR Min	Total m ³ /hr	Total gpm	FIR Min	Max Clad Surf T(C)	Max Cool Temp(C)
History Data for Test Problem 28 Calculated by PLTEMP/ANL V4.2 Using Input File of Table 4												
1	0.95424	0.11537476	7.5000	0.0000	7.5000	1.926	18.953	27.23946	119.93171	2.674	123.287	91.039
2*	1.12600	0.11537476	6.0000	0.0000	6.0000	1.200	12.934	21.79156	95.94537	1.721	170.848	116.556
With Only Global Hot Channel Factors						1.268	14.092			1.807		
History Data for Test Problem 28 Calculated by PLTEMP/ANL V3.6 Using Converged Input File of Table 5												
1	0.95424	0.11537476	7.5000	0.0000	7.5000	1.926	18.953	27.23946	119.93171			
2**	1.12600	0.11537476	6.0000	0.0000	6.0000	1.268	14.092	21.79156	95.94537			
With Global and Local Factors						1.200						

* With Global and Local Hot Channel Factors Applied

** With Only Global Hot Channel Factors Applied

TABLE XII-4. Input File for Test Problem 28 with Hot Channel Factors Option 2 That Uses Double Search Type 21

```

Test Problem: 2 assemblies (of identical geometry) producing 1 MWt
! Each assembly has 4 fuel plates and 5 coolant channels
! H2O coolant, Flow is calculated from input pressure drop
! Uses Earl's hot channel factors, All Arnie's hot channel factors must be 1.0
! No bypass flow, NCTYP=0
! 10 axial heat transfer nodes in the heated length of fuel plates
! 1 2 3 4 5 6 7 8 9 10 11 12 13 14 15 16 17 18 19 20 #Card 0200
0 0 0 1 0 1 1 1 0 0 0 0 0 0 2 0 1 Card(1)0200
1.18 1.25 1.20 Card(1)0201
21 0.1 0.5 1 6.0 Card(1)0203
0.2 3.0 1 1.2 Card(1)0204
2 3 0.50 1.00 1.00 1.00 3 Card(1)0300
! Using pressure driven mode
1.05 1.06 1.07 Card(1)0300A
1 20 1.00 Card(1)0301
1 1 1 Card(1)0302
1.20 1.20 Card(2)0303
30.0E-04 0.02955665 0.15 8.00 0.20 15.0E-03 Card(3)0304
30.0E-04 0.02955665 0.75 0.00 0.20 15.0E-03 Card(3)0304
30.0E-04 0.02955665 0.15 8.00 0.20 15.0E-03 Card(3)0304
! Use the code's built-in correlation for friction factor
0.00 0.00 0.00 Card(1)0305
5 3 0.00 0.75 0.50E-03 0.00 1.00E-03 100.00 Card(1)0306
6.00E-04 5.91133E-03 0.4060 0.20 0.20 3.00E-03 Card(5)0307
6.00E-04 5.91133E-03 0.4060 0.40 0.20 3.00E-03 Card(5)0307
6.00E-04 5.91133E-03 0.4060 0.40 0.20 3.00E-03 Card(5)0307
6.00E-04 5.91133E-03 0.4060 0.40 0.20 3.00E-03 Card(5)0307
6.00E-04 5.91133E-03 0.4060 0.20 0.20 3.00E-03 Card(5)0307
0.20 0.20 0.20 0.20 Card(1)0308
! Card 0308a not required
! Radial power peaking factor data by fuel plate for each assembly. Input flow data by
! channel for each assembly on Cards 0310 not required because WFGES(1) is non-zero
0.900 0.950 1.050 1.100 Card(2)0309
0.600 0.800 1.200 1.400 Card(2)0309
! DPO DDP DPMAX POWER TIN PIN
0.10 0.04 0.10 1.00 45.0 1.40 Card(1)0500
Card(2)0500
50 0.0001 25.0 0.00 1.00 Card(1)0600
11 Card(1)0700
0.00 0.80 Card(11)0701
0.10 0.88 Card(11)0701
0.20 0.96 Card(11)0701
0.30 1.04 Card(11)0701
0.40 1.12 Card(11)0701
0.50 1.20 Card(11)0701
0.60 1.12 Card(11)0701
0.70 1.04 Card(11)0701
0.80 0.96 Card(11)0701
0.90 0.88 Card(11)0701
1.00 0.80 Card(11)0701
0 Card(11)0702

```

**TABLE XII-5. Converged Input File for Test Problem 28 with Hot Channel Factors
Option 2 Without the Search Option**

```

Test Problem: 2 assemblies (of identical geometry) producing 1 MWt          Card 100
0 0 0 1 0 1 1 1 0 0 0 0 0 0 2 0 0 0 0 0 0 Card 200
1.18000E+00 1.25000E+00 1.20000E+00 Card 201
! 21 1.00000E-01 5.00000E-01 1 6.00000E+00
!2.00000E-01 3.00000E+00 1 1.20000E+00
2 3 5.00000E-01 1.00000E+00 1.00000E+00 1.00000E+00 3 0 0.00000E+00 Card 300
1.05000E+00 1.06000E+00 1.07000E+00 Card300A
1 20 1.00000E+00 Card 301
1 1 1 Card 302
1.20000E+00 1.20000E+00 Card 303
3.00000E-03 2.95567E-02 1.50000E-01 8.00000E+00 2.00000E-01 1.50000E-02 Card 304
3.00000E-03 2.95567E-02 7.50000E-01 0.00000E+00 2.00000E-01 1.50000E-02 Card 304
3.00000E-03 2.95567E-02 1.50000E-01 8.00000E+00 2.00000E-01 1.50000E-02 Card 304
0.00000E+00 0.00000E+00 0.00000E+00 0.00000E+00 0.00000E+00 Card 305
5 3 0.00000E+00 7.50000E-01 5.00000E-04 0.00000E+00 1.00000E-03 1.00000E+02 Card 306
6.00000E-04 5.91133E-03 4.06000E-01 2.00000E-01 2.00000E-01 3.00000E-03 Card 307
6.00000E-04 5.91133E-03 4.06000E-01 4.00000E-01 2.00000E-01 3.00000E-03 Card 307
6.00000E-04 5.91133E-03 4.06000E-01 4.00000E-01 2.00000E-01 3.00000E-03 Card 307
6.00000E-04 5.91133E-03 4.06000E-01 4.00000E-01 2.00000E-01 3.00000E-03 Card 307
2.00000E-01 2.00000E-01 2.00000E-01 2.00000E-01 Card 308
9.00000E-01 9.50000E-01 1.05000E+00 1.10000E+00 Card 309
6.00000E-01 8.00000E-01 1.20000E+00 1.40000E+00 Card 309
!-----
1.1537476E-1 4.00000E-02 1.00000E-019.5423889E-1 4.50000E+01 1.40000E+00 Card 500
.000000000000.000000000000 Card 500
17 1.00000E-04 2.50000E+01 0.00000E+00 1.00000E+00 Card 600
11 Card 700
0.00000E+00 8.00000E-01 Card 701
1.00000E-01 8.80000E-01 Card 701
2.00000E-01 9.60000E-01 Card 701
3.00000E-01 1.04000E+00 Card 701
4.00000E-01 1.12000E+00 Card 701
5.00000E-01 1.20000E+00 Card 701
6.00000E-01 1.12000E+00 Card 701
7.00000E-01 1.04000E+00 Card 701
8.00000E-01 9.60000E-01 Card 701
9.00000E-01 8.80000E-01 Card 701
1.00000E+00 8.00000E-01 Card 701
0
! end of input

```

**TABLE XII-7. Input File for Test Problem 29 Using Double Search Type 21
for 40 Target Values**

```

Test Problem: 2 assemblies (of identical geometry) producing 1 MWt
! Each assembly has 4 fuel plates and 5 coolant channels
! H2O coolant, Flow is calculated from input pressure drop
! Uses Earl's hot channel factors, All Arnie's hot channel factors must be 1.0
! No bypass flow, NCTYP=0
! 10 axial heat transfer nodes in the heated length of fuel plates
! 1 2 3 4 5 6 7 8 9 10 11 12 13 14 15 16 17 18 19 20 #Card 0200
0 0 0 1 0 1 1 1 0 0 0 0 0 0 2 0 1 Card(1)0200
1.18 1.25 1.20 Card(1)0201
21 0.1 0.5 10 6.0 6.5 7.0 7.5 Card(1)0203
8.0 9.0 10.0 11.0 12.0 12.5 Card(1)0203
0.2 3.0 4 1.2 1.5 2.0 2.5 Card(1)0204
2 3 0.50 1.00 1.00 1.00 3 Card(1)0300
! Using pressure driven mode
1.05 1.06 1.07 Card(1)0300A
1 20 1.00 Card(1)0301
1 1 1 Card(1)0302
1.20 1.20 Card(2)0303
30.0E-04 0.02955665 0.15 8.00 0.20 15.0E-03 Card(3)0304
30.0E-04 0.02955665 0.75 0.00 0.20 15.0E-03 Card(3)0304
30.0E-04 0.02955665 0.15 8.00 0.20 15.0E-03 Card(3)0304
! Use the code's built-in correlation for friction factor
0.00 0.00 0.00 Card(1)0305
5 3 0.00 0.75 0.50E-03 0.00 1.00E-03 100.00 Card(1)0306
6.00E-04 5.91133E-03 0.4060 0.20 0.20 3.00E-03 Card(5)0307
6.00E-04 5.91133E-03 0.4060 0.40 0.20 3.00E-03 Card(5)0307
6.00E-04 5.91133E-03 0.4060 0.40 0.20 3.00E-03 Card(5)0307
6.00E-04 5.91133E-03 0.4060 0.40 0.20 3.00E-03 Card(5)0307
6.00E-04 5.91133E-03 0.4060 0.20 0.20 3.00E-03 Card(5)0307
0.20 0.20 0.20 0.20 Card(1)0308
! Card 0308a not required
! Radial power peaking factor data by fuel plate for each assembly. Input flow data by
! channel for each assembly on Cards 0310 not required because WFGES(1) is non-zero
0.900 0.950 1.050 1.100 Card(2)0309
0.600 0.800 1.200 1.400 Card(2)0309
! DP0 DDP DPMAX POWER TIN PIN
0.10 0.04 0.10 1.00 45.0 1.40 Card(1)0500
Card(2)0500
50 0.0001 25.0 0.00 1.00 Card(1)0600
11 Card(1)0700
0.00 0.80 Card(11)0701
0.10 0.88 Card(11)0701
0.20 0.96 Card(11)0701
0.30 1.04 Card(11)0701
0.40 1.12 Card(11)0701
0.50 1.20 Card(11)0701
0.60 1.12 Card(11)0701
0.70 1.04 Card(11)0701
0.80 0.96 Card(11)0701
0.90 0.88 Card(11)0701
1.00 0.80 Card(11)0701
0 Card(11)0702

```

TABLE XII-8. History Data Printed by PLTEMP/ANL V4.2 for the Test Problem 29

===== BEGIN HISTORY RESULTS FOR ALL SEARCHES =====

I	Power MW	Delta P MPa	Core Flow kg/s	Bypass kg/s	Total kg/s	ONBR Min	DNBR Min	Total m ³ /hr	Total gpm	FIR Min	Max Clad Surf T(C)	Max Cool Temp(C)
1	0.95424	0.11537476	7.5000	0.0000	7.5000	1.926	18.953	27.23946	119.93171	2.674	123.287	91.039
2	1.12600	0.11537476	6.0000	0.0000	6.0000	1.200	12.934	21.79156	95.94537	1.721	170.848	116.556
1	1.01809	0.13475037	8.1250	0.0000	8.1250	1.926	17.908	29.50959	129.92680	2.704	123.139	90.418
2	1.20135	0.13475037	6.5000	0.0000	6.5000	1.200	12.211	23.60767	103.94144	1.740	170.664	115.577
1	1.08051	0.15558472	8.7499	0.0000	8.7499	1.927	16.997	31.77929	139.91999	2.733	122.975	89.826
2	1.27500	0.15558472	7.0000	0.0000	7.0000	1.200	11.580	25.42343	111.93599	1.759	170.455	114.657
1	1.14156	0.17788086	9.3749	0.0000	9.3749	1.928	16.191	34.04927	149.91442	2.760	122.796	89.262
2	1.34705	0.17788086	7.5000	0.0000	7.5000	1.200	11.022	27.23942	119.93154	1.776	170.221	113.783
1	1.20127	0.20163574	10.0000	0.0000	10.0000	1.928	15.473	36.31941	159.90953	2.786	122.605	88.728
2	1.41750	0.20163574	8.0000	0.0000	8.0000	1.200	10.526	29.05553	127.92763	1.793	169.959	112.944
1	1.31616	0.25350342	11.2500	0.0000	11.2500	1.930	14.250	40.85949	179.89891	2.835	122.150	87.692
2	1.55307	0.25350342	9.0000	0.0000	9.0000	1.200	9.683	32.68759	143.91913	1.825	169.360	111.322
1	1.42617	0.31115723	12.5001	0.0000	12.5001	1.931	13.230	45.39956	199.88823	2.879	121.658	86.731
2	1.68289	0.31115723	10.0001	0.0000	10.0001	1.200	8.979	36.31965	159.91058	1.854	168.654	109.819
1	1.53079	0.37457275	13.7500	0.0000	13.7500	1.932	12.363	49.93915	219.87546	2.920	121.101	85.801
2	1.80633	0.37457275	11.0000	0.0000	11.0000	1.200	8.382	39.95132	175.90037	1.880	167.839	108.369
1	1.62986	0.44375000	15.0000	0.0000	15.0000	1.933	11.612	54.47921	239.86473	2.958	120.478	84.902
2	1.92324	0.44375000	12.0000	0.0000	12.0000	1.200	7.868	43.58337	191.89179	1.905	166.913	106.958
1	1.67690	0.48052979	15.6250	0.0000	15.6250	1.934	11.272	56.74902	249.85840	2.976	120.136	84.460
2	1.97875	0.48052979	12.5000	0.0000	12.5000	1.200	7.637	45.39922	199.88672	1.917	166.403	106.265
1	0.72682	0.11635742	7.5000	0.0000	7.5000	2.430	25.528	27.23974	119.93295	3.498	106.885	80.196
2	0.85764	0.11635742	6.0000	0.0000	6.0000	1.500	18.555	21.79179	95.94636	2.248	145.405	99.751
1	0.77537	0.13587036	8.1250	0.0000	8.1250	2.431	24.107	29.50968	129.92719	3.537	106.761	79.718
2	0.91494	0.13587036	6.5000	0.0000	6.5000	1.500	17.494	23.60774	103.94176	2.275	145.245	98.990
1	0.82284	0.15685425	8.7500	0.0000	8.7500	2.432	22.869	31.77954	139.92111	3.576	106.622	79.259
2	0.97095	0.15685425	7.0000	0.0000	7.0000	1.500	16.568	25.42363	111.93689	2.299	145.068	98.278
1	0.86929	0.17930298	9.3750	0.0000	9.3750	2.433	21.775	34.04949	149.91538	3.612	106.472	78.822
2	1.02576	0.17930298	7.5000	0.0000	7.5000	1.500	15.751	27.23959	119.93230	2.322	144.867	97.601
1	0.91470	0.20321655	10.0000	0.0000	10.0000	2.434	20.800	36.31951	159.90996	3.646	106.315	78.410
2	1.07934	0.20321655	8.0000	0.0000	8.0000	1.500	15.023	29.05560	127.92797	2.344	144.648	96.954
1	1.00245	0.25541992	11.2501	0.0000	11.2501	2.435	19.132	40.85967	179.89971	3.709	105.959	77.627
2	1.18290	0.25541992	9.0001	0.0000	9.0001	1.500	13.781	32.68774	143.91976	2.386	144.145	95.719
1	1.08615	0.31342773	12.5000	0.0000	12.5000	2.437	17.748	45.39935	199.88733	3.767	105.552	76.885
2	1.28166	0.31342773	10.0000	0.0000	10.0000	1.500	12.752	36.31948	159.90986	2.424	143.559	94.554
1	1.16569	0.37723389	13.7501	0.0000	13.7501	2.438	16.573	49.93941	219.87660	3.820	105.095	76.175
2	1.37552	0.37723389	11.0000	0.0000	11.0000	1.500	11.882	39.95153	175.90128	2.459	142.885	93.442
1	1.24103	0.44680176	14.9999	0.0000	14.9999	2.440	15.554	54.47894	239.86356	3.870	104.585	75.486
2	1.46441	0.44680176	12.0000	0.0000	12.0000	1.500	11.135	43.58315	191.89085	2.491	142.123	92.358
1	1.27702	0.48375244	15.6250	0.0000	15.6250	2.440	15.093	56.74909	249.85871	3.894	104.306	75.142
2	1.50689	0.48375244	12.5000	0.0000	12.5000	1.500	10.795	45.39927	199.88697	2.507	141.704	91.822
1	0.51669	0.11736755	7.5000	0.0000	7.5000	3.282	36.731	27.23963	119.93249	4.903	90.691	70.102
2	0.60970	0.11736755	6.0000	0.0000	6.0000	2.000	27.647	21.79171	95.94599	3.149	120.082	84.082
1	0.55119	0.13702087	8.1250	0.0000	8.1250	3.284	34.672	29.50950	129.92642	4.960	90.593	69.756
2	0.65041	0.13702087	6.5000	0.0000	6.5000	2.000	26.059	23.60760	103.94114	3.187	119.953	83.534

TABLE XII-8. Continued

1	0.58466	0.15815430	8.7500	0.0000	8.7500	3.286	32.892	31.77937	139.92033	5.017	90.467	69.415
2	0.68990	0.15815430	7.0000	0.0000	7.0000	2.000	24.673	25.42349	111.93626	3.223	119.809	83.004
1	0.61765	0.18076172	9.3750	0.0000	9.3750	3.287	31.303	34.04947	149.91531	5.067	90.351	69.102
2	0.72883	0.18076172	7.5000	0.0000	7.5000	2.000	23.447	27.23958	119.93225	3.256	119.651	82.514
1	0.64988	0.20483398	10.0000	0.0000	10.0000	3.289	29.891	36.31937	159.90935	5.116	90.225	68.804
2	0.76686	0.20483398	8.0000	0.0000	8.0000	2.000	22.356	29.05549	127.92748	3.287	119.478	82.050
1	0.71223	0.25737305	11.2500	0.0000	11.2500	3.291	27.472	40.85924	179.89779	5.204	89.953	68.246
2	0.84043	0.25737305	9.0000	0.0000	9.0000	2.000	20.487	32.68739	143.91823	3.345	119.083	81.166
1	0.77166	0.31574707	12.5000	0.0000	12.5000	3.293	25.465	45.39913	199.88633	5.284	89.643	67.723
2	0.91055	0.31574707	10.0000	0.0000	10.0000	2.000	18.938	36.31930	159.90906	3.398	118.625	80.335
1	0.82818	0.37993164	13.7500	0.0000	13.7500	3.295	23.761	49.93917	219.87554	5.359	89.294	67.214
2	0.97725	0.37993164	11.0000	0.0000	11.0000	2.000	17.622	39.95134	175.90043	3.447	118.103	79.542
1	0.88167	0.44990234	14.9999	0.0000	14.9999	3.297	22.286	54.47890	239.86336	5.427	88.905	66.728
2	1.04037	0.44990234	11.9999	0.0000	11.9999	2.000	16.484	43.58312	191.89069	3.492	117.512	78.770
1	0.90732	0.48706055	15.6250	0.0000	15.6250	3.298	21.615	56.74903	249.85847	5.459	88.696	66.490
2	1.07063	0.48706055	12.5000	0.0000	12.5000	2.000	15.968	45.39923	199.88677	3.514	117.189	78.385
1	0.39934	0.11798706	7.5001	0.0000	7.5001	4.142	48.102	27.23975	119.93302	6.333	81.145	64.434
2	0.47122	0.11798706	6.0000	0.0000	6.0000	2.500	36.478	21.79180	95.94642	4.066	104.950	75.268
1	0.42600	0.13772583	8.1250	0.0000	8.1250	4.144	45.395	29.50961	129.92691	6.406	81.063	64.166
2	0.50268	0.13772583	6.5000	0.0000	6.5000	2.500	34.367	23.60769	103.94153	4.114	104.843	74.846
1	0.45208	0.15894775	8.7500	0.0000	8.7500	4.145	43.031	31.77942	139.92058	6.476	80.976	63.911
2	0.53345	0.15894775	7.0000	0.0000	7.0000	2.500	32.525	25.42354	111.93646	4.159	104.723	74.444
1	0.47758	0.18165283	9.3751	0.0000	9.3751	4.147	40.943	34.04980	149.91673	6.538	80.883	63.678
2	0.56355	0.18165283	7.5001	0.0000	7.5001	2.500	30.897	27.23984	119.93338	4.202	104.592	74.065
1	0.50252	0.20581665	10.0000	0.0000	10.0000	4.148	39.085	36.31928	159.90896	6.602	80.783	63.444
2	0.59298	0.20581665	8.0000	0.0000	8.0000	2.500	29.447	29.05542	127.92717	4.241	104.449	73.707
1	0.55073	0.25855713	11.2499	0.0000	11.2499	4.151	35.905	40.85899	179.89669	6.715	80.561	63.012
2	0.64986	0.25855713	8.9999	0.0000	8.9999	2.500	26.966	32.68719	143.91735	4.316	104.125	73.024
1	0.59673	0.31715088	12.5000	0.0000	12.5000	4.153	33.267	45.39928	199.88702	6.819	80.313	62.605
2	0.70414	0.31715088	10.0000	0.0000	10.0000	2.500	24.909	36.31943	159.90962	4.384	103.750	72.379
1	0.64048	0.38156738	13.7500	0.0000	13.7500	4.155	31.029	49.93939	219.87651	6.913	80.034	62.218
2	0.75577	0.38156738	11.0000	0.0000	11.0000	2.500	23.164	39.95151	175.90121	4.447	103.322	71.762
1	0.68192	0.45178223	15.0001	0.0000	15.0001	4.158	29.087	54.47965	239.86667	6.998	79.724	61.846
2	0.80467	0.45178223	12.0001	0.0000	12.0001	2.500	21.654	43.58372	191.89334	4.505	102.841	71.167
1	0.70174	0.48905029	15.6250	0.0000	15.6250	4.158	28.207	56.74904	249.85849	7.039	79.558	61.660
2	0.82805	0.48905029	12.5000	0.0000	12.5000	2.500	20.970	45.39923	199.88680	4.533	102.578	70.872

=====
 ===== END OF HISTORY RESULTS FOR SEARCHES =====

Total Elapsed Time = 9351.06 sec

**APPENDIX XIII. ANALYTICAL SOLUTION FOR RADIAL TEMPERATURE
DISTRIBUTION IN AN ASSEMBLY OF MULTIPLE FUEL TUBES
EACH MADE OF FIVE MATERIAL REGIONS**

(Coauthor: E. E. Feldman)

1. Description of the Analytical Solution

In nuclear reactors, the major heat source is the fuel meat of fuel tubes each of which is here modeled to have five material regions, i.e., inner cladding, inner gap, fuel meat, outer gap, and outer cladding. The innermost fuel tube could be a solid rod. The inner and outer gaps are not voids. Each gap is here intended to be used by the reactor analyst (i) to model the thickness and thermal resistance of a fuel-cladding gap as a given thickness of a mixture of fill and fission gases (assumed to remain stationary) of given thermal conductivity, or in other fuel tube/rod designs (ii) to model an additional solid region that is present in the fuel tube/rod. Some gamma radiation is deposited directly in all other regions, i.e., cladding, gap, and coolant, making them minor heat sources. An analytical solution for radial temperature distribution is obtained using *Mathematica* in radial geometry for a multi-tube fuel assembly with heat sources in all six materials, i.e., inner cladding, inner gap, fuel meat, outer gap, outer cladding, and coolant. The crud resistances at (1) the coolant-inner cladding interface and (2) the coolant-outer cladding interface of each fuel tube are included in the solution. Each crud resistance is modeled as a thermal resistance with no thickness. The gap resistances at (1) the meat-inner cladding interface and (2) the meat-outer cladding interface of each fuel tube are also included in the solution. This solution is implemented in the PLTEMP/ANL code, and verified for some sample problems.

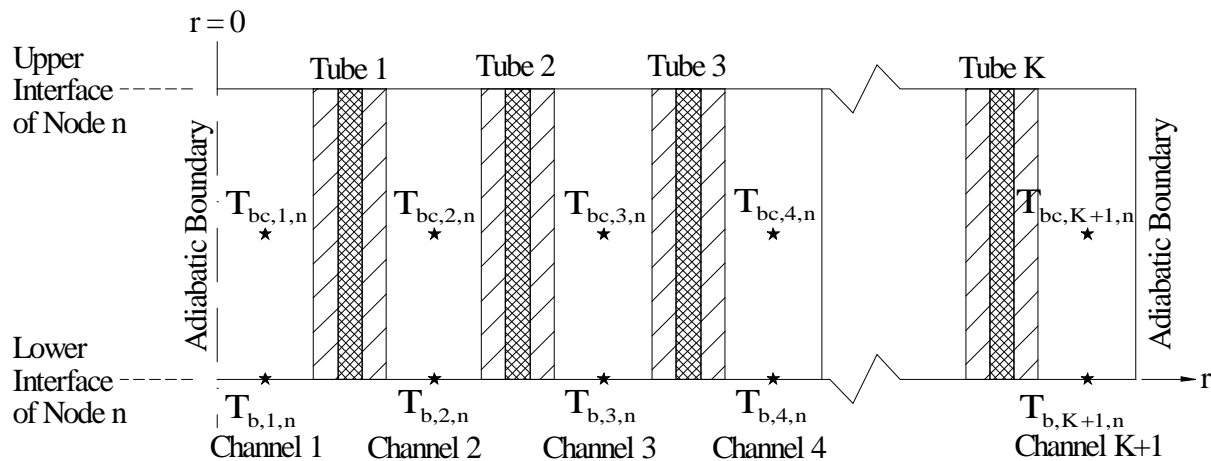


Fig. XIII-1. An Axial Slice of Fuel Assembly Showing a Heat Transfer Axial Node

Figure VIII-1 shows a vertical section of an experimental nuclear reactor fuel assembly consisting of several coaxial fuel tubes that are cooled by coolant channels of annular cross section. In this formulation, each fuel tube is assumed to be different from the others, and each coolant channel is assumed to have a different area and flow rate than the others. The method consists of setting up $K+1$ simultaneous linear algebraic equations in $K+1$ bulk coolant temperatures, $T_{bc,k,n}$ for $k = 1$ to $K+1$, in a slice of the fuel assembly shown in Fig. VIII-1.

Symbols Used:

- K = Number of fuel tubes in an assembly
 $T_{bc,k,n}$ = Coolant bulk temperature in channel k at the *center* of heat transfer axial node n , (C)
 $T_{b,k,n}$ = Coolant bulk temperature in channel k at the *entry* to heat transfer axial node n , (C)
 $g_{1,k}$ = Thickness of gap between the fuel meat and inner cladding, ($W/m^2 \cdot ^\circ C$)
 $g_{2,k}$ = Thickness of gap between the fuel meat and outer cladding, ($W/m^2 \cdot ^\circ C$)
 $h_{g1,k}$ = Gap conductance at the fuel meat and inner cladding interface, ($W/m^2 \cdot ^\circ C$)
 $h_{g2,k}$ = Gap conductance at the fuel meat and outer cladding interface, ($W/m^2 \cdot ^\circ C$)
 $h_{1,k,n}$ = Convective heat transfer coefficient on the inside of fuel tube k ($W/m^2 \cdot C$)
 $h_{2,k,n}$ = Convective heat transfer coefficient on the outside of fuel tube k ($W/m^2 \cdot C$)
 $K_{a,k}$ = Thermal conductivity of inner cladding of fuel tube k ($W/m \cdot C$)
 $K_{b,k}$ = Thermal conductivity of fuel meat in tube k ($W/m \cdot C$)
 $K_{c,k}$ = Thermal conductivity of outer cladding of fuel tube k ($W/m \cdot C$)
 $K_{d,k}$ = Thermal conductivity of the gas in inner gap of fuel tube k ($W/m \cdot C$)
 $K_{e,k}$ = Thermal conductivity of the gas in outer gap of fuel tube k ($W/m \cdot C$)
 P_n = Coolant pressure in a channel at the entry to heat transfer axial node n (Pa)
 $q_{a,k,n}$ = Volumetric heat source in inner cladding of tube k in axial node n (W/m^3)
 $q_{b,k,n}$ = Volumetric heat source in fuel meat of tube k in axial node n (W/m^3)
 $q_{c,k,n}$ = Volumetric heat source in outer cladding of tube k in axial node n (W/m^3)
 $q_{d,k,n}$ = Volumetric heat source in inner gap of tube k in axial node n (W/m^3)
 $q_{e,k,n}$ = Volumetric heat source in outer gap of tube k in axial node n (W/m^3)
 $q_{w,k,n}$ = Volumetric heat source in *coolant* (directly deposited in water) in coolant channel k in axial node n (W/m^3)
 r = Radial position coordinate with $r = 0$ at the common axis of fuel tubes (meter)
 $r_{a,k}$ = Inner radius of fuel tube k , (m)
 $r_{b,k}$ = Inner radius of meat in fuel tube k , (m)
 $r_{c,k}$ = Outer radius of meat in fuel tube k , (m)
 $r_{d,k}$ = Outer radius of fuel tube k , (m)
 $r_{e,k}$ = Outer radius of inner cladding in fuel tube k , (m)
 $r_{f,k}$ = Inner radius of outer cladding in fuel tube k , (m)
 r_{max} = Radial position of maximum fuel temperature (m)
 $R_{c1,k}$ = Crud resistance at the coolant and inner cladding interface, ($m^2 \cdot ^\circ C/W$).
It is *zero for unoxidized cladding surface* in research reactor fuels.
 $R_{c2,k}$ = Crud resistance at the coolant and outer cladding interface, ($m^2 \cdot ^\circ C/W$).
It is *zero for unoxidized cladding surface* in research reactor fuels.
 $R_{g1,k}$ = $1/h_{g1,k}$ = Gap resistance at the fuel meat and inner cladding interface, ($m^2 \cdot ^\circ C/W$).
It is *zero for good meat-cladding contact* present in research reactor fuels.
 $R_{g2,k}$ = $1/h_{g2,k}$ = Gap resistance at the fuel meat and outer cladding interface, ($m^2 \cdot ^\circ C/W$).
It is *zero for good meat-cladding contact* present in research reactor fuels.
 $t_{a,k}$ = Thickness of inner cladding of fuel tube k (meter)
 $t_{b,k}$ = Fuel meat thickness in tube k (meter)
 $t_{c,k}$ = Thickness of outer cladding of fuel tube k (meter)
 W_k = Coolant mass flow rate in channel k (kg/sec)
 X_k = Maximum fuel temperature's radial position expressed as the areal fraction
 $\frac{(r_{max,k}^2 - r_{b,k}^2)}{(r_{c,k}^2 - r_{b,k}^2)}$ of the meat cross sectional area. The subscript n is dropped for brevity.

The rather cumbersome algebraic solutions of heat conduction equations in the inner cladding, the fuel meat, the outer cladding, the inner gap, and the outer gap regions obtained with aid of *Mathematica* were further simplified manually. The manually simplified algebraic expressions were checked and verified by adding them to the end of the *Mathematica* program used to solve the heat conduction equations, and then numerical values of both the actual by *Mathematica* solution and the manually simplified solution were calculated and compared for several values of all the parameters of the problem. The values of the constants of integration and cladding surface heat fluxes matched to 20 significant digits. The solution of heat conduction equations in the inner cladding, the fuel meat, the outer cladding, the inner gap, and the outer gap of a fuel tube k are given below. For brevity, the index k has been dropped in Eqs. (1) to (32).

Temperature distribution in the inner cladding of fuel tube:

$$\frac{d}{dr} \left(r \frac{dT_a}{dr} \right) + \frac{q_a r}{K_a} = 0 \quad (1)$$

$$T_a(r) = A_2 + A_1 \text{Log}(r/r_b) - \frac{q_a r^2}{4K_a} \quad (r = r_a \text{ to } r = r_c = r_a + t_a), \quad (2)$$

Temperature distribution in the fuel meat:

$$\frac{d}{dr} \left(r \frac{dT_b}{dr} \right) + \frac{q_b r}{K_b} = 0 \quad (3)$$

$$T_b(r) = A_4 + A_3 \text{Log}(r/r_c) - \frac{q_b r^2}{4K_b} \quad (r = r_b \text{ to } r = r_c = r_b + t_b), \quad (4)$$

Temperature distribution in the outer cladding of fuel tube:

$$\frac{d}{dr} \left(r \frac{dT_c}{dr} \right) + \frac{q_c r}{K_c} = 0 \quad (5)$$

$$T_c(r) = A_6 + A_5 \text{Log}(r/r_d) - \frac{q_c r^2}{4K_c} \quad (r = r_f \text{ to } r = r_d = r_f + t_c), \quad (6)$$

Temperature distribution in the inner gap of fuel tube:

$$\frac{d}{dr} \left(r \frac{dT_d}{dr} \right) + \frac{q_d r}{K_d} = 0 \quad (7)$$

$$T_d(r) = A_8 + A_7 \text{Log}(r/r_b) - \frac{q_d r^2}{4K_d} \quad (r = r_e \text{ to } r = r_b = r_e + g_1), \quad (8)$$

Temperature distribution in the outer gap of fuel tube:

$$\frac{d}{dr} \left(r \frac{dT_e}{dr} \right) + \frac{q_e r}{K_e} = 0 \quad (9)$$

$$T_e(r) = A_{10} + A_9 \text{Log}(r/r_f) - \frac{q_e r^2}{4K_e} \quad (r = r_c \text{ to } r = r_f = r_c + g_2), \quad (10)$$

The ten constants of integration, $A_1, A_2, A_3, A_4, A_5, A_6, A_7, A_8, A_9,$ and A_{10} are determined by the following ten boundary and interface conditions: a convective boundary condition at the tube inner radius, a convective boundary condition at the tube outer radius, and two matching conditions (equal temperatures and equal heat fluxes) at each of the four material region interfaces. The interface conditions account for the temperature jump due to the crud resistances R_{c1} and R_{c2} , and gap resistances R_{g1} and R_{g2} . These boundary and interface conditions are shown below in Fig. VIII- 2 with the positions of their equality signs aligned with the corresponding boundary or interface.

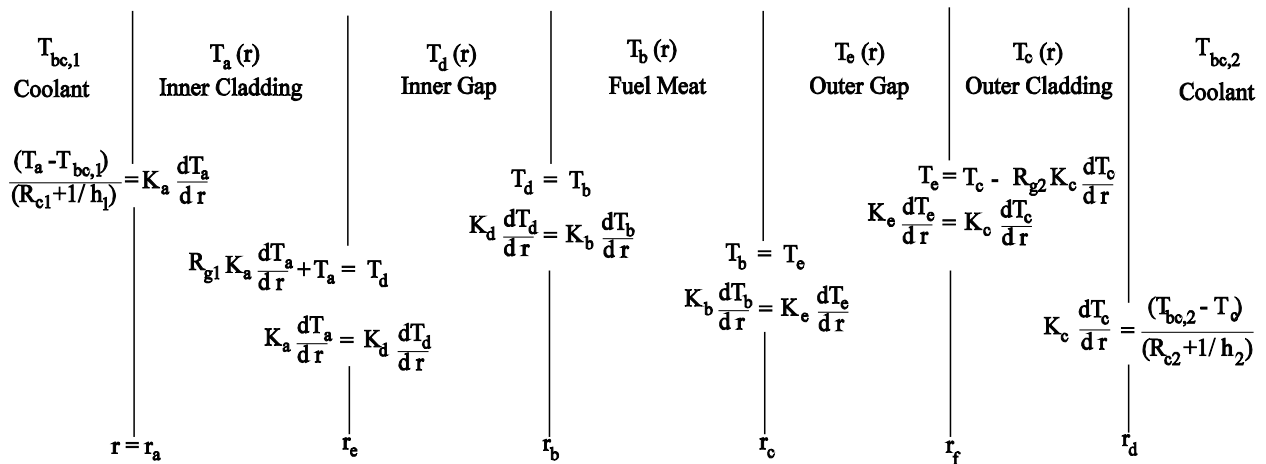


Fig. XIII-2. Boundary/Interface Conditions for Temperature and Heat Flux in a Fuel Tube

For a fuel assembly consisting of *single fuel tube*, the inner radius and the film coefficients at the inner and outer surfaces, i.e., parameters r_a, h_1 and h_2 , could be greater than zero or equal to zero. This leads mathematically to a total of 6 cases (types of boundary conditions) tabulated below.

Case	r_a	h_1	h_2	Physically Possible?
1	$r_a > 0$	$h_1 > 0$	$h_2 > 0$	Yes
2	$r_a > 0$	$h_1 = 0$	$h_2 > 0$	Yes
3	$r_a = 0$	h_1 irrelevant	$h_2 > 0$	Yes
4	$r_a > 0$	$h_1 > 0$	$h_2 = 0$	Yes
5	$r_a > 0$	$h_1 = 0$	$h_2 = 0$	Not Possible
6	$r_a = 0$	h_1 irrelevant	$h_2 = 0$	Not Possible

Out of these 6 cases, only the first four are physically possible because of two reasons: (1) Both heat transfer coefficients h_1 and h_2 cannot be zero together in a steady-state problem with heat source. If one of them is zero, then the other must be non-zero. (2) If r_a is zero, i.e., the innermost fuel tube is solid, then the outer heat transfer coefficients h_2 must be non-zero. This is because there is no material (contacting the inner radius r_a) to transfer the heat to.

The constants of integration $A_1, A_2, A_3, A_4, A_5, A_6, A_7, A_8, A_9$, and A_{10} were found with the aid of *Mathematica* for the four possible cases, and are given by Eqs. (11) through (24). Note that Log in these equations implies the natural logarithm.

$$\frac{2K_c S_1 A_5}{r_d r_f} = h_1 q_c r_a r_d r_e + h_2 S_2 + h_1 h_2 r_a r_e \left[\begin{aligned} & \frac{S}{2} + \frac{(q_b - q_d)r_b^2 + (q_e - q_b)r_c^2 + (q_d - q_a)r_e^2 + (q_c - q_e)r_f^2}{K_a} \text{Log}(r_e/r_a) \\ & + \frac{(q_e - q_b)r_c^2 + (q_c - q_e)r_f^2}{K_b} \text{Log}(r_c/r_b) + \frac{(q_c - q_e)r_f^2}{K_e} \text{Log}(r_f/r_c) \\ & + \frac{(q_b - q_d)r_b^2 + (q_e - q_b)r_c^2 + (q_c - q_e)r_f^2}{K_d} \text{Log}(r_b/r_e) \end{aligned} \right] \quad \text{if } r_a \neq 0 \quad (11a)$$

$$A_5 = \frac{-q_a r_e^2 + q_b (r_b^2 - r_c^2) + q_c r_f^2 + q_d (r_e^2 - r_b^2) + q_e (r_c^2 - r_f^2)}{2K_c} \quad \text{if } r_a = 0 \quad (11b)$$

$$S = \frac{q_a (r_e^2 - r_a^2)}{K_a} + \frac{q_b (r_c^2 - r_b^2)}{K_b} + \frac{q_c (r_d^2 - r_f^2)}{K_c} + \frac{q_d (r_b^2 - r_e^2)}{K_d} + \frac{q_e (r_f^2 - r_c^2)}{K_e} \quad (12)$$

$$S_1 = r_e r_f \{h_1 r_a + h_2 r_d\} + h_1 h_2 \{r_d r_e r_f R_{c1} + r_a r_e r_f R_{c2} + r_a r_d r_f R_{g1} + r_a r_d r_e R_{g2}\} + h_1 h_2 r_a r_d r_e r_f \left[\frac{\text{Log}(r_e/r_a)}{K_a} + \frac{\text{Log}(r_c/r_b)}{K_b} + \frac{\text{Log}(r_d/r_f)}{K_c} + \frac{\text{Log}(r_b/r_e)}{K_d} + \frac{\text{Log}(r_f/r_c)}{K_e} \right] \quad \text{if } r_a \neq 0 \quad (13a)$$

$$S_1 = h_2 r_d r_e r_f (1 + h_1 R_{c1}) \quad \text{if } r_a = 0 \quad (13b)$$

$$S_2 = h_1 q_c r_a r_e (r_d R_{c2} + r_f R_{g2}) + 2h_1 r_a r_e (T_{bc,2} - T_{bc,1}) + (r_e + h_1 r_e R_{c1}) q_a (r_a^2 - r_e^2) + (r_e + h_1 r_e R_{c1} + h_1 r_a R_{g1}) \{q_e (r_c^2 - r_f^2) + q_d (r_e^2 - r_b^2) + q_b (r_b^2 - r_c^2) + q_c r_f^2\} \quad \text{if } r_a \neq 0 \quad (14a)$$

$$S_2 = r_e (1 + h_1 R_{c1}) \{-q_a r_e^2 + q_e (r_c^2 - r_f^2) + q_d (r_e^2 - r_b^2) + q_b (r_b^2 - r_c^2) + q_c r_f^2\} \quad \text{if } r_a = 0 \quad (14b)$$

$$A_9 = \frac{(q_e - q_c) r_f^2 + 2K_c A_5}{2K_e} \quad (15)$$

$$A_3 = \frac{(q_b - q_e)r_c^2 + 2K_e A_9}{2K_b} \quad \text{if } r_b > 0, \quad A_3 = 0 \quad \text{if } r_b = 0 \quad (16)$$

$$A_7 = \frac{(q_d - q_b)r_b^2 + 2K_b A_3}{2K_d} \quad \text{if } r_e > 0, \quad A_7 = 0 \quad \text{if } r_e = 0 \quad (17)$$

$$A_1 = \frac{(q_a - q_d)r_e^2 + 2K_d A_7}{2K_a} \quad \text{if } r_a > 0, \quad A_1 = 0 \quad \text{if } r_a = 0 \quad (18)$$

$$A_6 = T_{bc,2} + \frac{q_c r_d^2}{4K_c} + (1 + h_2 R_{c2}) \left(\frac{q_c r_d}{2h_2} - \frac{A_5 K_c}{h_2 r_d} \right) \quad (19)$$

$$A_{10} = -\frac{q_c r_f^2}{4K_c} + \frac{q_e r_f^2}{4K_e} + \frac{q_c r_f R_{g2}}{2} - \frac{A_5 K_c R_{g2}}{r_f} + A_6 - A_5 \text{Log}(r_d/r_f) \quad (20)$$

$$A_4 = -\frac{q_e r_c^2}{4K_e} + \frac{q_b r_c^2}{4K_b} + A_{10} - A_9 \text{Log}(r_f/r_c) \quad (21)$$

$$A_8 = -\frac{q_b r_b^2}{4K_b} + \frac{q_d r_b^2}{4K_d} + A_4 - A_3 \text{Log}(r_c/r_b) \quad \text{if } r_b > 0, \quad A_8 = A_4 \quad \text{if } r_b = 0 \quad (22)$$

$$A_2 = -\frac{q_d r_e^2}{4K_d} + \frac{q_a r_e^2}{4K_a} + \frac{q_a r_e R_{g1}}{2} - \frac{A_1 K_a R_{g1}}{r_e} + A_8 - A_7 \text{Log}(r_b/r_e) \quad \text{if } r_e > 0 \quad (23a)$$

$$A_2 = -\frac{q_d r_e^2}{4K_d} + \frac{q_a r_e^2}{4K_a} + \frac{q_a r_e R_{g1}}{2} + A_8 \quad \text{if } r_e = 0 \quad (23b)$$

The following mathematically equivalent equation for A_2 is used only for testing purposes.

$$A_2 = T_{bc,1} + \frac{q_a r_a}{2} \left\{ \frac{r_a}{2K_a} - R_{c1} - \frac{1}{h_1} \right\} + A_1 \left\{ \frac{K_a R_{c1}}{r_a} + \frac{K_a}{h_1 r_a} + \text{Log}(r_e/r_a) \right\} \quad \text{if } r_a \neq 0 \quad (24)$$

For simplicity and brevity, the tube index k and the level index n have been omitted from the symbols used above in the analytical solution to find temperature profile in the thickness of a single fuel tube. As shown in Fig. VIII-3 for an axial slice n of the assembly, the heat fluxes from a tube k to its inner and outer adjacent coolant channels are defined as $q_{1,k,n}''$ and $q_{2,k,n}''$ respectively, and have corresponding heat transfer areas $A_{h1,k,n}$ and $A_{h2,k,n}$.

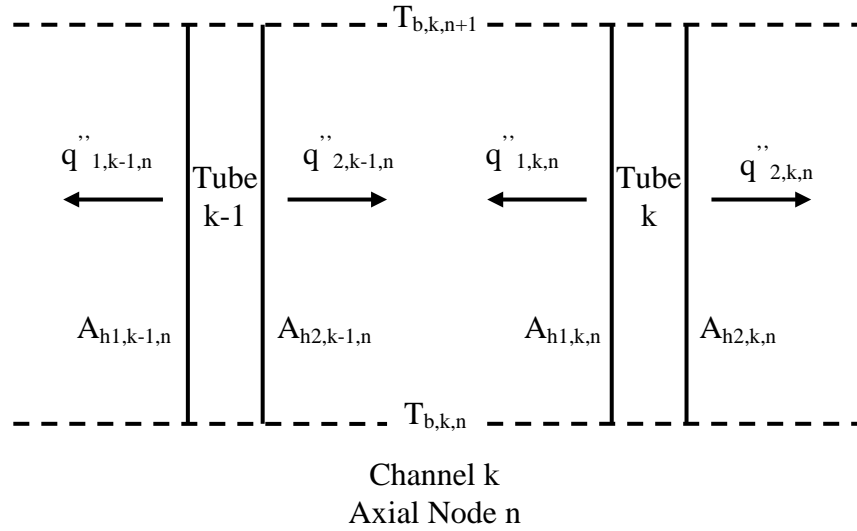


Fig. XIII-3. Heat Fluxes into a Coolant Heat Transfer Node

where

$$q_1'' = \{T_a(r_a) - T_{bc,1}\}/(R_{c1}+1/h_1) = \text{Heat flux into coolant on the inside of fuel tube } k \equiv q_{1,k,n}''$$

$$q_2'' = \{T_c(r_d) - T_{bc,2}\}/(R_{c2}+1/h_2) = \text{Heat flux into coolant on the outside of fuel tube } k \equiv q_{2,k,n}''$$

$A_{h1,k,n}$ = Surface area on the *inside* of fuel tube k for heat transfer into the coolant channel axial node n . It is the tube circumference (based on radius $r_{a,k}$) times the axial height of the node.

$A_{h2,k,n}$ = Surface area on the *outside* of fuel tube k for heat transfer into the coolant channel axial node n . It is the tube circumference (based on radius $r_{d,k}$) times the axial height of the node.

With the aid of Mathematica, these two heat fluxes can be expressed as

$$q_1'' = \alpha + R(T_{bc,2} - T_{bc,1}) \quad (25)$$

$$q_2'' = Q - (r_a/r_d)q_1'' \quad (26)$$

where Q , α , and R are given by

$$Q = \frac{q_a(r_e^2 - r_a^2) + q_b(r_c^2 - r_b^2) + q_c(r_d^2 - r_f^2) + q_d(r_b^2 - r_e^2) + q_e(r_f^2 - r_c^2)}{2r_d} \quad (27)$$

$$\alpha = -\frac{q_a r_a}{2} + \frac{S_3}{2S_1} \quad \text{if } r_a \neq 0, \quad \text{and } \alpha = 0 \quad \text{if } r_a = 0 \quad (28)$$

$$R = \frac{h_1 h_2 r_d r_e r_f}{S_1} \quad \text{if } r_a \neq 0, \quad \text{and } R = 0 \quad \text{if } r_a = 0 \quad (29)$$

The quantities S_3 and B used in Eq. (28) for α are given by Eqs. (30) and (31a) when r_a is not zero. If r_a is zero, then the inner heat flux q_1'' and the quantity R are zero, and the quantities S_3 and B are not used. Hence the quantities S_3 and B are set to zero if $r_a = 0$ as given by Eq. (30b). In this case ($r_a = 0$), the heat generated in all regions of the fuel tube comes out as a heat flux ($q_2'' = Q$) from the outer surface of the outer cladding at radius r_d , as given by Eq. (30b).

$$S_3 = h_1 h_2 r_d r_e r_f \left\{ B + S/2 + r_a q_a/h_1 + q_a (r_a R_{c1} + r_e R_{g1}) \right\} + h_1 r_e \left[\begin{array}{l} q_c (r_d^2 - r_f^2)(r_f + r_f h_2 R_{c2}) \\ + (r_f + r_f h_2 R_{c2} + r_d h_2 R_{g2}) \{ q_a r_e^2 + q_b (r_c^2 - r_b^2) + q_d (r_b^2 - r_e^2) + q_e (r_f^2 - r_c^2) \} \end{array} \right] \quad \text{if } r_a \neq 0 \quad (30)$$

$$B = \frac{(q_d - q_b)r_b^2 + (q_a - q_d)r_e^2}{K_b} \text{Log}(r_c/r_b) + \frac{(q_a - q_d)r_e^2}{K_d} \text{Log}(r_b/r_e) + \frac{(q_d - q_b)r_b^2 + (q_b - q_e)r_c^2 + (q_a - q_d)r_e^2 + (q_e - q_c)r_f^2}{K_c} \text{Log}(r_d/r_f) \quad \text{if } r_a \neq 0 \quad (31a) + \frac{(q_d - q_b)r_b^2 + (q_b - q_e)r_c^2 + (q_a - q_d)r_e^2}{K_e} \text{Log}(r_f/r_c)$$

$$S_3 = 0, \quad B = 0, \quad \text{and} \quad q_2'' = Q \quad \text{if } r_a = 0 \quad (31b)$$

Up to this point, the equations were written without an index for identifying the fuel tube and axial level. When the tube index k and the axial level index n are included, Eqs. (25) and (26) can be rewritten as follows:

$$q_{1,k,n}'' = \alpha_{k,n} + R_{k,n} (T_{bc,k+1,n} - T_{bc,k,n}) \quad (32)$$

$$q_{2,k,n}'' = Q_{k,n} - (r_{a,k}/r_{d,k}) q_{1,k,n}'' \quad (33)$$

The heat balance for coolant axial node n of channel k (between fuel tubes $k-1$ and k) can be written as Eq. (34) below, accounting for the coolant enthalpy dependence on both pressure and temperature. The quantity in the square parentheses on the left hand side of Eq. (34) is the change in coolant enthalpy $h(P,T)$ from the inlet to outlet of the axial node n . Equation (35) is obtained from Eq. (34) by expressing the enthalpy change in terms of the partial derivatives of enthalpy with respect to temperature and pressure.

$$W_k [h(P_{n+1}, T_{b,k,n+1}) - h(P_n, T_{b,k,n})] = q_{w,k,n} V_{k,n} + A_{h1,k,n} q_{1,k,n}'' + A_{h2,k-1,n} q_{2,k-1,n}'' \quad (34)$$

$$W_k [(T_{b,k,n+1} - T_{b,k,n}) C_{p,k,n} + C_{T,k,n} (P_{n+1} - P_n)] = q_{w,k,n} V_{k,n} + A_{h1,k,n} q_{1,k,n}'' + A_{h2,k-1,n} q_{2,k-1,n}'' \quad (35)$$

where

$C_{p,k,n}$ = Specific heat of coolant in channel k in axial node n, evaluated at the central bulk coolant temperature $T_{bc,k,n}$ (J/kg-C)

$C_{T,k,n}$ = Partial derivative of coolant enthalpy with respect to pressure at constant temperature, $\left(\frac{\partial h}{\partial P} \right)_T$, in channel k in axial node n (J/kg per Pa)

$V_{k,n}$ = Volume of coolant in node n of channel k

Using the heat fluxes found from Eqs. (32) and (33), and using Eq. (36) to replace the difference between coolant (upper and lower) node-boundary temperatures in Eq. (35), one obtains Eq.(26) for node-center coolant bulk temperatures of an assembly axial slice n.

$$T_{b,k,n+1} - T_{b,k,n} = 2 (T_{bc,k,n} - T_{b,k,n}) \quad (36)$$

The resulting final set of equations for node-center coolant bulk temperatures, $T_{bc,k,n}$, in channels (index k = 1 through K+1) in an axial slice (index n) of an assembly is given by Eqs. (37) through (41). These equations are of the form shown by the set of Eqs. (37) in which the coefficients a_k , b_k , c_k and d_k are known and given by Eqs. (38) through (41).

$$a_k T_{bc,k-1,n} + b_k T_{bc,k,n} + c_k T_{bc,k+1,n} = d_k \quad (\text{for channels } k = 1 \text{ through } K+1) \quad (37)$$

where

$$a_k = - \frac{r_{a,k-1} R_{k-1} A_{h2,k-1,n}}{r_{d,k-1}} \quad (38)$$

$$b_k = 2 W_k C_{p,k,n} + \frac{r_{a,k-1} R_{k-1} A_{h2,k-1,n}}{r_{d,k-1}} + R_k A_{h1,k,n} \quad (39)$$

$$c_k = -R_k A_{h1,k,n} \quad (40)$$

$$d_k = V_{k,n} q_{w,k,n} + A_{h2,k-1,n} \left(Q_{k-1} - \frac{r_{a,k-1}}{r_{d,k-1}} \alpha_{k-1} \right) + A_{h1,k,n} \alpha_k + 2 W_k C_{p,k,n} T_{b,k,n} - W_k C_{T,k,n} (P_{n+1} - P_n) \quad (41)$$

Equation (37) is a set of linear simultaneous algebraic equations for the node-center coolant bulk temperatures $T_{bc,k,n}$ of all channels in an axial slice n of the fuel assembly. The coefficients a_k , b_k , c_k and d_k are known. The coefficient matrix of the set of equations is tri-diagonal. A very simple and fast method employing Gaussian elimination is used to directly solve for the unknown temperatures $T_{bc,k,n}$. Once the node-center temperatures are obtained for the level n, Eq. (36) is used to obtain the node outlet temperatures $T_{b,k,n+1}$ which are the node inlet temperatures for the next axial slice, or the channel outlet temperatures of the assembly if level n is the last axial slice.

For a fuel assembly consisting of *two or more tubes*, it is possible in steady-state heat transfer to simultaneously have zero film coefficients on the inner surface of the innermost tube and the outer surface of the outermost tube. Therefore, the following six types of boundary conditions are physically possible for a fuel assembly of two or more tubes, and are handled in the PLTEMP code.

Case	r_a	h_1 of the Innermost Fuel Tube	h_2 of the Outermost Fuel Tube	Number of Effective Channels
1	$r_a > 0$	$h_1 > 0$	$h_2 > 0$	$K+1$
2	$r_a > 0$	$h_1 = 0$	$h_2 > 0$	K
3	$r_a = 0$	$h_1 = 0$	$h_2 > 0$	K
4	$r_a > 0$	$h_1 > 0$	$h_2 = 0$	K
5	$r_a > 0$	$h_1 = 0$	$h_2 = 0$	$K-1$
6	$r_a = 0$	$h_1 = 0$	$h_2 = 0$	$K-1$

If the film coefficient on the inner surface of the innermost fuel tube is zero, then the first coolant channel is thermally disconnected from the rest of the assembly, thus reducing the number of effective (i.e., heat removing) channels by 1, as shown in the above table. Similarly, if the film coefficient on the outer surface of the outermost tube is zero, then the last coolant channel is thermally disconnected from the rest of the assembly, thus reducing the number of effective channels by 1. These conditions are accounted for in the PLTEMP code.

After solving for these coolant temperatures, the fuel meat and cladding temperatures and other quantities like heat fluxes are evaluated using the closed-form solutions given above by Eqs. (2), (4), and (6). The radial location of the maximum fuel temperature is found by setting the derivative of $T_b(r)$, obtained from Eq. (4), equal to zero.

$$r_{\max,k} = \sqrt{\frac{2 A_3 K_{b,k}}{q_{b,k}}} \quad (42)$$

Equation (42) is used only if the fuel region has a non-zero heat source ($q_{b,k} > 0$). If $q_{b,k}$ is zero, then the radial location of the maximum fuel temperature is either the inner or the outer radius of the fuel region (r_b or r_c). The radial location found by Eq. (42) may or may not be in the fuel meat thickness, i.e., may or may not satisfy the condition $r_b \leq r_{\max} \leq r_c$. If r_{\max} is in the fuel meat thickness, the maximum fuel temperature is found by setting $r = r_{\max}$ in Eq. (4). If r_{\max} is *not* in the fuel meat thickness, the maximum fuel temperature is found by choosing the greater of the two fuel interface temperatures $T_b(r_b)$ and $T_b(r_c)$. Accordingly, r_{\max} is also redefined as r_b or r_c in this case. The fractional fuel meat cross sectional area, X_{\max} , inside the radial location of the maximum fuel temperature is given by

$$X_k = \frac{r_{\max,k}^2 - r_{b,k}^2}{r_{c,k}^2 - r_{b,k}^2} \quad (43)$$

2. Sub-Channel Flow Mixing Model

Using known values of coolant temperatures by stripe (or sub-channel) at the inlet to an axial node n , $T_{b,k,n}$, the above method is used to calculate the coolant temperatures by sub-channel at the exit of the axial node n , $T_{b,k,n+1}$, and the coolant temperatures by sub-channel at the center of the axial node, $T_{bc,k,n}$. These are each sub-channel's own mixed-mean coolant temperatures calculated without any mixing among the sub-channels of a coolant channel. The effect of sub-channel coolant mixing on the temperatures $T_{b,k,n+1}$ and $T_{bc,k,n}$ is included using a simple one-parameter (X_{mix}) mixing model described below. The mixing model calculation is done for each axial node as the heat transfer calculation proceeds node after node.

It is noted that the hydraulics model of the code, which calculates a single flow rate through a coolant channel and does not model sub-channels within a channel, was not changed with the implementation of the above heat transfer method. The currently implemented mixing model fits in this restriction of the hydraulics model. The sum of the flow rates of all sub-channels in a channel k equals the hydraulics model-calculated flow in the channel k which is not changed by the mixing model.

$$W_k = \sum_{\text{all } m} W_{k,m} \quad (44)$$

In the mixing model, each sub-channel's flow rate $W_{k,m}$ (k is channel index, and m is sub-channel index) remains unchanged after mixing. The fraction of *another* sub-channel's flow that mixes with the flow of sub-channel M is assumed to be $X_{mix} W_{k,M} / W_k$ where W_k is the total flow in coolant channel k . The remainder of sub-channel M flow comes from itself.

Based these assumptions, the flow from a sub-channel m that

$$\text{mixes with sub-channel } M = \frac{X_{mix} W_{k,M} W_{k,m}}{W_k} \quad (45)$$

The sum of the flow rates from all *other* sub-channels that

$$\begin{aligned} \text{go to sub-channel } M &= \sum_{m \neq M} \left(\frac{X_{mix} W_{k,M} W_{k,m}}{W_k} \right) = \frac{X_{mix} W_{k,M}}{W_k} \sum_{k \neq M} W_{k,m} \\ &= \frac{X_{mix} W_{k,M}}{W_k} (W_k - W_{k,M}) \end{aligned} \quad (46)$$

The flow rate of sub-channel M that remains in the

sub-channel itself after mixing = (Flow in sub-channel M) – Eq. (46)

$$= W_{k,M} - \frac{X_{mix} W_{k,M}}{W_k} (W_k - W_{k,M}) \quad (47)$$

Equations (45) to (46) describe what goes to collect in a given sub-channel M due to mixing. Based on these equations, one can write equations for how the flow of a given sub-channel m

splits into different sub-channels. For the mixing model to be consistent, the split flow rates must sum to the flow in sub-channel m before mixing ($W_{k,m}$). This consistency check follows.

Based on Eq. (45), the flow from the sub-channel m that goes to sub-channel m'

$$= \frac{X_{\text{mix}} W_{k,m'} W_{k,m}}{W_k} \quad (48)$$

Based on Eq. (46), the flow rate of sub-channel m that remains in the sub-channel itself

$$\text{after mixing} = W_{k,m} - \frac{X_{\text{mix}} W_{k,m}}{W_k} (W_k - W_{k,m}) \quad (49)$$

The sum of split flow rates = The sum of Eqs. (48) and (49) over m'

$$= \sum_{m' \neq m} \frac{X_{\text{mix}} W_{k,m} W_{k,m'}}{W_k} + W_{k,m} - \frac{X_{\text{mix}} W_{k,m}}{W_k} (W_k - W_{k,m}) \quad (50)$$

Equation (50) simplifies to Eq. (51) which verifies the consistency of the mixing model.

The sum of split flow rates of sub-channel m

$$= \frac{X_{\text{mix}} W_{k,m}}{W_k} \sum_{m' \neq m} W_{k,m'} + W_{k,m} - \frac{X_{\text{mix}} W_{k,m}}{W_k} (W_k - W_{k,m}) = W_{k,m} \quad (51)$$

In all prior heat transfer methods in the PLTEMP/ANL code, we have assumed perfect mixing over the whole cross section of a coolant channel, i.e., perfect mixing among all the sub-channels of a coolant channel. This assumption makes the reactor look safer than it actually might be, i.e., it is not a conservative assumption. This is one extreme. Assuming no mixing among the sub-channels of a channel (in the above calculation) is the other extreme. Therefore, a partial mixing model with an input parameter X_{mix} to specify the degree of mixing is considered suitable. The parameter can vary from zero to 1.0 where $X_{\text{mix}} = 0.0$ gives no mixing, and $X_{\text{mix}} = 1.0$ gives perfect mixing. The model is preliminary at this time, and eventually X_{mix} will need to be calibrated with some experimental data or fluid flow code calculated results. With an intermediate value of the parameter (e.g., $X_{\text{mix}} = 0.5$), the sub-channel temperatures still vary over the channel cross section, from sub-channel to sub-channel, but the variation is milder than that in the no mixing case. One may set $X_{\text{mix}} = 1.0$, making all sub-channel temperatures equal in a coolant channel.

In summary, PLTEMP/ANL has three coolant temperature arrays, $TTB_S(k,m)$, $TTB_M(k)$, and $TTB_P(k,m)$ where k is channel index, and m is stripe index. TTB_S are temperatures computed with *no mixing*, TTB_M are *perfectly mixed* temperatures, and TTB_P are temperatures with *partial mixing* using the input value of X_{mix} . It should be noted that the coolant temperatures edited in the code output are TTB_P .

3. Programming Notes

A new subroutine SLICHTR5 was developed to implement the above analytical solution for temperature distribution in a fuel assembly made of 5-layer fuel tubes, with the axial power shape varying from stripe to stripe. The subroutine was incorporated in the PLTEMP/ANL code

as option IEND = 1. During implementation, the old single power shape array QVZ was set to a user-specified stripe's axial power shape, for now, instead of changing and then verifying the older methods. The older analytical and Broyden methods for heat transfer calculation have been kept unchanged (as option IEND = 0) for use in 3-layer plates/tubes. These methods are not executed when the option IEND = 1. The code was tested to reproduce (to 14 significant digits) the *Mathematica* values of the intermediate parameters B, Q, R, S, S₁, S₂, S₃, α , q₁, q₂, and the ten integration constants A₁ through A₁₀ for the one-axial-node problem that was used to develop the closed-form analytical solution. The new code was also tested for the old set of 26 standard problems and found to reproduce their output files. It was also tested for the innermost tube modeling a solid rod ($r_a = 0$, or $r_e = r_a = 0$, or $r_b = r_e = r_a = 0$).

The above one-parameter mixing model is implemented at the end of subroutine SLICHTR5. The geometry data, power shapes, and computed results for the 5-layer fuel plates are kept in arrays separate from those for the 3-layer fuel plates. The results of the subroutine SLICHTR5 are stored in arrays (names ending in _S) different from those used by the older methods. They are saved in a temporary direct access binary file on unit 11 separate from those used by the older methods. The coolant mixed-mean temperatures are also written on the direct access file on unit 19 in the natural circulation calculation option for use by the existing natural circulation subroutine NATCIRC. By doing this, the subroutine NATCIRC itself did not require any change for the implementation of the natural circulation calculation based on the coolant temperatures calculated by the subroutine SLICHTR5.

To edit the results, the temperature and heat flux distribution data of each user-specified stripe are filled (one stripe at a time) into the data arrays of the six existing edit routines FINLEDIT, FINLEDIT2, FINLEDIT3, FINLEDIT4, FINLEDIT6, and UPDAT2. The data filling is done in subroutine GETDATA. This avoids rewriting new edit routines.

4. Technique Used if Input Data Has the Outermost Tube First

The method in Section 1 assumes that the fuel tubes are numbered from the innermost to the outermost (see Fig. XIII-1). In order to handle an input data file having the outermost tube numbered as 1, the code internally rearranges the input data that depend on the *numbering* of fuel tubes and coolant channels, then solves the problem using the method of Section 1, and finally rearranges the solution. The input data card types 307, 308, 308A, 309 and 310 contain all the tube-numbering-dependent input data. The calculated data that are saved in the direct access file written on logical units 19 and 20 are rearranged after the solution. All rearranging is done in the subroutine SLICE1, using variables with the suffix _R (for example, AFF_R, DFF_R). It is noted that during this whole technique, the input data arrays read from the input file are never changed, and are presented in the code output as provided in the input file.

The verification of the implementation of the method described above is reported in Ref. [1].

REFERENCES

1. Kalimullah, A. P. Olson, and E. E. Feldman, "Verification in PLTEMP/ANL Version 4.2 of the Analytical Solution Method for Radial Temperature Distribution in an Assembly of Multiple Fuel Tubes Each Made of 5 Material Regions," Intra-Laboratory Memorandum to J. E. Matos, Global Threat Reduction Initiative (GTRI) – Conversion Program, Nuclear Engineering Division, Argonne National Laboratory, IL, USA (Undocumented work).

APPENDIX XIV. NORMALIZATION OF POWER IN LONGITUDINAL STRIPES OF A FIVE-LAYER THICK FUEL PLATE

1. Normalization of Power in Radial Geometry (IGOM = 1)

The purpose of this work is to find a normalization constant factor C_{ijk} for each fuel plate at a given reactor operating power (W) so that C_{ijk}^* (the input relative power density Q_{ijkmn} in a stripe axial node) equals the operating power density (W/m^3) in the node (i,j,k,m,n). The final equation for C_{ijk} is given by Eq. (12) for the radial geometry and by Eq. (34) for the slab geometry.

Notations

i	= Fuel type number
j	= Fuel assembly number
k	= Fuel plate number
m	= Longitudinal stripe number
n	= Axial node number
NN	= Number of interfaces of axial nodes
$NN-1$	= Number of axial nodes
$NELF(i)$	= Number of fuel assemblies of type i
C_{ijk}	= Normalization constant for a fuel plate (i,j,k)
$CIRCF(i,k)$	= Width or arc length of fuel plate (i,k), meter
$F_{urad,ijk}$	= FACTF = Input values (usually un-normalized) of radial power peaking factor of plate (i,j,k)
$F_{rad,ijk}$	= Normalized radial power peaking factor of plate (i,j,k) $\equiv Q_{meat,ijk}/Q_{meat,c}$
L_i	= Fueled length of plates, meter
P_o	= POWER = Reactor operating power, W
P_{ijk}	= Operating power of a fuel plate (i,j,k), W
P_{ijkmn}	= Operating power (W) in the plate thickness (meat and claddings) of a stripe axial node (i,j,k,m,n)
Q_{ijkmn}	= QAVEZ = Input relative power density in <i>meat</i> of a stripe axial node (i,j,k,m,n)
$Q_{ave,c}$	$\equiv P_o/V_{meat,c}$ = Average power density in meat of the reactor core, W/m^3
$Q_{ave,ijk}$	= Average power density in meat of a fuel plate (i,j,k), W/m^3
Q_{fc}	= Fraction of reactor power P_o that is generated in the coolant channels due to gamma heating
$QWC(i,j,k,m,n)$	= Power density in a stripe axial node (i,j,k,m,n) of coolant channel k , W/m^3
Q_{c1}	= QFCLAD1 = Power density in the left cladding as a fraction of the power density in meat
Q_{g1}	= QFGAP1 = Power density in the left gap as a fraction of the power density in meat
Q_{c2}	= QFCLAD2 = Power density in the right cladding as a fraction of power density in meat
Q_{g2}	= QFGAP2 = Power density in the right gap as a fraction of power density in meat
$TAEMO(i,k)$	= Meat thickness in fuel plate (i,k), meter
$UNFUEL(i)$	= Unfueled width or arc length on each edge of fuel plate (i,k), meter
$V_{meat,c}$	= Total volume of fuel meat in reactor core, m^3

$V_{\text{meat,ik}}$ = Volume of meat in a fuel plate (i,k), m^3
 $V_{\text{meat,ijkmn}}$ = Volume of fuel meat in a stripe axial node (i,j,k,m,n), m^3
 $W_{\text{s,ikm}}$ = Fraction of plate width CIRCFC(i,k) that is in the m-th longitudinal stripe
 ΔZ_n = Length of axial node n, meter

In the radial geometry, the volume of meat in a stripe axial node (i,j,k,m,n), i.e., the axial node n of the m-th stripe of the k-th fuel plate in the j-th fuel assembly of the i-th type, is obtained from the reactor geometry as follows. The quantity CIRCFC(i,k)* $W_{\text{s,ikm}}$ in Eq. (1) is the *fuelled* arc length of the fuel tube (i,j,k).

$$V_{\text{meat,ijkmn}} = \text{TAEM0}(i,k) * \Delta Z_n * \text{CIRCFC}(i,k) * W_{\text{s,ikm}} \quad (1a)$$

The six radii r_a through r_f in a fuel tube (see Fig. 4 on page 32) are found from the input data as follows:

r_b = $\text{RMID}(I,K) - 0.5 * \text{TAEM0}(I,K)$ = Inner radius of the meat in the fuel tube
 r_e = $\text{RMID}(I,K) - 0.5 * \text{TAEM0}(I,K) - \text{GAP1}(I,K)$
 = Outer radius of the inner cladding of the fuel tube
 r_a = $\text{TUBERE} - \text{CLAD1}(I,K)$ = Inner radius of the K^{th} fuel tube
 r_c = $\text{RMID}(I,K) + 0.5 * \text{TAEM0}(I,K)$ = Outer radius of meat in the fuel tube
 r_f = $\text{RMID}(I,K) + 0.5 * \text{TAEM0}(I,K) + \text{GAP2}(I,K)$
 = Inner radius of the outer cladding of the fuel tube
 r_d = $\text{TUBERF} + \text{CLAD2}(I,K)$ = Outer radius of the fuel tube

The volumes of inner and outer claddings and gaps in the stripe axial node (i,j,k,m,n) are obtained by replacing the meat thickness and arc length in Eq. (1) by the thickness and arc length of the respective materials (inner cladding, etc). The arc length of a material (inner cladding, etc) can be found by scaling the meat arc length by a factor equal to the ratio of the mean radius of the material to the mean radius of the meat. This is because the meat and the inner and outer claddings and gaps each subtends the same angle at the common center.

$$V_{\text{includ,ijkmn}} = \text{CLAD1} * \Delta Z_n * \text{CIRCFC}(i,k) * W_{\text{s,ikm}} * (r_a + r_e) / [2 * \text{RMID}(i,k)] \quad (1b)$$

$$V_{\text{ingap,ijkmn}} = \text{GAP1} * \Delta Z_n * \text{CIRCFC}(i,k) * W_{\text{s,ikm}} * (r_e + r_b) / [2 * \text{RMID}(i,k)] \quad (1c)$$

$$V_{\text{outclad,ijkmn}} = \text{CLAD2} * \Delta Z_n * \text{CIRCFC}(i,k) * W_{\text{s,ikm}} * (r_f + r_d) / [2 * \text{RMID}(i,k)] \quad (1d)$$

$$V_{\text{outgap,ijkmn}} = \text{GAP2} * \Delta Z_n * \text{CIRCFC}(i,k) * W_{\text{s,ikm}} * (r_c + r_f) / [2 * \text{RMID}(i,k)] \quad (1e)$$

Assuming a normalization constant factor C_{ijk} , the operating power (W) in the meat of the stripe axial node (i,j,k,m,n) is given by $C_{ijk} * Q_{ijkmn} * V_{\text{meat,ijkmn}}$. Using Eq. (1a) for the volume of meat in the node, we get

$$P_{\text{meat,ijkmn}} = C_{ijk} * Q_{ijkmn} * \Delta Z_n * \text{CIRCFC}(i,k) * W_{\text{s,ikm}} * \text{TAEM0}(i,k) \quad (2a)$$

Similarly, the operating power (W) in the inner and outer claddings and gaps of the stripe axial node (i,j,k,m,n) are given by

$$P_{\text{in clad},ijkmn} = C_{ijk} * Q_{ijkmn} * \Delta Z_n * Q_{c1} * \text{CIRCF}(i,k) * W_{s,ikm} * \text{CLAD1}(i,k) * (r_a + r_e) / [2 * \text{RMID}(i,k)] \quad (2b)$$

$$P_{\text{in gap},ijkmn} = C_{ijk} * Q_{ijkmn} * \Delta Z_n * Q_{g1} * \text{CIRCF}(i,k) * W_{s,ikm} * \text{GAP1}(i,k) * (r_e + r_b) / [2 * \text{RMID}(i,k)] \quad (2c)$$

$$P_{\text{out clad},ijkmn} = C_{ijk} * Q_{ijkmn} * \Delta Z_n * Q_{c2} * \text{CIRCF}(i,k) * W_{s,ikm} * \text{CLAD2}(i,k) * (r_f + r_d) / [2 * \text{RMID}(i,k)] \quad (2d)$$

$$P_{\text{out gap},ijkmn} = C_{ijk} * Q_{ijkmn} * \Delta Z_n * Q_{g2} * \text{CIRCF}(i,k) * W_{s,ikm} * \text{GAP2}(i,k) * (r_c + r_f) / [2 * \text{RMID}(i,k)] \quad (2e)$$

The operating power (W) in the plate thickness (meat, gaps, and claddings) of a stripe axial node (i,j,k,m,n) is obtained by adding Eqs. (2a) through (2e).

$$P_{ijkmn} = C_{ijk} * Q_{ijkmn} * \text{CIRCF}(i,k) * W_{s,ikm} * \Delta Z_n * [2 * \text{RMID}(i,k) * \text{TAEM0}(i,k) + Q_{c1} * \text{CLAD1}(i,k) * (r_a + r_e) + Q_{g1} * \text{GAP1}(i,k) * (r_e + r_b) + Q_{c2} * \text{CLAD2}(i,k) * (r_f + r_d) + Q_{g2} * \text{GAP2}(i,k) * (r_c + r_f)] / [2 * \text{RMID}(i,k)] \quad (3)$$

The operating power (W) of the whole fuel plate (i,j,k) is obtained by summing Eq. (3) over all axial nodes and stripes.

$$P_{ijk} = C_{ijk} * \text{CIRCF}(i,k) * [2 * \text{RMID}(i,k) * \text{TAEM0}(i,k) + Q_{c1} * \text{CLAD1}(i,k) * (r_a + r_e) + Q_{g1} * \text{GAP1}(i,k) * (r_e + r_b) + Q_{c2} * \text{CLAD2}(i,k) * (r_f + r_d) + Q_{g2} * \text{GAP2}(i,k) * (r_c + r_f)] / [2 * \text{RMID}(i,k)] * \sum_{m=1}^{\text{NLSTR}(i)} \sum_{n=1}^{\text{NN}-1} Q_{ijkmn} * \Delta Z_n * W_{s,ikm} \quad (4)$$

The operating power (W) of the fuel plate (i,j,k) can also be obtained from the normalized radial power factors $F_{\text{rad},ijk}$ (the array FACTF input on Cards 0309 is un-normalized) and the reactor operating power. The radial power factors should be calculated assuming that all power is produced in the fuel meat, even in cases which model power production in cladding and coolant. The *normalized* radial power factors are defined as

$$F_{\text{rad},ijk} \equiv \frac{\text{Average power density in meat of plate } (i, j, k)}{\text{Average power density in meat of the reactor core}} = \frac{Q_{\text{ave},ijk}}{Q_{\text{ave},c}} \quad (5)$$

Note that the user-input radial power factors may be un-normalized, and hence is normalized by the code. Assuming that all power is produced in the fuel meat:

Average power density in meat of the reactor core = $\frac{\text{Reactor operating power}}{\text{Volume of meat in reactor core}}$

$$Q_{\text{ave,c}} = \frac{P_0}{V_{\text{meat,c}}} \quad (6)$$

where the volume of meat in the core and in a fuel plate (i,j,k) are given by Eqs. (7) and (8).

$$V_{\text{meat,c}} = \sum_{i=1}^{\text{NFTYP}} \text{NELF}(i) * \sum_{k=1}^{\text{NCHNF}(i)} V_{\text{meat,ik}} \quad (7)$$

$$V_{\text{meat,ik}} = [\text{CIRCF}(i,k) - 2 * \text{UNFUEL}(i)] * \text{TAEM0}(i,k) * L_i \quad (8)$$

The average power density in meat of the plate (i,j,k) can be obtained from Eqs. (5) and (6).

$$\text{Average power density in meat of plate (i,j,k)} = F_{\text{rad,ijk}} * Q_{\text{ave,c}} = \frac{F_{\text{rad,ijk}} * P_0}{V_{\text{meat,c}}} \quad (9)$$

The operating power of fuel plate (i,j,k) is given by Eq. (9) multiplied by the volume of meat in the plate.

$$P_{\text{ijk}} = \frac{F_{\text{rad,ijk}} * P_0 * V_{\text{meat,ik}}}{V_{\text{meat,c}}} \quad (10)$$

The normalization constant C_{ijk} is found by equating the operating power of fuel plate (i,j,k) obtained in Eqs. (4) and (10).

$$C_{\text{ijk}} = \frac{F_{\text{rad,ijk}} * P_0 * V_{\text{meat,ik}}}{f_1 f_2 * V_{\text{meat,c}}} \quad (11)$$

$$f_1 = \sum_{m=1}^{\text{NLSTR}(i)} \sum_{n=1}^{\text{NN}-1} Q_{\text{ijkmn}} \Delta Z_n * W_{s,ikm} \quad (11a)$$

$$f_{2,ik} = [2 * \text{RMID}(i,k) * \text{TAEM0}(i,k) + Q_{c1} * (r_a + r_e) * \text{CLAD1}(i,k) + Q_{g1} * \text{GAP1}(i,k) * (r_e + r_b) + Q_{c2} * \text{CLAD2}(i,k) * (r_f + r_d) + Q_{g2} * \text{GAP2}(i,k) * (r_c + r_f)] * \text{CIRCF}(i,k) / \{ 2 * \text{RMID}(i,k) \} \quad (11b)$$

Using Eq. (22) of the next Section, the normalized power peaking factor $F_{\text{rad,ijk}}$ of Eq. (11) can be replaced by the corresponding un-normalized power factor $F_{\text{urad,ijk}}$.

$$C_{\text{ijk}} = \frac{F_{\text{urad,ijk}} * P_0 * V_{\text{meat,ik}}}{f_1 f_{2,ik} * \sum_{i,j,k} F_{\text{urad,ijk}} V_{\text{meat,ik}}} \quad (12)$$

2. Distribution of Power Generated in Coolant Channels

In this heat transfer model, a fraction Q_{fc} of the input reactor power P_0 is assumed to be directly deposited in the coolant channels. The axial distribution of the deposited heat source and its split by stripe in coolant channels is calculated using the axial power shapes of fuel plate stripes, and assuming that a fraction $0.5*Q_{fc}$ of each fuel plate's power calculated by Eq. (12) goes into the two adjacent channels. The deposited heat source in an interior channel k (that is located between plates $k-1$ and k) is calculated from the power density distributions of plates $k-1$ and k . The flow area of **sub-channel m** is assumed to be a fraction $0.5*(W_{s,i,k-1,m} + W_{s,ikm})$ of the flow area of channel k .

Equation (3) gives the power (W) in the metal of **fuel plate k** in a stripe axial node (i,j,k,m,n) before accounting for the fraction Q_{fc} deposited in coolant. To account for the heat deposited in coolant, the normalization factors obtained from Eq. (12) are reduced by a factor of $(1 - Q_{fc})$ to get the power density in the **metal** of fuel plates: $C_{ijk}^{metal} = (1 - Q_{fc}) C_{ijk}$, and the power density in an axial node (i,j,k,m,n) of **sub-channel m** in coolant channel k is obtained as follows.

$$QWC(i, j, k, m, n) = \frac{0.5 * Q_{fc} (P_{ij,k-1,mn} + P_{ij,k,mn})}{AFF(i, k) * 0.5 * \{W_{s,i,k-1,m} + W_{s,ikm}\} * \Delta Z_n} \quad (13)$$

Equation (13) simplifies to Eq. (14) on substituting the following rewritten form of Eq. (3).

$$P_{ij,k,mn} = C_{ijk} * Q_{ijkmn} * CIRCF(i,k) * W_{s,ikm} * \Delta Z_n * f_{2,ik} \quad (3)$$

$$QWC(i, j, k, m, n) = \frac{Q_{fc} \{C_{ij,k-1} Q_{ij,k-1,mn} f_{2,i,k-1} * CIRCF(i,k-1) * W_{s,i,k-1,m} + C_{ijk} Q_{ijkmn} f_{2,ik} * CIRCF(i,k) * W_{s,ikm}\}}{AFF(i,k) * \{W_{s,i,k-1,m} + W_{s,ikm}\}} \quad (14)$$

3. Normalization of Radial Power Peaking Factors of Fuel Plates

Since input data, FACTF(I,J,K) denoted here by $F_{urad,ijk}$, for radial power peaking factors are usually un-normalized but proportional to their actual normalized values $F_{rad,ijk}$, these two arrays must be related by a constant factor independent of the indices i , j , and k . The purpose here is to find this factor of normalization. Assuming this factor to be C_0 , we have

$$F_{rad,ijk} = C_0 F_{urad,ijk} \quad (15)$$

The normalized radial power peaking factors $F_{rad,ijk}$ are defined as

$$F_{rad,ijk} = \frac{Q_{ave,ijk}}{Q_{ave,c}} \quad (16)$$

Eliminating $F_{rad,ijk}$ from Eqs. (15) and (16), we get

$$C_0 F_{\text{urad,ijk}} = \frac{Q_{\text{ave,ijk}}}{Q_{\text{ave,c}}} \quad (17)$$

Multiplying both sides of Eq. (17) by volume of meat in plate (i,j,k) and then summing over all fuel plates k of all fuel assemblies j of all types i, we get

$$\sum_{i,j,k} (C_0 F_{\text{urad,ijk}} V_{\text{meat,ik}}) = \sum_{i,j,k} \left(\frac{Q_{\text{ave,ijk}} V_{\text{meat,ik}}}{Q_{\text{ave,c}}} \right) \quad (18)$$

Since C_0 and $Q_{\text{ave,c}}$ do not depend on the indices (i, j, k), they can be pulled out of the summations in Eq. (18).

$$C_0 \sum_{i,j,k} F_{\text{urad,ijk}} V_{\text{meat,ik}} = \frac{1}{Q_{\text{ave,c}}} \sum_{i,j,k} Q_{\text{ave,ijk}} V_{\text{meat,ik}} \quad (19)$$

Noting that the product $Q_{\text{ave,ijk}} V_{\text{meat,ik}}$ equals the power produced in plate (i,j,k), the summation over all plates on the right hand side of Eq. (19) equals the total reactor power P_0 . By definition, we have $P_0 = V_{\text{meat,c}} Q_{\text{ave,c}}$. Therefore, the right hand side of Eq. (19) equals $V_{\text{meat,c}}$, the total volume of meat in core.

$$C_0 \sum_{i,j,k} F_{\text{urad,ijk}} V_{\text{meat,ik}} = V_{\text{meat,c}} \quad (20)$$

The constant of normalization is obtained from Eq. (20) as follows.

$$\sum_{i,j,k} F_{\text{urad,ijk}} (V_{\text{meat,ik}} / V_{\text{meat,c}}) = \frac{1}{C_0} \quad (21)$$

Using this value of the normalization constant in Eq. (17), we can find the normalized power peaking factors from the un-normalized power peaking factors, as follows.

$$F_{\text{rad,ijk}} = \frac{F_{\text{urad,ijk}}}{\sum_{i,j,k} F_{\text{urad,ijk}} (V_{\text{meat,ik}} / V_{\text{meat,c}})} \quad (22)$$

4. Normalization of Power in Slab Geometry (IGOM = 0)

The purpose of this work is to find the normalization constant factor C_{ijk} for a given reactor operating power (W) so that C_{ijk}^* (the input relative power density Q_{ijkmn} in a stripe axial node) equals the operating power density (W/m^3) in the node. The volume of meat in a stripe axial node (i,j,k,m,n), i.e., the axial node n of the m-th stripe of the k-th fuel plate in the j-th fuel assembly of the i-th type, is obtained from the reactor geometry as follows.

$$V_{\text{meat},ijkmn} = \text{CIRCF}(i,k) * W_{s,ikm} * \text{TAEM0}(i,k) * \Delta Z_n \quad (23)$$

Assuming a normalization constant factor C_{ijk} , the operating power (W) in the meat of the stripe axial node (i,j,k,m,n) is given by $C_{ijk} * Q_{ijkmn} * V_{\text{meat},ijkmn}$. Using Eq. (23) for the volume of meat in the node, we get

$$P_{\text{meat},ijkmn} = C_{ijk} * Q_{ijkmn} * \text{CIRCF}(i,k) * W_{s,ikm} * \text{TAEM0}(i,k) * \Delta Z_n \quad (24a)$$

Similarly, the operating power (W) in the left and right side claddings and gaps of the stripe axial node (i,j,k,m,n) are given by

$$P_{\text{leftclad},ijkmn} = C_{ijk} * Q_{ijkmn} * Q_{c1} * \text{CIRCF}(i,k) * W_{s,ikm} * \text{CLAD1}(i,k) * \Delta Z_n \quad (24b)$$

$$P_{\text{leftgap},ijkmn} = C_{ijk} * Q_{ijkmn} * Q_{g1} * \text{CIRCF}(i,k) * W_{s,ikm} * \text{GAP1}(i,k) * \Delta Z_n \quad (24c)$$

$$P_{\text{rightclad},ijkmn} = C_{ijk} * Q_{ijkmn} * Q_{c2} * \text{CIRCF}(i,k) * W_{s,ikm} * \text{CLAD2}(i,k) * \Delta Z_n \quad (24d)$$

$$P_{\text{rightgap},ijkmn} = C_{ijk} * Q_{ijkmn} * Q_{g2} * \text{CIRCF}(i,k) * W_{s,ikm} * \text{GAP2}(i,k) * \Delta Z_n \quad (24e)$$

The operating power (W) in the plate thickness (meat, gap, and claddings) of a stripe axial node (i,j,k,m,n) can be obtained by adding Eqs. (24a) through (24e).

$$P_{ijkmn} = C_{ijk} * Q_{ijkmn} * \text{CIRCF}(i,k) * W_{s,ikm} * \Delta Z_n * [\text{TAEM0}(i,k) + Q_{c1} * \text{CLAD1}(i,k) + Q_{g1} * \text{GAP1}(i,k) + Q_{c2} * \text{CLAD2}(i,k) + Q_{g2} * \text{GAP2}(i,k)] \quad (25)$$

The operating power (W) of the whole fuel plate (i,j,k) is obtained by summing Eq. (25) over all axial nodes and stripes.

$$P_{ijk} = C_{ijk} * \text{CIRCF}(i,k) * [\text{TAEM0}(i,k) + Q_{c1} * \text{CLAD1}(i,k) + Q_{g1} * \text{GAP1}(i,k) + Q_{c2} * \text{CLAD2}(i,k) + Q_{g2} * \text{GAP2}(i,k)] * \sum_{m=1}^{\text{NLSTR}(i)} \sum_{n=1}^{\text{NN}-1} Q_{ijkmn} \Delta Z_n * W_{s,ikm} \quad (26)$$

The operating power (W) of the fuel plate (i,j,k) can also be obtained from the normalized radial power factors $F_{\text{rad},ijk}$ and the reactor operating power. The radial power factors should be calculated assuming that all power is produced in the fuel meat, even in cases which model power production in cladding and coolant. The radial power factors are defined as

$$F_{\text{rad},ijk} = \frac{\text{Average power density in meat of plate } (i, j, k)}{\text{Average power density in meat of the reactor core}} \quad (27)$$

Assuming that all power is produced in the fuel meat:

Average power density in meat of the reactor core = $\frac{\text{Reactor operating power}}{\text{Volume of meat in reactor core}}$

$$Q_{\text{ave,c}} = \frac{P_0}{V_{\text{meat,c}}} \quad (28)$$

where the volume of meat in the core and in a fuel plate (i,j,k) are given by Eqs. (29) and (30).

$$V_{\text{meat,c}} = \sum_{i=1}^{\text{NFTYP}} \text{NELF}(i) * \sum_{k=1}^{\text{NCHNF}(i)} V_{\text{meat,ik}} \quad (29)$$

$$V_{\text{meat,ik}} = [\text{CIRCF}(i,k) - 2 * \text{UNFUEL}(i)] * \text{TAEM0}(i,k) * L_i \quad (30)$$

The average power density in meat of the plate (i,j,k) can be obtained from Eqs. (27) and (28).

$$\text{Average power density in meat of plate (i,j,k)} = F_{\text{rad,ijk}} * Q_{\text{ave,c}} = \frac{F_{\text{rad,ijk}} * P_0}{V_{\text{meat,c}}} \quad (31)$$

The operating power of fuel plate (i,j,k) is given by Eq. (31) multiplied by the volume of meat in the plate.

$$P_{\text{ijk}} = \frac{F_{\text{rad,ijk}} * P_0 * V_{\text{meat,ik}}}{V_{\text{meat,c}}} \quad (32)$$

The normalization constant C_{ijk} is found by equating the operating power of fuel plate (i,j,k) obtained in Eqs. (26) and (32).

$$C_{\text{ijk}} = \frac{F_{\text{rad,ijk}} * P_0 * V_{\text{meat,ik}}}{f_1 f_2 * V_{\text{meat,c}}} \quad (33)$$

$$f_1 = \sum_{m=1}^{\text{NLSTR}(i)} \sum_{n=1}^{\text{NN}-1} Q_{\text{ijkmn}} \Delta Z_n * W_{s,ikm} \quad (33a)$$

$$f_{2,ik} = \{ \text{TAEM0}(i,k) + Q_{c1} * \text{CLAD1}(i,k) + Q_{g1} * \text{GAP1}(i,k) + Q_{c2} * \text{CLAD2}(i,k) + Q_{g2} * \text{GAP2}(i,k) \} * \text{CIRCF}(i,k) \quad (33b)$$

Using Eq. (22) of the previous Section, the normalized power peaking factor $F_{\text{rad,ijk}}$ of Eq. (33) can be replaced by the corresponding un-normalized power factor $F_{\text{urad,ijk}}$.

$$C_{\text{ijk}} = \frac{F_{\text{urad,ijk}} * P_0 * V_{\text{meat,ik}}}{f_1 f_{2,ik} * \sum_{i,j,k} F_{\text{urad,ijk}} V_{\text{meat,ik}}} \quad (34)$$